A UNITED STATES DEPARTMENT OF COMMERCE PUBLICATION

EASTROPAC ATLAS

U.S. DEPARTMENT OF COMMERCE
National Oceanic and Atmospheric Administration
National Marine Fisheries Service

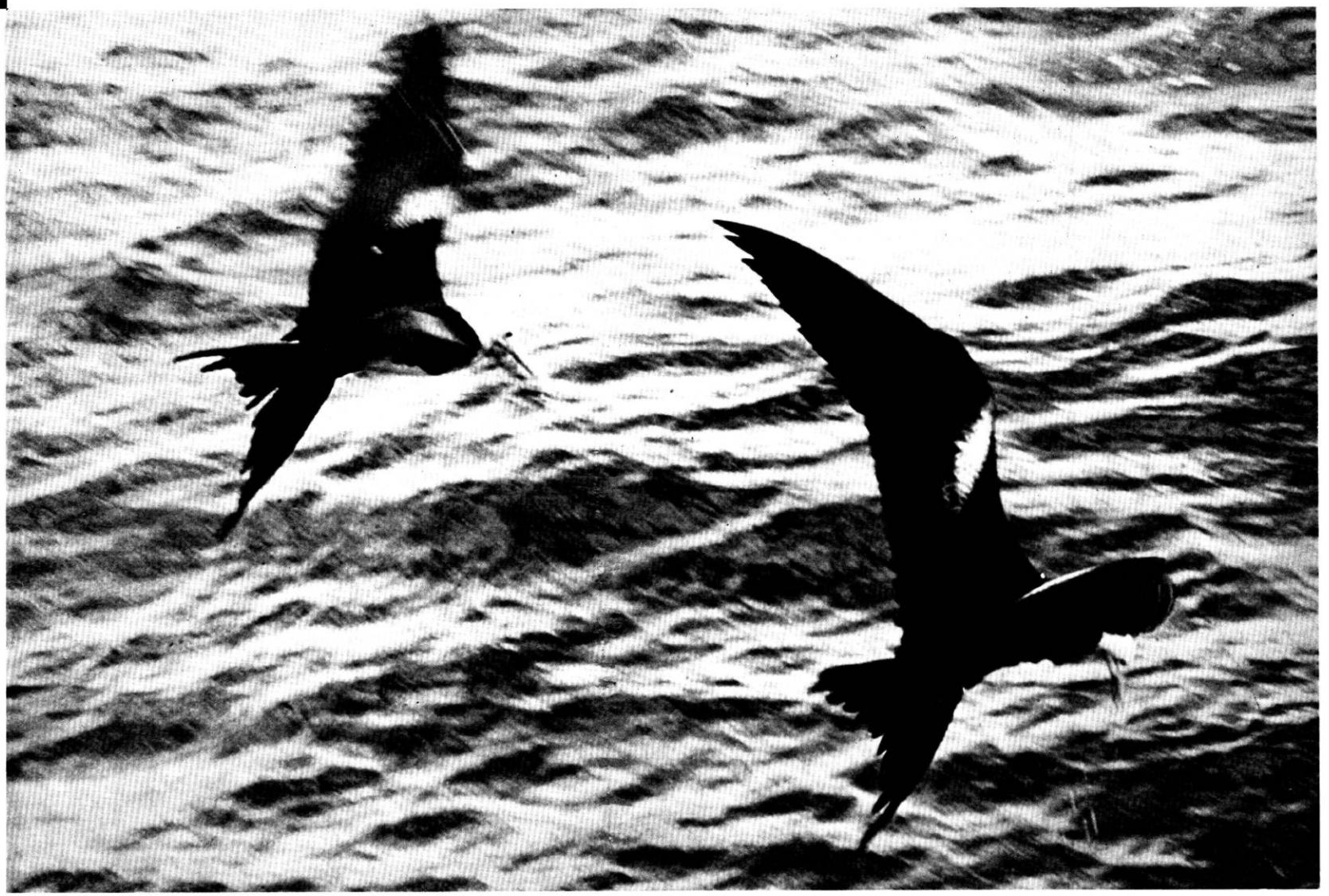

CIRCULAR
330
VOLUME 3
SEPTEMBER
1971

EASTROPAC *Atlas*

Volume 1	Physical oceanographic and meteorological data from principal participating ships, first survey cruise, February-March 1967.	In preparation
Volume 2	Biological and nutrient chemistry data from principal participating ships, first survey cruise, February-March 1967.	Published April 1971
Volume 3	Physical oceanographic and meteorological data from principal participating ships, first and second monitor cruises, April-July 1967.	Published September 1971
Volume 4	Biological and nutrient chemistry data from principal participating ships, first and second monitor cruises, April-July 1967.	Published November 1970
Volume 5	Physical oceanographic and meteorological data from principal participating ships, second survey cruise, August-September 1967.	In preparation
Volume 6	Biological and nutrient chemistry data from principal participating ships, second survey cruise, August-September 1967.	In preparation
Volume 7	Physical oceanographic and meteorological data from principal participating ships and *Oceanographer*, third and fourth monitor cruises, October 1967-January 1968.	In preparation
Volume 8	Biological and nutrient chemistry data from principal participating ships and *Oceanographer*, third and fourth monitor cruises, October 1967-January 1968.	In preparation
Volume 9	Physical oceanographic and meteorological data from principal participating ships, third survey cruise, February-March 1968.	In preparation
Volume 10	Biological and nutrient chemistry data from principal participating ships, third survey cruise, February-March 1968.	In preparation
Volume 11	Data from Latin American cooperating ships and ships of opportunity, all cruises, February 1967-March 1968.	In preparation

Cover. Immature magnificent frigatebirds near Cocos Island.
Photo by John H. Taylor, Scripps Institution of Oceanography.

ABSTRACT

This atlas contains charts depicting the distribution of physical, chemical, and biological oceanographic properties and associated meteorological properties observed during EASTROPAC. EASTROPAC was an international cooperative investigation of the eastern tropical Pacific Ocean (20° N. to 20° S., and from the west coasts of the American continents to 119° W.) which was intended to provide data necessary for a more effective use of the marine resources of the area, especially tropical tunas, and also to increase knowledge of the ocean circulation, air-sea interaction, and ecology. The Bureau of Commercial Fisheries (now National Marine Fisheries Service) was the coordinating agency. The field work, from February 1967 through March 1968, was divided into seven 2-month cruise periods. During each cruise period one or more ships were operating in the study area.

On completion of the field work the data seemed too numerous for a classical data report. Instead, it was decided to produce an 11-volume atlas of the results, with 5 volumes containing physical oceanographic and meteorological data from the principal participating ships, 5 volumes containing biological and nutrient chemistry data from the same ships, and 1 volume containing all data from Latin American cooperating ships and ships of opportunity. Extensive use was made of a computer and automatic plotter in preparation of the atlas charts. Methods used to collect and process the data upon which the atlas is based are described in detail by the contributors of the following categories of charts: temperature, salinity, and derived quantities; thickness of the upper mixed layer; dissolved oxygen; meteorology; nutrient chemistry; phytoplankton standing stocks and production; zooplankton and fish larvae; micronekton; birds, fish schools, and marine mammals.

U.S. DEPARTMENT OF COMMERCE
National Oceanic and Atmospheric Administration
National Marine Fisheries Service
Fishery-Oceanography Center
8604 La Jolla Shores Drive
P.O. Box 271
La Jolla, California 92037

September 1971

NOTICE TO RECIPIENTS OF THE EASTROPAC ATLAS

VOLUME 3

In the Introduction to this volume the reader is referred to Volume 1 for background information on the EASTROPAC Project, processing of the data, and preparation of the atlas. Volume 1 has not yet been published, but the introductory material referred to has been placed in Volume 4 which was published in November 1970.

Cuthbert M. Love, Editor
EASTROPAC Atlas

EASTROPAC Atlas

VOLUME 3

ERRATA

November 1971

FIGURE 20-δ-v4 The short contour near the surface between 15°-16° N. should be labeled 650 instead of 550.

FIGURE 20-S-v1 The short, heavy contour near the surface between 4°-5° N. should be labeled 34.0.

UNITED STATES DEPARTMENT OF COMMERCE
Maurice H. Stans, *Secretary*

NATIONAL OCEANIC AND ATMOSPHERIC ADMINISTRATION
Robert M. White, *Administrator*

NATIONAL MARINE FISHERIES SERVICE
Philip M. Roedel, *Director*

EASTROPAC ATLAS

VOLUME 3

PHYSICAL OCEANOGRAPHIC AND METEOROLOGICAL DATA FROM
PRINCIPAL PARTICIPATING SHIPS
FIRST AND SECOND MONITOR CRUISES, APRIL-JULY 1967

CUTHBERT M. LOVE, *Editor*

CIRCULAR 330
WASHINGTON, D.C.
SEPTEMBER 1971

For sale by the Superintendent of Documents, U.S. Government Printing Office, Washington, D.C. 20402—Price $4.75 per volume

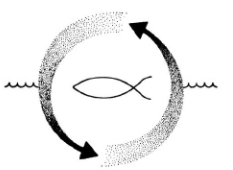

COORDINATOR, EASTROPAC PROJECT

WARREN S. WOOSTER, Scripps Institution of Oceanography, June 27, 1966-May 15, 1967
ALAN R. LONGHURST, National Marine Fisheries Service, May 15, 1967-June 30, 1970

ATLAS CONTRIBUTORS

ELBERT H. AHLSTROM—National Marine Fisheries Service, Fish Larvae
MAURICE BLACKBURN—Scripps Institution of Oceanography, Micronekton
WITOLD L. KLAWE—Inter-American Tropical Tuna Commission, Scombroid Larvae
R. MICHAEL LAURS—National Marine Fisheries Service, Zooplankton, Micronekton, Bird and Mammal Observations
FORREST R. MILLER—Inter-American Tropical Tuna Commission, Meteorology
ROBERT W. OWEN, Jr.—National Marine Fisheries Service, Phytoplankton, Oxygen, Mixed Layer Depth
BRUCE A. TAFT—Scripps Institution of Oceanography, Physical Oceanography
WILLIAM H. THOMAS—Scripps Institution of Oceanography, Nutrient Chemistry
MIZUKI TSUCHIYA—Scripps Institution of Oceanography, Physical Oceanography
BERNT ZEITZSCHEL—Scripps Institution of Oceanography, Phytoplankton

EDITORIAL COMMITTEE

CUTHBERT M. LOVE, National Marine Fisheries Service
BRUCE A. TAFT, Scripps Institution of Oceanography
R. MICHAEL LAURS, National Marine Fisheries Service

National Marine Fisheries Service
Fishery-Oceanography Center
La Jolla, California 92037

Scripps Institution of Oceanography
University of California, San Diego
La Jolla, California 92037

Inter-American Tropical Tuna Commission
% Scripps Institution of Oceanography
La Jolla, California 92037

INTRODUCTION

EASTROPAC was an international cooperative investigation of the eastern tropical Pacific Ocean which was intended to provide data necessary for a more effective use of the marine resources of the area, especially tropical tunas, and also to increase knowledge of the ocean circulation, air-sea interaction, and ecology. The National Marine Fisheries Services (NMFS)—the Bureau of Commercial Fisheries (BCF) at the time of the investigations—was the coordinating agency. The field work, from February 1967 through March 1968, was divided into seven 2-month cruise periods.

At a meeting of the EASTROPAC Coordinating Committee held at La Jolla in April 1968, it was decided that the data derived from the cruises were so numerous as to render classical data reports impractical and that a comprehensive atlas of the physical and biological results of the project should be produced instead. The atlas has been divided into 11 volumes, with five volumes containing physical oceanographic and meteorological data from the principal participating ships, five volumes containing biological and nutrient chemistry data from the same ships, and one volume containing all data from Latin-American cooperating ships and ships of opportunity.

Volume 3 contains physical oceanographic and meteorological data collected mainly by the principal participating ships during the first and second monitor cruise periods: cruise 20, April-May 1967, and cruise 30, June-July 1967. The companion volume presenting the corresponding biological and nutrient chemistry data is Volume 4. The locations of stations occupied by participating ships are shown in figure 20-TC and figure 30-TC.

Information concerning the history and organization of the EASTROPAC Project, a description of the cruises undertaken, the program of observations, the methods used for preparation of the charts, and remarks on the organization of the atlas are contained in Volume 1 with descriptions by the contributing scientists of the methods used to collect and process the data upon which the atlas charts are based.

CUTHBERT M. LOVE
Editor

Abbreviations used in figure designation system

Cruise or cruise period

Numbers 11, 12, 13, etc., indicate principal cruises. See figure 1.

Letters or letter-number combinations indicate cruises of Latin American cooperating ships or ships of opportunity, as follows:

MZ-4	*Yolanda*, MZ-4
MZ-5	*Yolanda*, MZ-5
MZ-6	*Yolanda*, MZ-6
MZ-7	*Defiance*, MZ-7
MZ-8	*Tuxpan*, MZ-8
H1	*Huayaipe*-1
H2	*Huayaipe*-2
H3	*Huayaipe*-3
U1	*Unanue* 6702
U2	*Unanue* 6708
U3	*Unanue* 6802
Y5	*Yelcho* MARCHILE V
Y6	*Yelcho* MARCHILE VI
Y7	*Yelcho* MARCHILE VII
E6	*Esmeralda* BE VI
OP	*Oceanographer*
CD	*Charles H. Davis*
T3	*Te Vega* 13
T4	*Te Vega* 14
T5	*Te Vega* 15
T6	*Te Vega* 16
T7	*Te Vega* 17

Numbers 10, 20, 30, 40, 50, 60, 70, indicate 2-month cruise periods.

Property represented

T	Temperature
S	Salinity
δ	Thermosteric anomaly (δ_T)
G	Geostrophic velocity
O_2	Oxygen concentration
O_2Sa	Oxygen saturation
ML	Thickness of the mixed layer
δ300	300 cl./t. thermosteric anomaly surface
AP	Acceleration Potential
P	Phosphate-phosphorus
Si	Silicate-silicon
NO_3	Nitrate-nitrogen
NO_2	Nitrite-nitrogen
NH_3	Ammonia-nitrogen
Ch	Chlorophyll-a
Ph	Phaeophytin
PP	Primary production
EL	Thickness of the euphotic layer
FCp	Fish and cephalopod standing stock
Cr	Crustacean standing stock
Nk	Total micronekton standing stock
ZhN	Zooplankton standing stock from 50-cm. net hauls, night
Z1N	Zooplankton standing stock from 1-m. net hauls, night
ZhD	Zooplankton standing stock from 50-cm. net hauls, day
Z1D	Zooplankton standing stock from 1-m. net hauls, day
FLN	Total fish larvae, night hauls
FLD	Total fish larvae, day hauls
FE	Total fish eggs
FS	Total skipjack tuna larvae
FA	Total *Auxis* larvae
FC	Total *Coryphaena* larvae
FMN	Total myctophid larvae, night hauls
FMD	Total myctophid larvae, day hauls
FGN	Total gonostomatid and sternoptychid larvae, night hauls
FGD	Total gonostomatid and sternoptychid larvae, day hauls
BP	Relative abundance of plankton-feeding birds
BF	Relative abundance of fish and cephalopod-feeding birds
SP	Porpoise sightings
SW	Whale sightings
ST	Tuna school sightings, all cruises
UA	Upper atmosphere meteorology
MW	Surface meteorological analysis, winds and pressure
MC	Surface meteorological analysis, clouds, dewpoint, temperature
MT	Surface meteorological analysis, sea temperature, sea-air temperature difference, sea temperature anomaly
RM	Reference map
TC	Track chart

Mnemonic to explain choice of letters

Zooplankton, half-meter, Night
Zooplankton, 1-meter, Night
Zooplankton, half-meter, Day
Zooplankton, 1-meter, Day
Fish Larvae, Night
Fish Larvae, Day
Fish, Skipjack
Fish, *Auxis*
Fish, *Coryphaena*
Fish, Myctophid, Night
Fish, Myctophid, Day
Fish, Gonostomatid, Night
Fish, Gonostomatid, Day
Birds, Plankton-feeding
Birds, Fish-feeding
Sightings, Porpoise
Sightings, Whales
Sightings, Tuna
Meteorology, Winds
Meteorology, Clouds
Meteorology, Temperature

Indicator for vertical sections or type of horizontal surface

v1, v2, etc., indicate vertical sections.

Vertical sections are assigned consecutive numbers within each cruise which follow the chronological order in which the ship ran the sections.

Number 10 or 100 following O_2Sa or horizontal P, Si, NO_3, NO_2, or NH_3 charts indicates distribution at that depth (m.).

s	Distribution at the sea surface
δ300	Distribution on the surface where δ_T=300 cl./t.
ei	Distribution integrated over the euphotic layer
150i	Distribution integrated to 150 m. depth
z	Depth of a surface

Number 1 or 2 following SP or SW charts indicates one of two 6-month periods into which those observations were divided.

Numbers 1 to 4 or 1 to 6 following MT or MW charts indicate one of the approximate 2-week periods into which those observations were divided. For all cruise periods except 40, the MT and MW charts were drawn for four 2-week periods. For the 40 cruise period these charts were drawn for six periods ranging from 12 to 16 days in length, but with several days overlap between some periods. Number 1 or 2 following MC charts indicates one of the monthly periods for which those charts were drawn.

LIST OF FIGURES

FIGURE 20-MC-1.—Analyses of the surface dew-point temperature of the air and total cloud cover based on 2-degree (latitude-longitude) averages from all available ship observations for the month of April 1967. Solid lines depict the monthly mean total cloud cover in oktas; the lines are dashed where data are sparse. Dash-dot lines are isotherms of the mean monthly dew-point temperature at 2-degree (C.) intervals. Areas where 15 percent or more of the ships reported rain of any type at or within sight of the ship are shaded. Dew-point temperature (°C. × 10) averaged for 5-degree squares is plotted above the mean position of the square, with total cloud cover (oktas) below and rainfall frequency (%) to the right of the symbol.

FIGURE 20-MC-2.—Analyses of the surface dew-point temperature of the air and total cloud cover based on 2-degree (latitude-longitude) averages from all available ship observations for the month of May 1967. Solid lines depict the monthly mean total cloud cover in oktas; the lines are dashed where data are sparse. Dash-dot lines are isotherms of the mean monthly dew-point temperature at 2-degree (C.) intervals. Areas where 15 percent or more of the ships reported rain of any type at or within sight of the ship are shaded. Dew-point temperature (°C. × 10) averaged for 5-degree squares is plotted above the mean position of the square, with total cloud cover (oktas) below and rainfall frequency (%) to the right of the symbol.

Temperature and salinity—White pages

FIGURE 20-T-v1.—Vertical distribution of temperature (°C.) along 119°20′ W., April 13-21, 1967.

FIGURE 20-T-v2.—Vertical distribution of temperature (°C.) along 112°20′ W., April 23-29, 1967.

FIGURE 20-T-v3.—Vertical distribution of temperature (°C.) along a section from 12° N., 112°20′ W. to Manzanillo, April 29-May 2, 1967.

FIGURE 20-T-v4.—Vertical distribution of temperature (°C.) along a section from Acapulco to 12° N., 105°20′ W., May 7-10, 1967.

FIGURE 20-T-v5.—Vertical distribution of temperature (°C.) along 105°20′ W., May 10-15, 1967.

FIGURE 20-T-v6.—Vertical distribution of temperature (°C.) along 98°20′ W., May 17-24, 1967.

FIGURE 20-S-v1.—Vertical distribution of salinity (‰) along 119°20′ W., April 13-21, 1967.

FIGURE 20-S-v2.—Vertical distribution of salinity (‰) along 112°20′ W., April 23-29, 1967.

FIGURE 20-S-v3.—Vertical distribution of salinity (‰) along a section from 12° N., 112°20′ W. to Manzanillo, April 29-May 2, 1967.

FIGURE 20-S-v4.—Vertical distribution of salinity (‰) along a section from Acapulco to 12° N., 105°20′ W., May 7-10, 1967.

FIGURE 20-S-v5.—Vertical distribution of salinity (‰) along 105°20′ W., May 10-15, 1967.

FIGURE 20-S-v6.—Vertical distribution of salinity (‰) along 98°20′ W., May 17-24, 1967.

Thermosteric anomaly and geostrophic velocity—Yellow pages

FIGURE 20-δ-v1.—Vertical distribution of thermosteric anomaly, δ_T, (cl./t.) along 119°20′ W., April 13-21, 1967.

FIGURE 20-δ-v2.—Vertical distribution of thermosteric anomaly, δ_T, (cl./t.) along 112°20′ W., April 23-29, 1967.

FIGURE 20-δ-v3.—Vertical distribution of thermosteric anomaly, δ_T, (cl./t.) along a section from 12° N., 112°20′ W. to Manzanillo, April 29-May 2, 1967.

FIGURE 20-δ-v4.—Vertical distribution of thermosteric anomaly, δ_T, (cl./t.) along a section from Acapulco to 12° N., 105°20′ W., May 7-10, 1967.

FIGURE 20-δ-v5.—Vertical distribution of thermosteric anomaly, δ_T, (cl./t.) along 105°20′ W., May 10-15, 1967.

FIGURE 20-δ-v6.—Vertical distribution of thermosteric anomaly, δ_T, (cl./t.) along 98°20′ W., May 17-24, 1967.

FIGURE 20-G-v1.—Vertical distribution of the zonal component of geostrophic velocity (cm./sec.), relative to 500 db., along 119°20′ W., April 13-21, 1967. Dark shading indicates eastward flow with a velocity greater than 5 cm./sec.; light shading indicates westward flow with a velocity greater than 5 cm./sec.

FIGURE 20-G-v2.—Vertical distribution of the zonal component of geostrophic velocity (cm./sec.), relative to 500 db., along 112°20′ W., April 24-29, 1967. Dark shading indicates eastward flow with a velocity greater than 5 cm./sec.; light shading indicates westward flow with a velocity greater than 5 cm./sec.

FIGURE 20-G-v3.—Vertical distribution of the component of geostrophic velocity (cm./sec.), relative to 500 db., normal to a section from 12° N., 112°20′ W. to Manzanillo, April 29-May 2, 1967. Dark shading indicates flow toward the southeast with a velocity greater than 5 cm./sec.; light shading indicates flow toward the northwest with a velocity greater than 5 cm./sec.

FIGURE 20-G-v4.—Vertical distribution of the component of geostrophic velocity (cm./sec.), relative to 500 db., normal to a section from Acapulco to 12° N., 105°20′ W., May 7-10, 1967. The dark shading indicates flow toward the southeast with a velocity greater than 5 cm./sec.

FIGURE 20-G-v5.—Vertical distribution of the zonal component of geostrophic velocity (cm./sec.), relative to 500 db., along 105°20′ W., May 10-15, 1967. Dark shading indicates eastward flow with a velocity greater than 5 cm./sec.; light shading indicates westward flow with a velocity greater than 5 cm./sec.

FIGURE 20-G-v6.—Vertical distribution of the zonal component of geostrophic velocity (cm./sec.), relative to 500 db., along 98°20′ W., May 17-24, 1967. Dark shading indicates eastward flow with a velocity greater than 5 cm./sec.; light shading indicates westward flow with a velocity greater than 5 cm./sec.

Oxygen—Green pages

FIGURE 20-O_2-v1.—Vertical distribution of oxygen (ml./l.) along 119°20′ W., April 13-21, 1967.

FIGURE 20-O_2-v2.—Vertical distribution of oxygen (ml./l.) along 112°20′ W., April 23-29, 1967.

FIGURE 20-O_2-v3.—Vertical distribution of oxygen (ml./l.) along a section from 12° N., 112°20′ W. to Manzanillo, April 29-May 2, 1967.

FIGURE 20-O_2-v4.—Vertical distribution of oxygen (ml./l.) along a section from Acapulco to 12° N., 105°20′ W., May 7-10, 1967.

FIGURE 20-O_2-v5.—Vertical distribution of oxygen (ml./l.) along 105°20′ W., May 10-15, 1967.

FIGURE 20-O_2-v6.—Vertical distribution of oxygen (ml./l.) along 98°20′ W., May 17-24, 1967.

Meteorology—Blue pages

FIGURE 20-UA-v1.—Vertical section of the atmosphere along 119°20′ W., April 14-20, 1967. Solid lines are isotherms of air temperature (°C.). Dashed lines are isopleths of mixing ratio of the air (g./kg.). Surface air temperature is plotted above surface mixing ratio and below a base line representing the surface pressure (mb.). The computed height (m.) of each standard pressure surface is plotted for the northernmost radiosonde station of the section. At other stations the difference of computed height minus the corresponding height at the northern station is shown at each standard level.

FIGURE 20-UA-v2.—Vertical section of the atmosphere along 112°20′ W., April 24-29, 1967. Solid lines are isotherms of air temperature (°C.). Dashed lines are isopleths of mixing ratio of the air (g./kg.). Surface air temperature is plotted above surface mixing ratio and below a base line representing the surface pressure (mb.). The computed height (m.) of each standard pressure surface is plotted for the northernmost radiosonde station of the section. At other stations the difference of computed height minus the corresponding height at the northern station is shown at each standard level.

FIGURE 20-UA-v5.—Vertical section of the atmosphere along 105°20′ W., May 9-16, 1967. Solid lines are isotherms of air temperature (°C.). Dashed lines are isopleths of mixing ratio of the air (g./kg.). Surface air temperature is plotted above surface mixing ratio and below a base line representing the surface pressure (mb.). The computed height (m.) of each standard pressure surface is plotted for the northernmost radiosonde station of the section. At other stations the difference of computed height minus the corresponding height at the northern station is shown at each standard level.

FIGURE 20-UA-v6.—Vertical section of the atmosphere along 98°20′ W., May 17-24, 1967. Solid lines are isotherms of air temperature (°C.). Dashed lines are isopleths of mixing ratio of the air (g./kg.). Surface air temperature is plotted above surface mixing ratio and below a base line representing the surface pressure (mb.). The computed height (m.) of each standard pressure surface is plotted for the northernmost radiosonde station of the section. At other stations the difference of computed height minus the corresponding height at the northern station is shown at each standard level.

Surface and near-surface properties—Pages of various colors

FIGURE 30-T-s.—Temperature (°C.) at the sea surface, June-July 1967. These contours are based on Nansen cast data.

FIGURE 30-ML.—Thickness of the mixed layer in meters, June-July 1967. Dashed lines indicate portions of the cruise track where such data were collected.

FIGURE 30-S-s.—Salinity (‰) at the sea surface, June-July 1967. These contours are based on Nansen cast data.

FIGURE 30-O_2Sa-10.—Oxygen saturation (%) at 10 meters, June-July 1967. Areas with less than 100 percent saturation are shaded.

Properties on isanosteric surfaces—Pages of various colors

FIGURE 30-δ300-z.—Depth (m.) of the surface where $\delta_T = 300$ cl./t., June-July 1967.

FIGURE 30-S-δ300.—Salinity (‰) on the surface where $\delta_T = 300$ cl./t., June-July 1967. The table shows the temperature corresponding to each isohaline on the chart.

FIGURE 30-AP-δ300.—Acceleration potential (j./kg.), relative to 500 db., on the surface where $\delta_T = 300$ cl./t., June-July 1967. For computing acceleration potential, thermosteric anomaly, δ_T, was used instead of specific volume anomaly, δ.

FIGURE 30-O_2-δ300.—Oxygen (ml./l.) on the surface where $\delta_T = 300$ cl./t., June-July 1967.

FIGURE 30-δ250-z.—Depth (m.) of the surface where $\delta_T = 250$ cl./t., June-July 1967.

FIGURE 30-S-δ250.—Salinity (‰) on the surface where $\delta_T = 250$ cl./t., June-July 1967. The table shows the temperature corresponding to each isohaline on the chart.

FIGURE 30-AP-δ250.—Acceleration potential (j./kg.), relative to 500 db., on the surface where $\delta_T = 250$ cl./t., June-July 1967. For computing acceleration potential, thermosteric anomaly, δ_T, was used instead of specific volume anomaly, δ.

FIGURE 30-O_2-δ250.—Oxygen (ml./l.) on the surface where $\delta_T = 250$ cl./t., June-July 1967.

FIGURE 30-δ200-z.—Depth (m.) of the surface where $\delta_T = 200$ cl./t., June-July 1967.

FIGURE 30-S-δ200.—Salinity (‰) on the surface where $\delta_T = 200$ cl./t., June-July 1967. The table shows the temperature corresponding to each isohaline on the chart.

FIGURE 30-AP-δ200.—Acceleration potential (j./kg.), relative to 500 db., on the surface where $\delta_T = 200$ cl./t., June-July 1967. For computing acceleration potential, thermosteric anomaly, δ_T, was used instead of specific volume anomaly, δ.

FIGURE 30-O_2-δ200.—Oxygen (ml./l.) on the surface where $\delta_T = 200$ cl./t., June-July 1967.

FIGURE 30-δ160-z.—Depth (m.) of the surface where $\delta_T = 160$ cl./t., June-July 1967.

FIGURE 30-S-δ160.—Salinity (‰) on the surface where $\delta_T = 160$ cl./t., June-July 1967. The table shows the temperature corresponding to each isohaline on the chart.

FIGURE 30-AP-δ160.—Acceleration potential (j./kg.), relative to 500 db., on the surface where $\delta_T = 160$ cl./t., June-July 1967. For computing acceleration potential, thermosteric anomaly, δ_T, was used instead of specific volume anomaly, δ.

FIGURE 30-O_2-δ160.—Oxygen (ml./l.) on the surface where $\delta_T = 160$ cl./t., June-July 1967.

Meteorology—Blue pages

FIGURE 30-MW-1.—Analyses of the surface air pressure and surface winds from all available ship observations, averaged over 2-degree (latitude-longitude) squares for the period June 1-16, 1967. Heavy dashed lines are isobars. Solid lines are streamlines showing the mean resultant direction of wind flow. Light dash-dot lines are isotachs indicating mean resultant wind speed (kn.). Pressure (mb.) averaged for 5-degree squares is plotted above the mean position of the square, and resultant wind direction followed by speed (kn.) is plotted below. The monthly climatological position of the intertropical convergence zone is shown by a wide dashed band.

FIGURE 30-MW-2.—Analyses of the surface air pressure and surface winds from all available ship observations, averaged over 2-degree (latitude-longitude) squares for the period June 17-30, 1967. Heavy dashed lines are isobars. Solid lines are streamlines showing the mean resultant direction of wind flow. Light dash-dot lines are isotachs indicating mean resultant wind speed (kn.). Pressure (mb.) averaged for 5-degree squares is plotted above the mean position of the square, and resultant wind direction followed by speed (kn.) is plotted below. The monthly climatological position of the intertropical convergence zone is shown by a wide dashed band.

FIGURE 30-MW-3.—Analyses of the surface air pressure and surface winds from all available ship observations, averaged over 2-degree (latitude-longitude) squares for the period July 1-15, 1967. Heavy dashed lines are isobars. Solid lines are streamlines showing the mean resultant direction of wind flow. Light dash-dot lines are isotachs indicating mean resultant wind speed (kn.). Pressure (mb.) averaged for 5-degree squares is plotted above the mean position of the square, and resultant wind direction followed by speed (kn.) is plotted below. The monthly climatological position of the intertropical convergence zone is shown by a wide dashed band.

FIGURE 30-MW-4.—Analyses of the surface air pressure and surface winds from all available ship observations, averaged over 2-degree (latitude-longitude) squares for the period July 16-31, 1967. Heavy dashed lines are isobars. Solid lines are streamlines showing the mean resultant direction of wind flow. Light dash-dot lines are isotachs indicating mean resultant wind speed (kn.). Pressure (mb.) averaged for 5-degree squares is plotted above the mean position of the square, and resultant wind direction followed by speed (kn.) is plotted below. The monthly climatological position of the intertropical convergence zone is shown by a wide dashed band.

FIGURE 30-MT-1.—Analysis of sea surface temperatures based on averages for 2-degree (latitude-longitude) squares from all available ship observations for the period June 1-16, 1967. Solid lines are sea surface isotherms (°C.); the isotherms are dashed where data are sparse. Dark hatching outlines areas with positive temperature anomalies (computed from mean sea surface temperatures averaged over 22 years) greater than 1°C.; light hatchings shows areas with negative anomalies greater than 1°C. Sea surface temperature (°C. × 10) averaged for 5-degree squares is plotted above the mean position of the square; sea temperature minus air temperature difference (°C. × 10) is plotted below the symbol.

FIGURE 30-MT-2.—Analysis of sea surface temperatures based on averages for 2-degree (latitude-longitude) squares from all available ship observations for the period June 17-30, 1967. Solid lines are sea surface isotherms (°C.); the isotherms are dashed where data are sparse. Dark hatching outlines areas with positive temperature anomalies (computed from mean sea surface temperatures averaged over 22 years) greater than 1°C.; light hatchings shows areas with negative anomalies greater than 1°C. Sea surface temperature (°C. × 10) averaged for 5-degree squares is plotted above the mean position of the square; sea temperature minus air temperature difference (°C. × 10) is plotted below the symbol.

FIGURE 30-MT-3.—Analysis of sea surface temperatures based on averages for 2-degree (latitude-longitude) squares from all available ship observations for the period July 1-15, 1967. Solid lines are sea surface isotherms (°C.); the isotherms are dashed where data are sparse. Dark hatching outlines areas with positive temperature anomalies (computed from mean sea surface temperatures averaged over 22 years) greater than 1°C.; light hatchings shows areas with negative anomalies greater than 1°C. Sea surface temperature (°C. × 10) averaged for 5-degree squares is plotted above the mean position of the square; sea temperature minus air temperature difference (°C. × 10) is plotted below the symbol.

FIGURE 30-MT-4.—Analysis of sea surface temperatures based on averages for 2-degree (latitude-longitude) squares from all available ship observations for the period July 16-31, 1967. Solid lines are sea surface isotherms (°C.); the isotherms are dashed where data are sparse. Dark hatching outlines areas with positive temperature anomalies (computed from mean sea surface temperatures averaged over 22 years) greater than 1°C.; light hatchings shows areas with negative anomalies greater than 1°C. Sea surface temperature (°C. × 10) averaged for 5-degree squares is plotted above the mean position of the square; sea temperature minus air temperature difference (°C. × 10) is plotted below the symbol.

FIGURE-30-MC-1.—Analyses of the surface dew-point temperature of the air and total cloud cover based on 2-degree (latitude-longitude) averages from all available ship observations for the month of June 1967. Solid lines depict the monthly mean total cloud cover in oktas; the lines are dashed where data are sparse. Dash-dot lines are isotherms of the mean monthly dew-point temperature at 2-degree (C.) intervals. Areas where 15 percent or more of the ships reported rain of any type at or within sight of the ship are shaded. Dew-point temperature (°C. × 10) averaged for 5-degree squares is plotted above the mean position of the square, with total cloud cover (oktas) below and rainfall frequency (%) to the right of the symbol.

FIGURE 30-MC-2.—Analyses of the surface dew-point temperature of the air and total cloud cover based on 2-degree (latitude-longitude) averages from all available ship observations for the month of July 1967. Solid lines depict the monthly mean total cloud cover in oktas; the lines are dashed where data are sparse. Dash-dot lines are isotherms of the mean monthly dew-point temperature at 2-degree (C.) intervals. Areas where 15 percent or more of the ships reported rain of any type at or within sight of the ship are shaded. Dew-point temperature (°C. × 10) averaged for 5-degree squares is plotted above the mean position of the square, with total cloud cover (oktas) below and rainfall frequency (%) to the right of the symbol.

Temperature and salinity—White pages

FIGURE 30-T-v1.—Vertical distribution of temperature (°C.) along 118°30′ W., June 16-26, 1967.

FIGURE 30-T-v2.—Vertical distribution of temperature (°C.) along 111°30′ W., June 28-July 3, 1967.

FIGURE 30-T-v3.—Vertical distribution of temperature (°C.) along a section from 12° N., 111°30′ W. to Manzanillo, July 4-7, 1967. The contours from stations 132-148 are based on Nansen cast data only.

FIGURE 30-T-v4.—Vertical distribution of temperature (°C.) along a section from Acapulco to 12° N., 104°30′ W., July 10-13, 1967. These contours are based on Nansen cast data only.

FIGURE 30-T-v5.—Vertical distribution of temperature (°C.) along 104°30′ W., July 13-18, 1967. These contours are based on Nansen cast data only.

FIGURE 30-T-v6.—Vertical distribution of temperature (°C.) along 97°30′ W., July 20-27, 1967. These contours are based on Nansen cast data only.

FIGURE 30-S-v1.—Vertical distribution of salinity (‰) along 118°30′ W., June 16-26, 1967.

FIGURE 30-S-v2.—Vertical distribution of salinity (‰) along 111°30′ W., June 28-July 3, 1967.

FIGURE 30-S-v3.—Vertical distribution of salinity (‰) along a section from 12° N., 111°30′ W. to Manzanillo, July 4-7, 1967. The contours from stations 132-148 are based on Nansen cast data only.

FIGURE 30-S-v4.—Vertical distribution of salinity (‰) along a section from Acapulco to 12° N., 104°30′ W., July 10-13, 1967. These contours are based on Nansen cast data only.

FIGURE 30-S-v5.—Vertical distribution of salinity (‰) along 104°30′ W., July 13-18, 1967. These contours are based on Nansen cast data only.

FIGURE 30-S-v6.—Vertical distribution of salinity (‰) along 97°30′ W., July 20-27, 1967. These contours are based on Nansen cast data only.

Thermosteric anomaly and geostrophic velocity—Yellow pages

FIGURE 30-δ-v1.—Vertical distribution of thermosteric anomaly, δ_T, (cl./t.) along 118°30′ W., June 16-26, 1967.

FIGURE 30-δ-v2.—Vertical distribution of thermosteric anomaly, δ_T, (cl./t.) along 111°30′ W., June 28-July 3, 1967.

FIGURE 30-δ-v3.—Vertical distribution of thermosteric anomaly, δ_T, (cl./t.) along a section from 12° N., 111°30′ W. to Manzanillo, July 4-7, 1967. The contours from stations 132-148 are based on Nansen cast data only.

FIGURE 30-δ-v4.—Vertical distribution of thermosteric anomaly, δ_T, (cl./t.) along a section from Acapulco to 12° N., 104°30′ W., July 10-13, 1967. These contours are based on Nansen cast data only.

FIGURE 30-δ-v5.—Vertical distribution of thermosteric anomaly, δ_T, (cl./t.) along 104°30′ W., July 13-18, 1967. These contours are based on Nansen cast data only.

FIGURE 30-δ-v6.—Vertical distribution of thermosteric anomaly, δ_T, (cl./t.) along 97°30′ W., July 20-27, 1967. These contours are based on Nansen cast data only.

FIGURE 30-G-v1.—Vertical distribution of the zonal component of geostrophic velocity (cm./sec.), relative to 500 db., along 118°30′ W., June 17-26, 1967. Dark shading indicates eastward flow with a velocity greater than 5 cm./sec.; light shading indicates westward flow with a velocity greater than 5 cm./sec.

FIGURE 30-G-v2.—Vertical distribution of the zonal component of geostrophic velocity (cm./sec.), relative to 500 db., along 111°30′ W., June 28-July 3, 1967. Dark shading indicates eastward flow with a velocity greater than 5 cm./sec.; light shading indicates westward flow with a velocity greater than 5 cm./sec.

FIGURE 30-G-v3.—Vertical distribution of the component of geostrophic velocity (cm./sec.), relative to 500 db., normal to a section from 12° N., 111°30′ W. to Manzanillo, July 4-7, 1967. Dark shading indicates flow toward the southeast with a velocity greater than 5 cm./sec.; light shading indicates flow toward the northwest with a velocity greater than 5 cm./sec.

FIGURE 30-G-v4.—Vertical distribution of the component of geostrophic velocity (cm./sec.), relative to 500 db., normal to a section from Acapulco to 12° N., 104°30′ W., July 10-12, 1967. Dark shading indicates flow toward the southeast with a velocity greater than 5 cm./sec.; light shading indicates flow toward the northwest with a velocity greater than 5 cm./sec.

FIGURE 30-G-v5.—Vertical distribution of the zonal component of geostrophic velocity (cm./sec.), relative to 500 db., along 104°30′ W., July 13-18, 1967. Dark shading indicates eastward flow with a velocity greater than 5 cm./sec.; light shading indicates westward flow with a velocity greater than 5 cm./sec.

FIGURE 30-G-v6.—Vertical distribution of the zonal component of geostrophic velocity (cm./sec.), relative to 500 db., along 97°30′ W., July 20-26, 1967. Dark shading indicates eastward flow with a velocity greater than 5 cm./sec.; light shading indicates westward flow with a velocity greater than 5 cm./sec.

Oxygen—Green pages

FIGURE 30-O_2-v1.—Vertical distribution of oxygen (ml./l.) along 118°30′ W., June 17-26, 1967.

FIGURE 30-O_2-v2.—Vertical distribution of oxygen (ml./l.) along 111°30′ W., June 28-July 4, 1967.

FIGURE 30-O_2-v3.—Vertical distribution of oxygen (ml./l.) along a section from 12° N., 111°30′ W. to Manzanillo, July 4-7, 1967.

FIGURE 30-O_2-v4.—Vertical distribution of oxygen (ml./l.) along a section from Acapulco to 12° N., 104°30′ W., July 10-13, 1967.

FIGURE 30-O_2-v5.—Vertical distribution of oxygen (ml./l.) along 104°30′ W., July 13-18, 1967.

FIGURE 30-O_2-v6.—Vertical distribution of oxygen (ml./l.) along 97°30′ W., July 20-27, 1967.

Meteorology—Blue pages

FIGURE 30-UA-v1.—Vertical section of the atmosphere along 118°30′ W., June 16-27, 1967. Solid lines are isotherms of air temperature (°C.). Dashed lines are isopleths of mixing ratio of the air (g./kg.). Surface air temperature is plotted above surface mixing ratio and below a base line representing the surface pressure (mb.). The computed height (m.) of each standard pressure surface is plotted for the northernmost radiosonde station of the section. At other stations the difference of computed height minus the corresponding height at the northern station is shown at each standard level.

FIGURE 30-UA-v2.—Vertical section of the atmosphere along 111°30′ W., June 28-July 7, 1967. Solid lines are isotherms of air temperature (°C.). Dashed lines are isopleths of mixing ratio of the air (g./kg.). Surface air temperature is plotted above surface mixing ratio and below a base line representing the surface pressure (mb.). The computed height (m.) of each standard pressure surface is plotted for the northernmost radiosonde station of the section. At other stations the difference of computed height minus the corresponding height at the northern station is shown at each standard level.

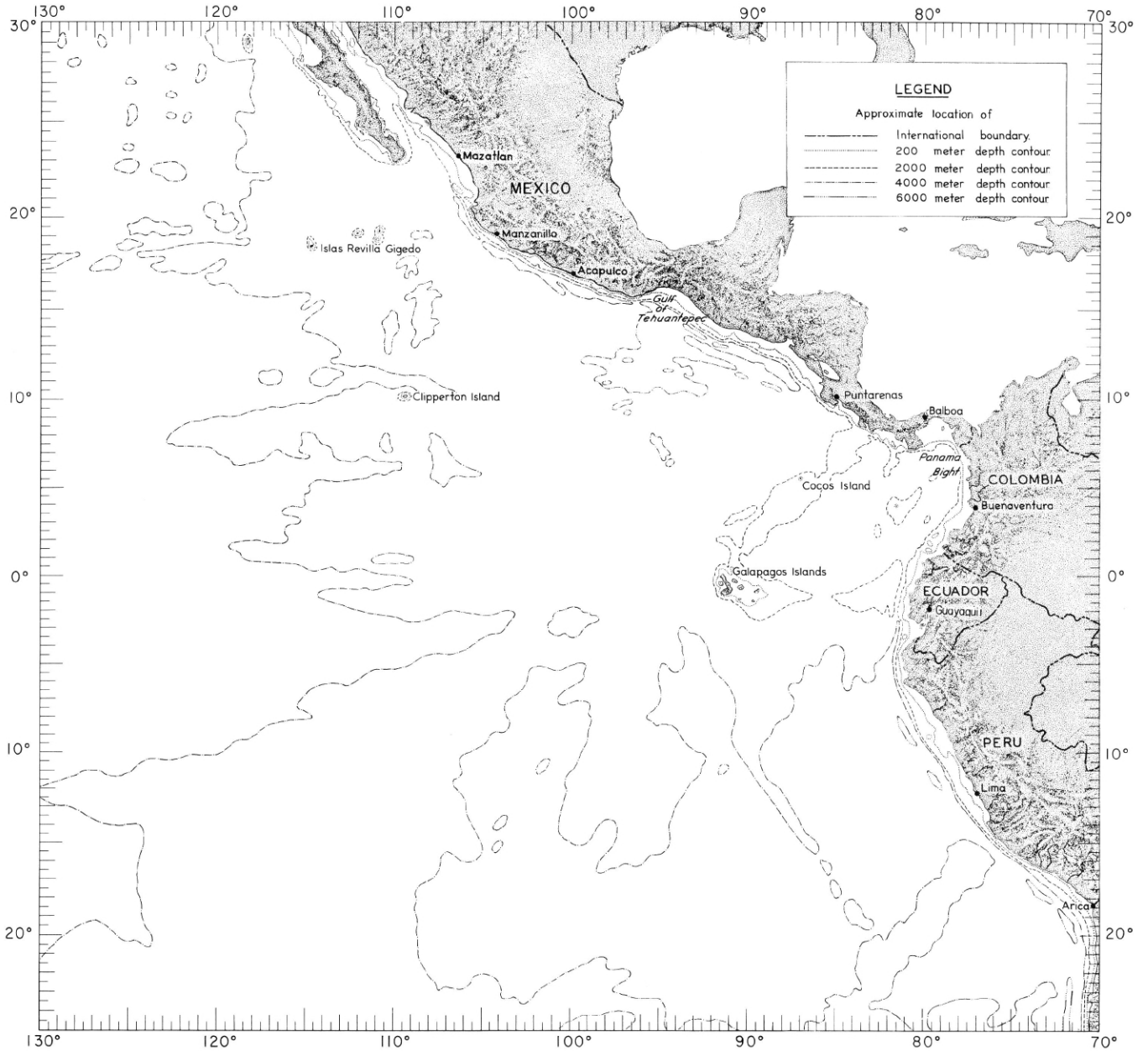

RM-a.

FIGURE RM-a. — Reference map of the main portion of the EASTROPAC area. The topographic shading and bathymetric contours are approximate only and should not be considered as portraying the latest available information.

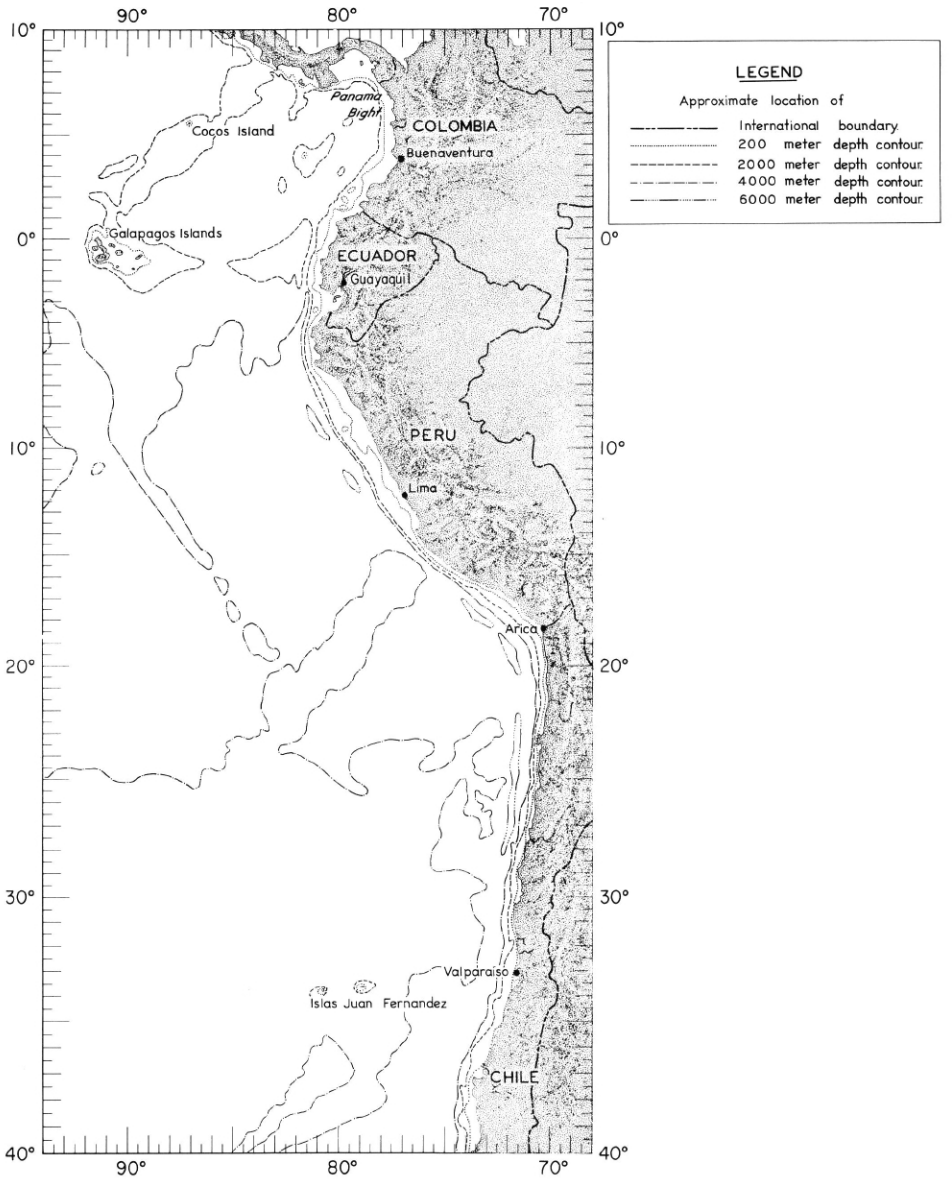

FIGURE RM-b — Reference map of the southern coastal portion of the EASTROPAC area. The topographic shading and bathymetric contours are approximate only and should not be considered as portraying the latest available information.

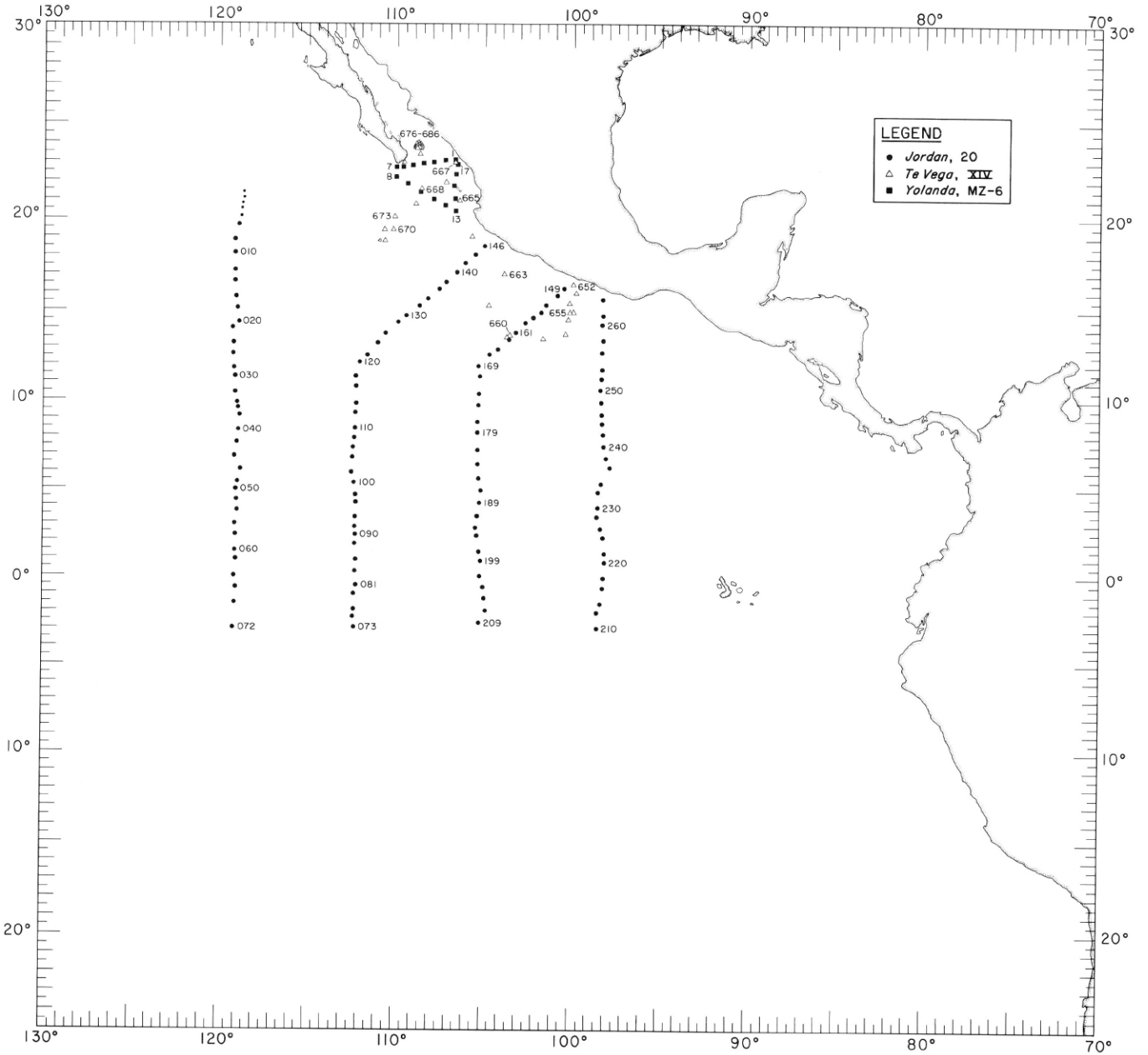

FIGURE 20-TC. — Locations of stations occupied by participating ships during the first monitor period, April-May 1967.

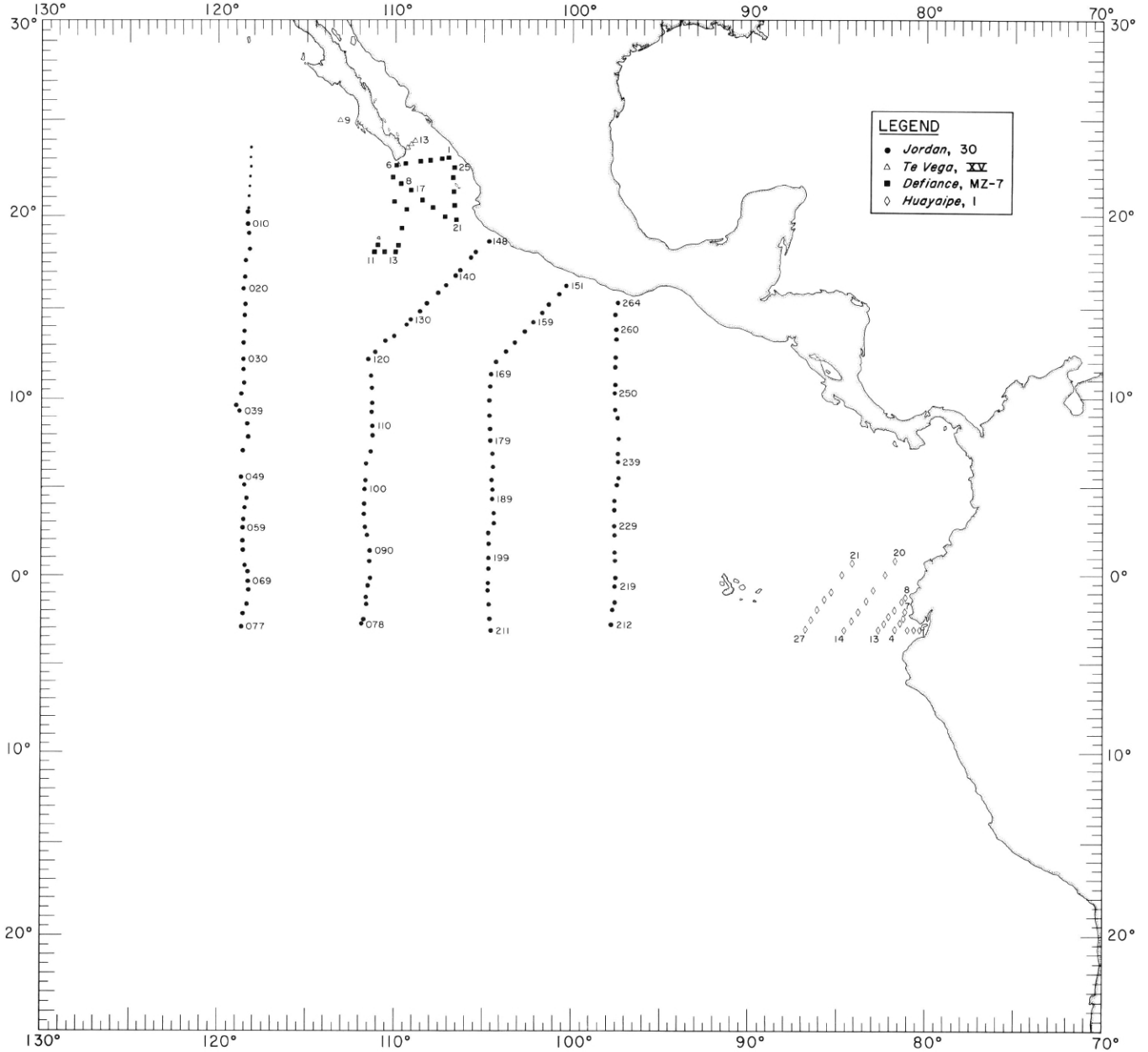

30-TC.

FIGURE 30-TC. — Locations of stations occupied by participating ships during the second monitor period, June-July 1967.

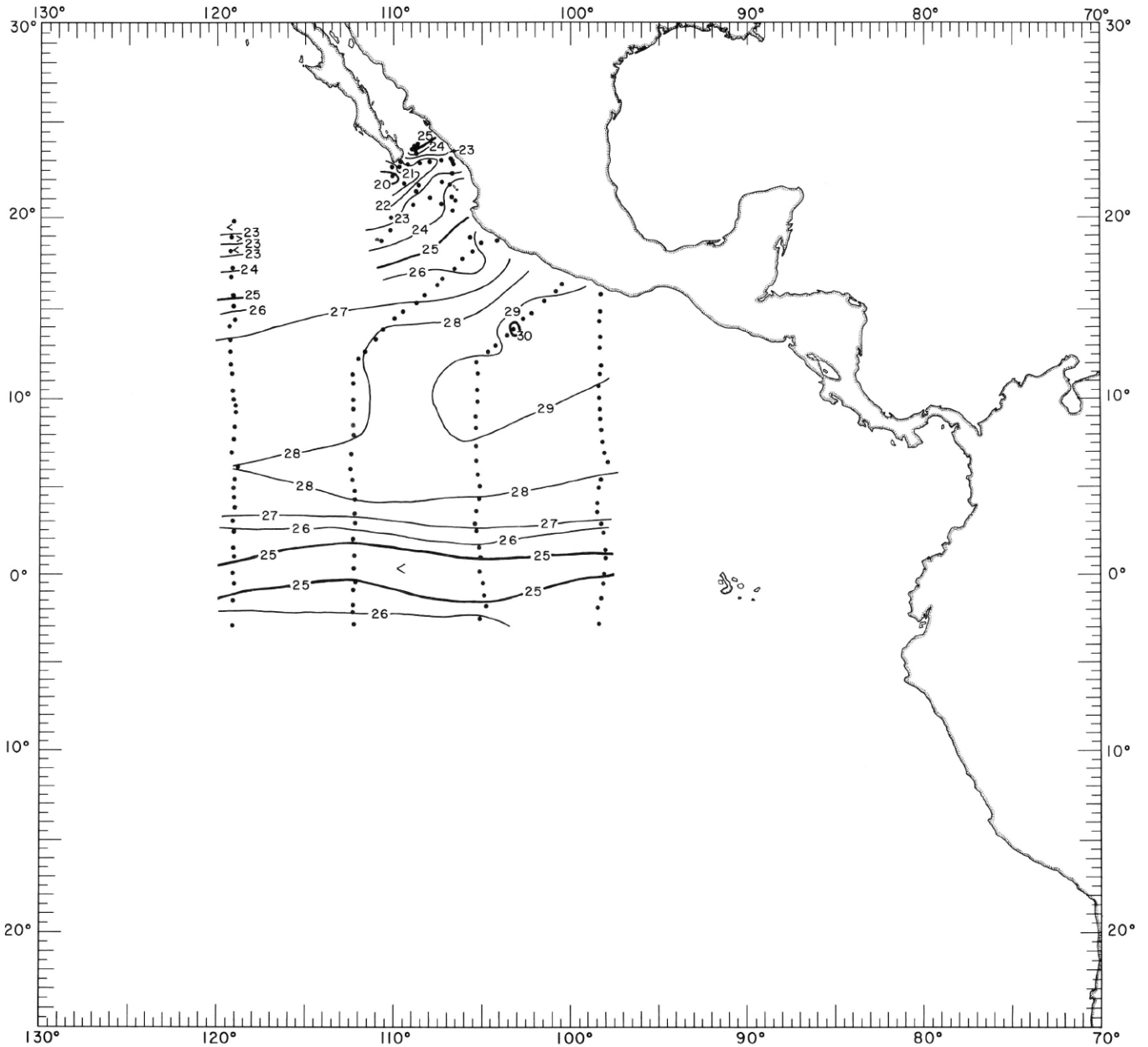

20-T-s.

FIGURE 20-T-s. — Temperature (°C) at the sea surface, April-May 1967. These contours are based on Nansen cast data.

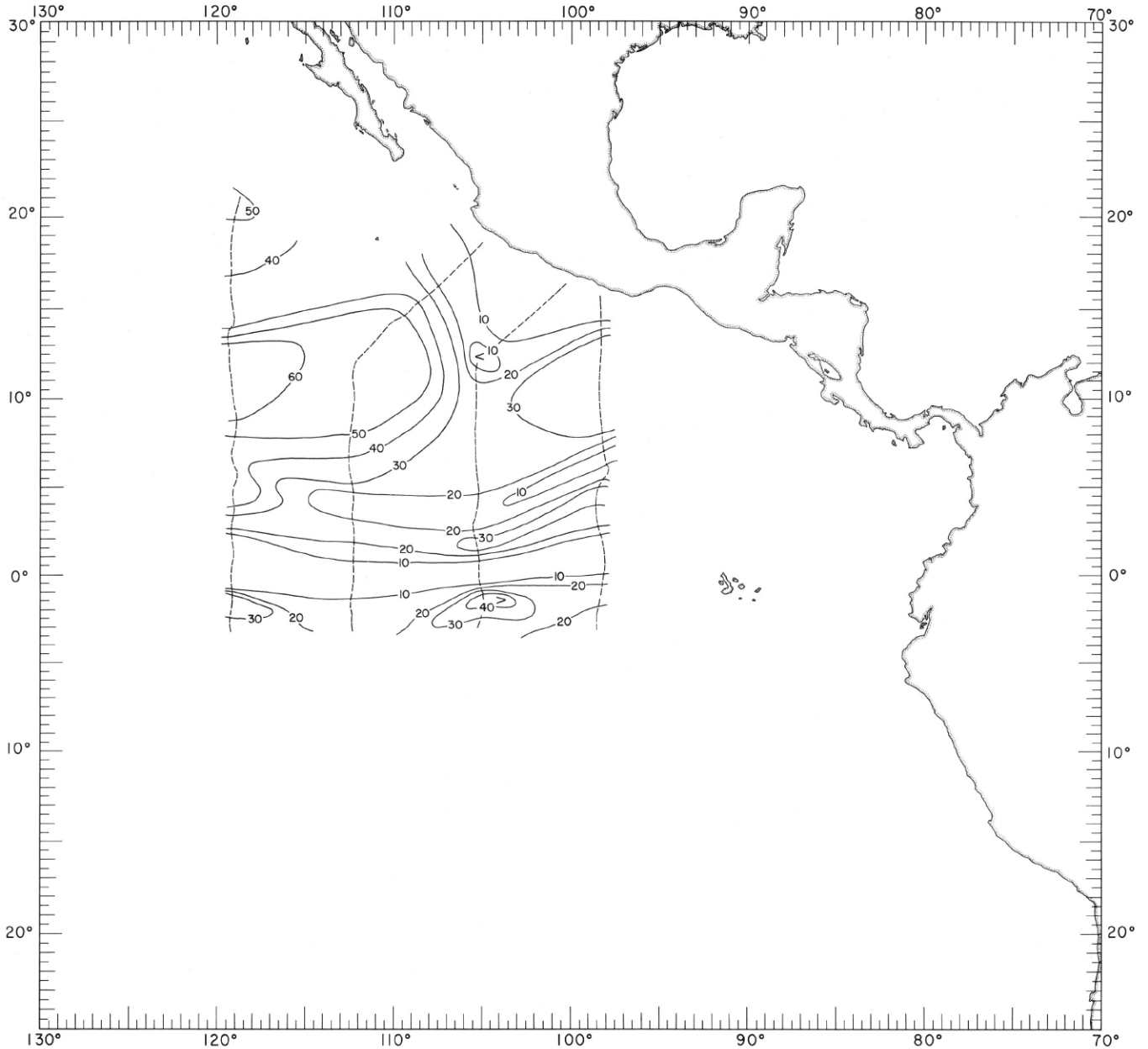

20-ML.

FIGURE 20-ML. — Thickness of the mixed layer in meters, April-May 1967. Dashed lines indicate portions of the cruise track where such data were collectetl.

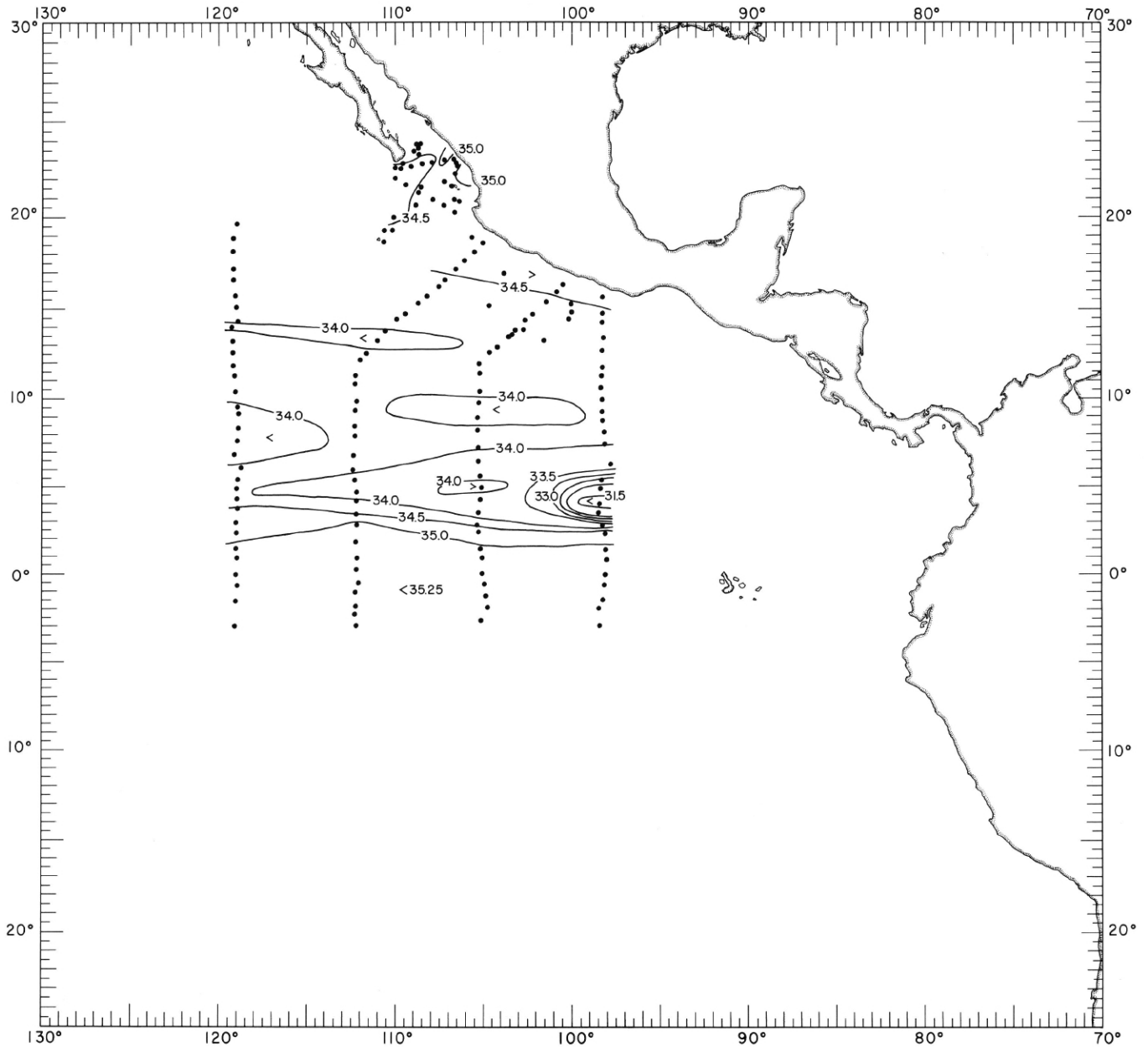

20-S-s.

FIGURE 20-S-s.—Salinity (‰) at the sea surface, April-May 1967. These contours are based on Nansen cast data.

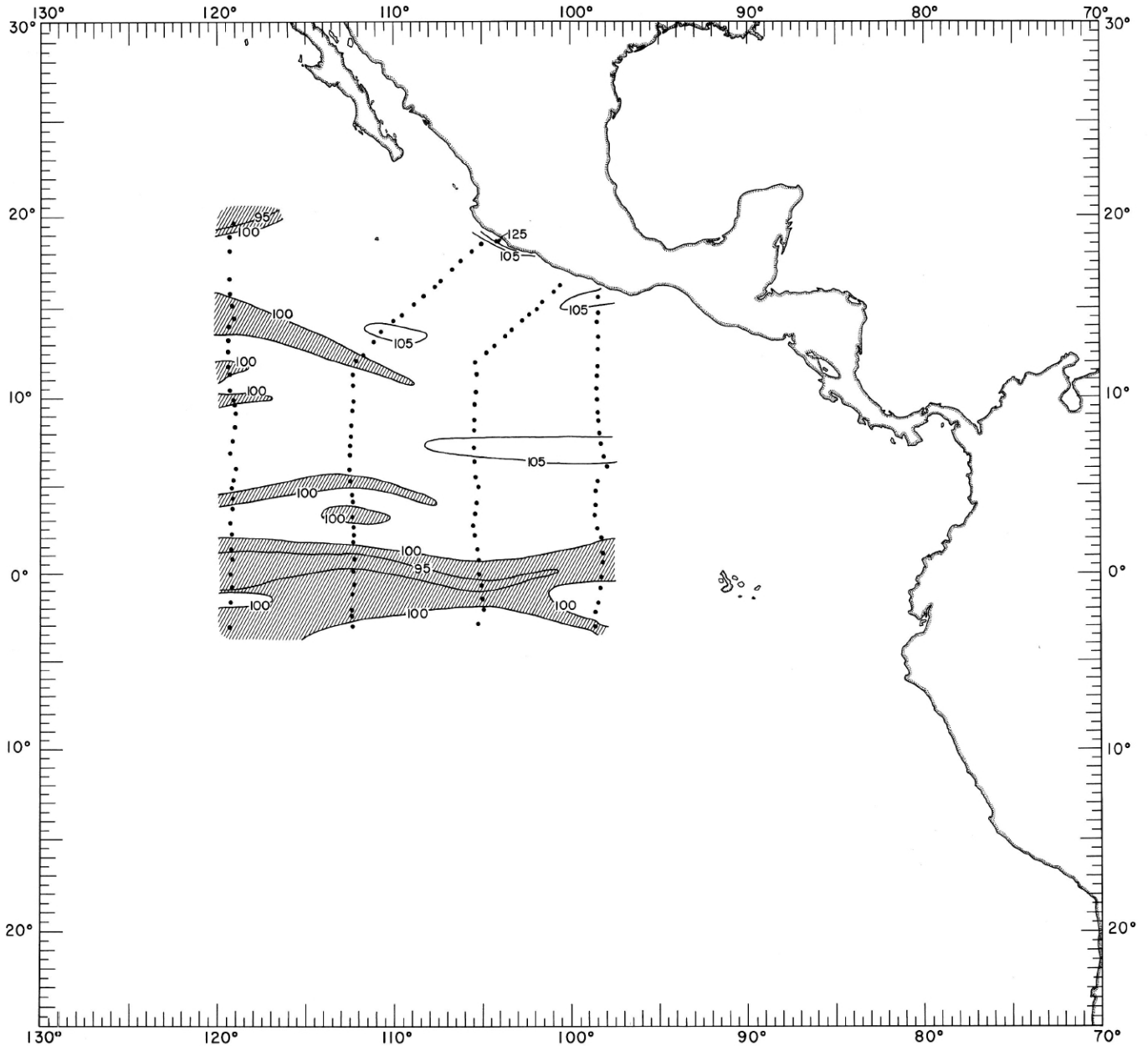

FIGURE 20-O_2Sa-10. — Oxygen saturation (%) at 10 meters, April-May 1967. Areas with less than 100% saturation are shaded.

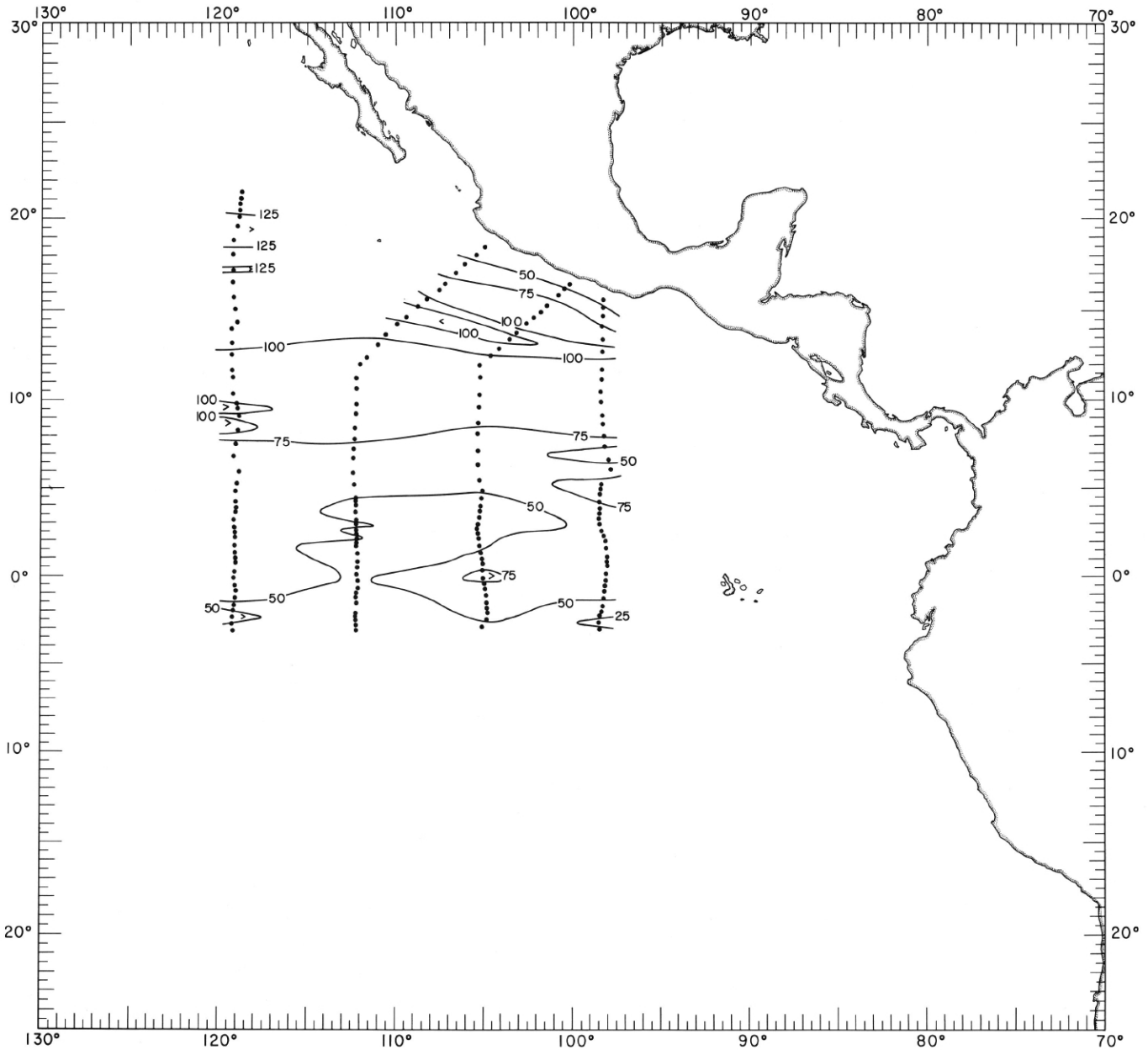

FIGURE 20-δ300-z.—Depth (m.) of the surface where $\delta_T = 300$ cl./t., April-May 1967.

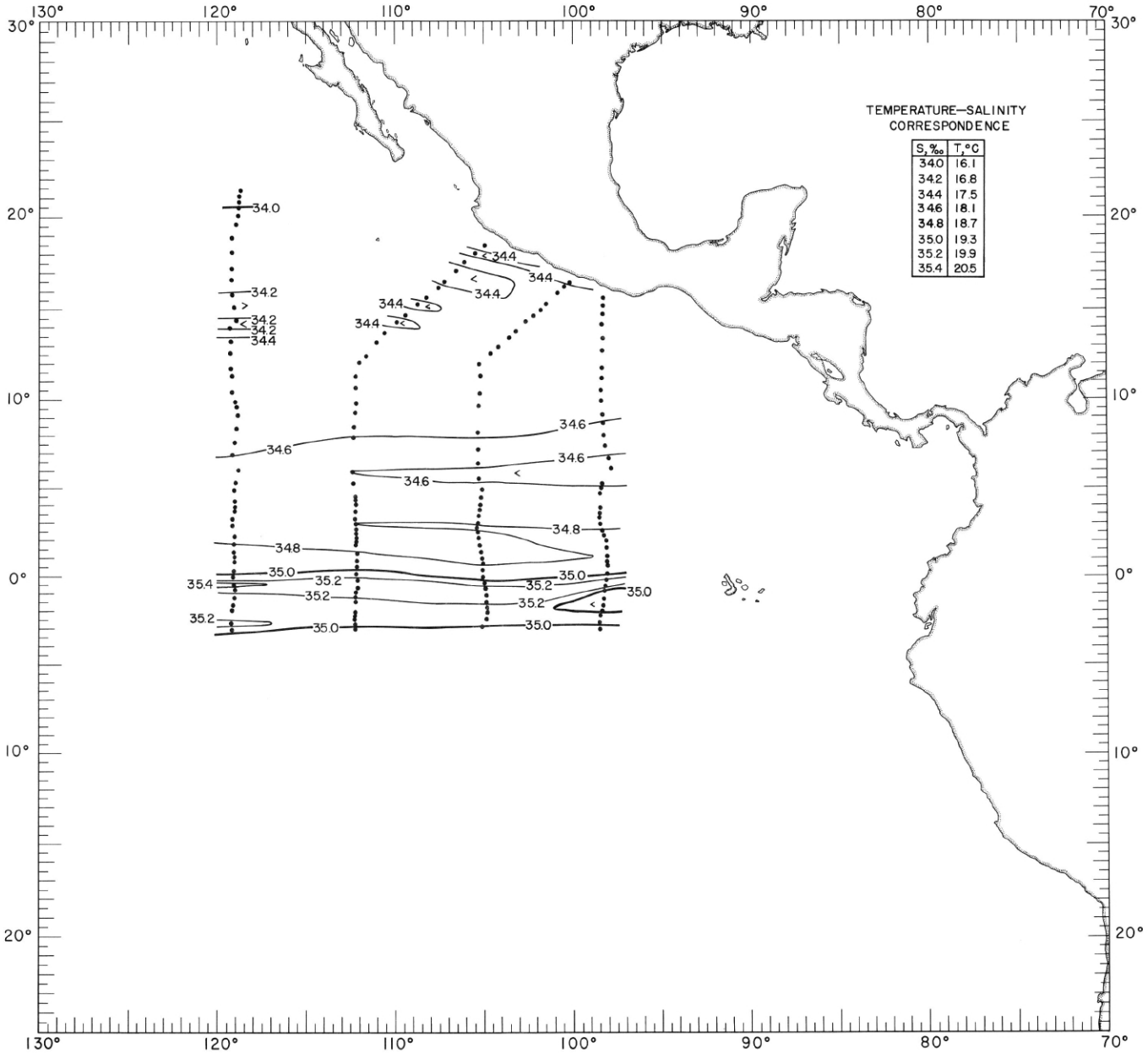

FIGURE 20-S-ß300.—Salinity (‰) on the surface where δ_r = 300 cl./t., April-May 1967. The table shows the temperature corresponding to each isohaline on the chart.

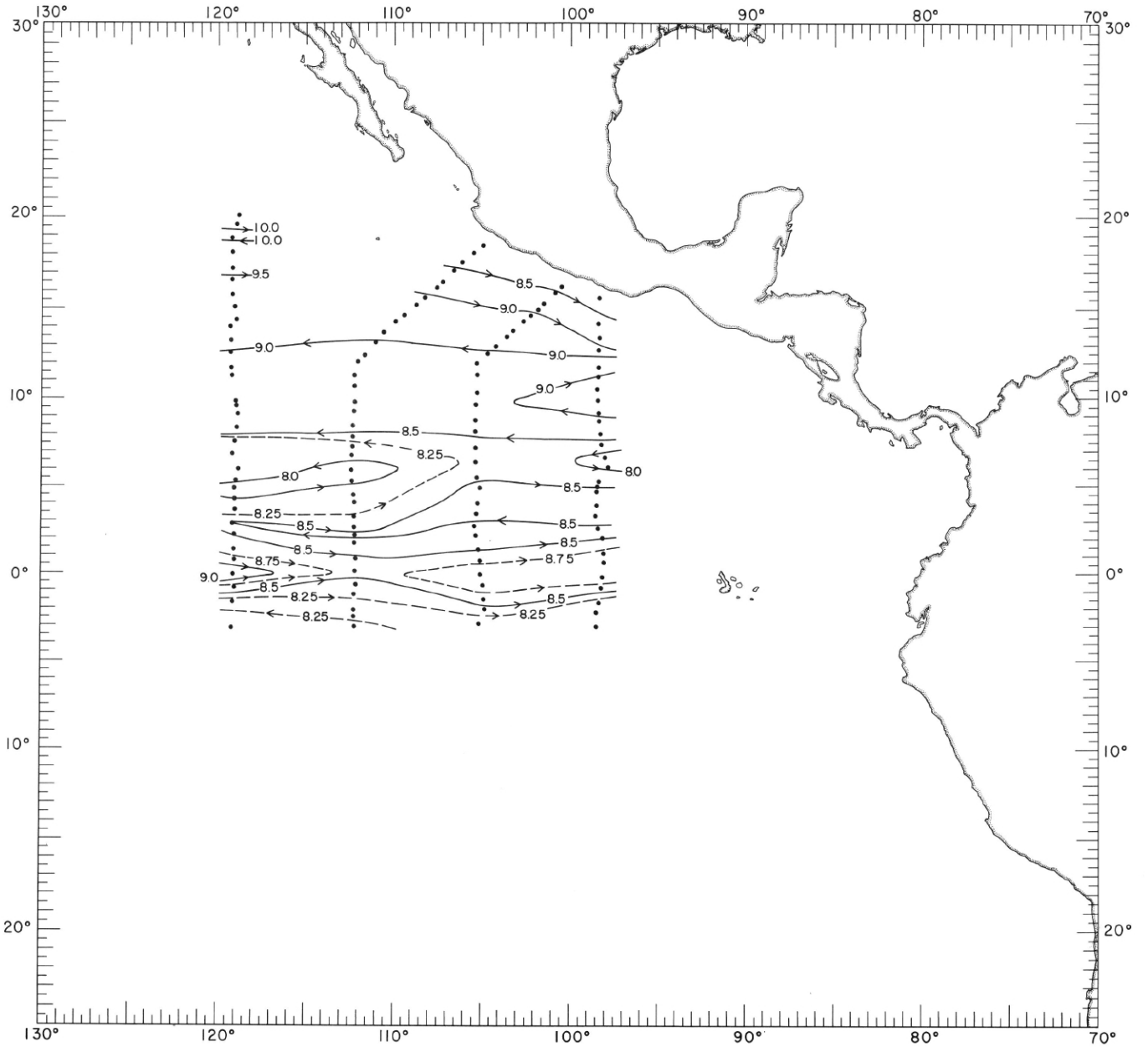

FIGURE 20-AP-δ300.—Acceleration potential (j./kg.), relative to 500 db., on the surface where δ_T = 300 cl./t., April-May 1967. For computing acceleration potential, thermosteric anomaly, δ_T, was used instead of specific volume anomaly, δ.

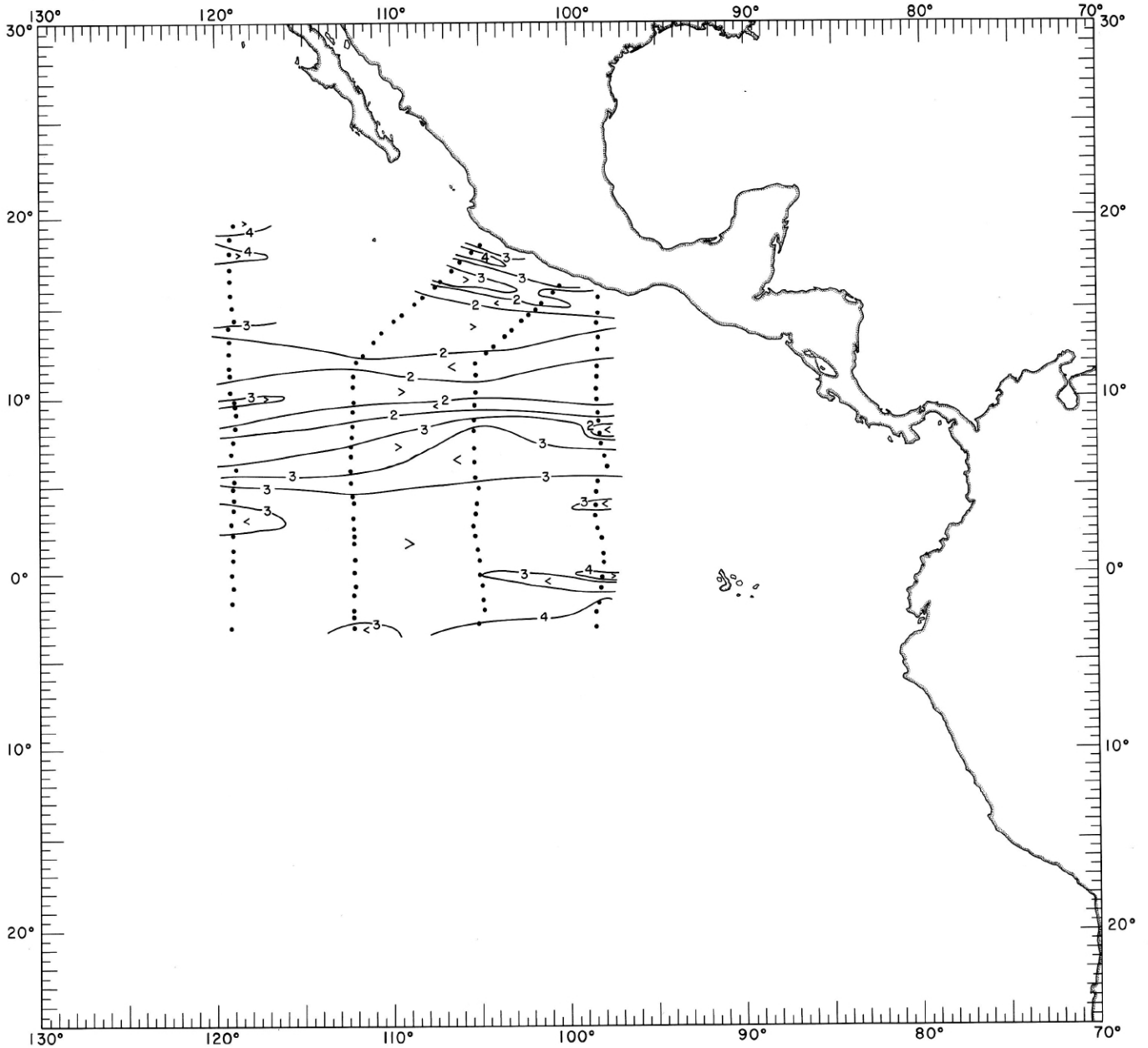

FIGURE 20-O_2-δ300.—Oxygen (ml./l.) on the surface where $\delta_t = 300$ cl./t., April-May 1967.

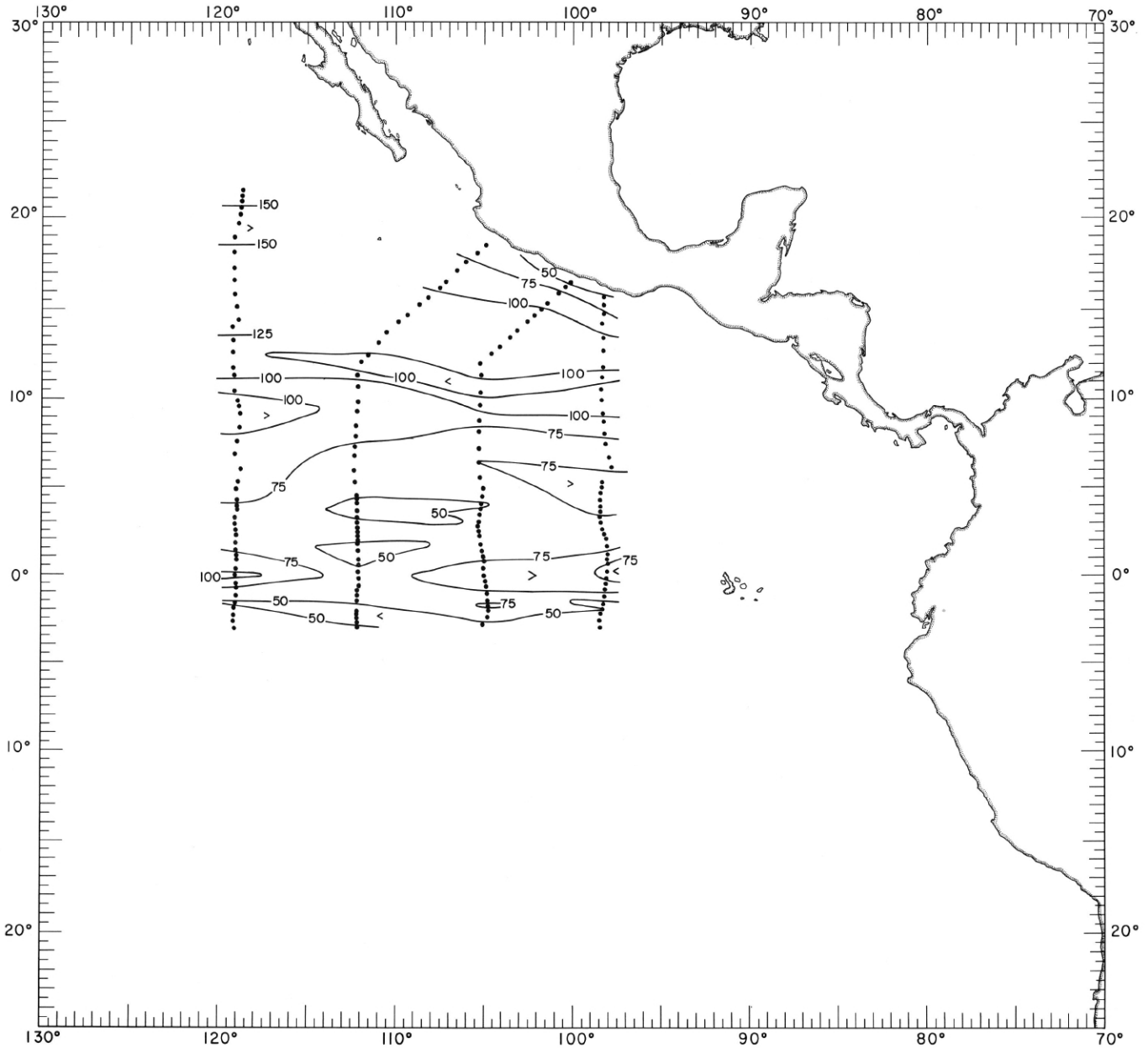

FIGURE 20-δ250-z.—Depth (m.) of the surface where $\delta_T = 250$ cl./t., April-May 1967.

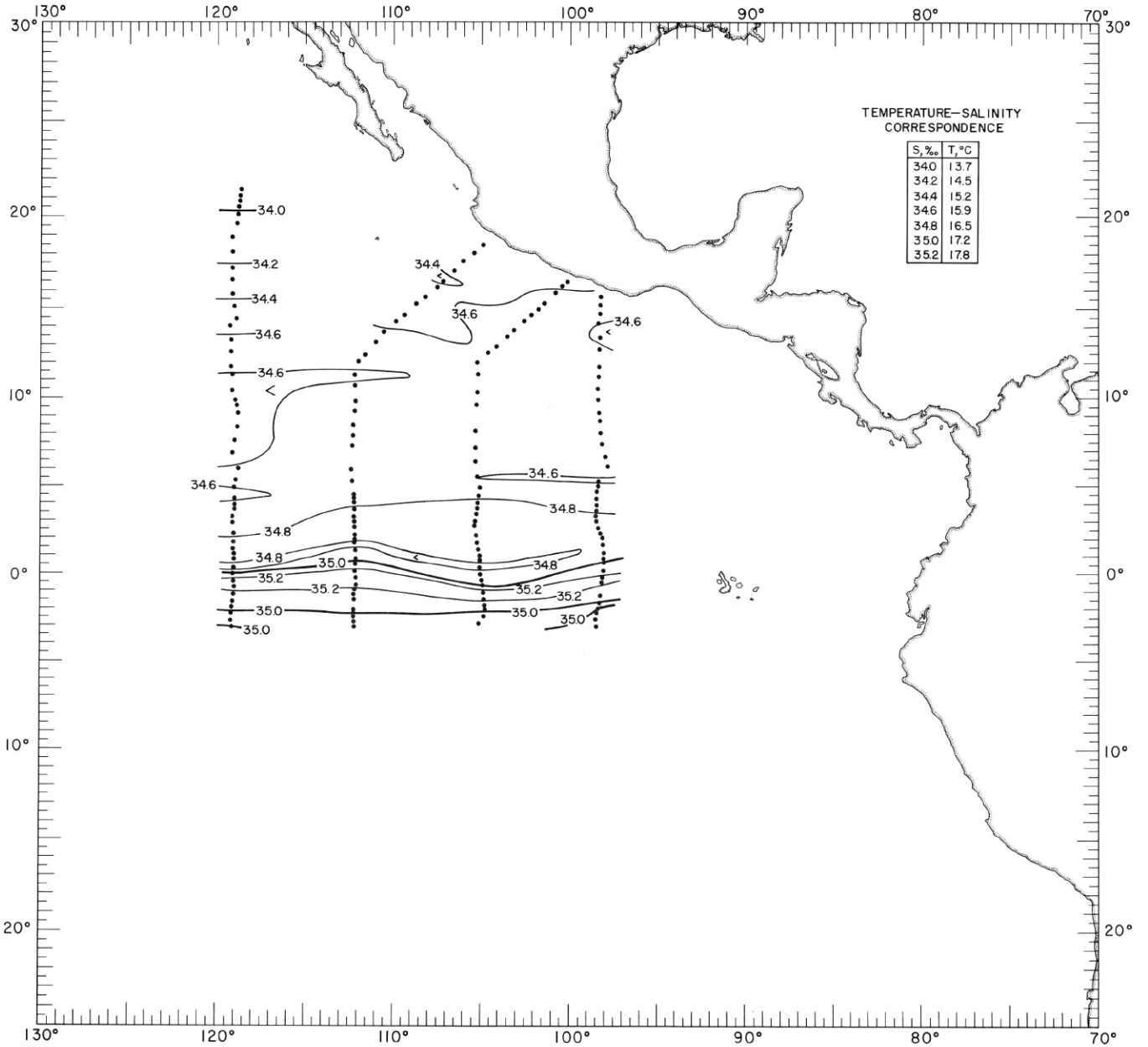

FIGURE 20-S-8250.—Salinity (‰) on the surface where $\delta_T = 250$ cl./t., April-May 1967. The table shows the temperature corresponding to each isohaline on the chart.

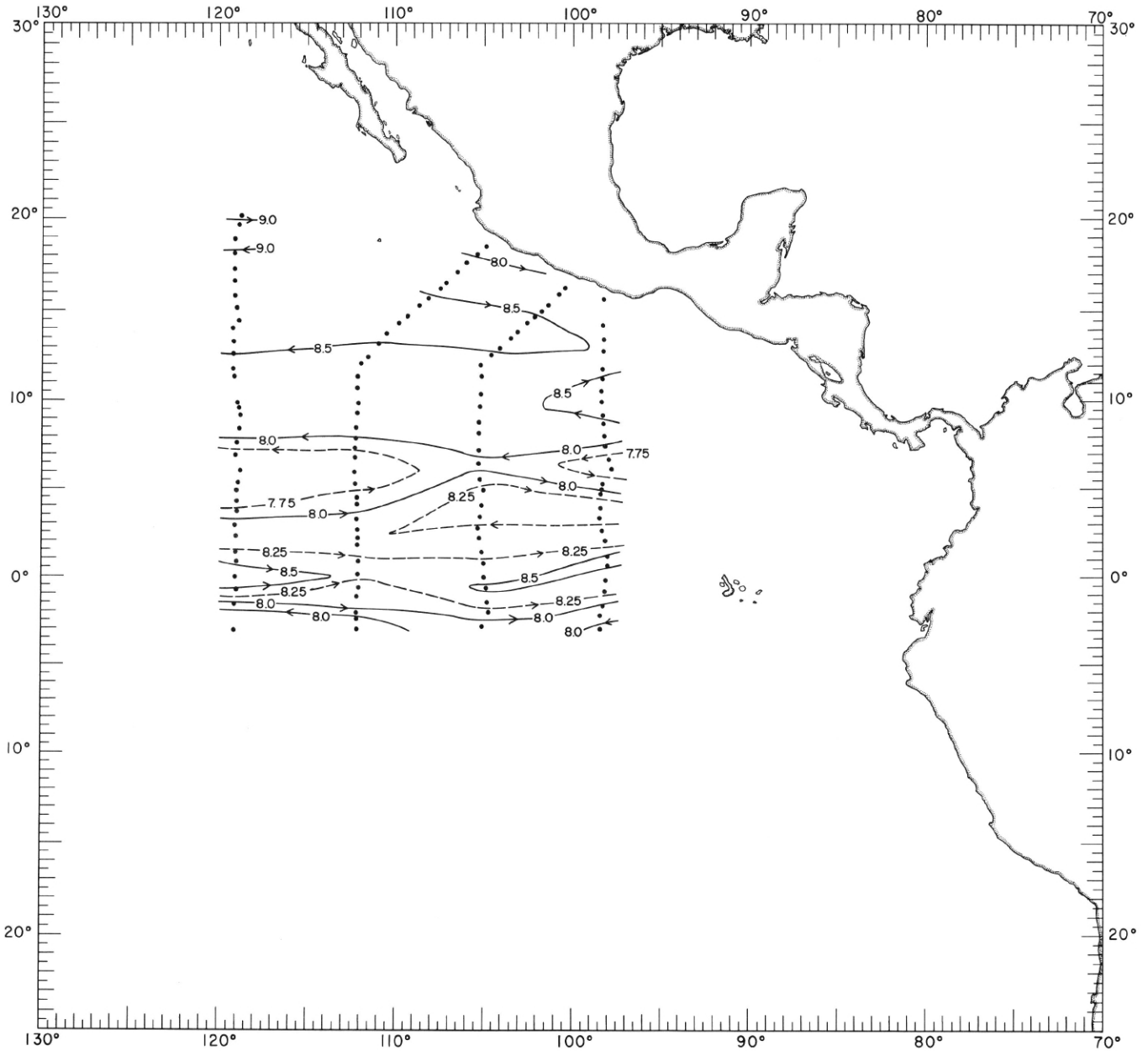

FIGURE 20-AP-δ250.—Acceleration potential (j./kg.), relative to 500 db., on the surface where δ_T = 250 cl./t., April-May 1967. For computing acceleration potential, thermosteric anomaly, δ_T, was used instead of specific volume anomaly, δ.

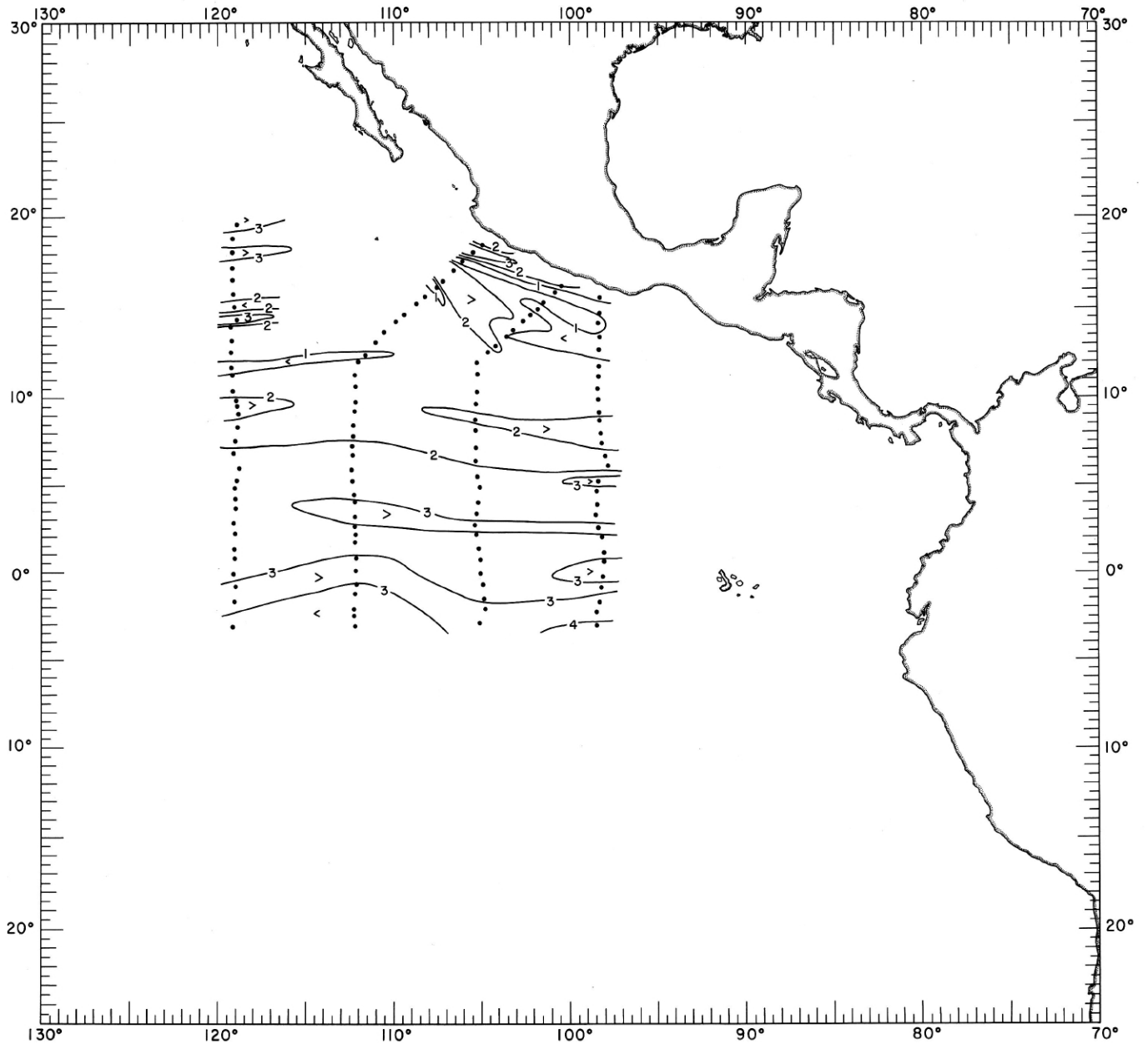

FIGURE 20-O_2-δ250.—Oxygen (ml./l.) on the surface where $\delta_T = 250$ cl./t., April-May 1967.

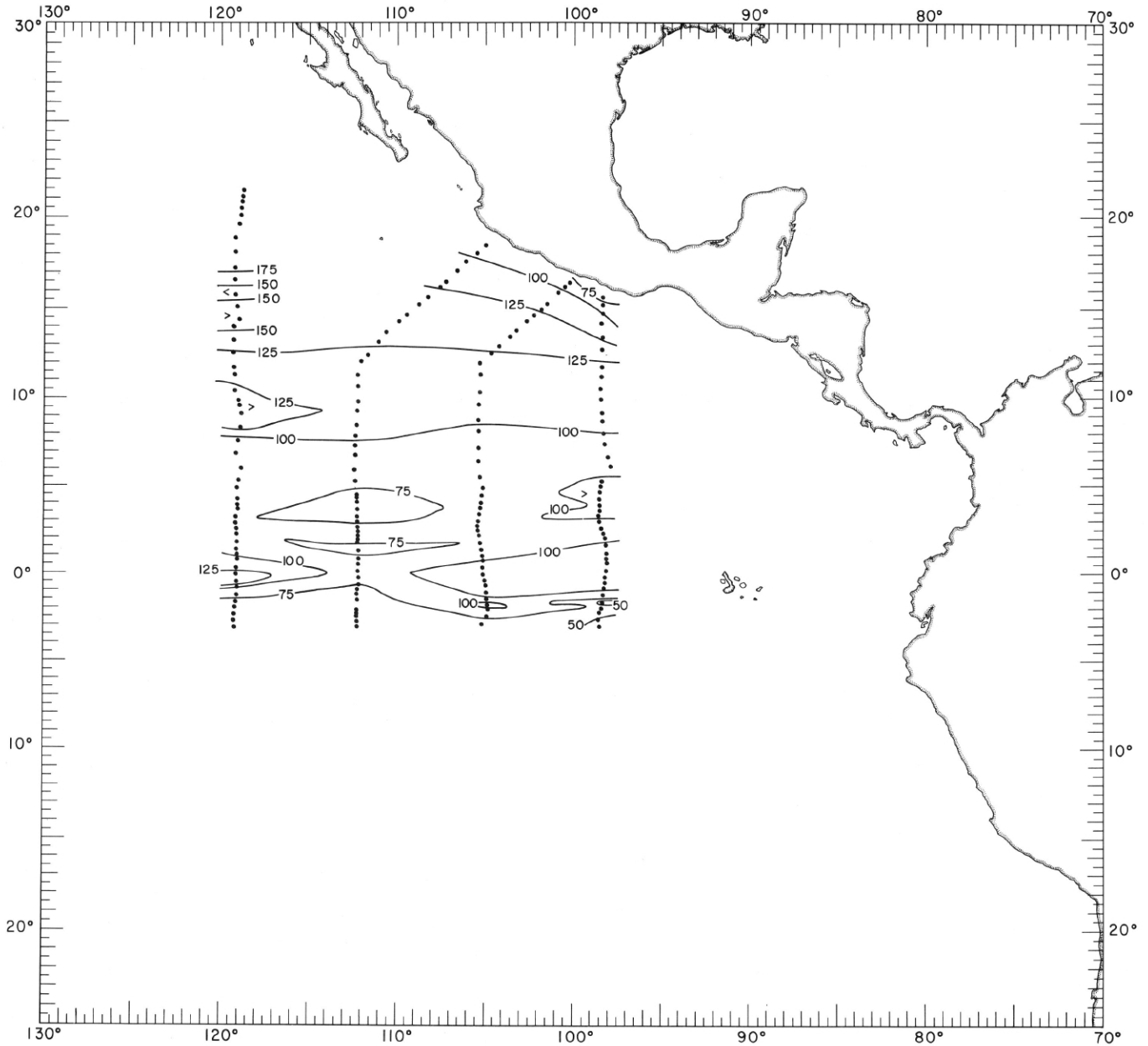

FIGURE 20-δ200-z.—Depth (m.) of the surface where $\delta_T = 200$ cl./t., April-May 1967.

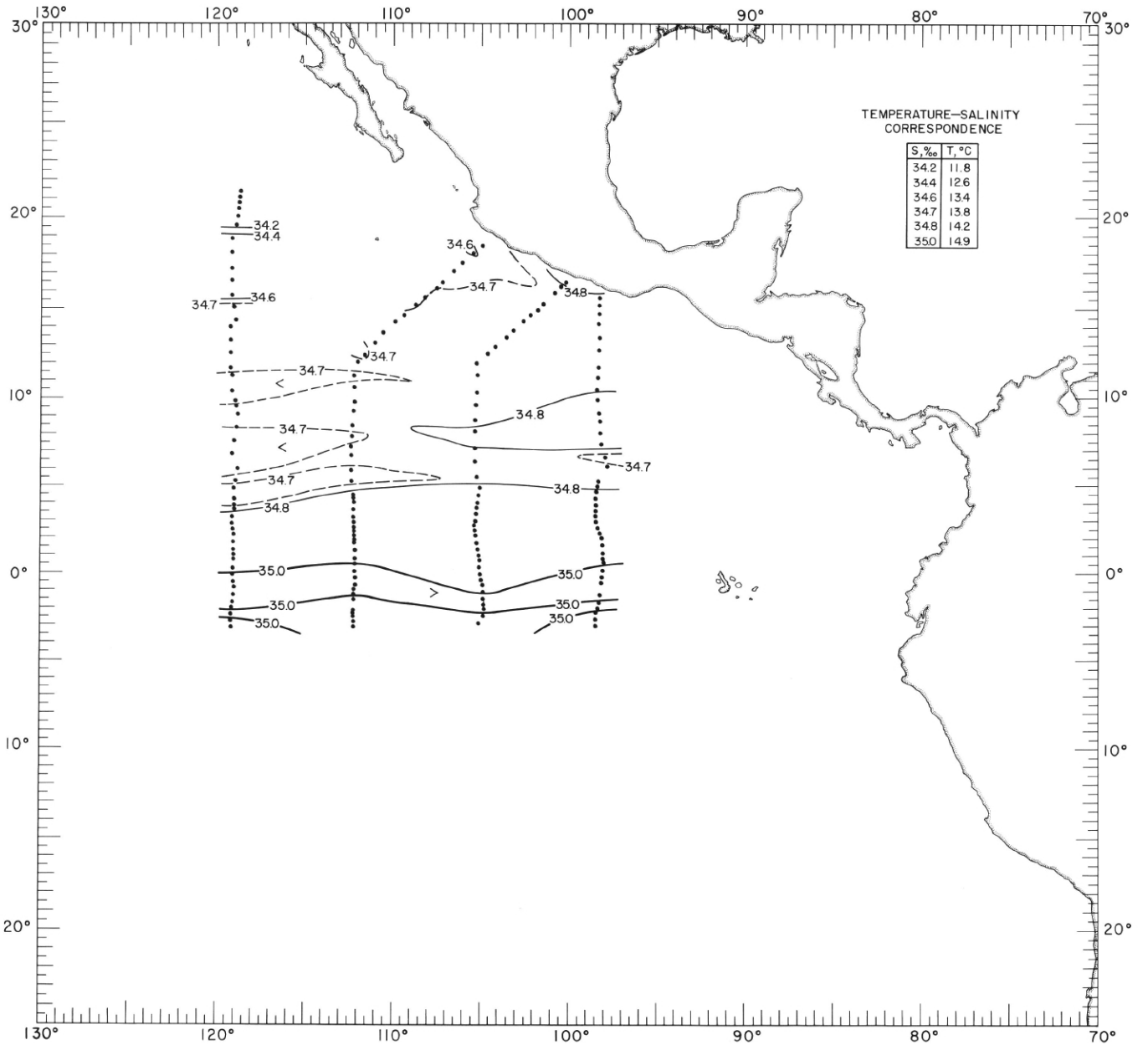

20-S-8200.

FIGURE 20-S-8200.—Salinity (‰) on the surface where $\delta_r = 200$ cl./t., April-May 1967. The table shows the temperature corresponding to each isohaline on the chart.

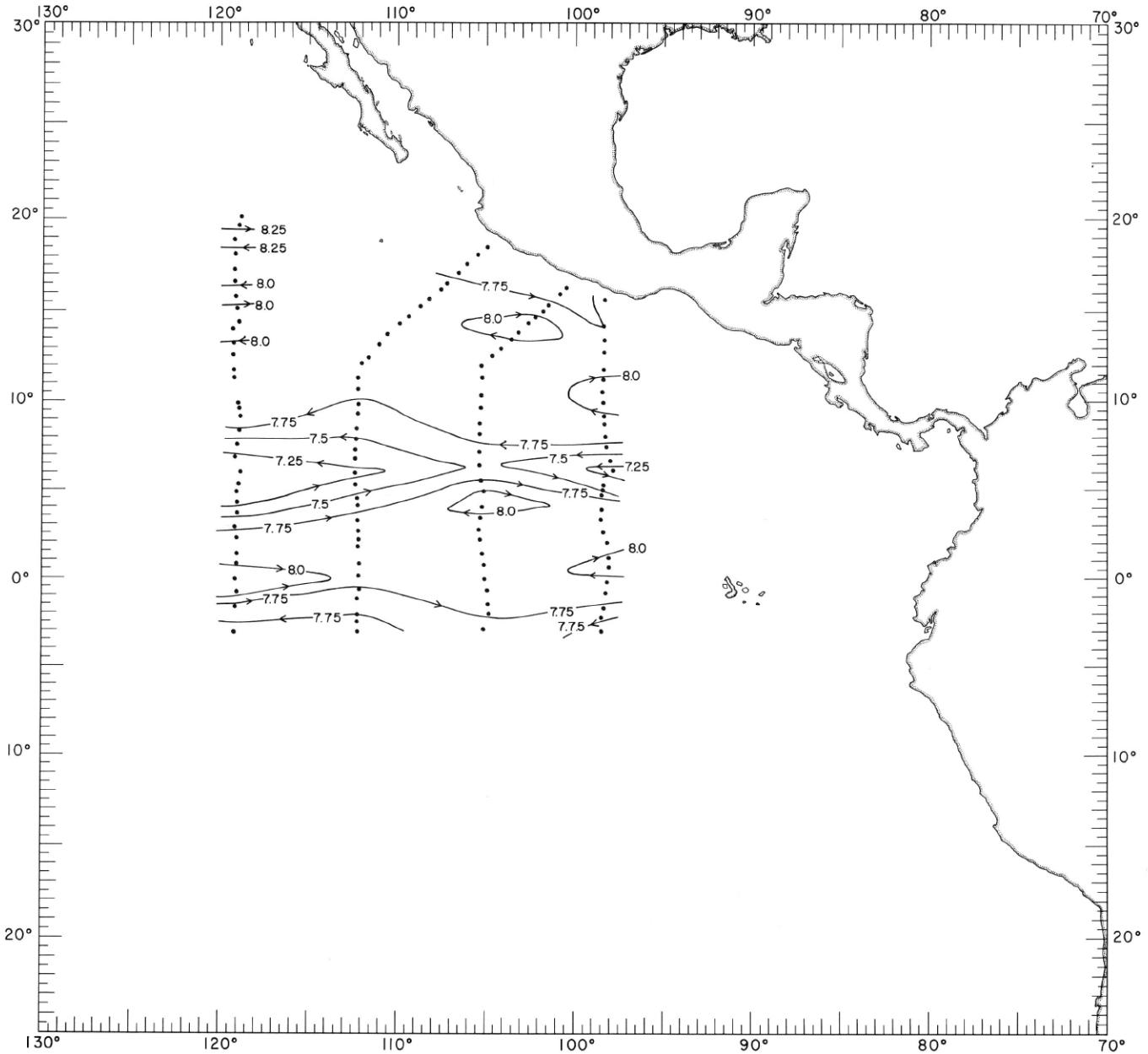

FIGURE 20-AP-δ200.—Acceleration potential (j./kg.), relative to 500 db., on the surface where δ_T = 200 cl./t., April-May 1967. For computing acceleration potential, thermosteric anomaly, δ_T, was used instead of specific volume anomaly, δ.

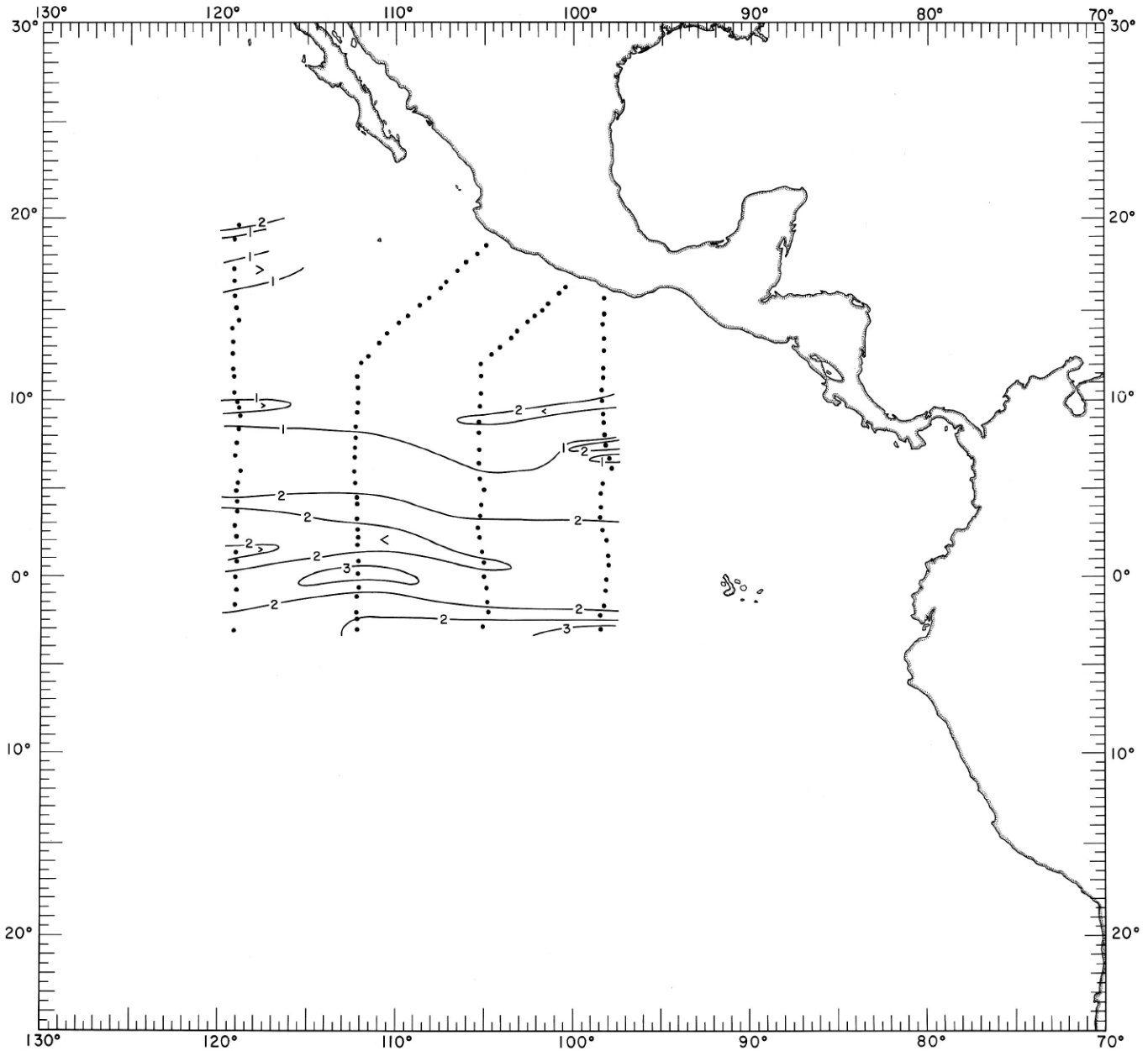

20-O_2-δ200.

FIGURE 20-O_2-δ200.—Oxygen (ml./l.) on the surface where $\delta_T = 200$ cl./t., April-May 1967.

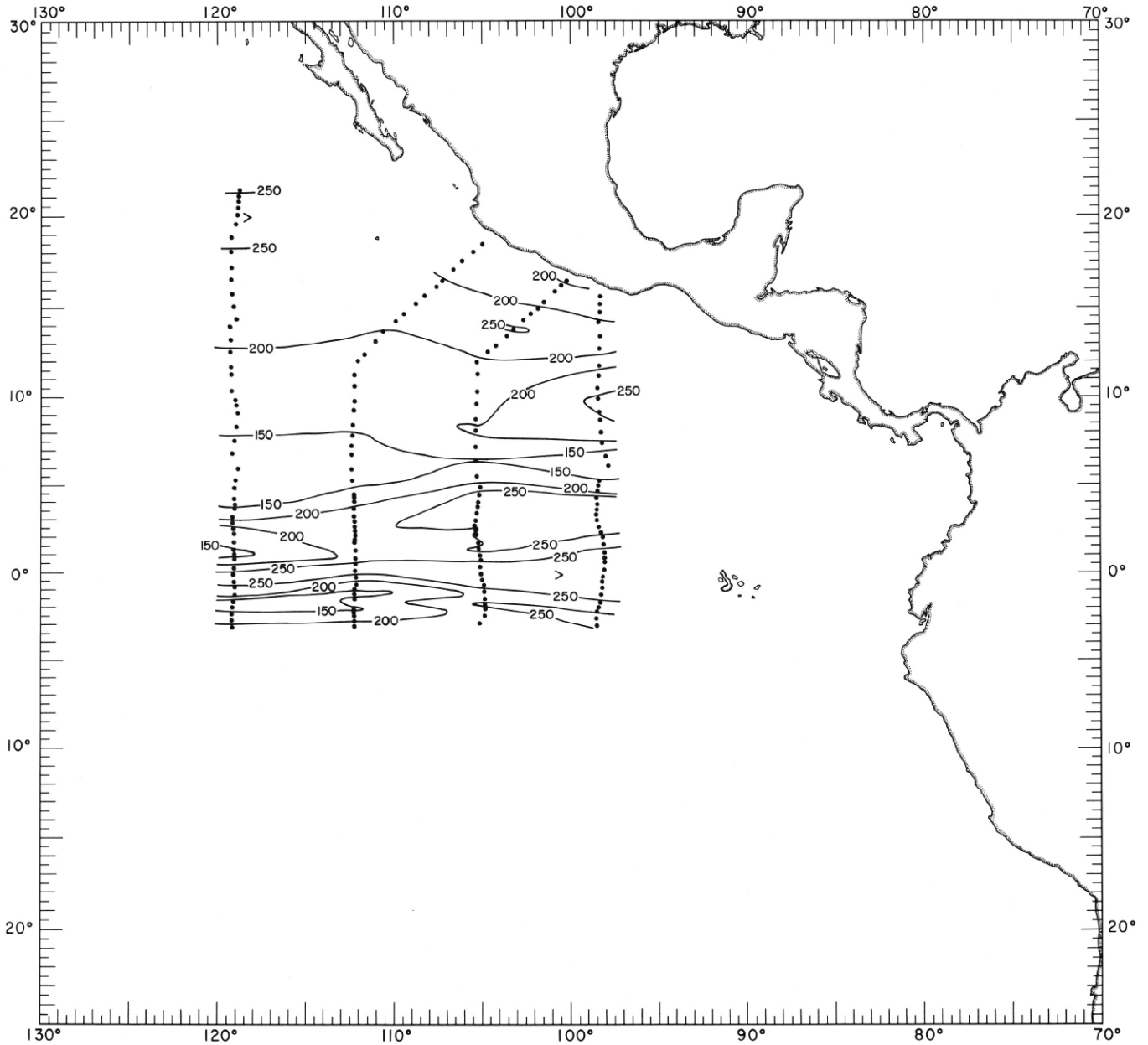

FIGURE 20-δ160-z.—Depth (m.) of the surface where $\delta_T = 160$ cl./t., April-May 1967.

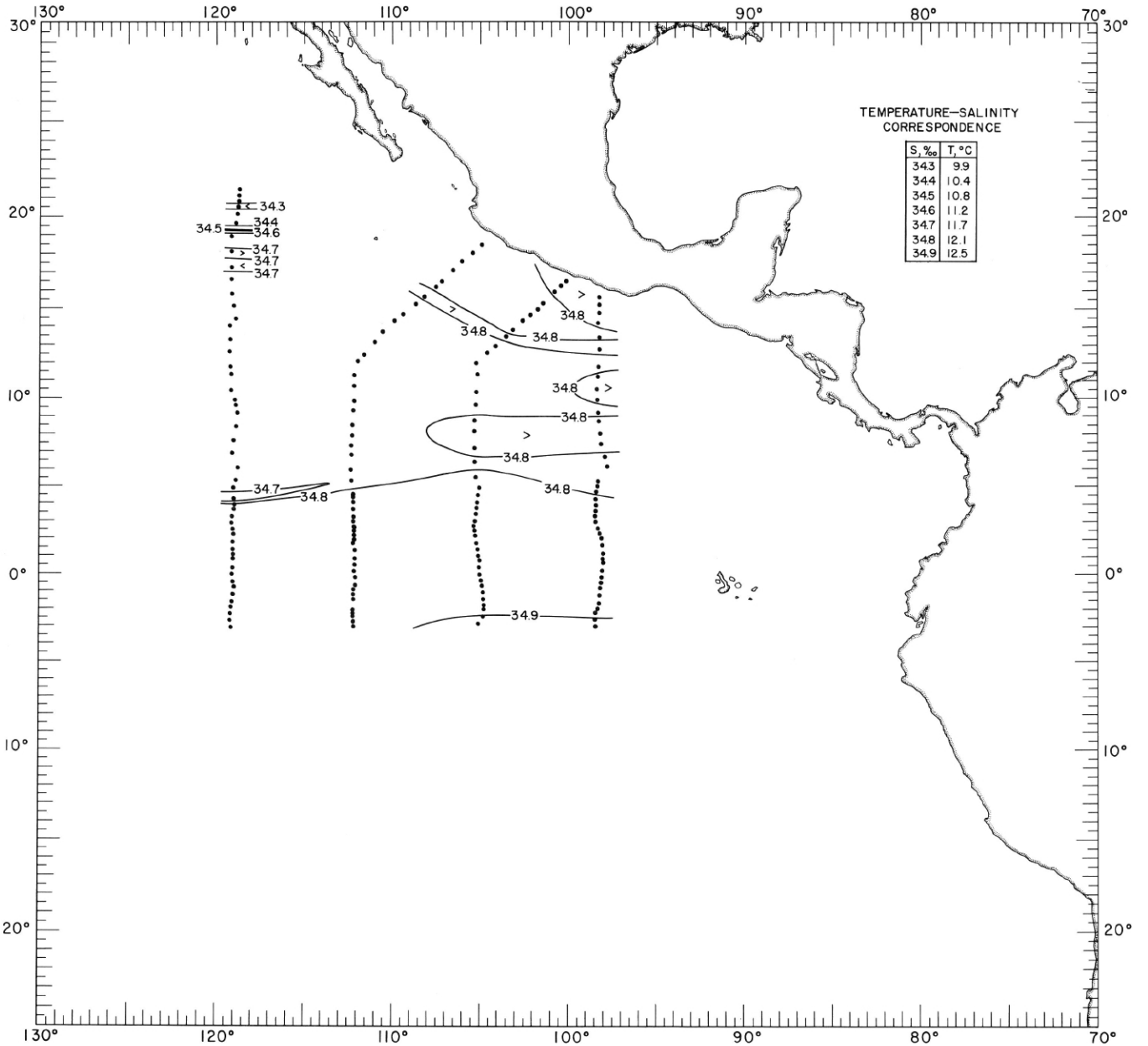

20-S-δ160.

FIGURE 20-S-δ160.—Salinity (‰) on the surface where δ_T = 160 cl./t., April-May 1967. The table shows the temperature corresponding to each isohaline on the chart.

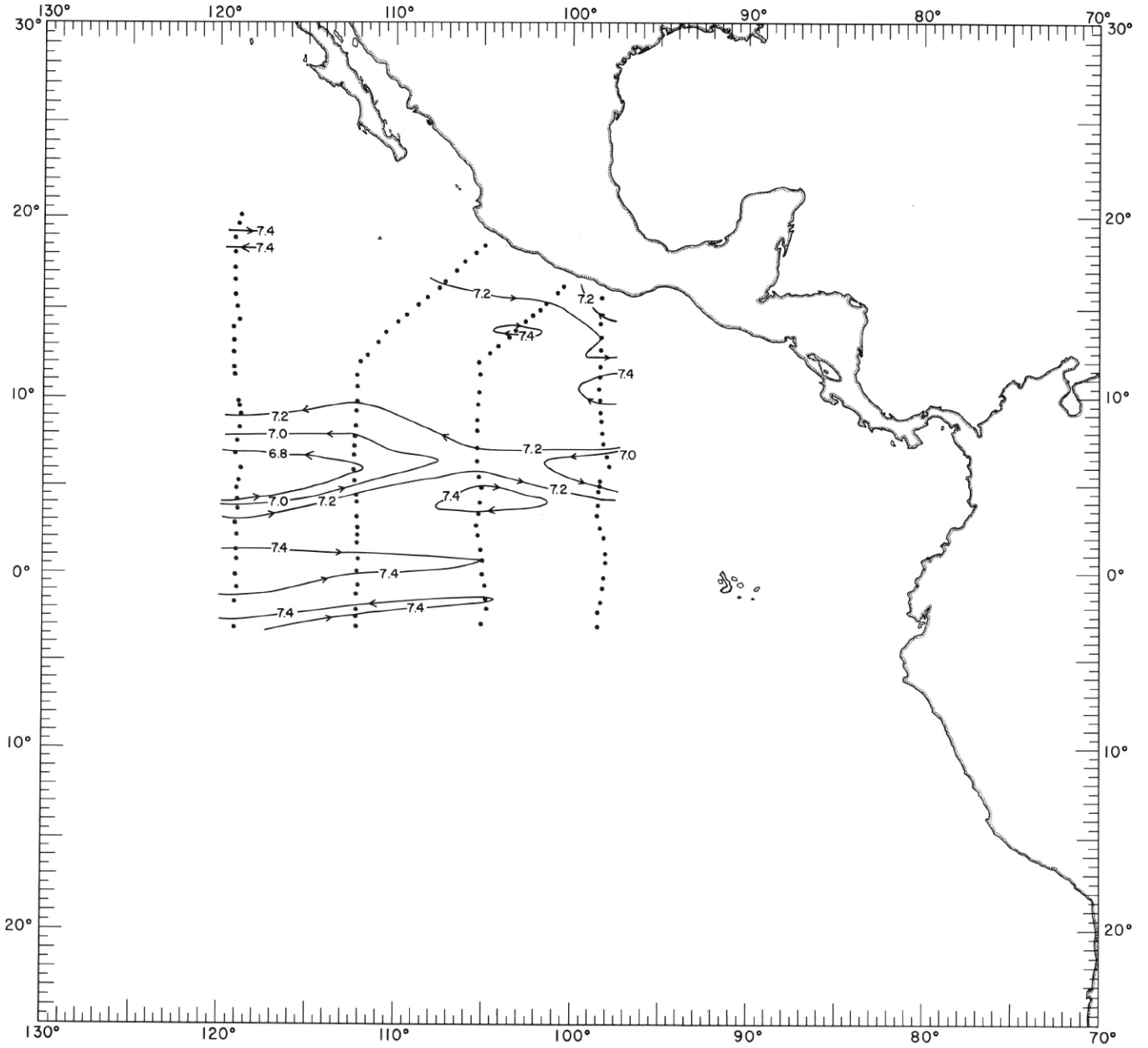

FIGURE 20-AP-δ160.—Acceleration potential (j./kg.), relative to 500 db., on the surface where δ_T = 160 cl./t., April-May 1967. For computing acceleration potential, thermosteric anomaly, δ_T, was used instead of specific volume anomaly, δ.

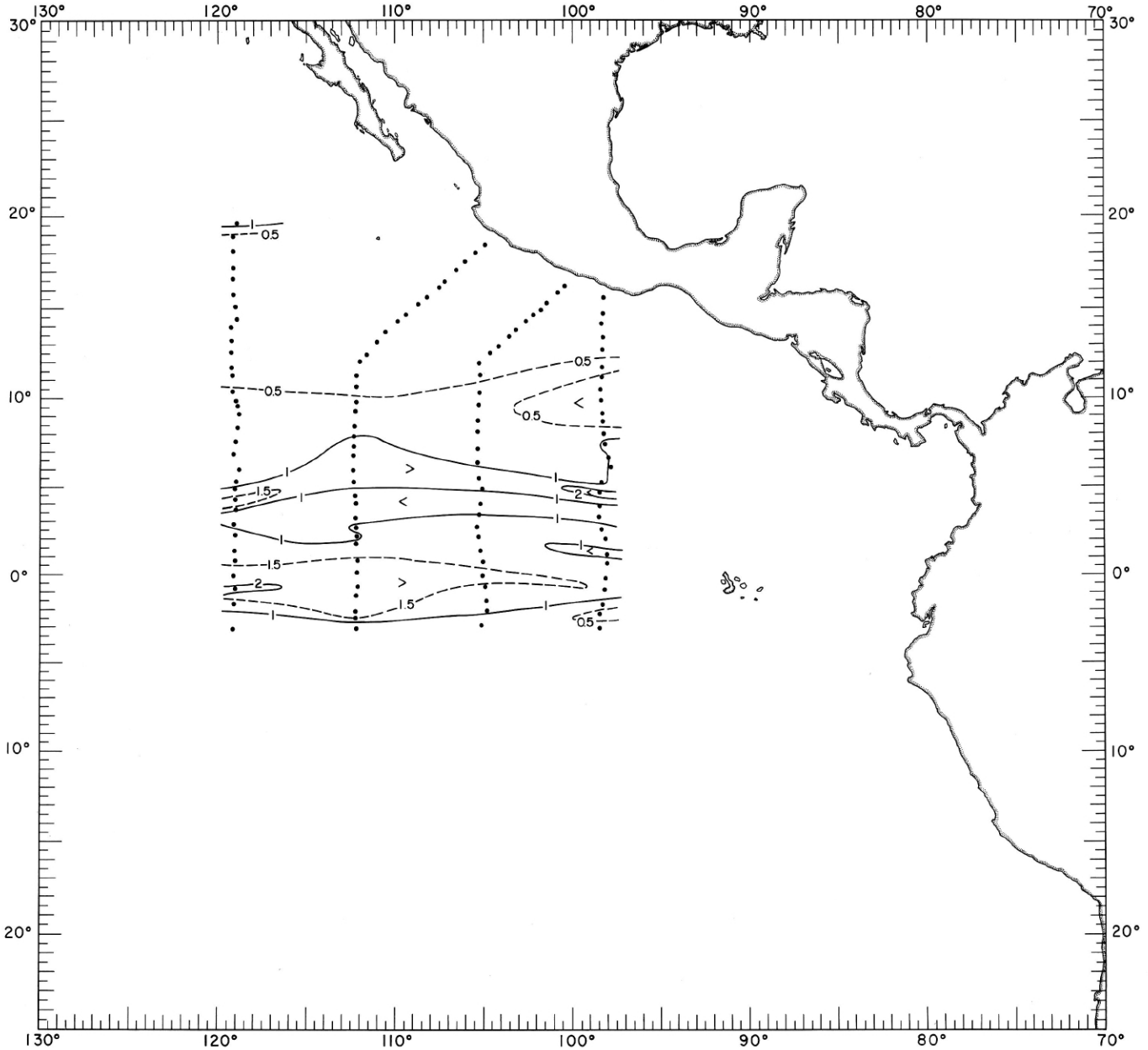

FIGURE 20-O$_2$-δ160.—Oxygen (ml./l.) on the surface where $\delta_T = 160$ cl./t., April-May 1967.

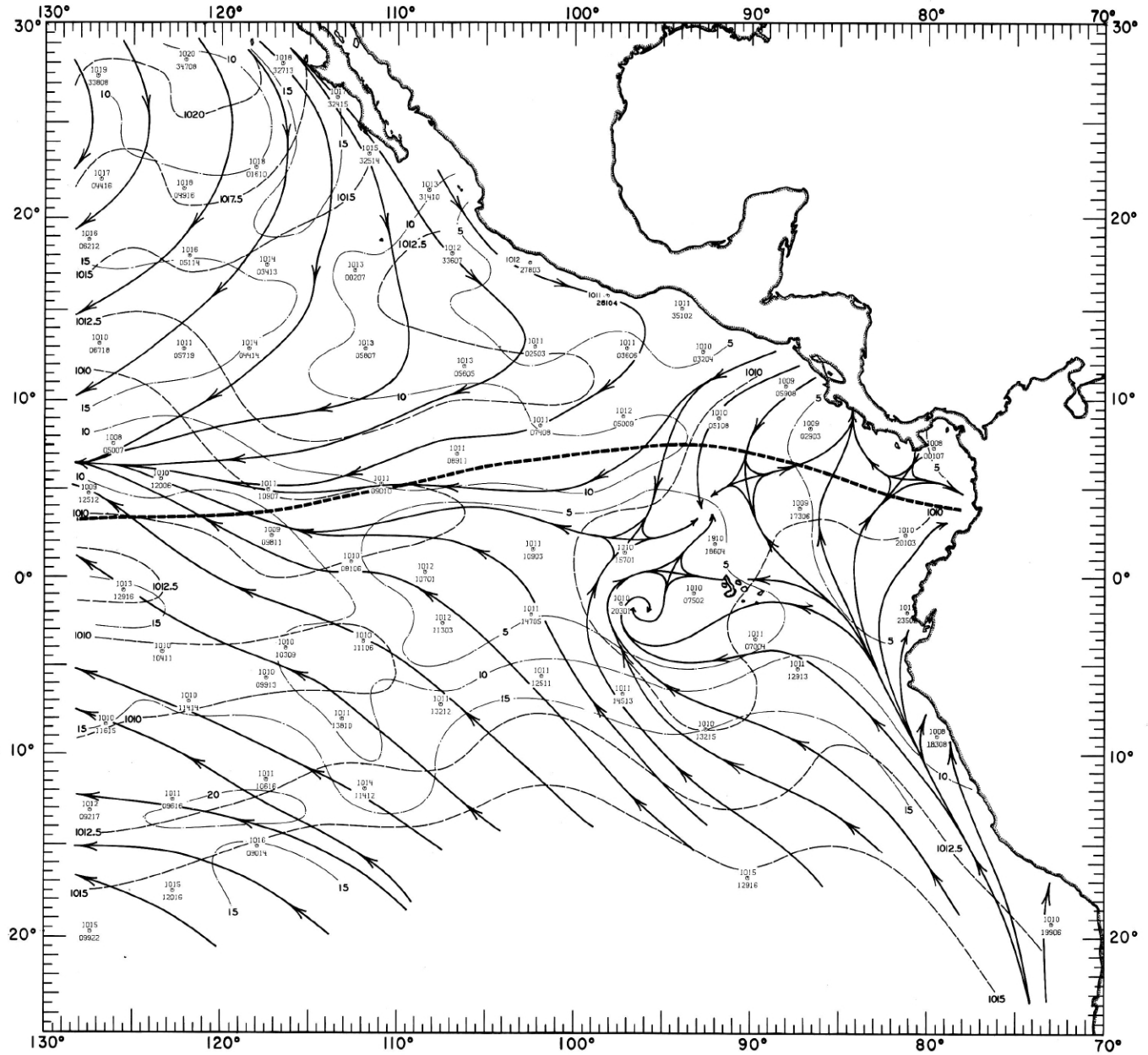

FIGURE 20-MW-1. — Analyses of the surface air pressure and surface winds from all available ship observations, averaged over 2-degree (latitude-longitude) squares for the period April 1-15, 1967. Heavy dashed lines are isobars. Solid lines are streamlines showing the mean resultant direction of wind flow. Light dash-dot lines are isotachs indicating mean resultant wind speed (kn.). Pressure (mb.) averaged for 5-degree squares is plotted above the mean position of the square, and resultant wind direction followed by speed (kn.) is plotted below. The monthly climatological position of the intertropical convergence zone is shown by a wide dashed band.

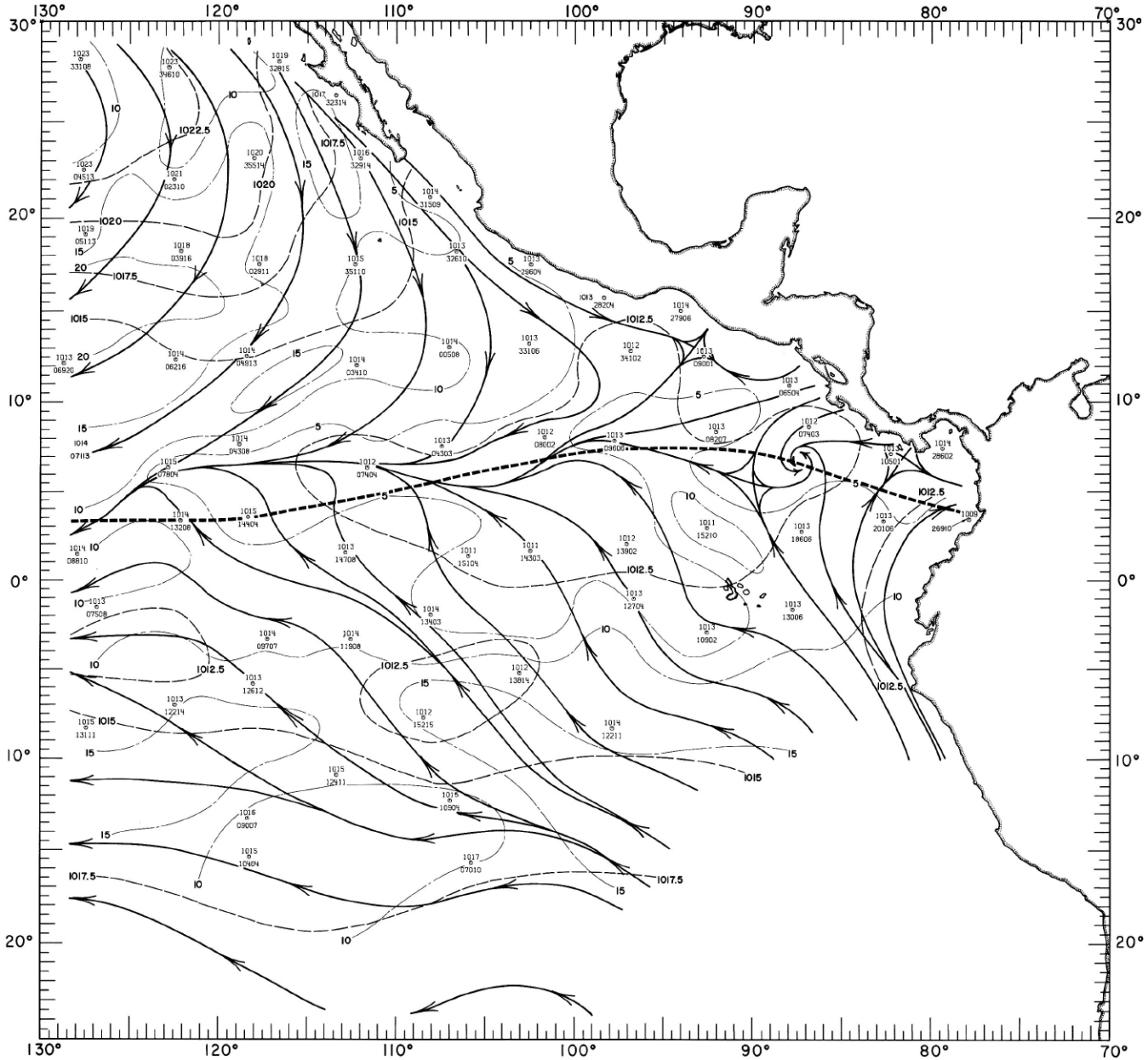

20-MW-2.

FIGURE 20-MW-2. — Analyses of the surface air pressure and surface winds from all available ship observations, averaged over 2-degree (latitude-longitude) squares for the period April 16-30, 1967. Heavy dashed lines are isobars. Solid lines are streamlines showing the mean resultant direction of wind flow. Light dash-dot lines are isotachs indicating mean resultant wind speed (kn.). Pressure (mb.) averaged for 5-degree squares is plotted above the mean position of the square, and resultant wind direction followed by speed (kn.) is plotted below. The monthly climatological position of the intertropical convergence zone is shown by a wide dashed band.

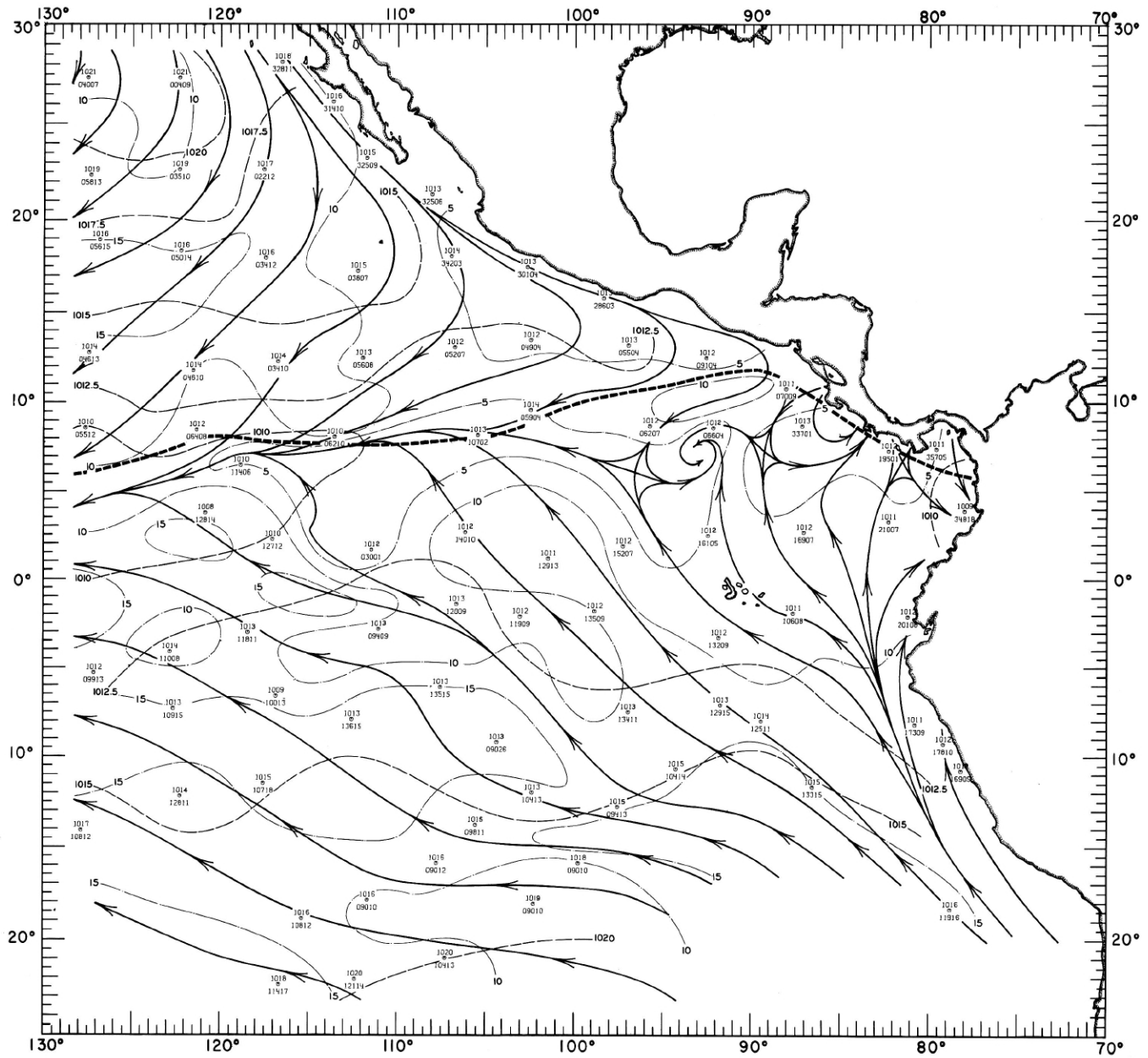

20-MW-3.

FIGURE 20-MW-3. — Analyses of the surface air pressure and surface winds from all available ship observations, averaged over 2-degree (latitude-longitude) squares for the period May 1-16, 1967. Heavy dashed lines are isobars. Solid lines are streamlines showing the mean resultant direction of wind flow. Light dash-dot lines are isotachs indicating mean resultant wind speed (kn.). Pressure (mb.) averaged for 5-degree squares is plotted above the mean position of the square, and resultant wind direction followed by speed (kn.) is plotted below. The monthly climatological position of the intertropical convergence zone is shown by a wide dashed band.

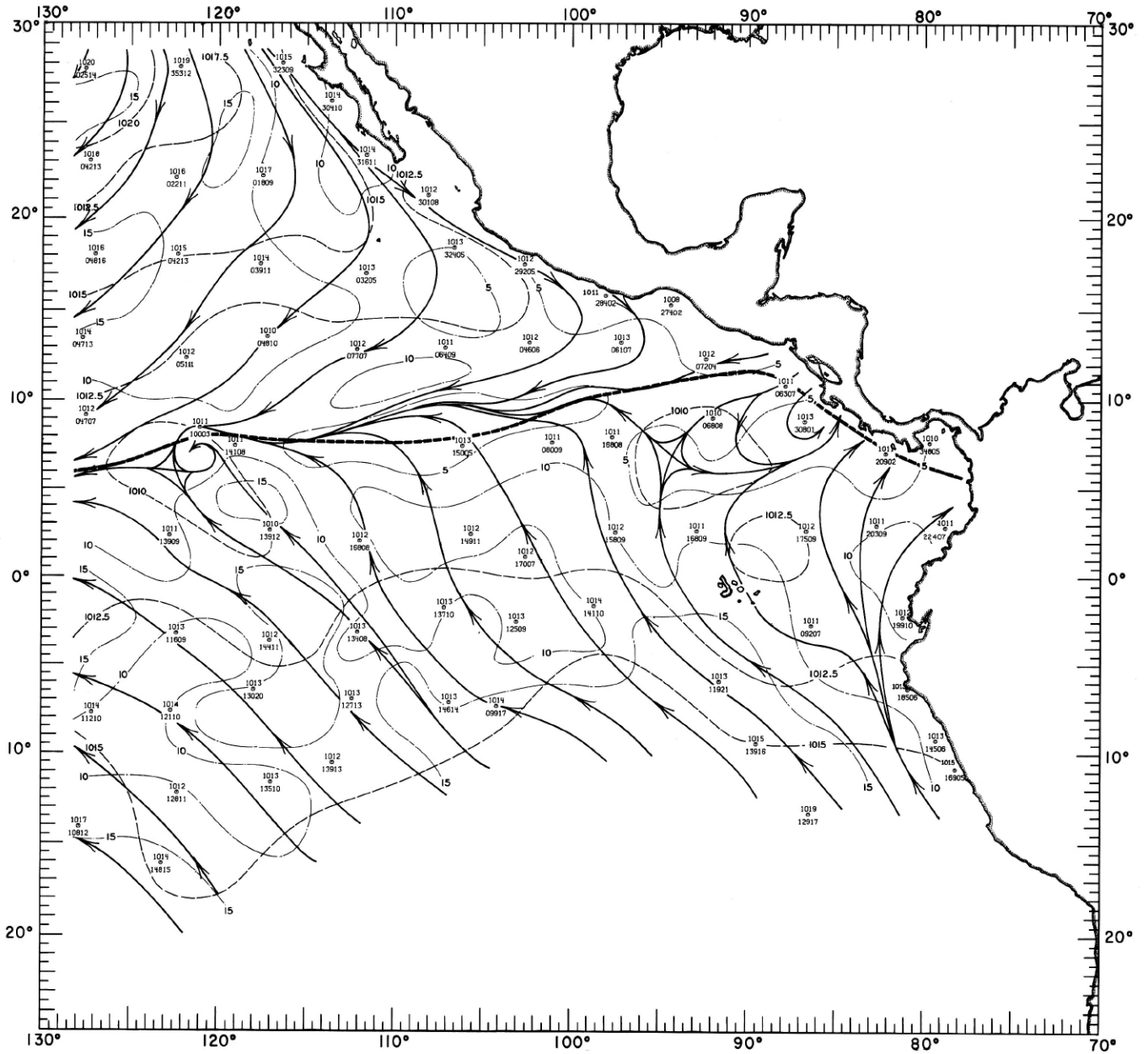

20-MW-4.

FIGURE 20-MW-4. — Analyses of the surface air pressure and surface winds from all available ship observations, averaged over 2-degree (latitude-longitude) squares for the period May 17-31, 1967. Heavy dashed lines are isobars. Solid lines are streamlines showing the mean resultant direction of wind flow. Light dash-dot lines are isotachs indicating mean resultant wind speed (kn.). Pressure (mb.) averaged for 5-degree squares is plotted above the mean position of the square, and resultant wind direction followed by speed (kn.) is plotted below. The monthly climatological position of the intertropical convergence zone is shown by a wide dashed band.

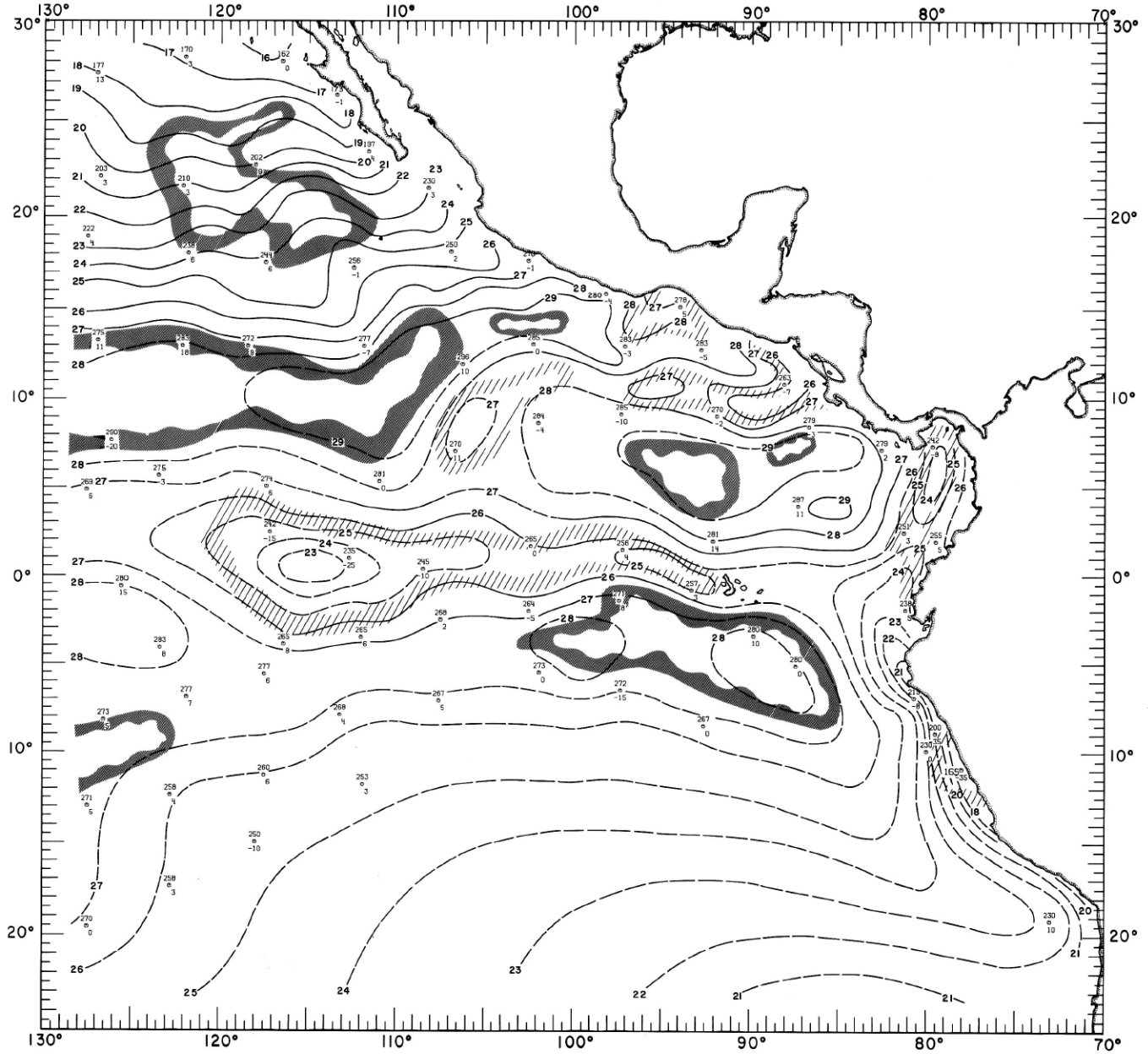

20-MT-1.

FIGURE 20-MT-1. — Analysis of sea surface temperatures based on averages for 2-degree (latitude-longitude) squares from all available ship observations for the period April 1-15, 1967. Solid lines are sea surface isotherms (°C.); the isotherms are dashed where data are sparse. Dark hatching outlines areas with positive temperature anomalies (computed from mean sea surface temperatures averaged over 22 years) greater than 1°C.; light hatching shows areas with negative anomalies greater than 1° C. Sea surface temperature (°C. x 10) averaged for 5-degree squares is plotted above the mean position of the square; sea temperature minus air temperature difference (°C. x 10) is plotted below the symbol.

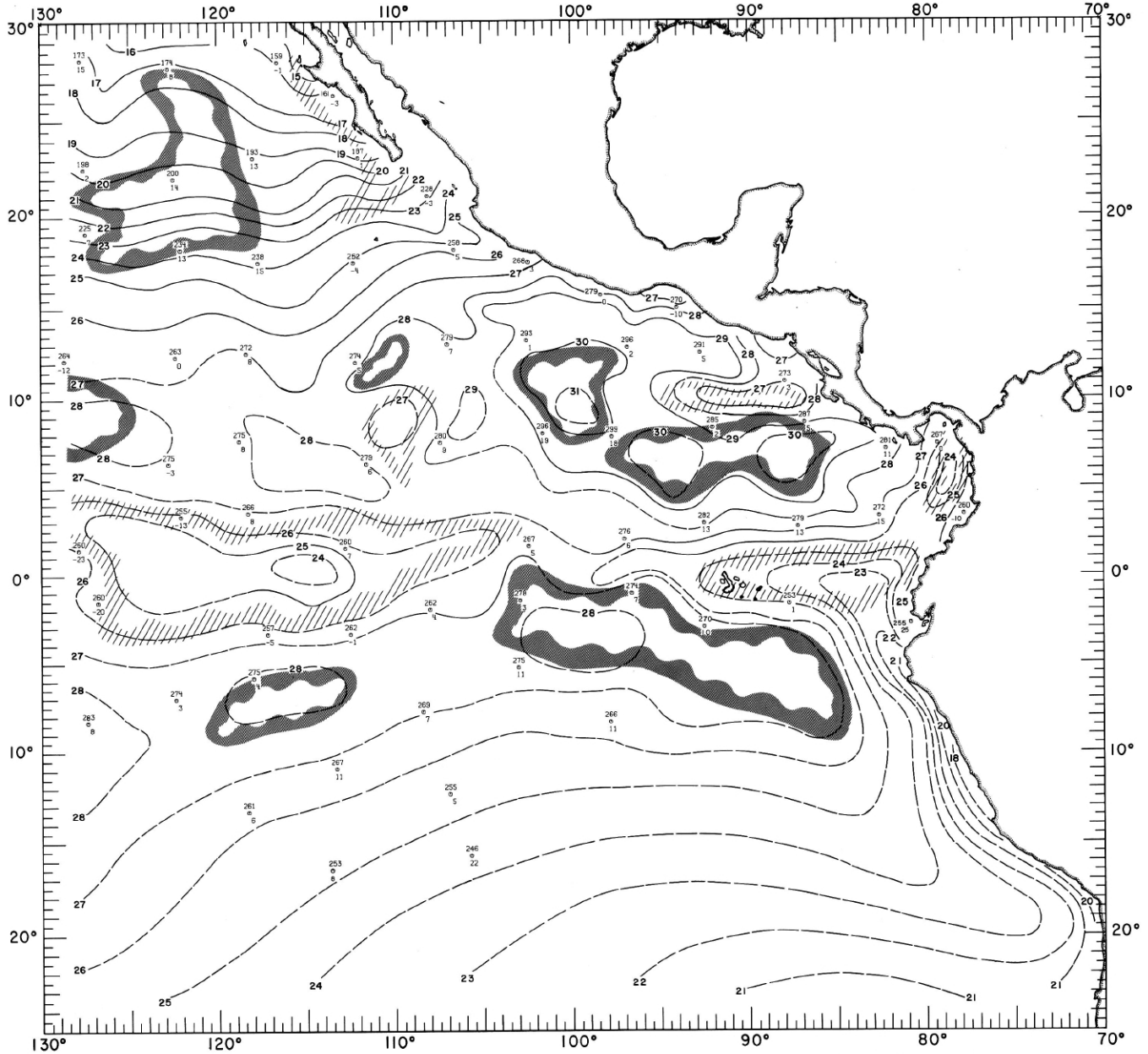

FIGURE 20-MT-2. — Analysis of sea surface temperatures based on averages for 2-degree (latitude-longitude) squares from all available ship observations for the period April 16-30, 1967. Solid lines are sea surface isotherms (°C.); the isotherms are dashed where data are sparse. Dark hatching outlines areas with positive temperature anomalies (computed from mean sea surface temperatures averaged over 22 years) greater than 1°C.; light hatching shows areas with negative anomalies greater than 1° C. Sea surface temperature (°C. x 10) averaged for 5-degree squares is plotted above the mean position of the square; sea temperature minus air temperature difference (°C. x 10) is plotted below the symbol.

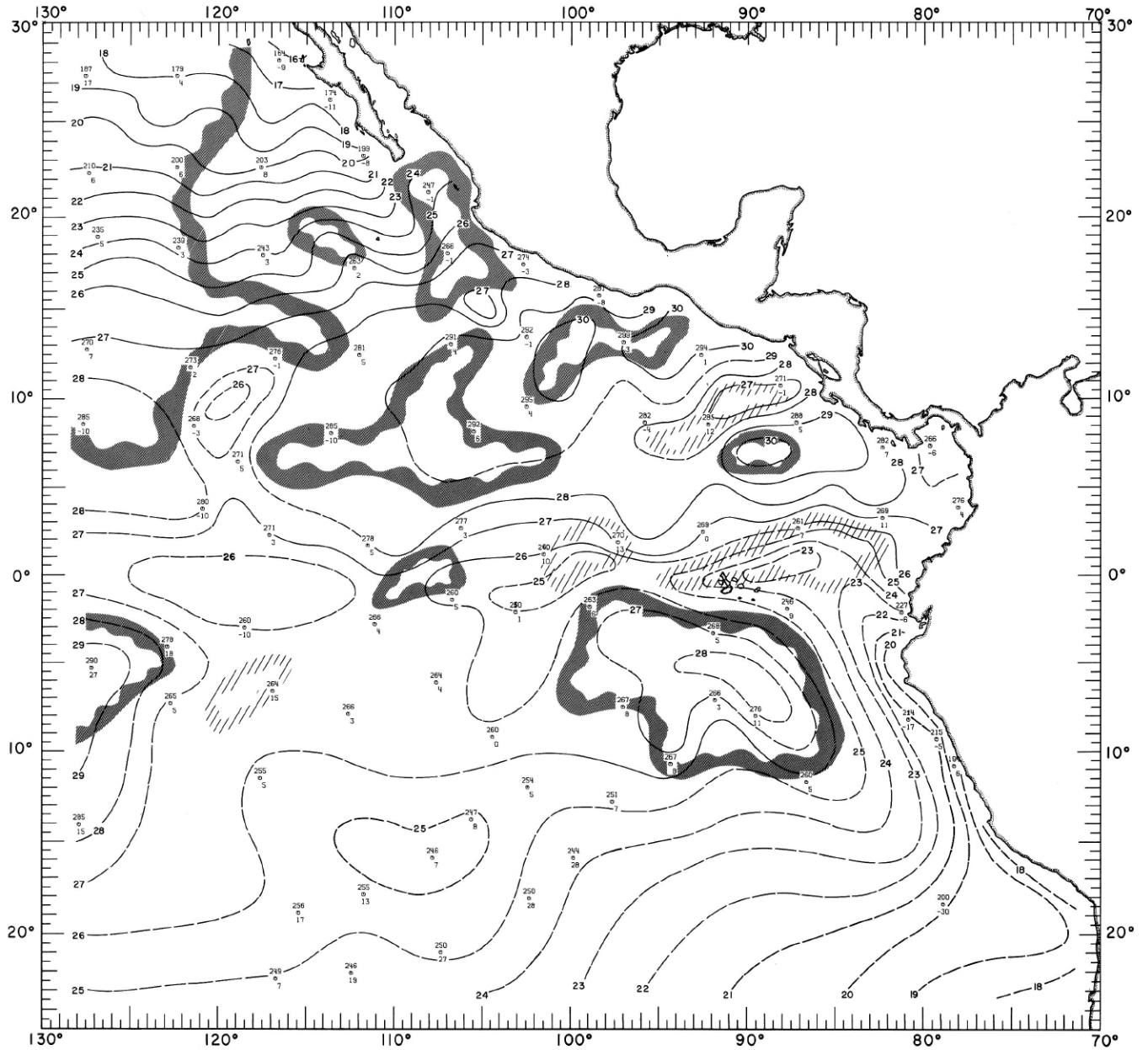

20-MT-3.

FIGURE 20-MT-3. — Analysis of sea surface temperatures based on averages for 2-degree (latitude-longitude) squares from all available ship observations for the period May 1-16, 1967. Solid lines are sea surface isotherms (°C.); the isotherms are dashed where data are sparse. Dark hatching outlines areas with positive temperature anomalies (computed from mean sea surface temperatures averaged over 22 years) greater than 1°C.; light hatching shows areas with negative anomalies greater than 1° C. Sea surface temperature (°C. x 10) averaged for 5-degree squares is plotted above the mean position of the square; sea temperature minus air temperature difference (°C. x 10) is plotted below the symbol.

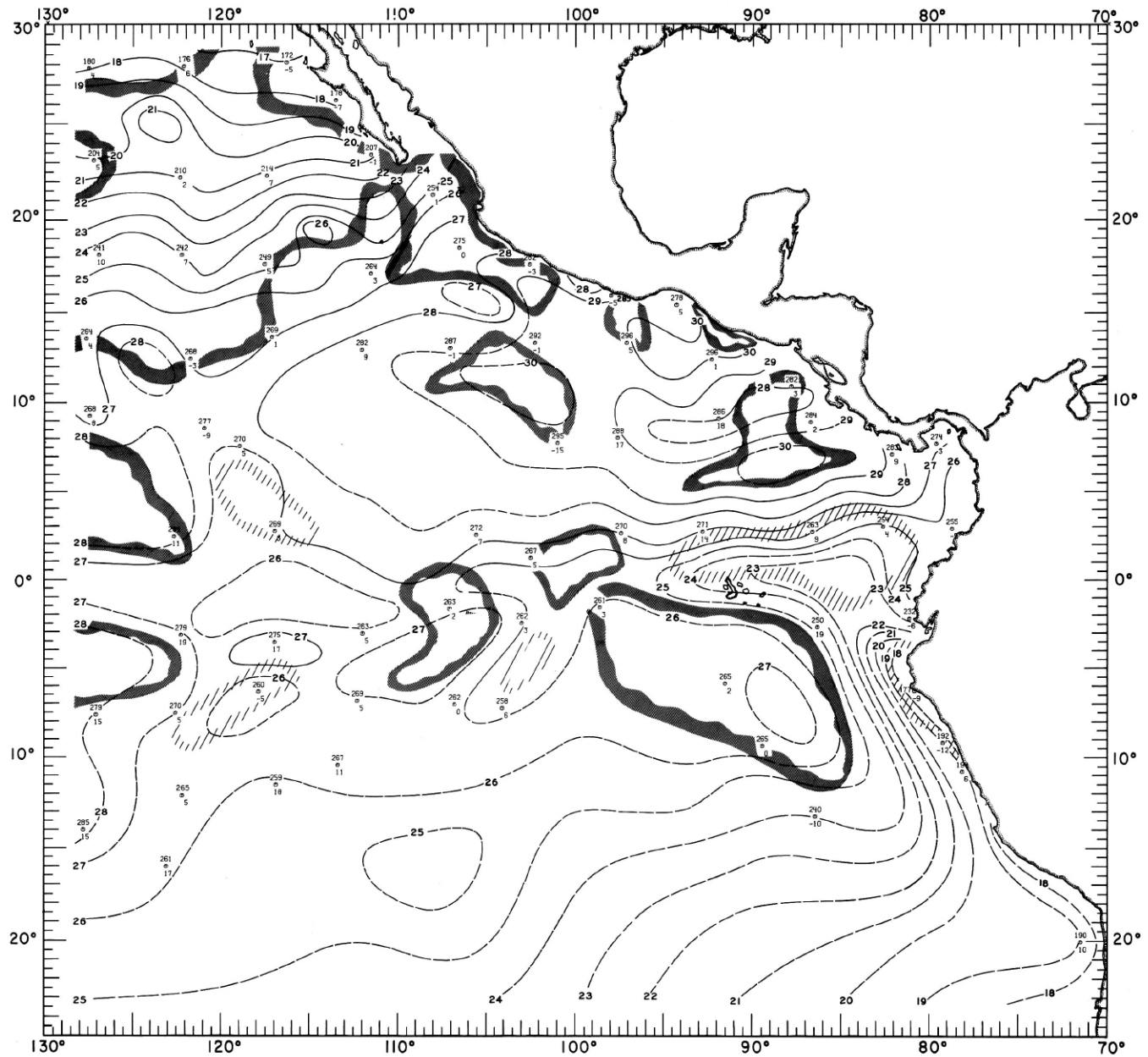

20-MT-4.

FIGURE 20-MT-4. — Analysis of sea surface temperatures based on averages for 2-degree (latitude-longitude) squares from all available ship observations for the period May 17-31, 1967. Solid lines are sea surface isotherms (°C.); the isotherms are dashed where data are sparse. Dark hatching outlines areas with positive temperature anomalies (computed from mean sea surface temperatures averaged over 22 years) greater than 1°C.; light hatching shows areas with negative anomalies greater than 1° C. Sea surface temperature (°C. x 10) averaged for 5-degree squares is plotted above the mean position of the square; sea temperature minus air temperature difference (°C. x 10) is plotted below the symbol.

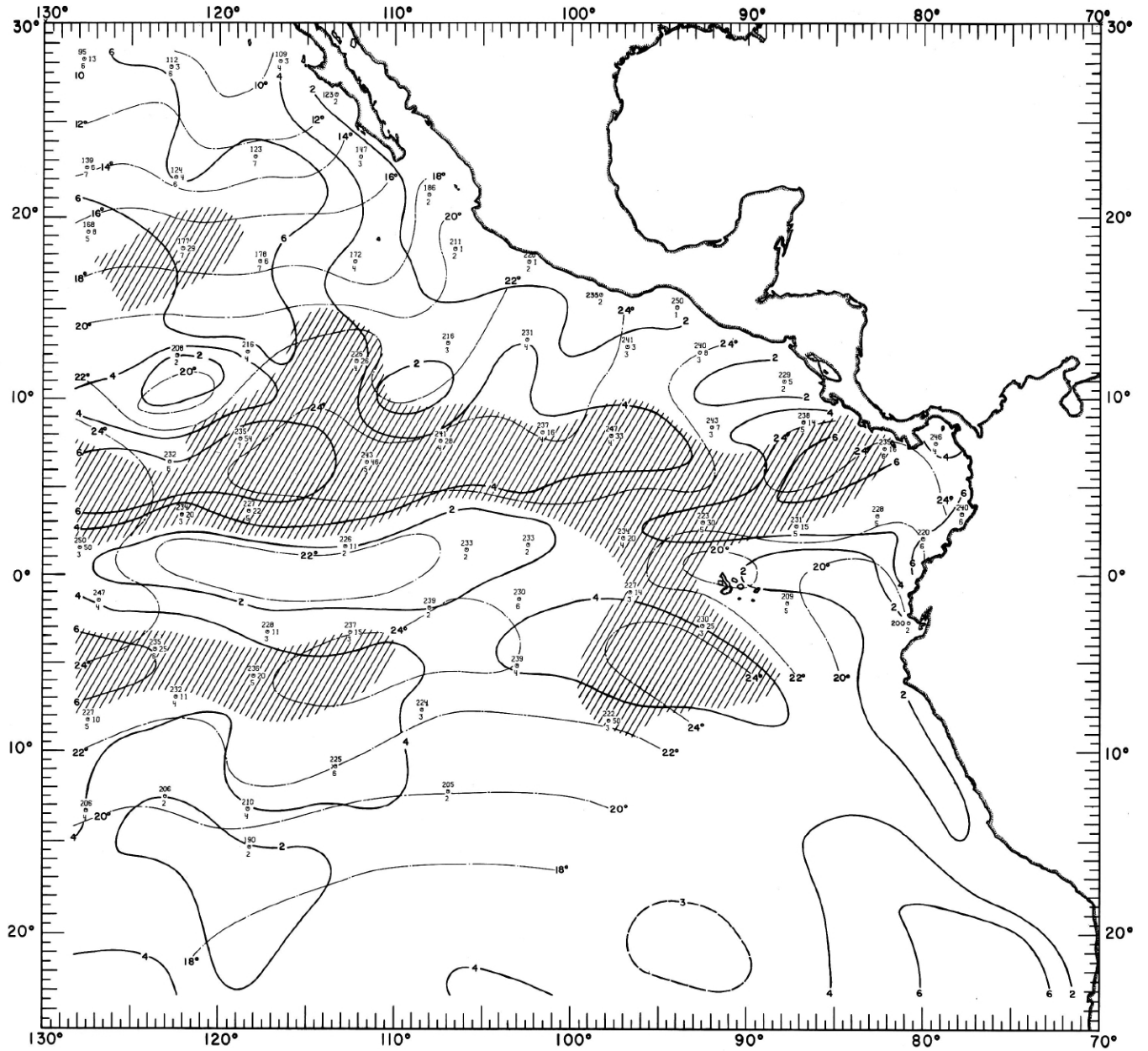

20-MC-1.

FIGURE 20-MC-1. — Analyses of the surface dew-point temperature of the air and total cloud cover based on 2 degree (latidude-longitude) averages from all available ship observations for the month of April 1967. Solid lines depict the monthly mean total cloud cover in oktas; the lines are dashed where data are sparse. Dash-dot lines are isotherms of the mean monthly dew-point temperature at 2-degree (C.) intervals Areas where 15 percent or more of the ships reported rain of any type at or within sight of the ship are shaded. Dew-point temperature (°C. x 10) averaged for 5-degree squares is plotted above the mean position of the square, with total cloud cover (oktas) below and rainfall frequency (%) to the right of the symbol.

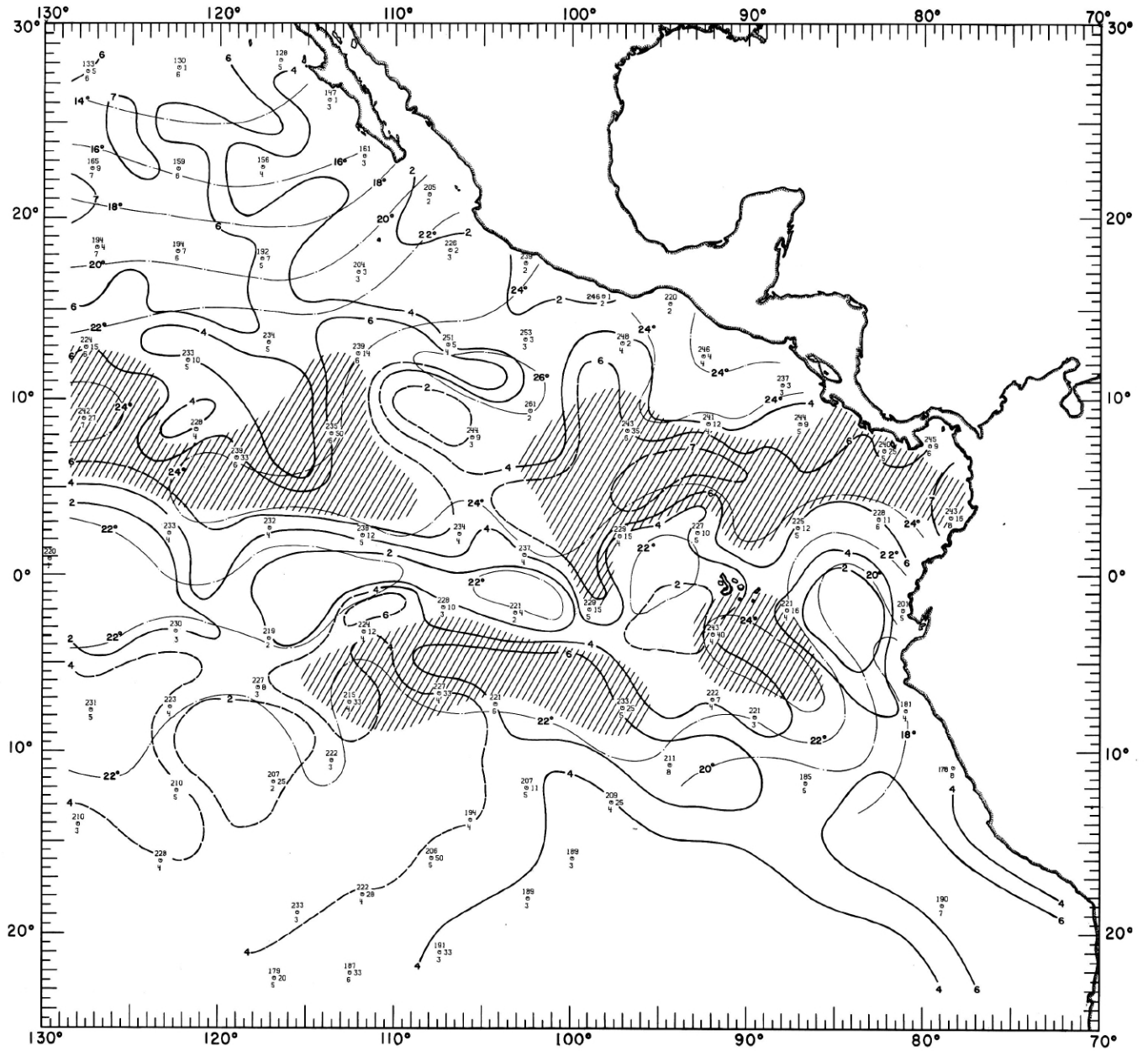

20-MC-2.

FIGURE 20-MC-2. — Analyses of the surface dew-point temperature of the air and total cloud cover based on 2 degree (latidude-longitude) averages from all available ship observations for the month of May 1967. Solid lines depict the monthly mean total cloud cover in oktas; the lines are dashed where data are sparse. Dash-dot lines are isotherms of the mean monthly dew-point temperature at 2-degree (C.) intervals. Areas where 15 percent or more of the ships reported rain of any type at or within sight of the ship are shaded. Dew-point temperature (°C. x 10) averaged for 5-degree squares is plotted above the mean position of the square, with total cloud cover (oktas) below and rainfall frequency (%) to the right of the symbol.

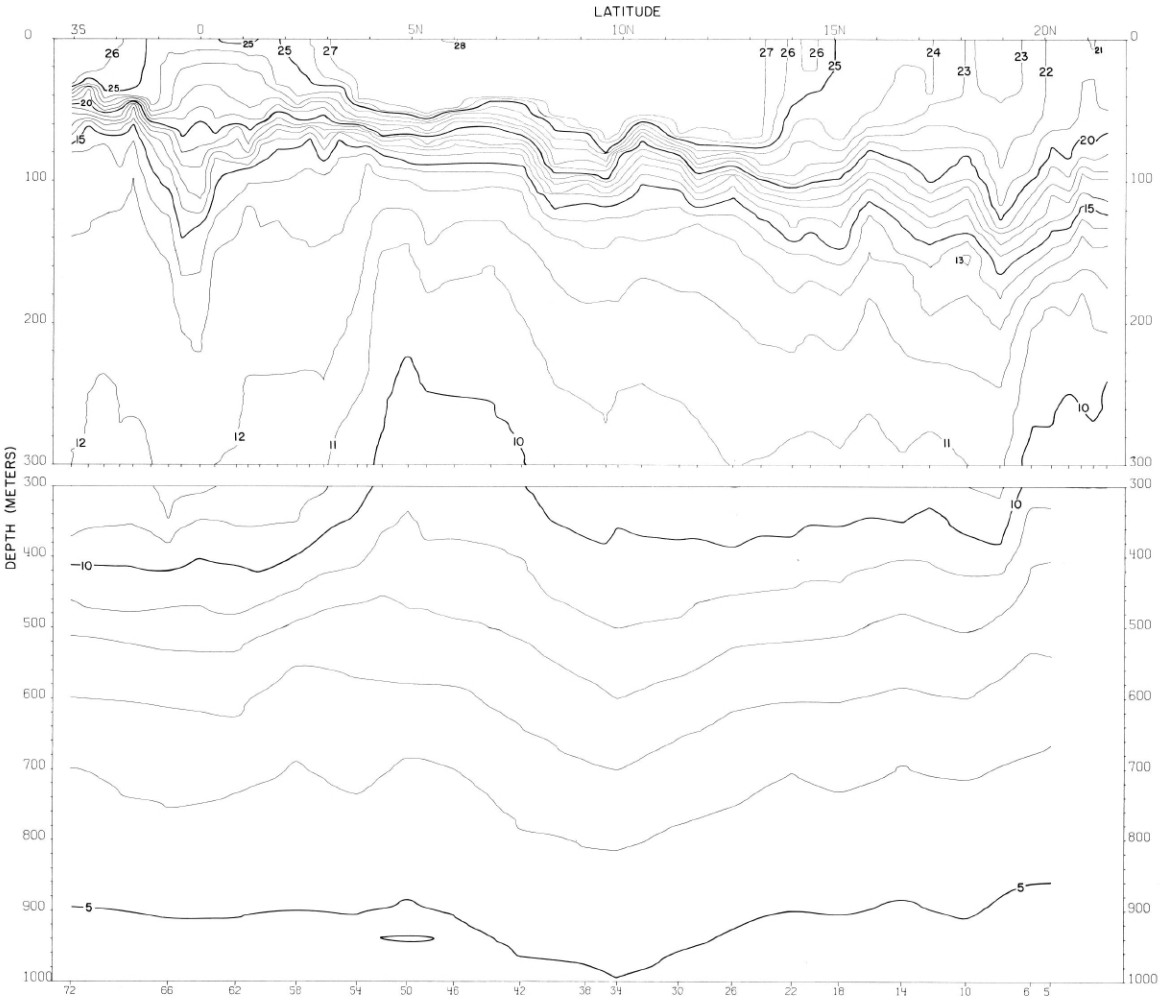

FIGURE 20-T-vl.—Vertical distribution of temperature (°C.) along 119°20′ W., April 13-21, 1967.

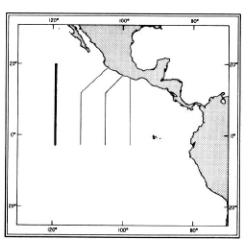

20-T-vl.

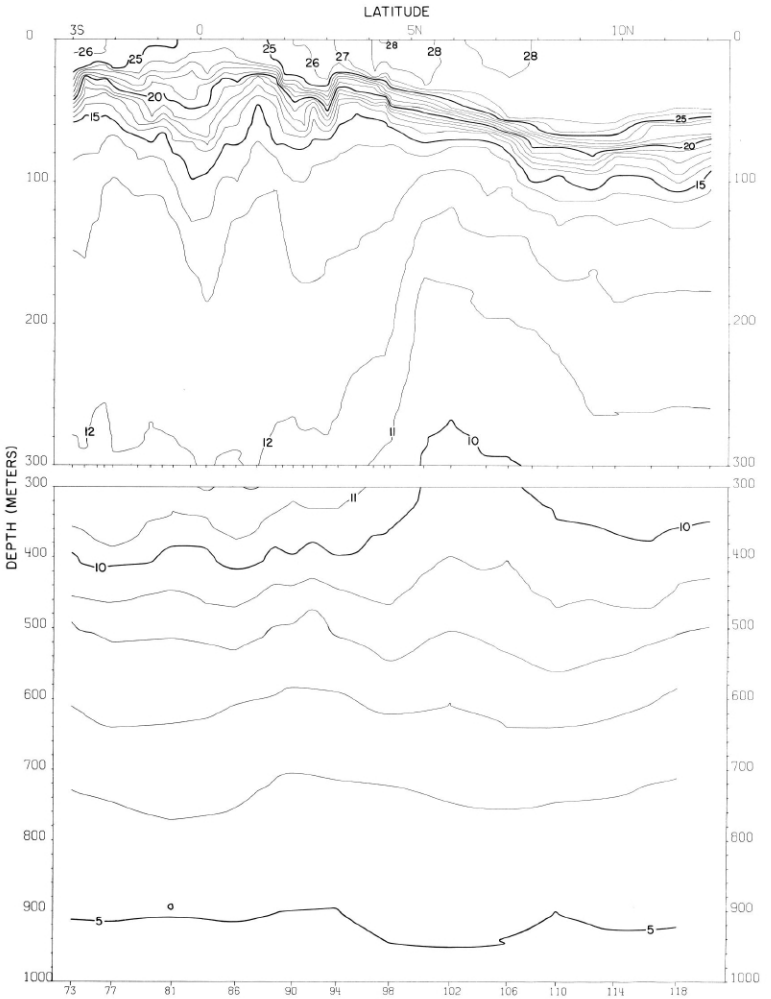

FIGURE 20-T-v2.—Vertical distribution of temperature (°C.) along 112°20′ W., April 23-29, 1967.

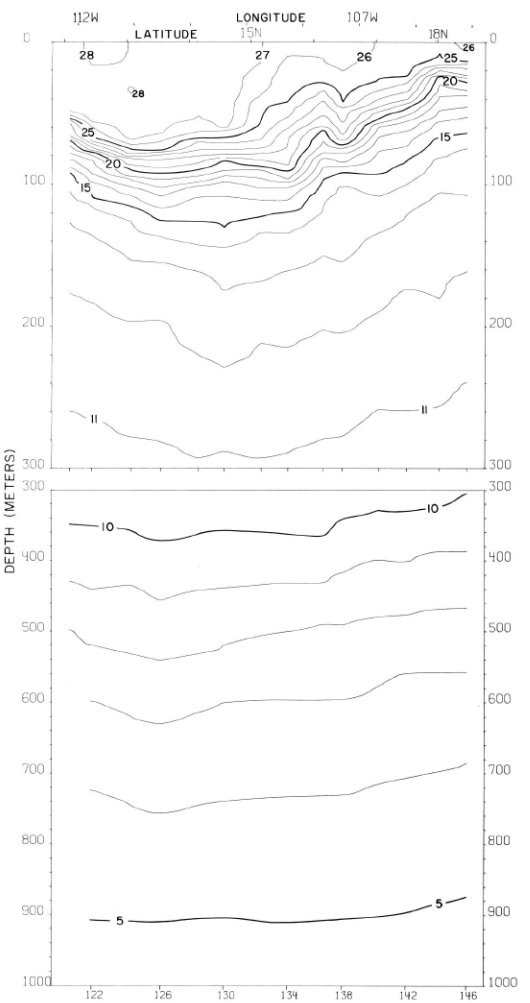

FIGURE 20-T-v3.—Vertical distribution of temperature (°C.) along a section from 12° N., 112°20′ W. to Manzanillo, April 29-May 2, 1967.

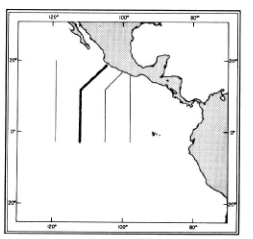

20-T-v2.

20-T-v3.

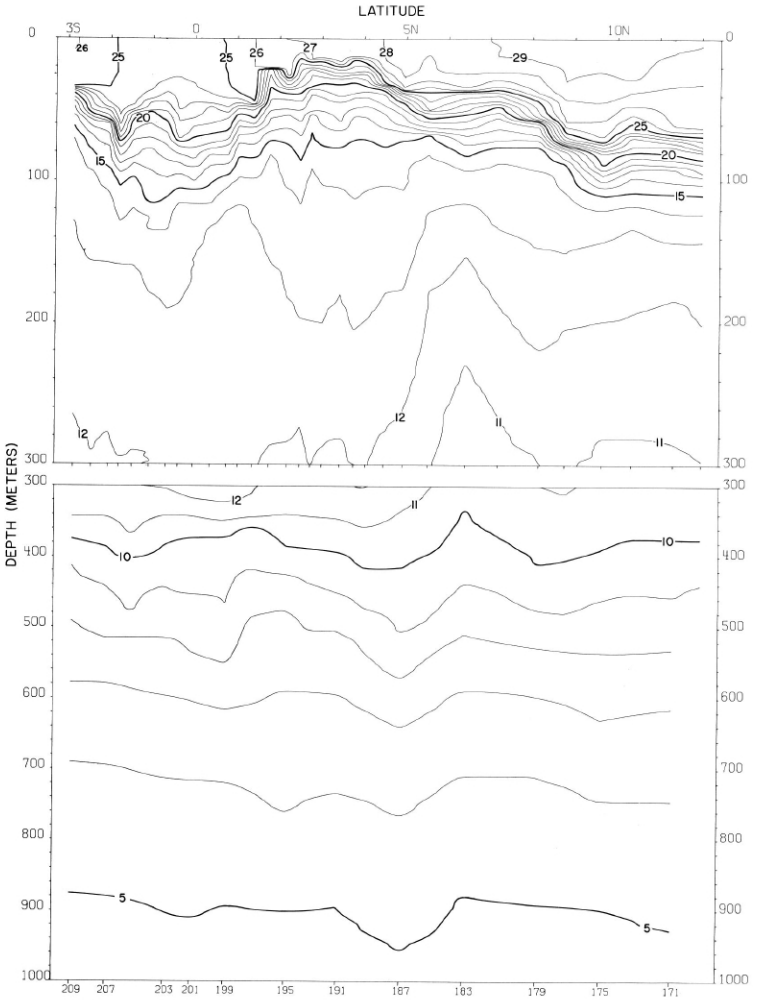

FIGURE 20-T-v5.—Vertical distribution of temperature (°C.) along 105°20′ W., May 10-15, 1967.

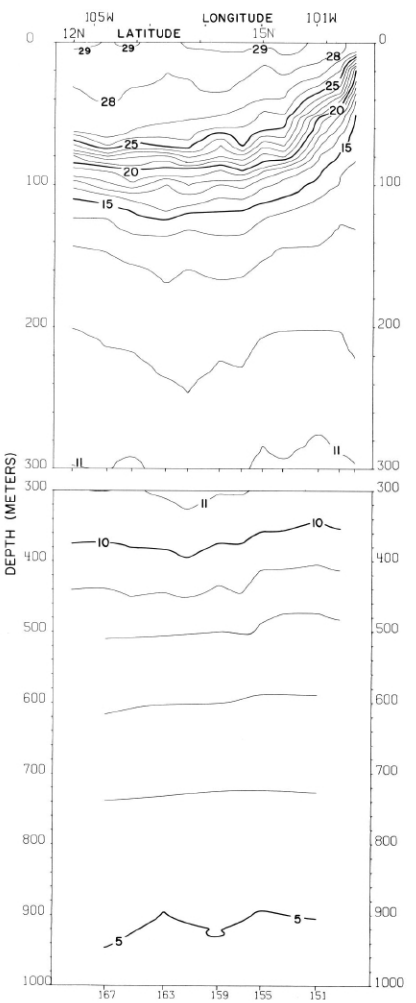

FIGURE 20-T-v4.—Vertical distribution of temperature (°C.) along a section from Acapulco to 12° N., 105°20′ W., May 7-10, 1967.

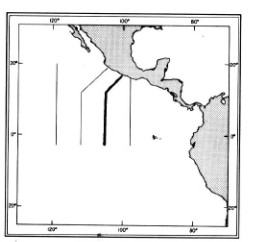

20-T-v4.

20-T-v5.

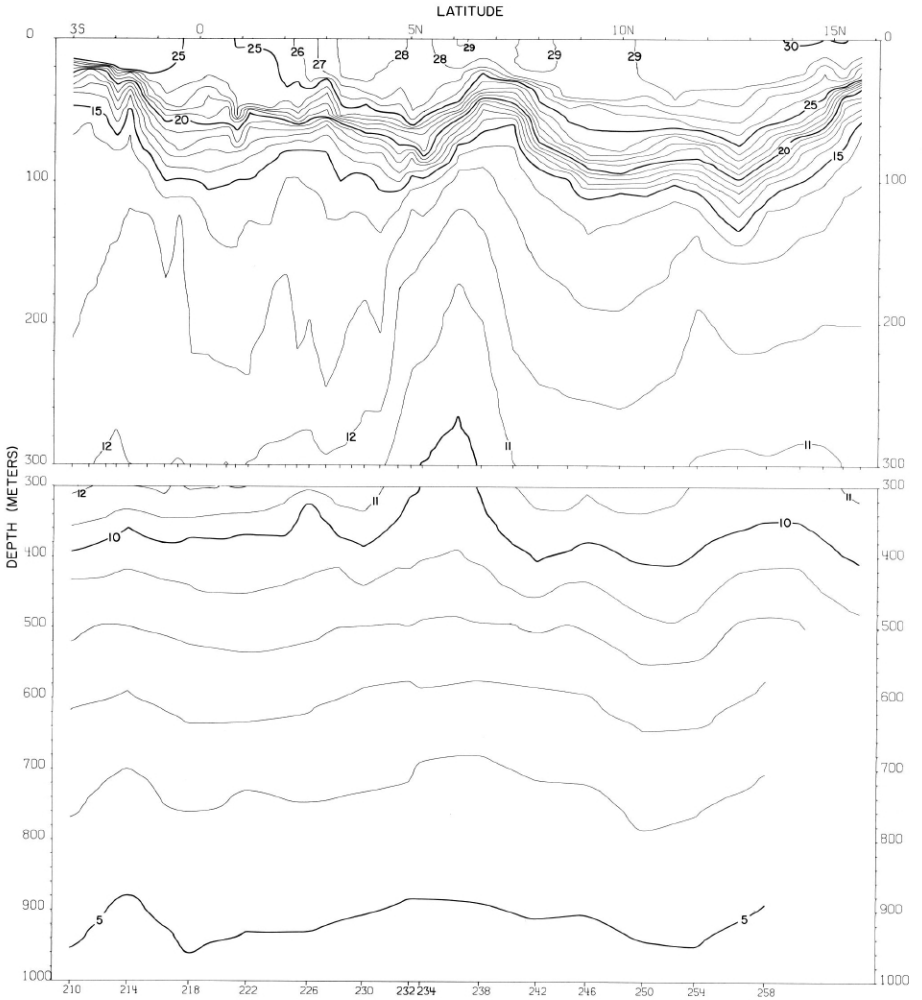

FIGURE 20-T-v6.—Vertical distribution of temperature (°C.) along 98°20′ W., May 17-24, 1967.

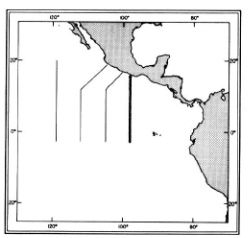

20-T-v6.

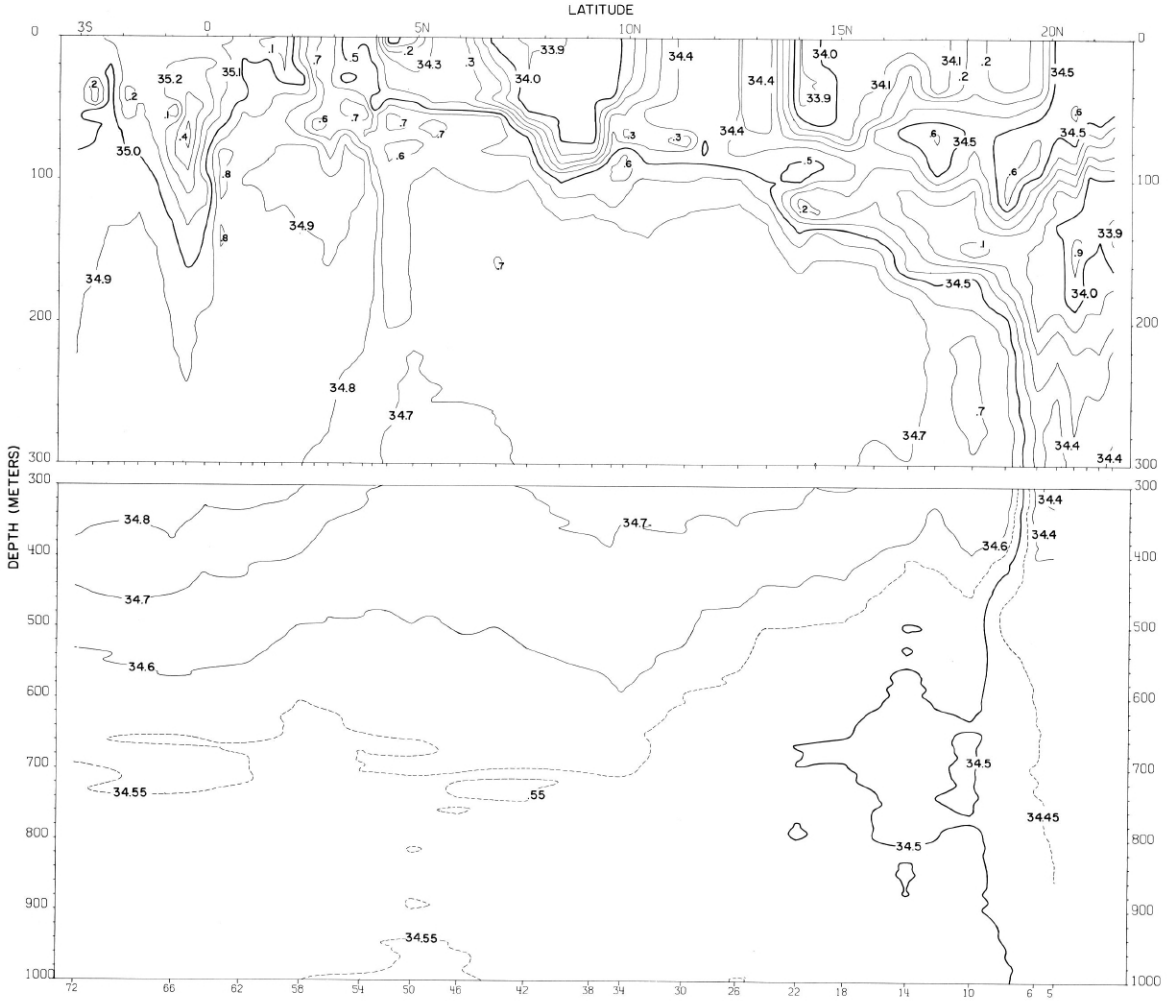

FIGURE 20-S-vl.—Vertical distribution of salinity (‰) along 119°20′ W., April 13-21, 1967.

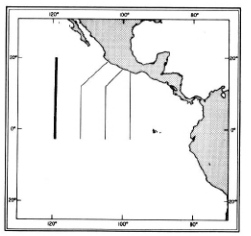

20-S-vl.

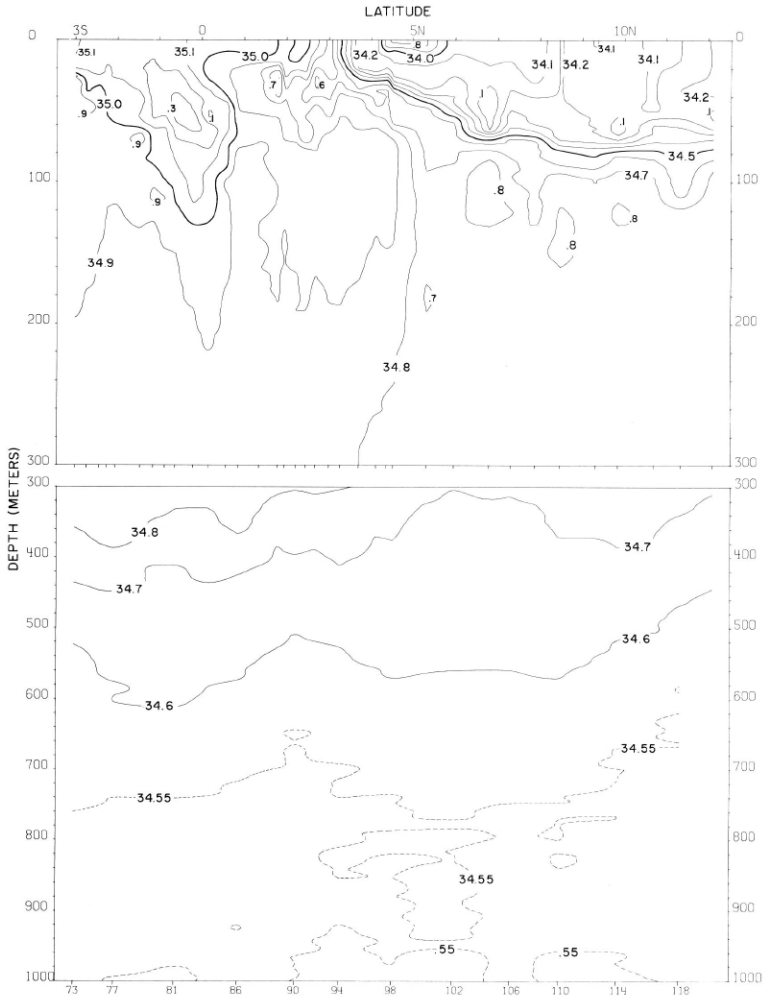

FIGURE 20-S-v2.—Vertical distribution of salinity (‰) along 112°20′ W., April 23-29, 1967.

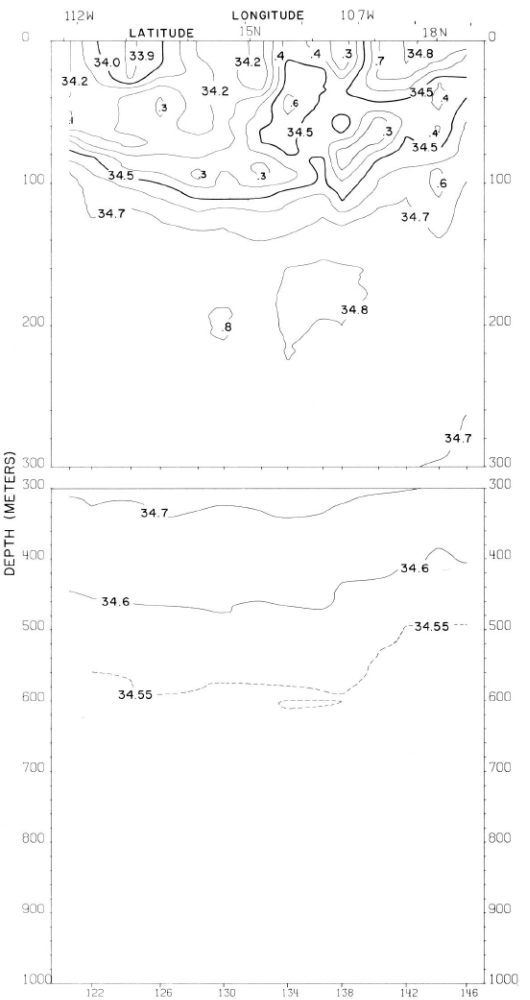

FIGURE 20-S-v3.—Vertical distribution of salinity (‰) along a section from 12° N., 112°20′ W. to Manzanillo, April 29-May 2, 1967.

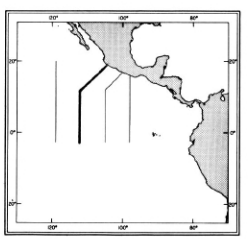

20-S-v2.

20-S-v3.

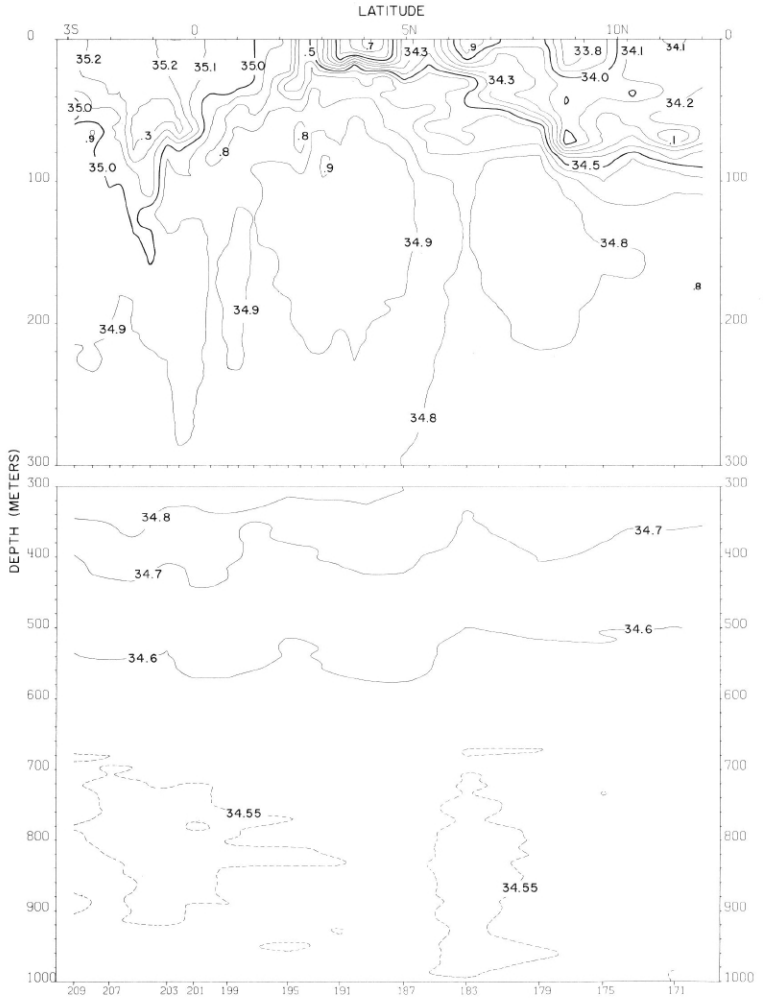

FIGURE 20-S-v5.—Vertical distribution of salinity (‰) along 105°20′ W., May 10-15, 1967.

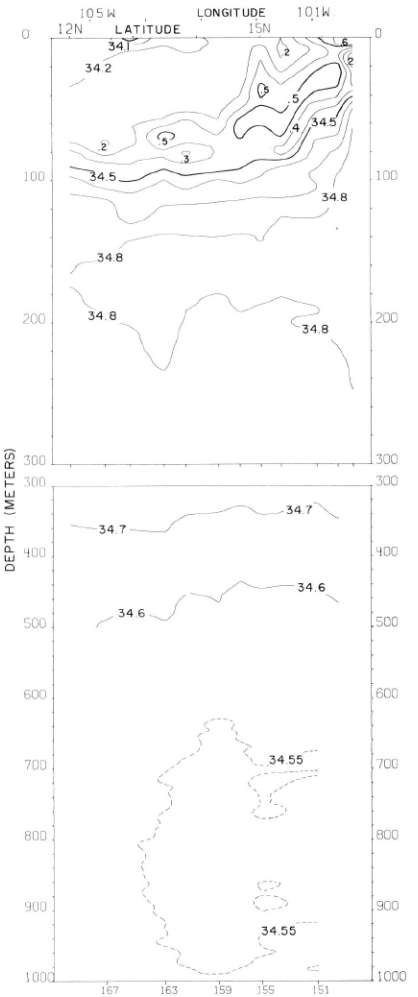

FIGURE 20-S-v4.—Vertical distribution of salinity (‰) along a section from Acapulco to 12° N., 105°20′ W., May 7-10, 1967.

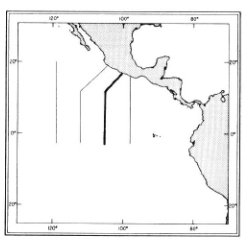

20-S-v4.

20-S-v5.

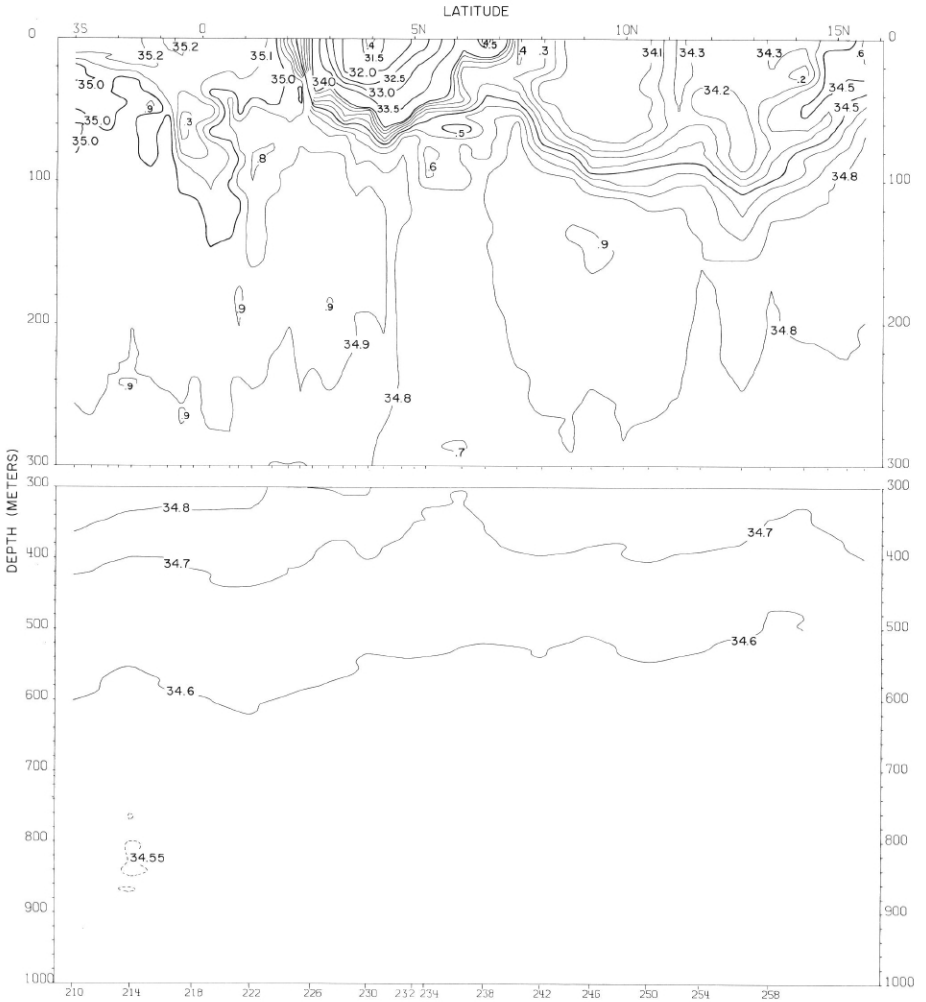

FIGURE 20-S-v6.—Vertical distribution of salinity (‰) along 98° 20′ W., May 17-24, 1967.

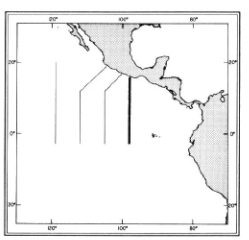

20-S-v6.

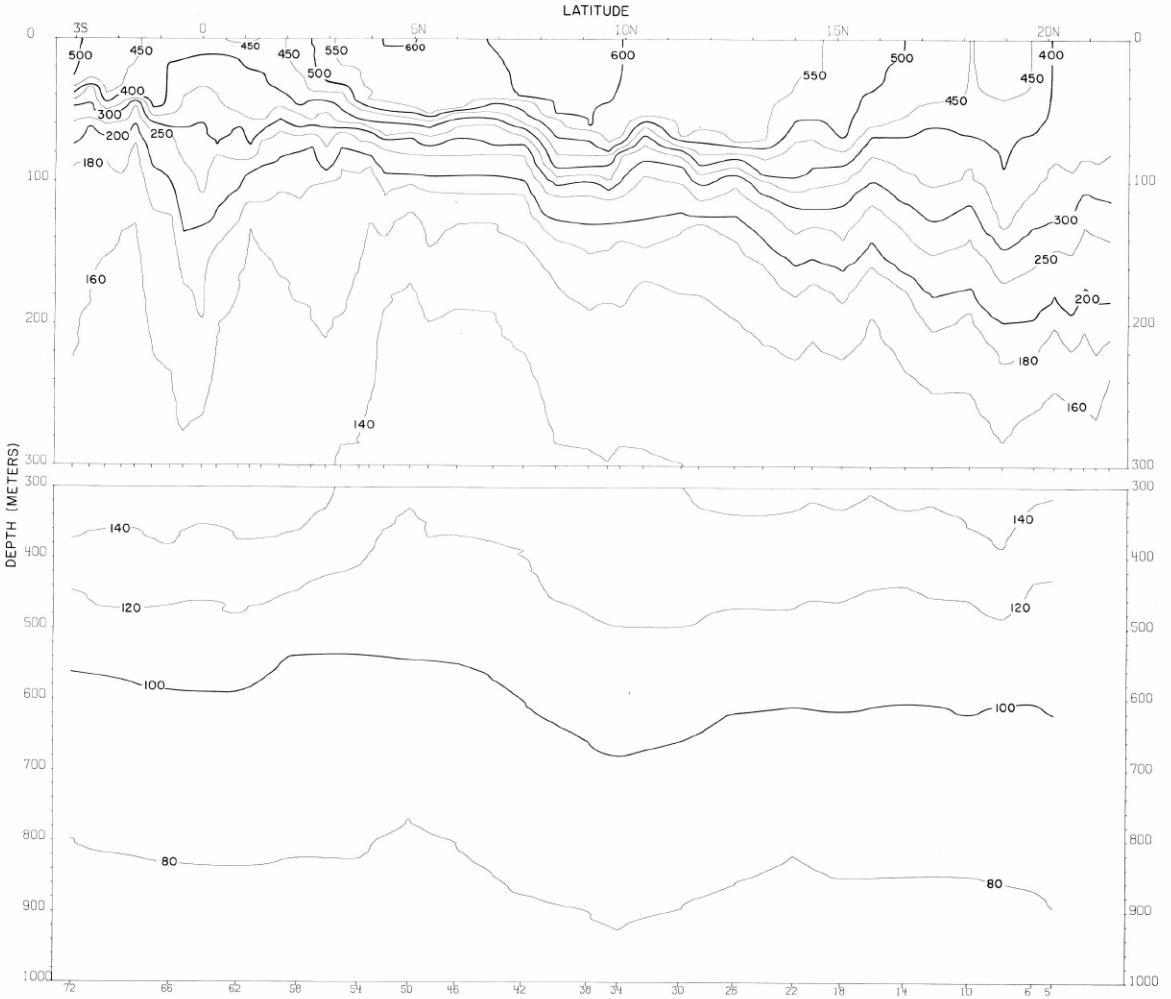

FIGURE 20-δ-vl.—Vertical distribution of thermosteric anomaly, δ_T, (cl./t.) along 119°20′ W., April 13-21, 1967.

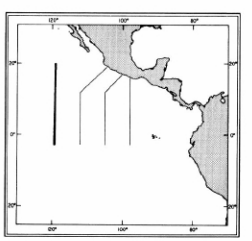

20-δ-vl.

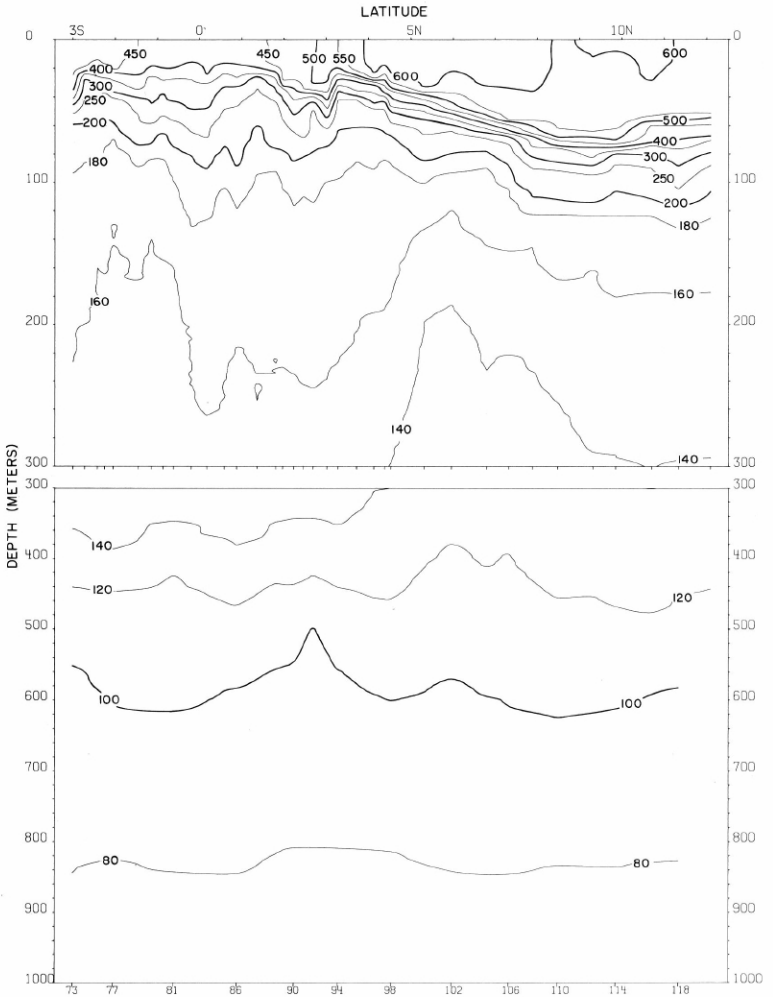

FIGURE 20-δ-v2.—Vertical distribution of thermosteric anomaly, δ_T, (cl./t.) along 112°20′ W., April 23-29, 1967.

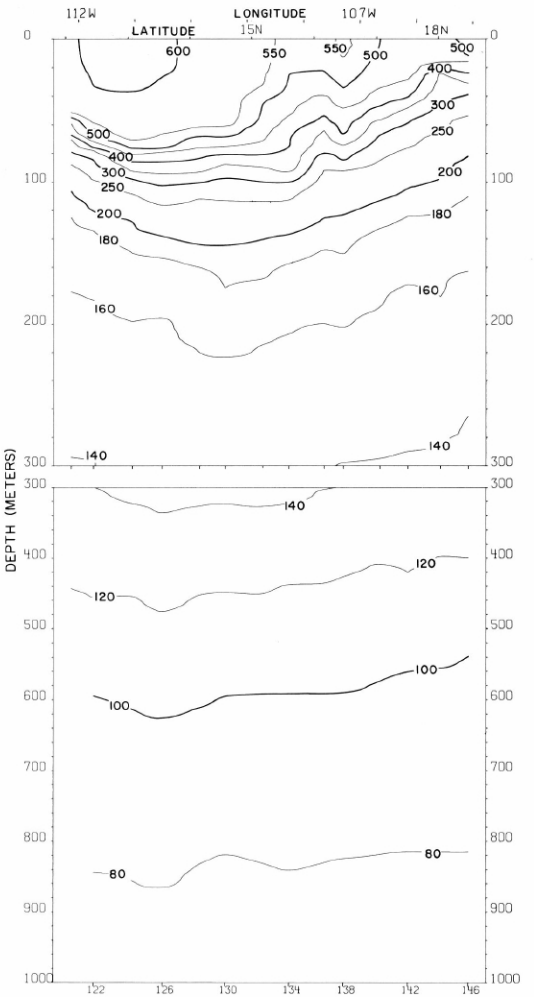

FIGURE 20-δ-v3.—Vertical distribution of thermosteric anomaly, δ_T, (cl./t.) along a section from 12° N., 112°20′ W. to Manzanillo, April 29-May 2, 1967.

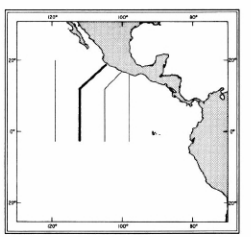

20-δ-v2.

20-δ-v3.

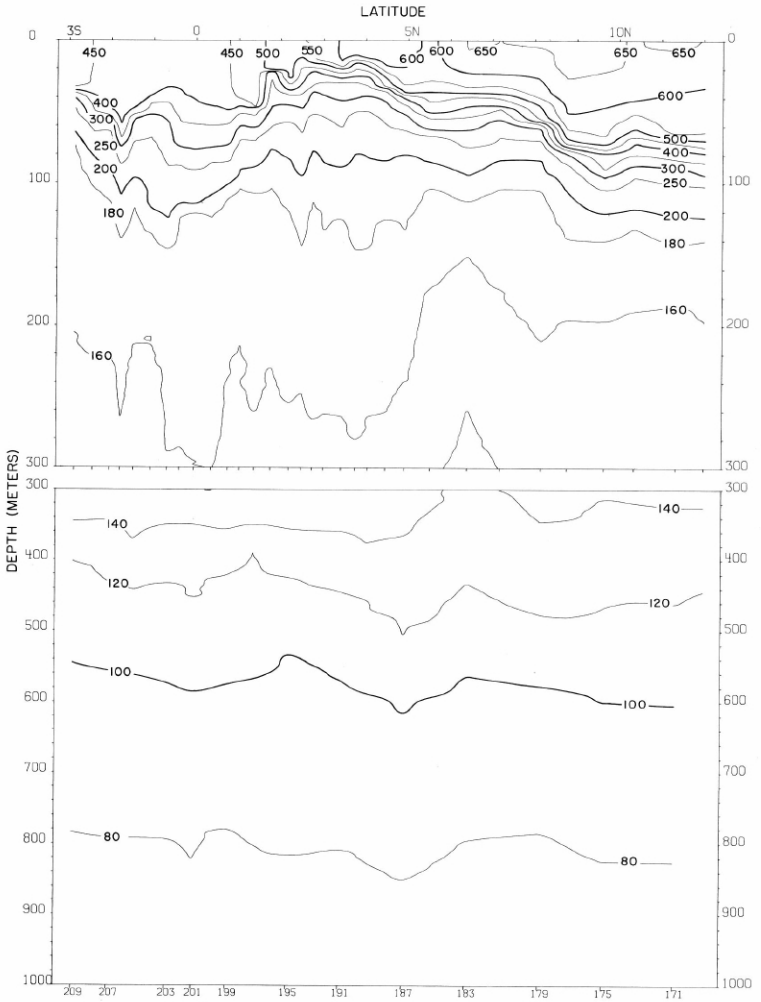

FIGURE 20-δ-v5.—Vertical distribution of thermosteric anomaly, δ_T, (cl./t.) along 105°20′ W., May 10-15, 1967.

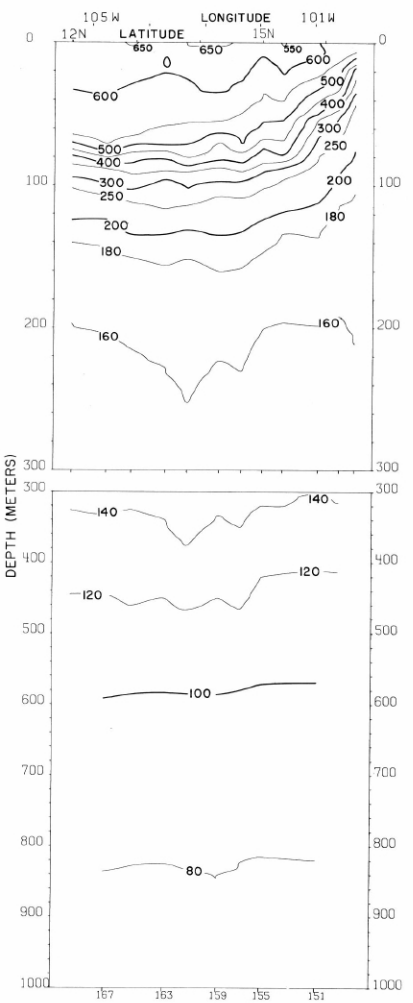

FIGURE 20-δ-v4.—Vertical distribution of thermosteric anomaly, δ_T, (cl./t.) along a section from Acapulco to 12° N., 105°20′ W., May 7-10, 1967.

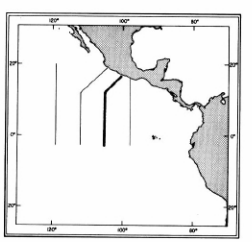

20-δ-v4.

20-δ-v5.

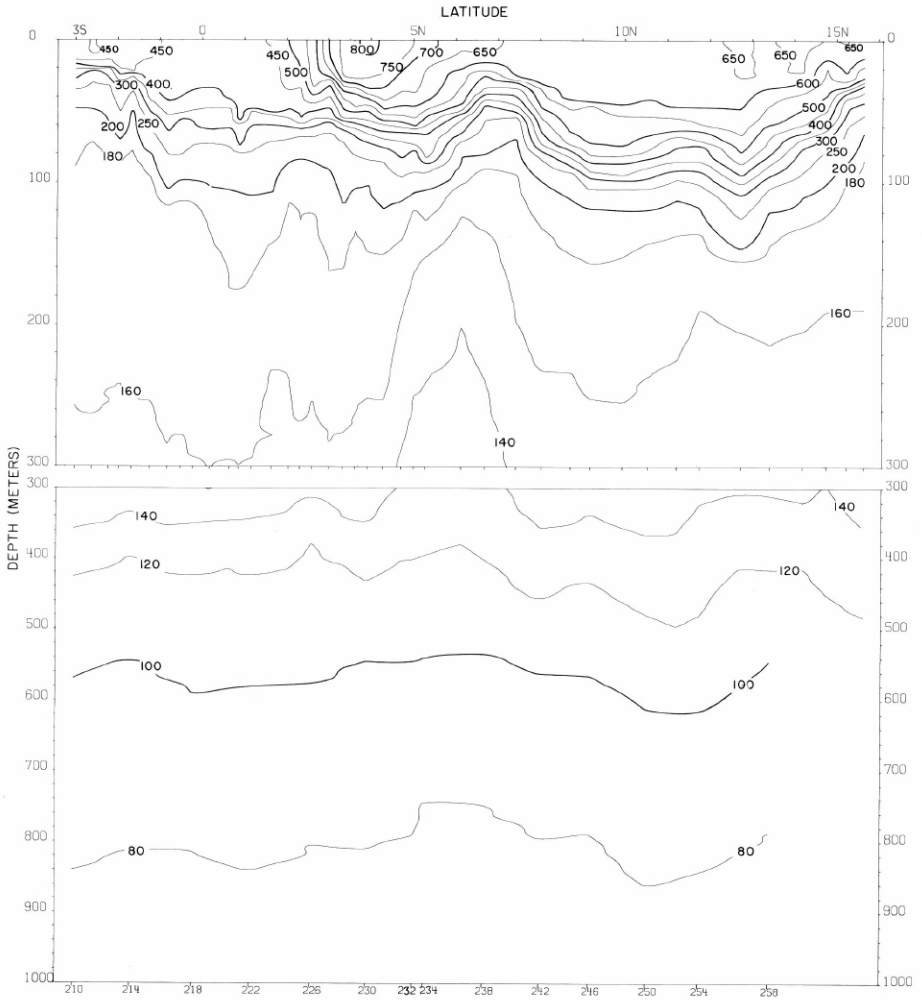

FIGURE 20-δ-v6.—Vertical distribution of thermosteric anomaly, δ_T, (cl./t.) along 98°20′ W., May 17-24, 1967.

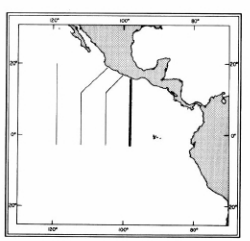

20-δ-v6.

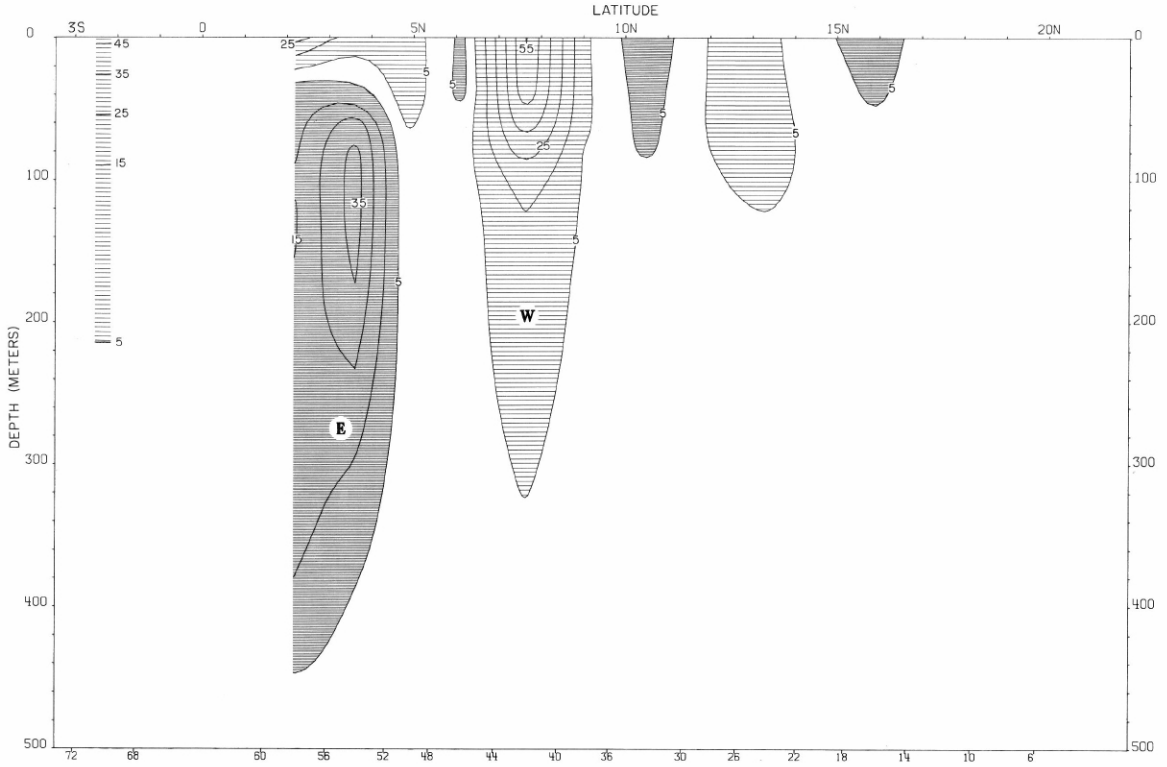

FIGURE 20-G-vl.—Vertical distribution of the zonal component of geostrophic velocity (cm./sec.), relative to 500 db., along 119°20′ W., April 13-21, 1967. Dark shading indicates eastward flow with a velocity greater than 5 cm./sec.; light shading indicates westward flow with a velocity greater than 5 cm./sec.

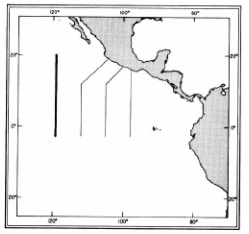

20-G-vl.

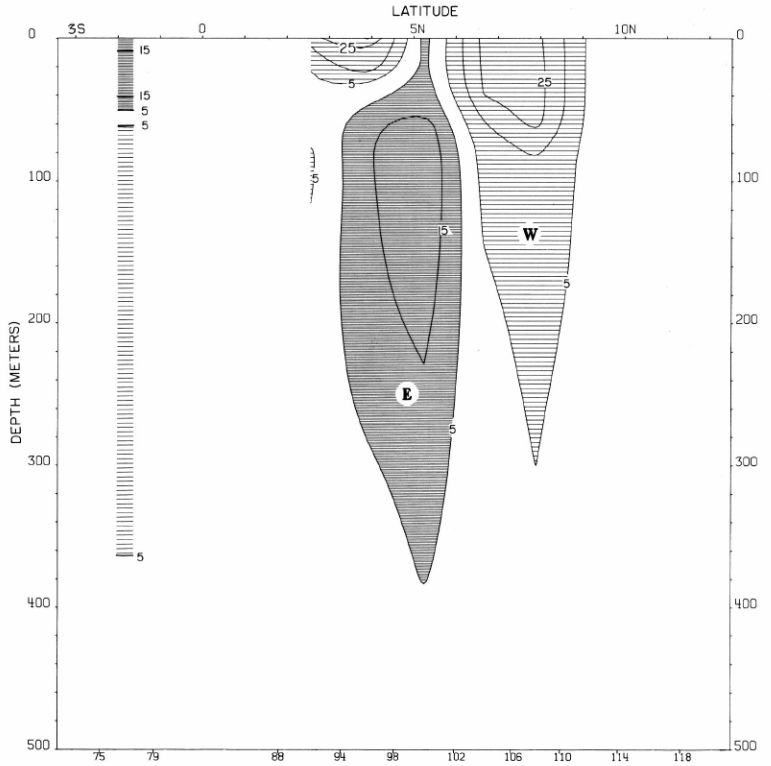

FIGURE 20-G-v2.—Vertical distribution of the zonal component of geostrophic velocity (cm./sec.), relative to 500 db., along 112°20′ W., April 24-29, 1967. Dark shading indicates eastward flow with a velocity greater than 5 cm./sec.; light shading indicates westward flow with a velocity greater than 5 cm./sec.

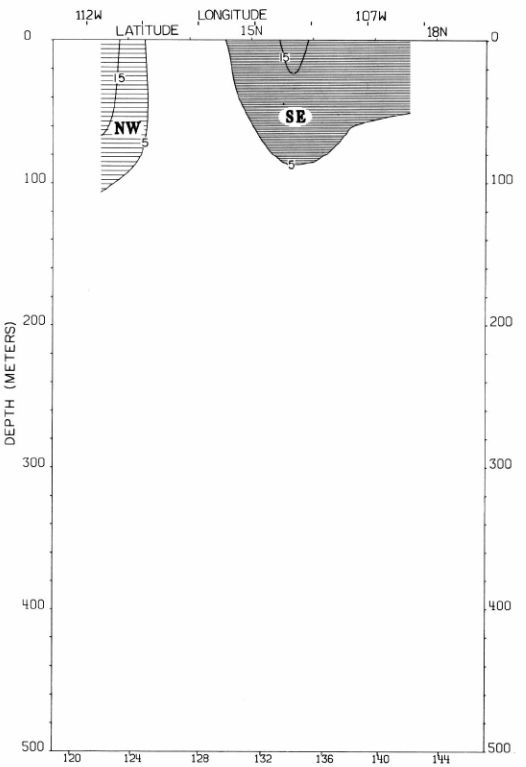

FIGURE 20-G-v3.—Vertical distribution of the component of geostrophic velocity (cm./sec.), relative to 500 db., normal to a section from 12° N., 112°20′ W., to Manzanillo, April 29-May 2, 1967. Dark shading indicates flow toward the southeast with a velocity greater than 5 cm./sec.; light shading indicates flow toward the northwest with a velocity greater than 5 cm./sec.

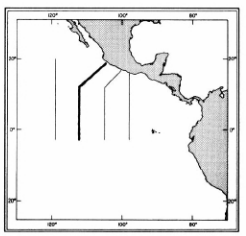

20-G-v2.

20-G-v3.

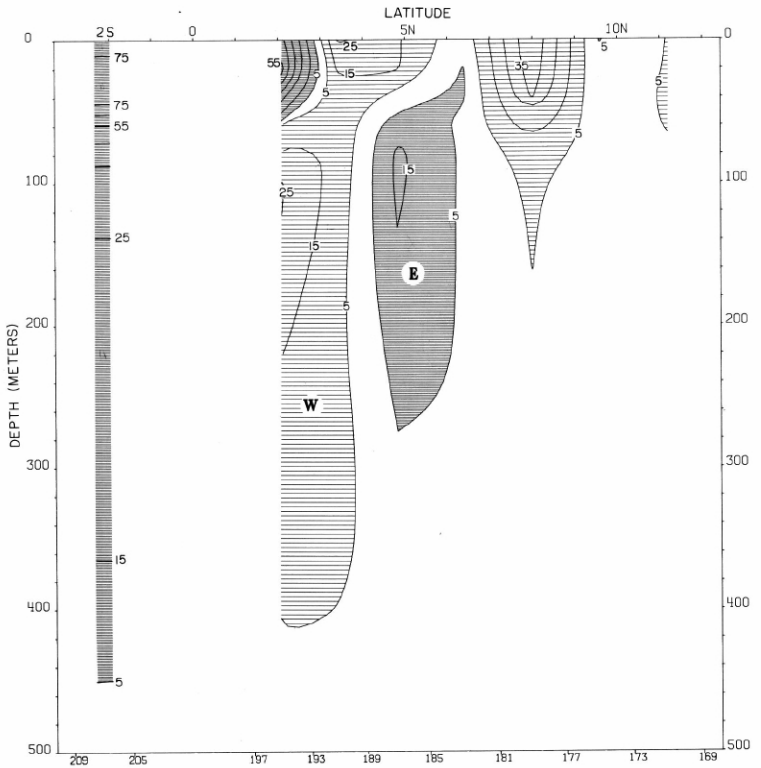

FIGURE 20-G-v5.—Vertical distribution of the zonal component of geostrophic velocity (cm./sec.), relative to 500 db., along 105°20′ W., May 10-15, 1967. Dark shading indicates eastward flow with a velocity greater than 5 cm./sec.; light shading indicates westward flow with a velocity greater than 5 cm./sec.

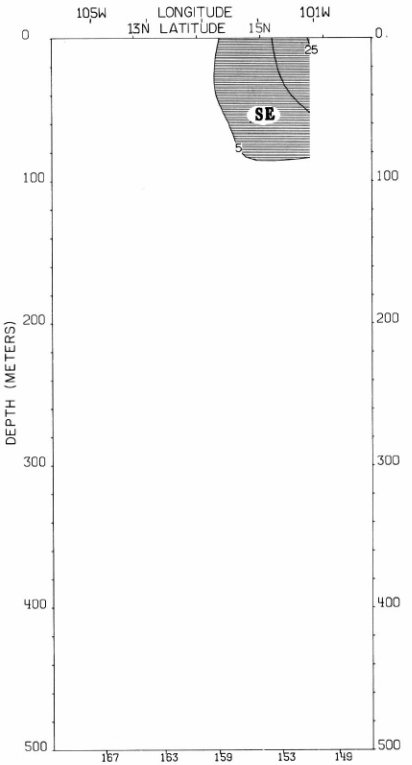

FIGURE 20-G-v4.—Vertical distribution of the component of geostrophic velocity (cm./sec.), relative to 500 db., normal to a section from Acapulco to 12° N., 105°20′ W., May 7-10, 1967. The dark shading indicates flow toward the southeast with a velocity greater than 5 cm./sec.

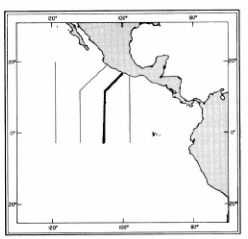

20-G-v4.

20-G-v5.

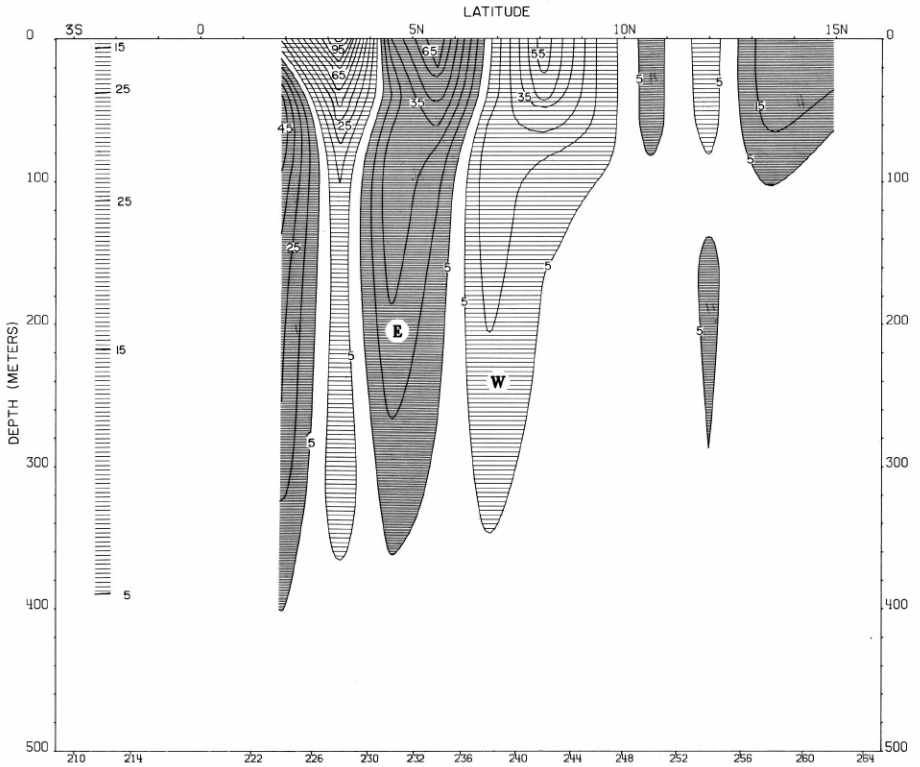

FIGURE 20-G-v6.—Vertical distribution of the zonal component of geostrophic velocity (cm./sec.), relative to 500 db., along 98°20′ W., May 17-24, 1967. Dark shading indicates eastward flow with a velocity greater than 5 cm./sec.; light shading indicates westward flow with a velocity greater than 5 cm./sec.

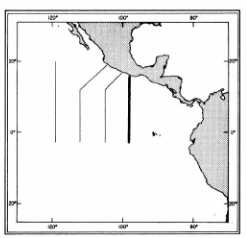

20-G-v6.

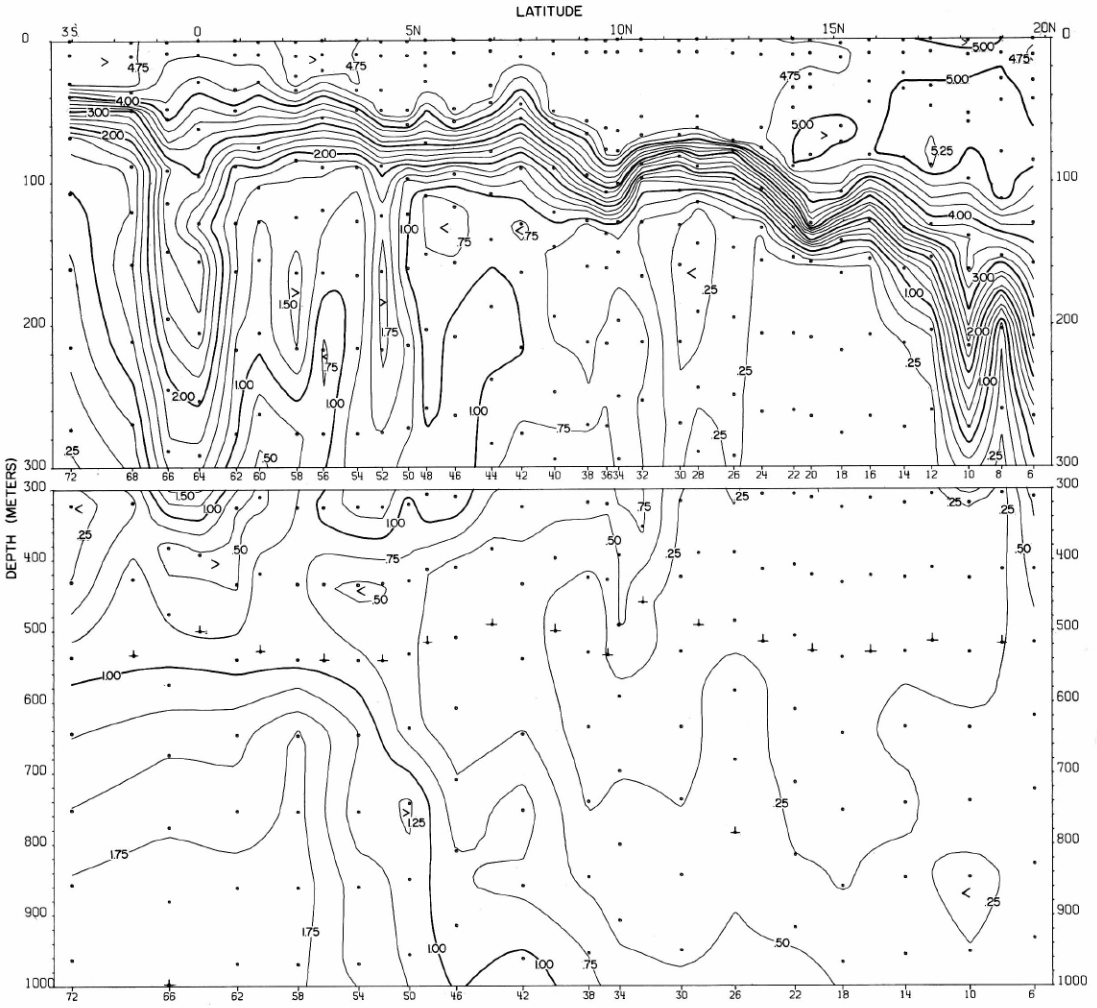

FIGURE 20-O2-v1.—Vertical distribution of oxygen (ml./l.) along 119°20′ W., April 13-21, 1967.

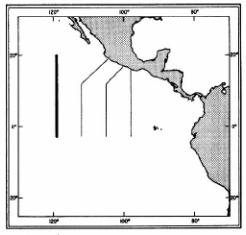

20-O2-v1.

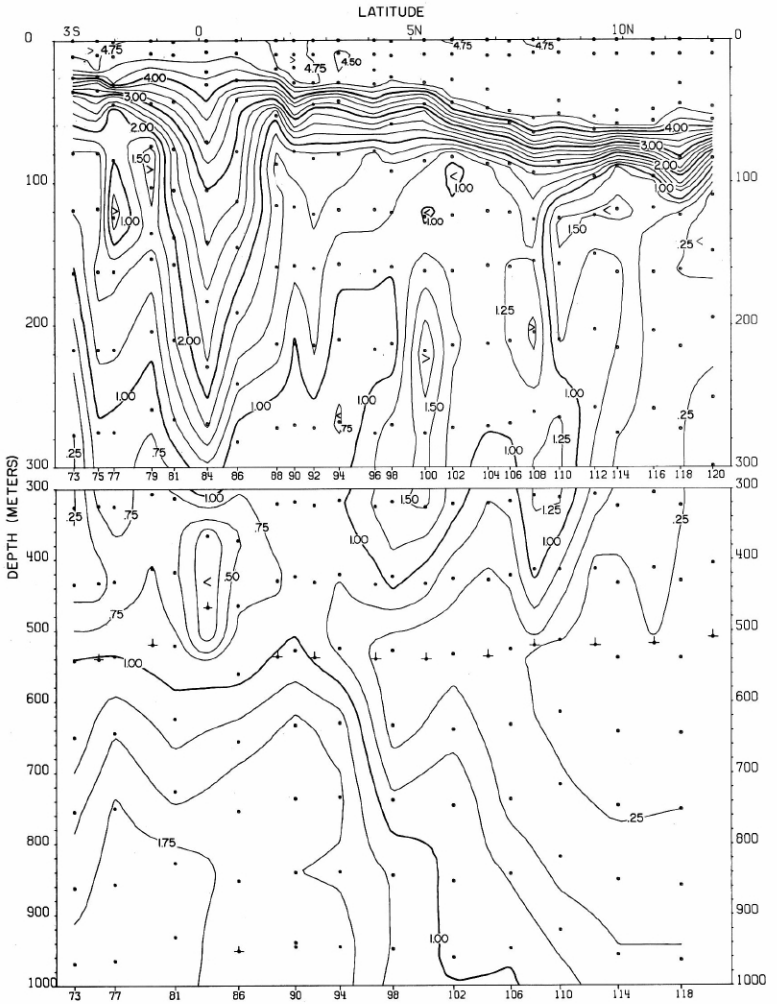

FIGURE 20-O₂-v2.—Vertical distribution of oxygen (ml./l.) along 112°20′ W., April 23-29, 1967.

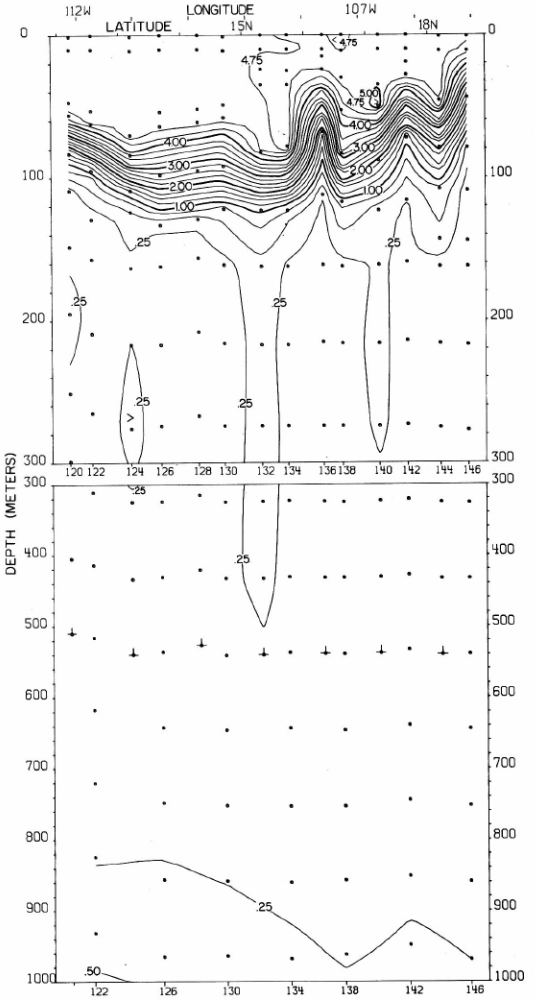

FIGURE 20-O₂-v3.—Vertical distribution of oxygen (ml./l.) along a section from 12° N., 112°20′ W. to Manzanillo, April 29-May 2, 1967.

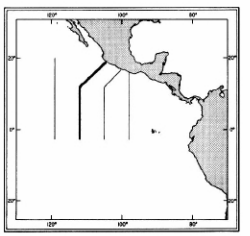

20-O₂-v2.

20-O₂-v3.

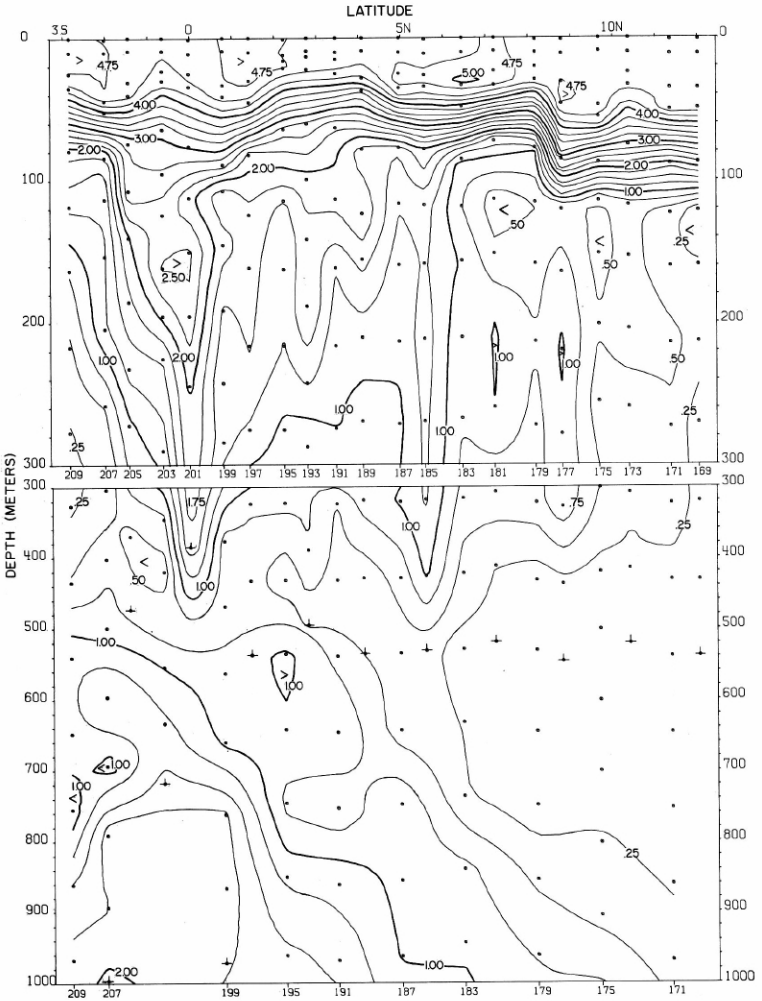

FIGURE 20-O2-v5.—Vertical distribution of oxygen (ml./l.) along 105°20′ W., May 10-15, 1967.

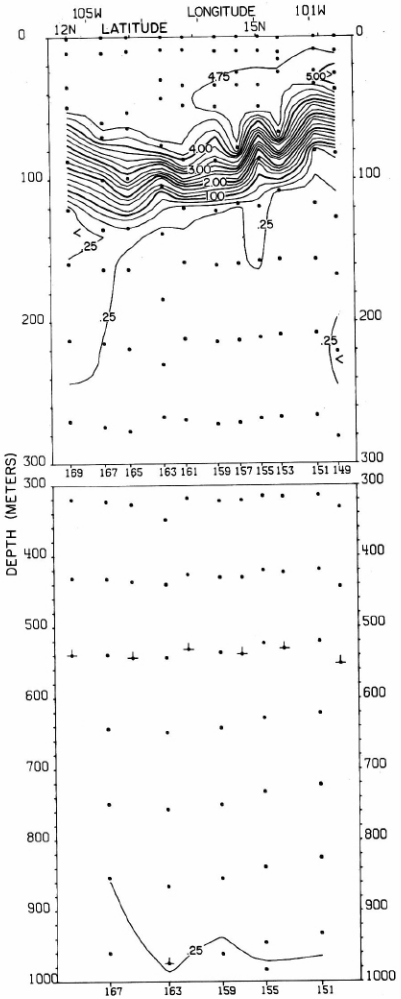

FIGURE 20-O2-v4.—Vertical distribution of oxygen (ml./l.) along a section from Acapulco to 12° N., 105°20′ W., May 7-10, 1967.

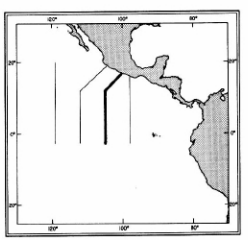

20-O2-v4.

20-O2-v5.

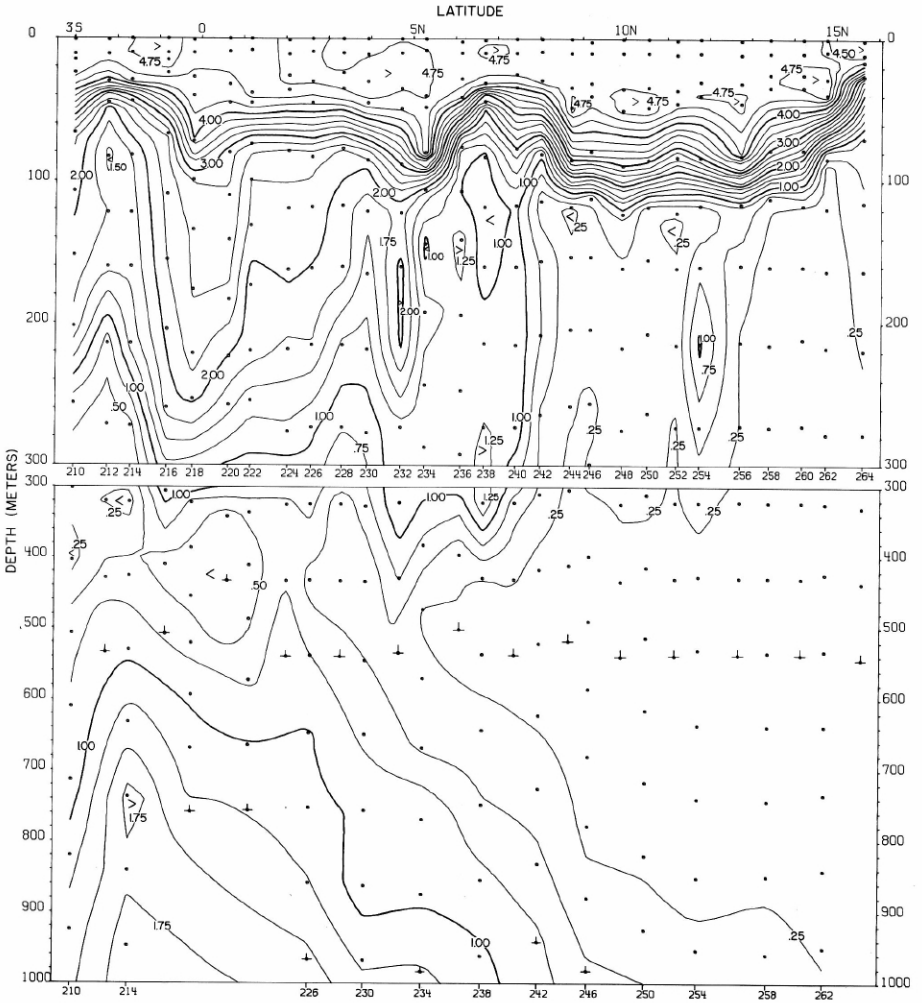

FIGURE 20-O₂-v6.—Vertical distribution of oxygen (ml./l.) along 98°20′ W., May 17-24, 1967.

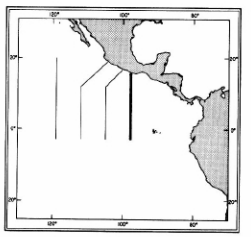

20-O₂-v6.

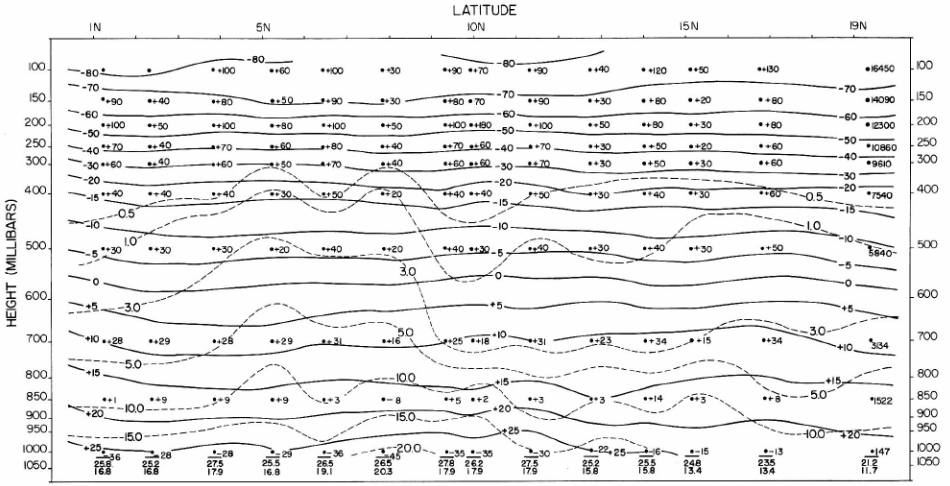

FIGURE 20-UA-vl.—Vertical section of the atmosphere along 119°20′ W., April 14-20, 1967. Solid lines are isotherms of air temperature (°C.). Dashed lines are isopleths of mixing ratio of the air (g./kg.). Surface air temperature is plotted above surface mixing ratio and below a base line representing the surface pressure (mb.). The computed height (m.) of each standard pressure surface is plotted for the northernmost radiosonde station of the section. At other stations the difference of computed height minus the corresponding height at the northern station is shown at each standard level.

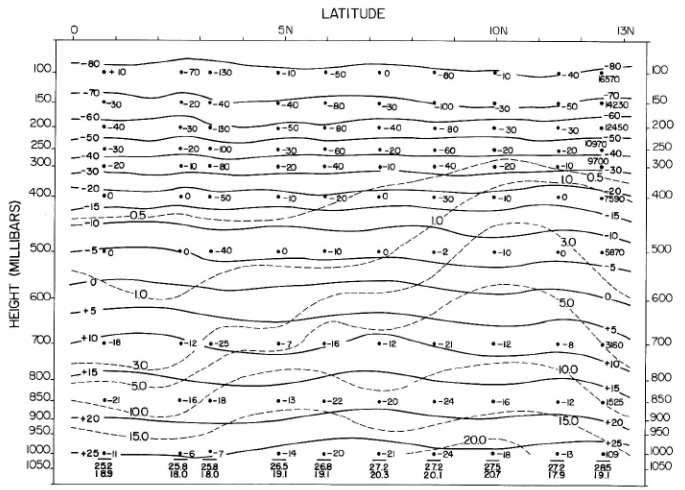

FIGURE 20-UA-v2.—Vertical section of the atmosphere along 112°20′ W., April 24-29, 1967. Solid lines are isotherms of air temperature (°C.). Dashed lines are isopleths of mixing ratio of the air (g./kg.). Surface air temperature is plotted above surface mixing ratio and below a base line representing the surface pressure (mb.). The computed height (m.) of each standard pressure surface is plotted for the northernmost radiosonde station of the section. At other stations the difference of computed height minus the corresponding height at the northern station is shown at each standard level.

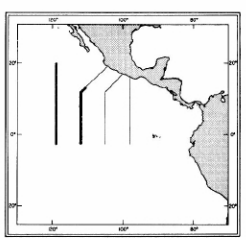

20-UA-vl.

20-UA-v2.

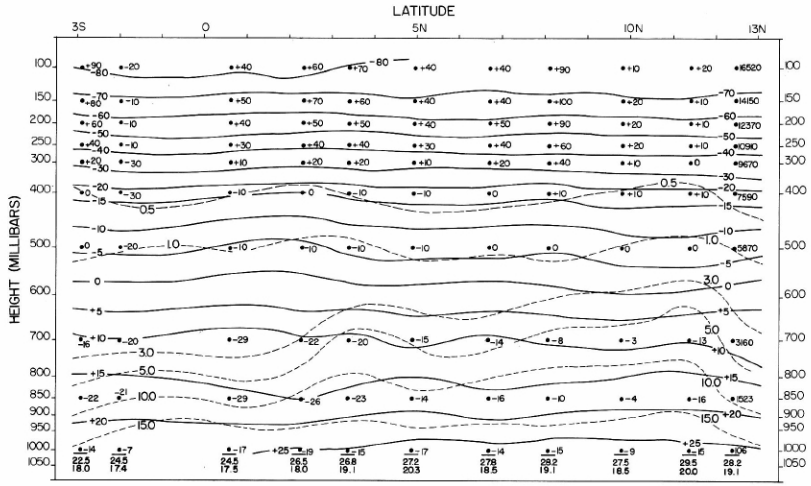

FIGURE 20-UA-v5.—Vertical section of the atmosphere along 105°20′ W., May 9-16, 1967. Solid lines are isotherms of air temperature (°C.). Dashed lines are isopleths of mixing ratio of the air (g./kg.). Surface air temperature is plotted above surface mixing ratio and below a base line representing the surface pressure (mb.). The computed height (m.) of each standard pressure surface is plotted for the northernmost radiosonde station of the section. At other stations the difference of computed height minus the corresponding height at the northern station is shown at each standard level.

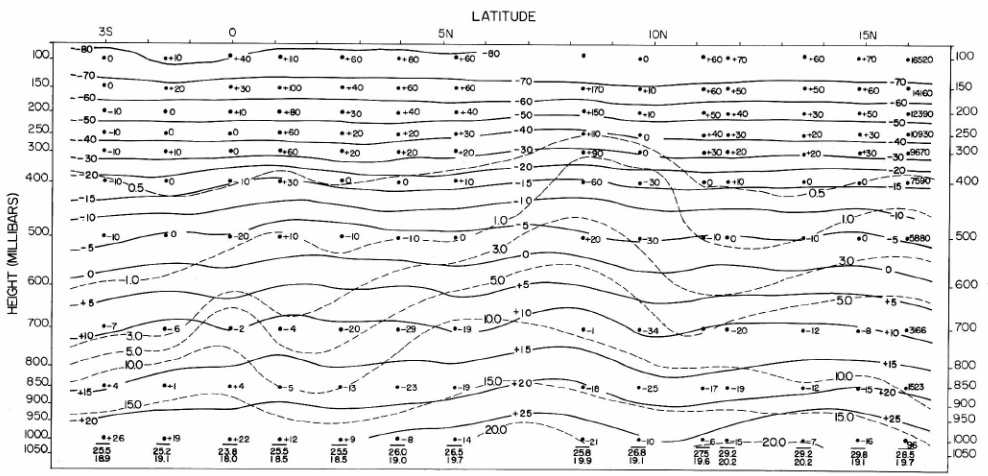

FIGURE 20-UA-v6.—Vertical section of the atmosphere along 98°20′ W., May 17-24, 1967. Solid lines are isotherms of air temperature (°C.). Dashed lines are isopleths of mixing ratio of the air (g./kg.). Surface air temperature is plotted above surface mixing ratio and below a base line representing the surface pressure (mb.). The computed height (m.) of each standard pressure surface is plotted for the northernmost radiosonde station of the section. At other stations the difference of computed height minus the corresponding height at the northern station is shown at each standard level.

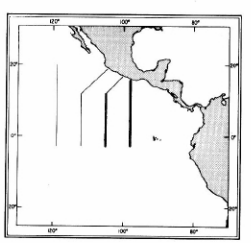

20-UA-v5.

20-UA-v6.

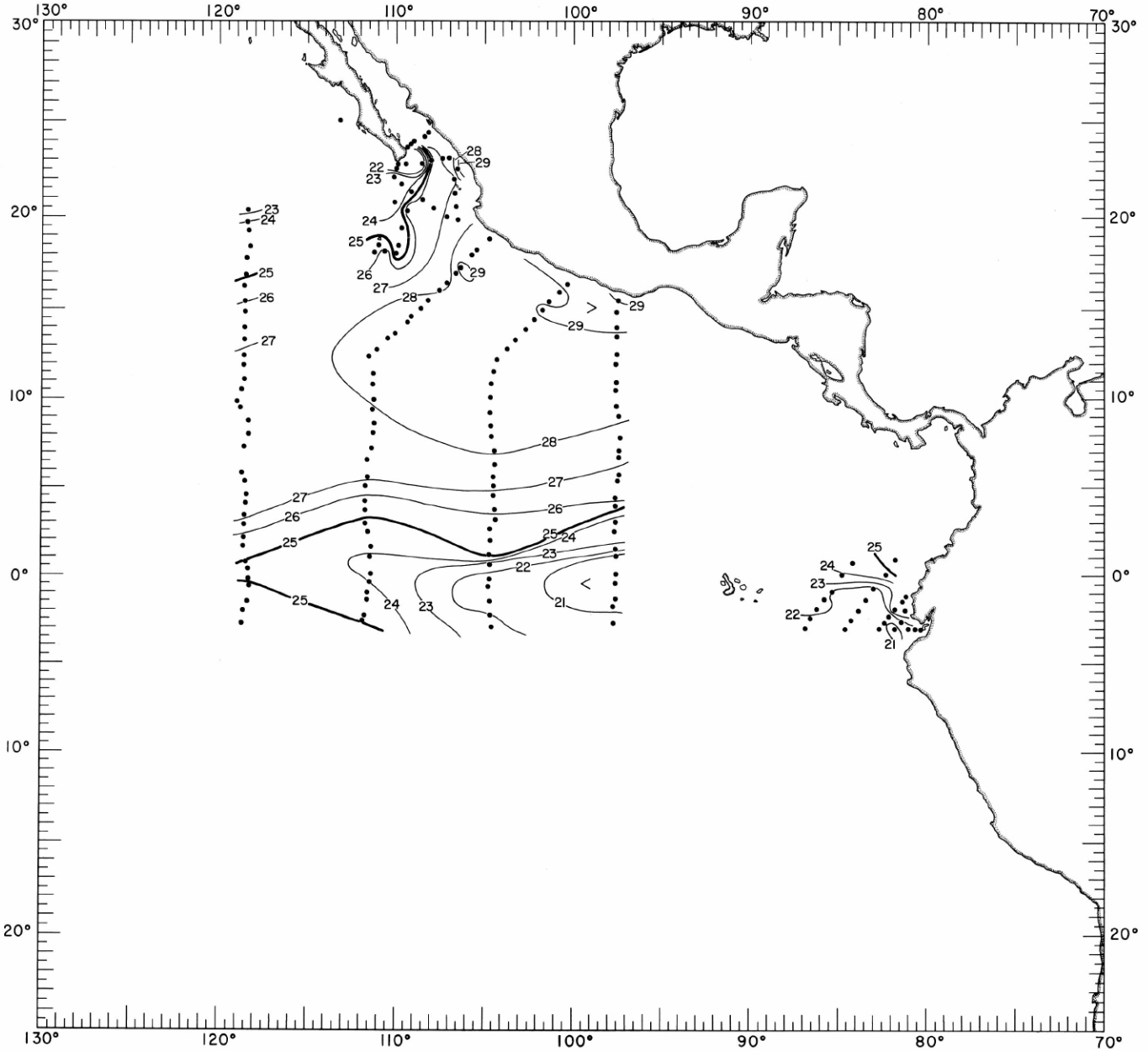

30-T-s.

FIGURE 30-T-s. — Temperature (°C.) at the sea surface, June-July 1967. These contours are based on Nansen cast data.

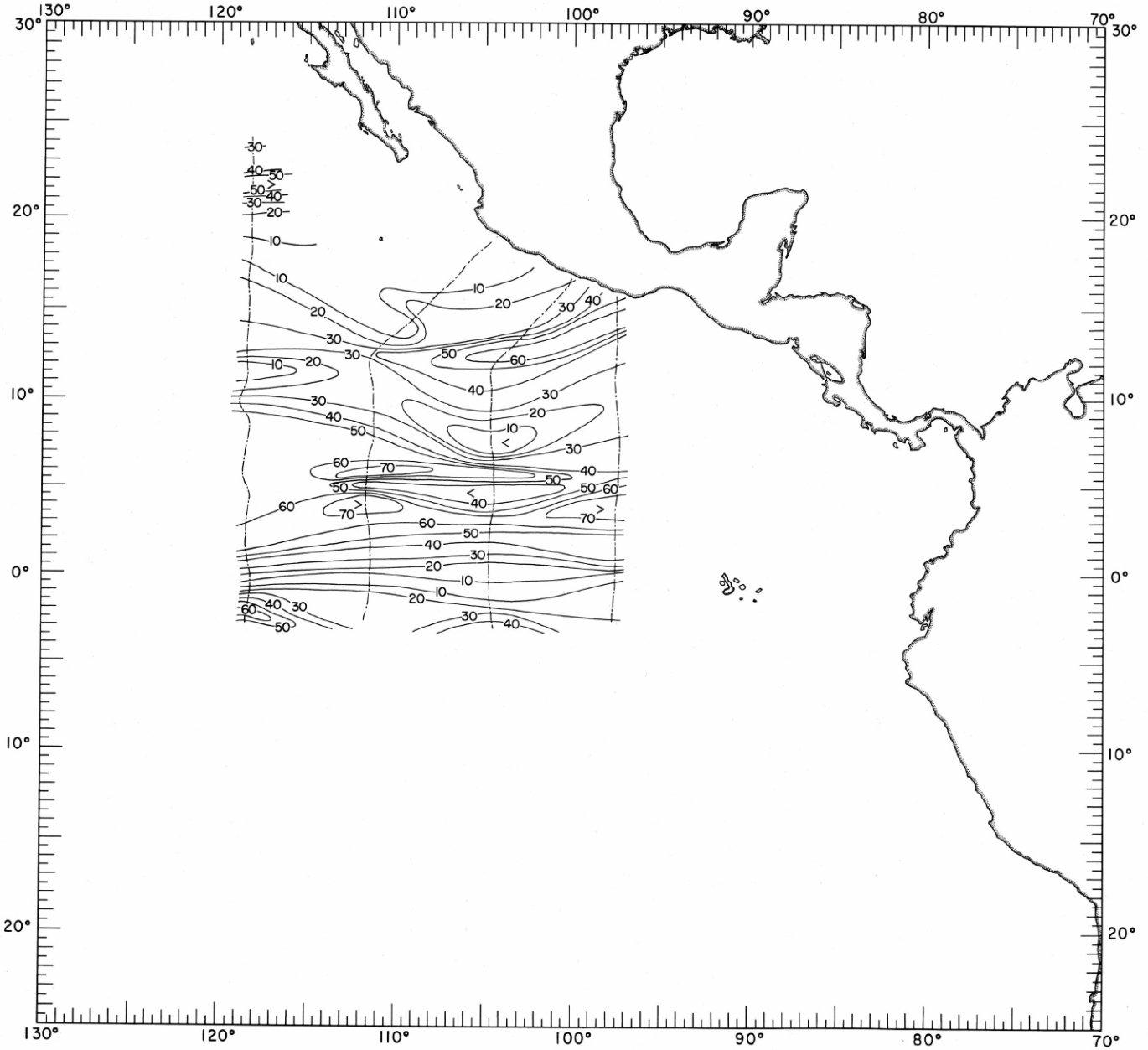

30-ML.

FIGURE 30-ML. — Thickness of the mixed layer in meters, June-July 1967. Dashed lines indicate portions of the cruise track where such data were collected.

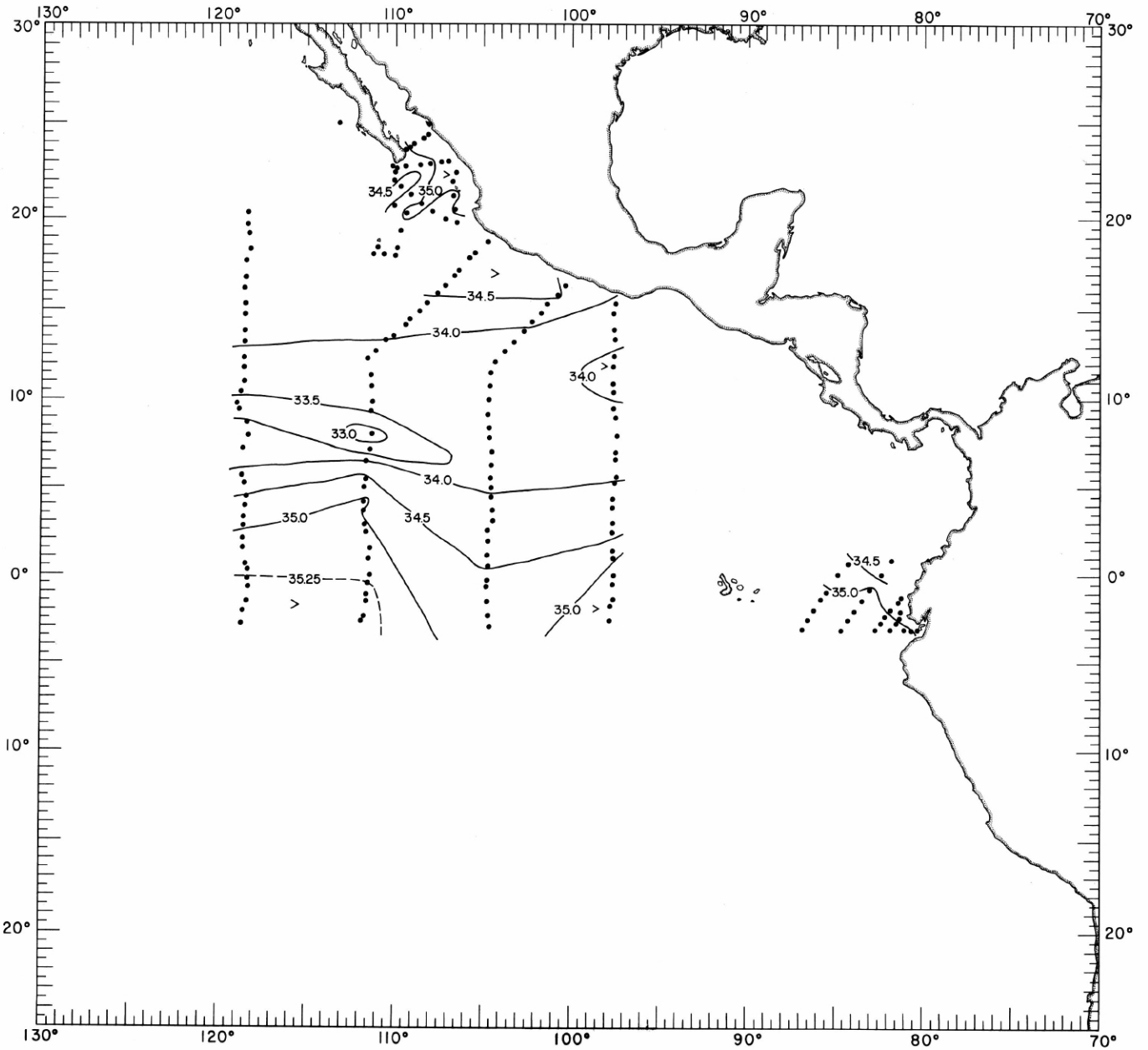

FIGURE 30-S-s.—Salinity (‰) at the sea surface, June-July 1967. These contours are based on Nansen cast data.

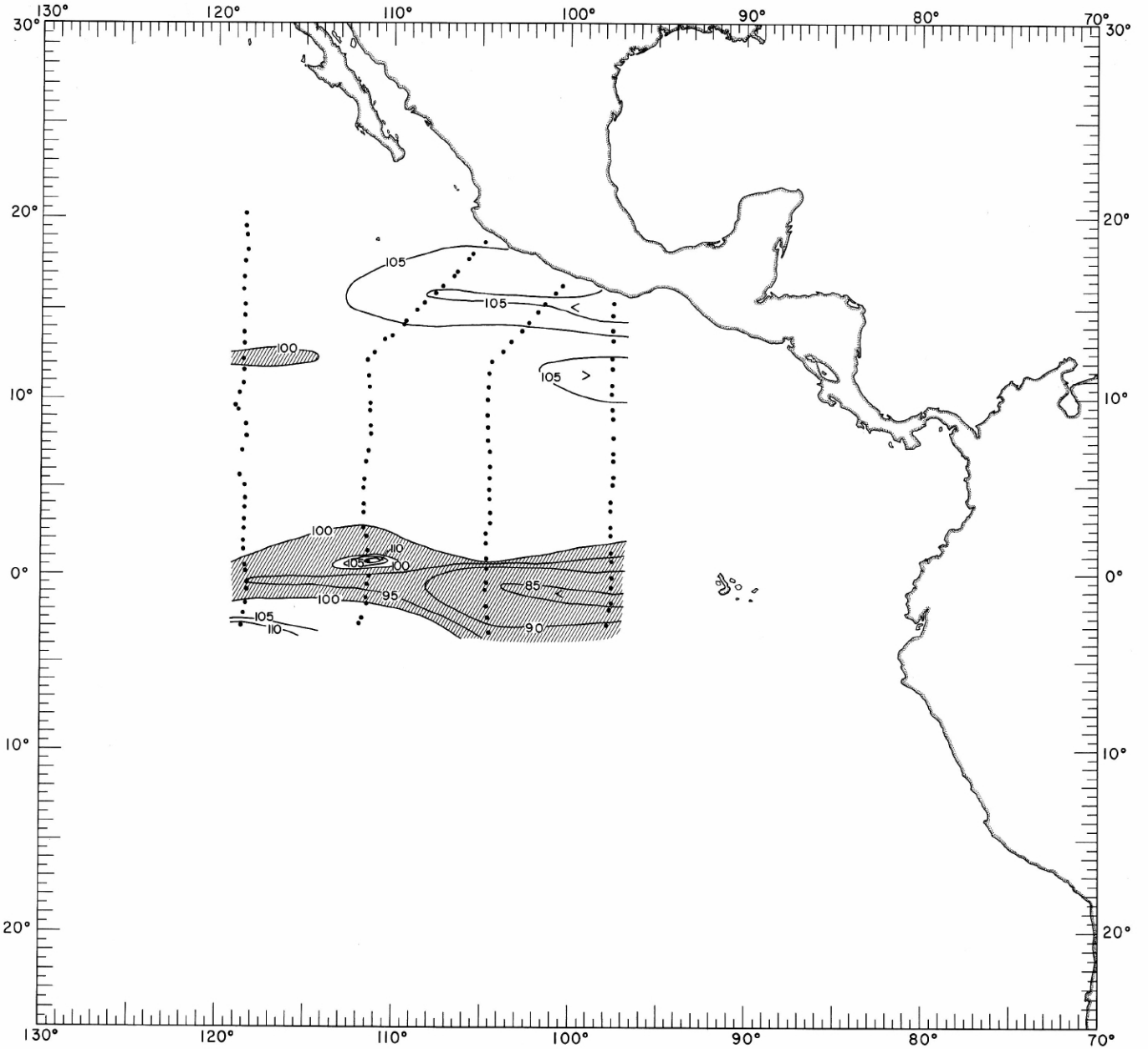

FIGURE 30-O_2Sa-10. — Oxygen saturation (%) at 10 meters, June-July 1967. Areas with less than 100% saturation are shaded.

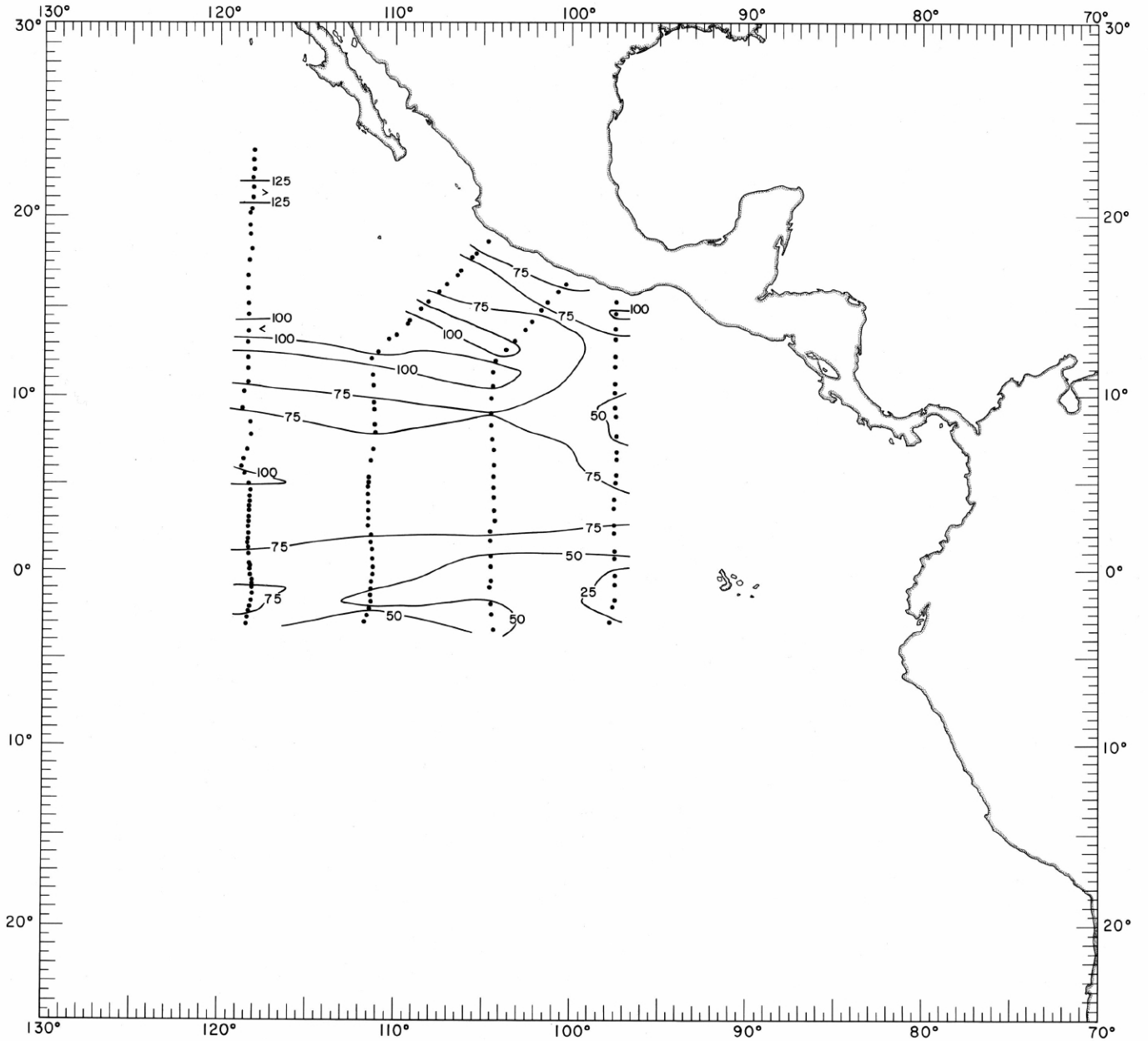

FIGURE 30-δ300-z.—Depth (m.) of the surface where $\delta_T = 300$ cl./t., June-July 1967.

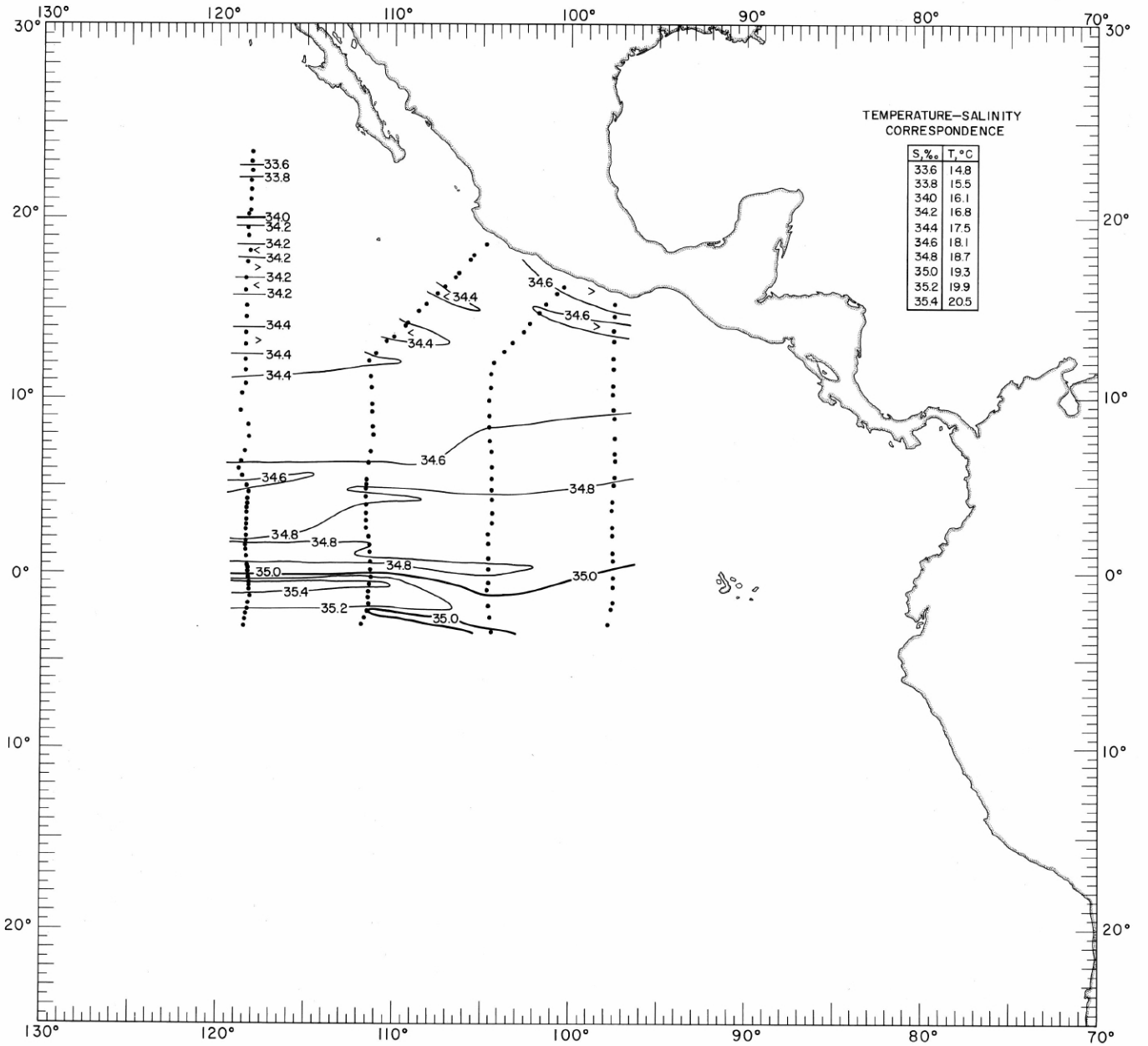

FIGURE 30-S-δ300.—Salinity (‰) on the surface where $\delta_r = 300$ cl./t., June-July 1967. The table shows the temperature corresponding to each isohaline on the chart.

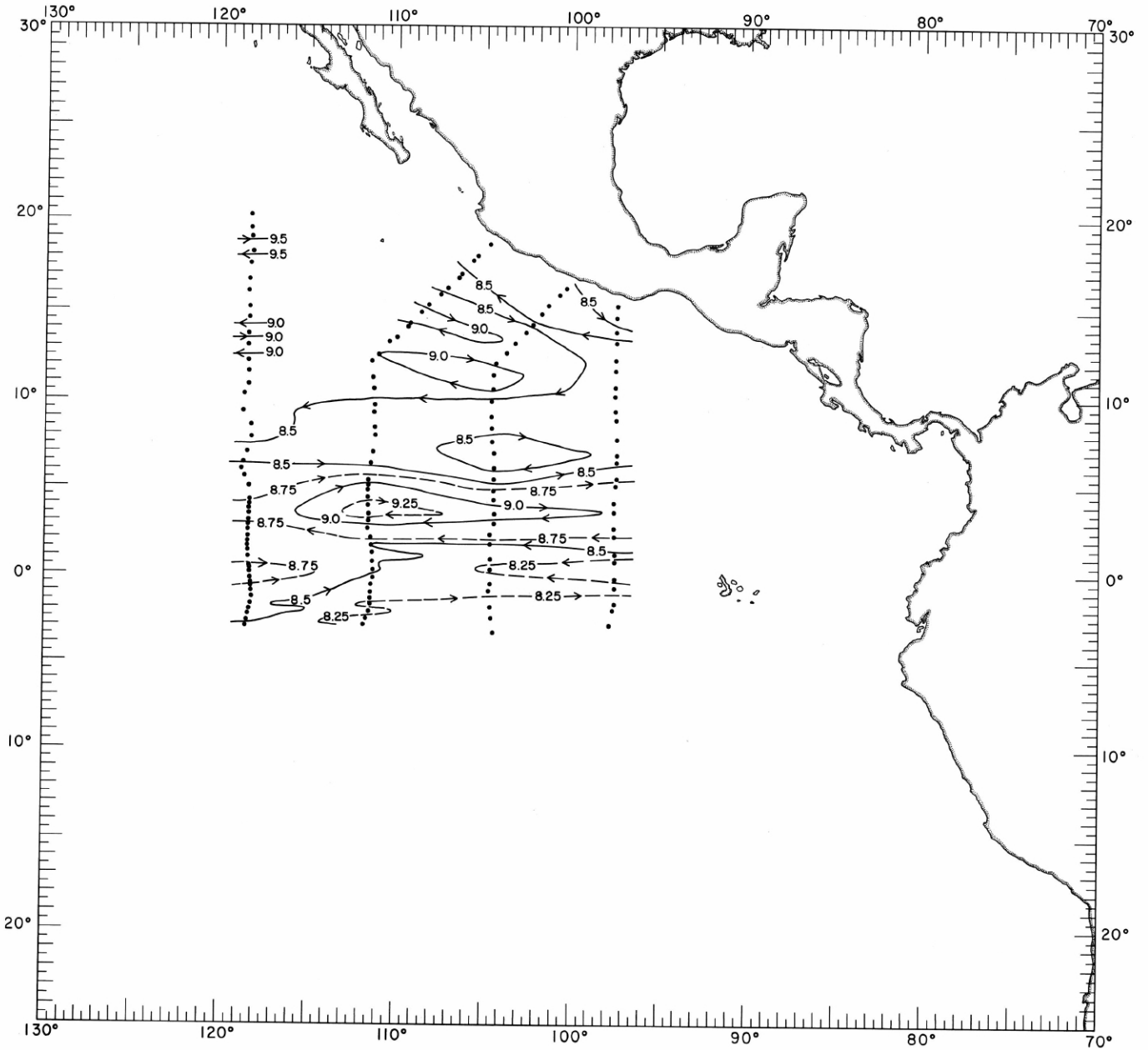

FIGURE 30-AP-δ300.—Acceleration potential (j./kg.), relative to 500 db., on the surface where δ_T = 300 cl./t., June-July 1967. For computing acceleration potential, thermosteric anomaly, δ_T, was used instead of specific volume anomaly, δ.

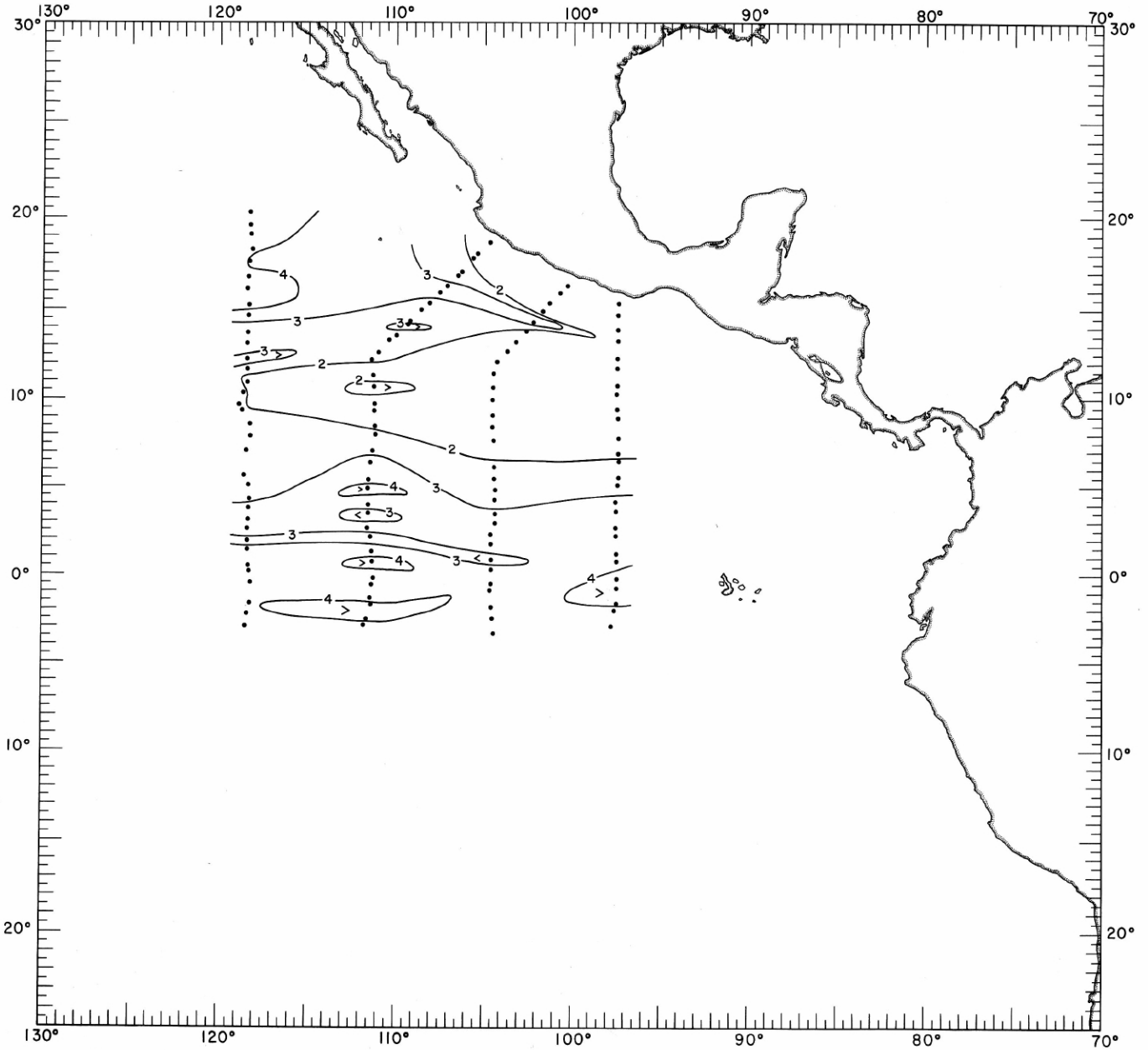

FIGURE 30-O_2-δ300.—Oxygen (ml./l.) on the surface where $\delta_r = 300$ cl./t., June-July 1967.

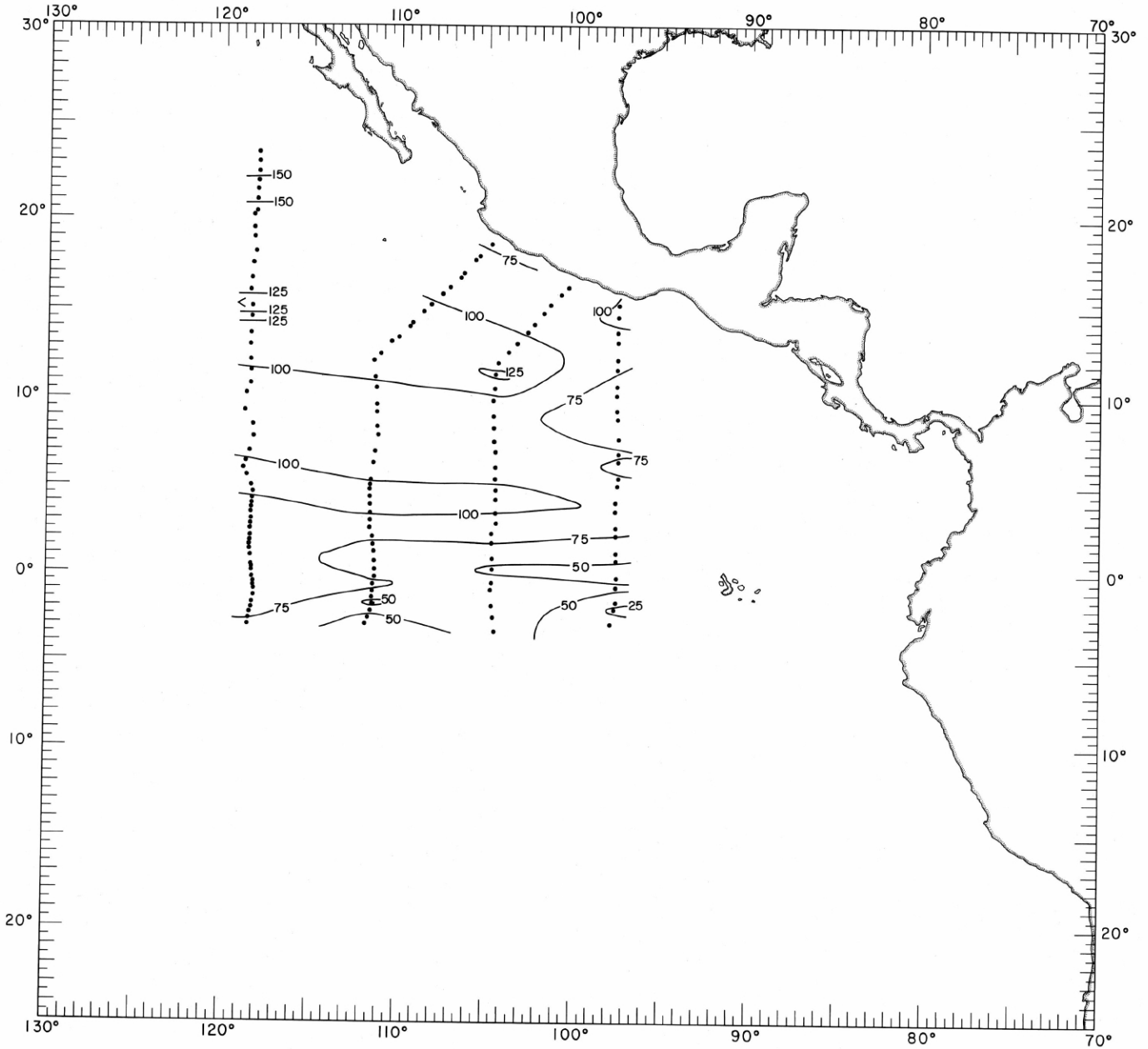

FIGURE 30-δ250-z.—Depth (m.) of the surface where $\delta_T = 250$ cl./t., June-July 1967.

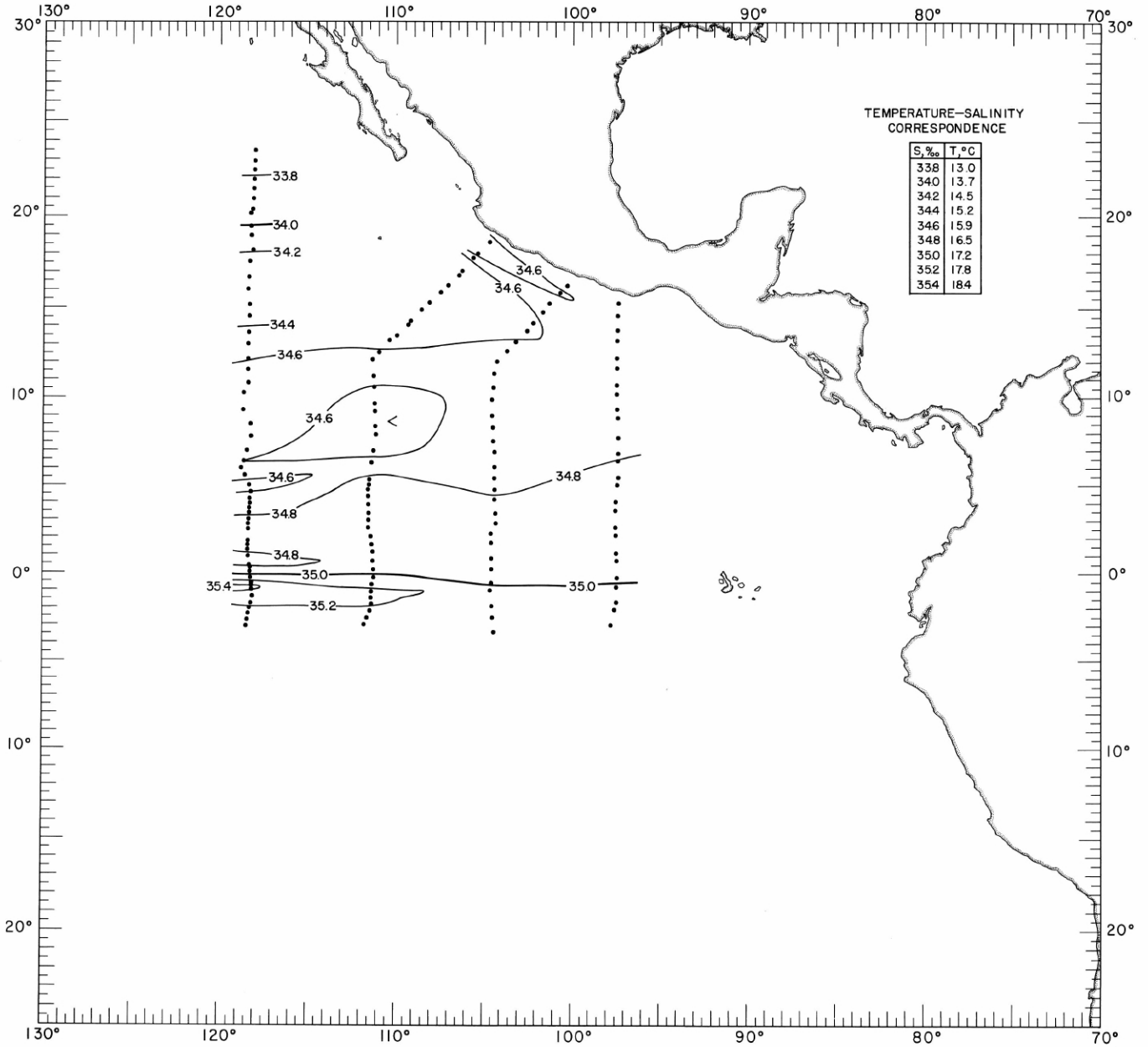

30-S-δ250.

FIGURE 30-S-δ250.—Salinity (‰) on the surface where $\delta_T = 250$ cl./t., June-July 1967. The table shows the temperature corresponding to each isohaline on the chart.

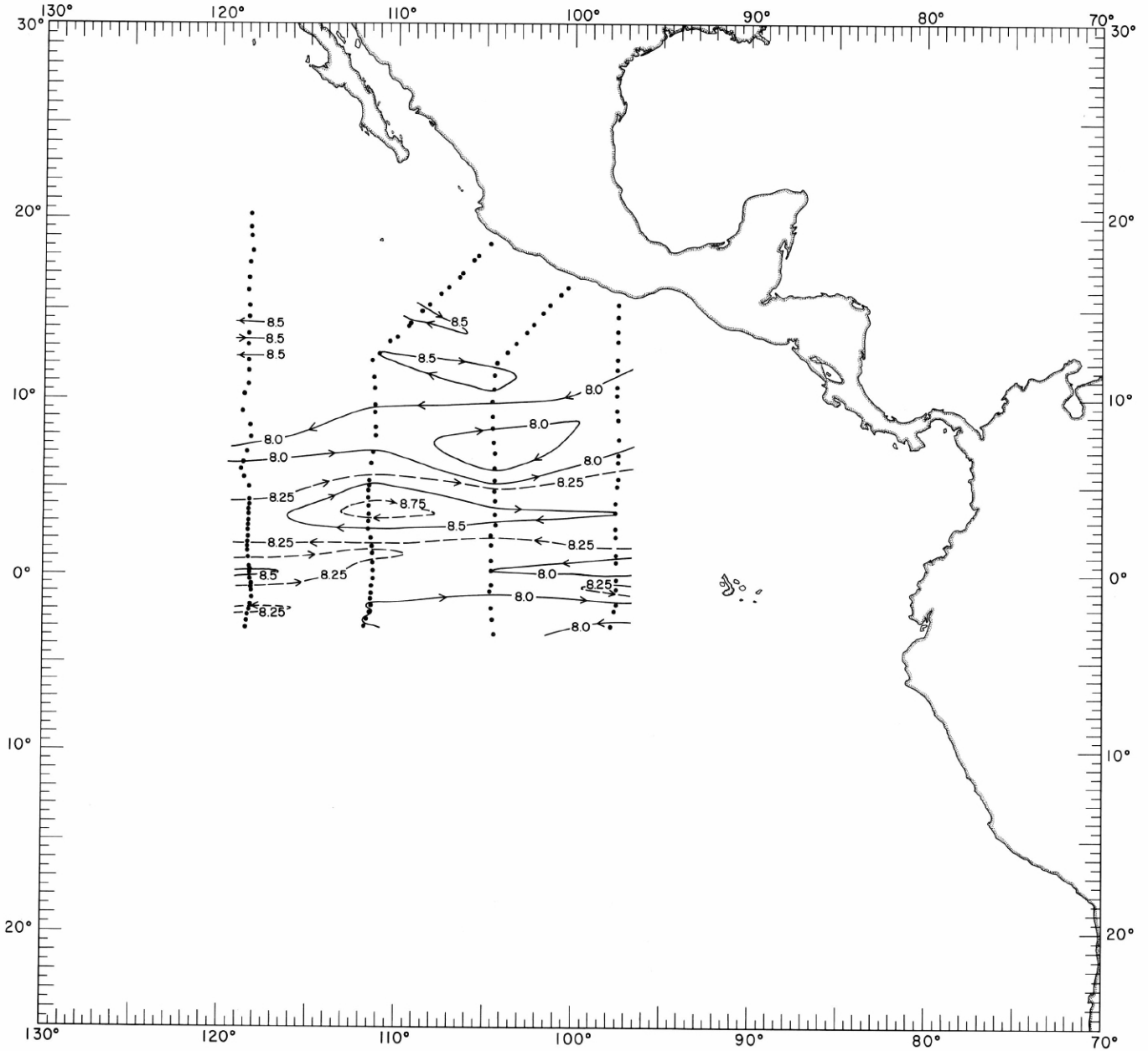

FIGURE 30-AP-δ250.—Acceleration potential (j./kg.), relative to 500 db., on the surface where δ_r = 250 cl./t., June-July 1967. For computing acceleration potential, thermosteric anomaly, δ_r, was used instead of specific volume anomaly, δ.

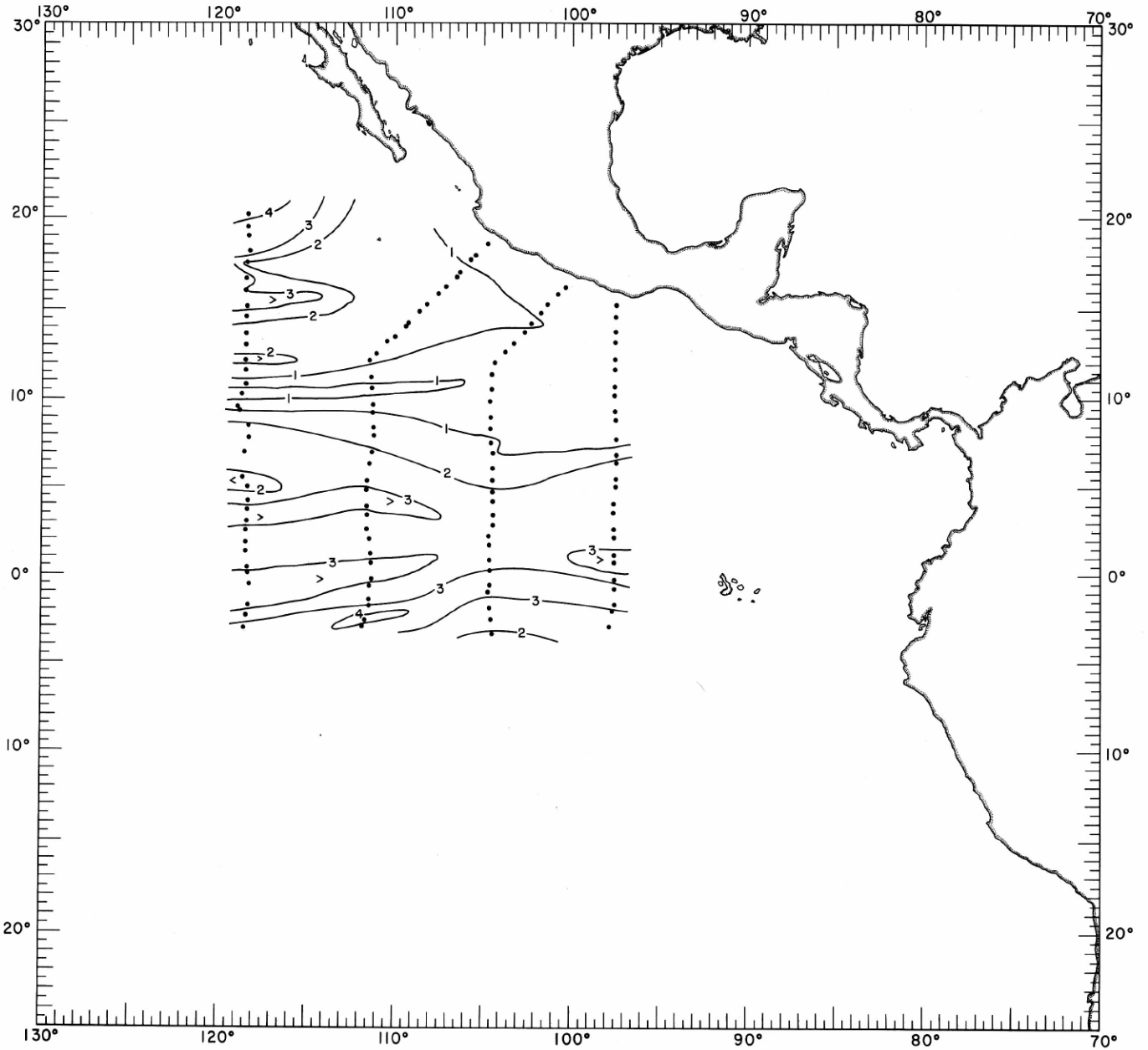

FIGURE 30-O_2-δ250.—Oxygen (ml./l.) on the surface where $\delta_r = 250$ cl./t., June-July 1967.

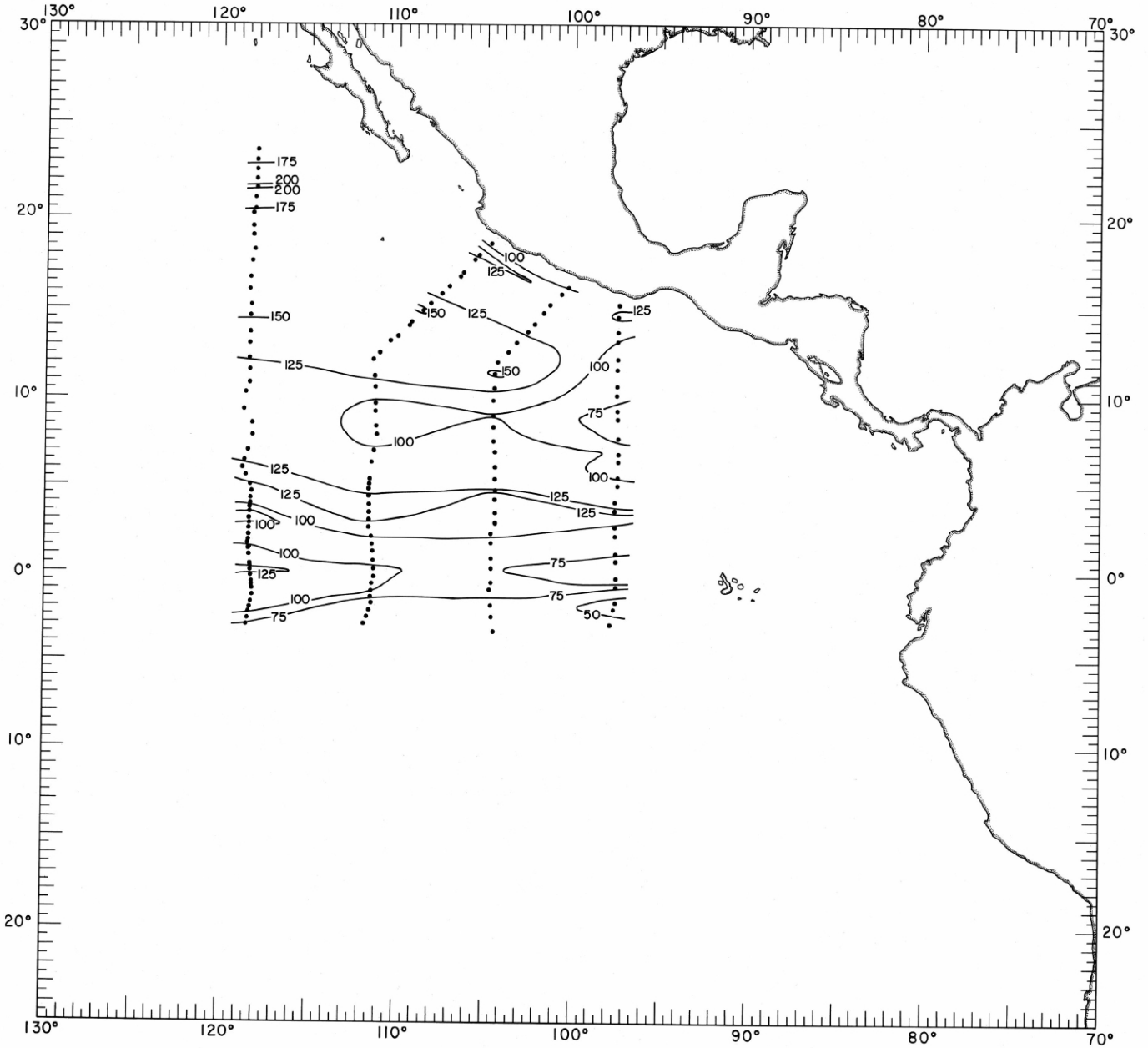

FIGURE 30-δ200-z.—Depth (m.) of the surface where $\delta_T = 200$ cl./t., June-July 1967.

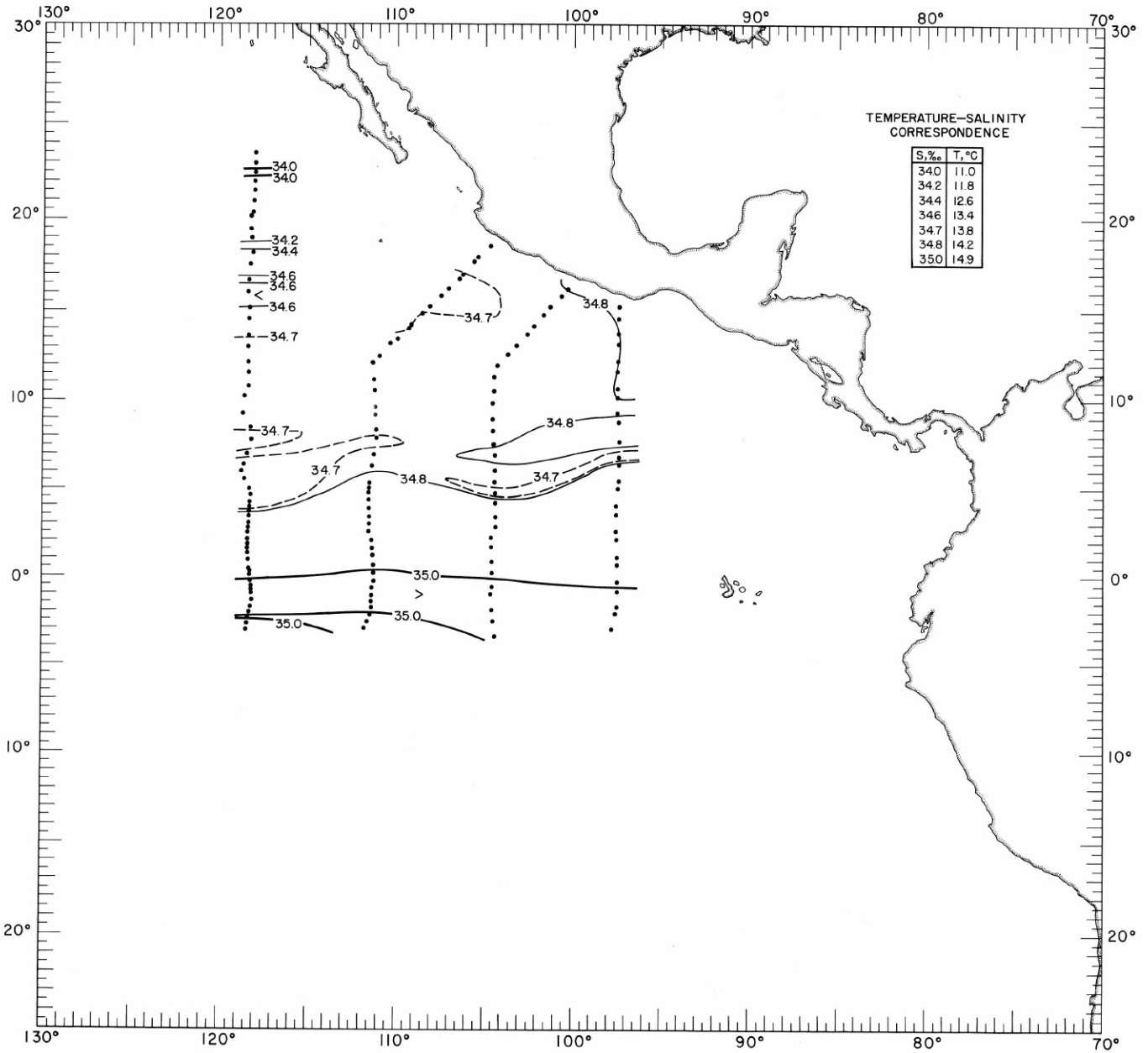

30-S-δ200.

FIGURE 30-S-δ200.—Salinity (‰) on the surface where $\delta_T = 200$ cl./t., June-July 1967. The table shows the temperature corresponding to each isohaline on the chart.

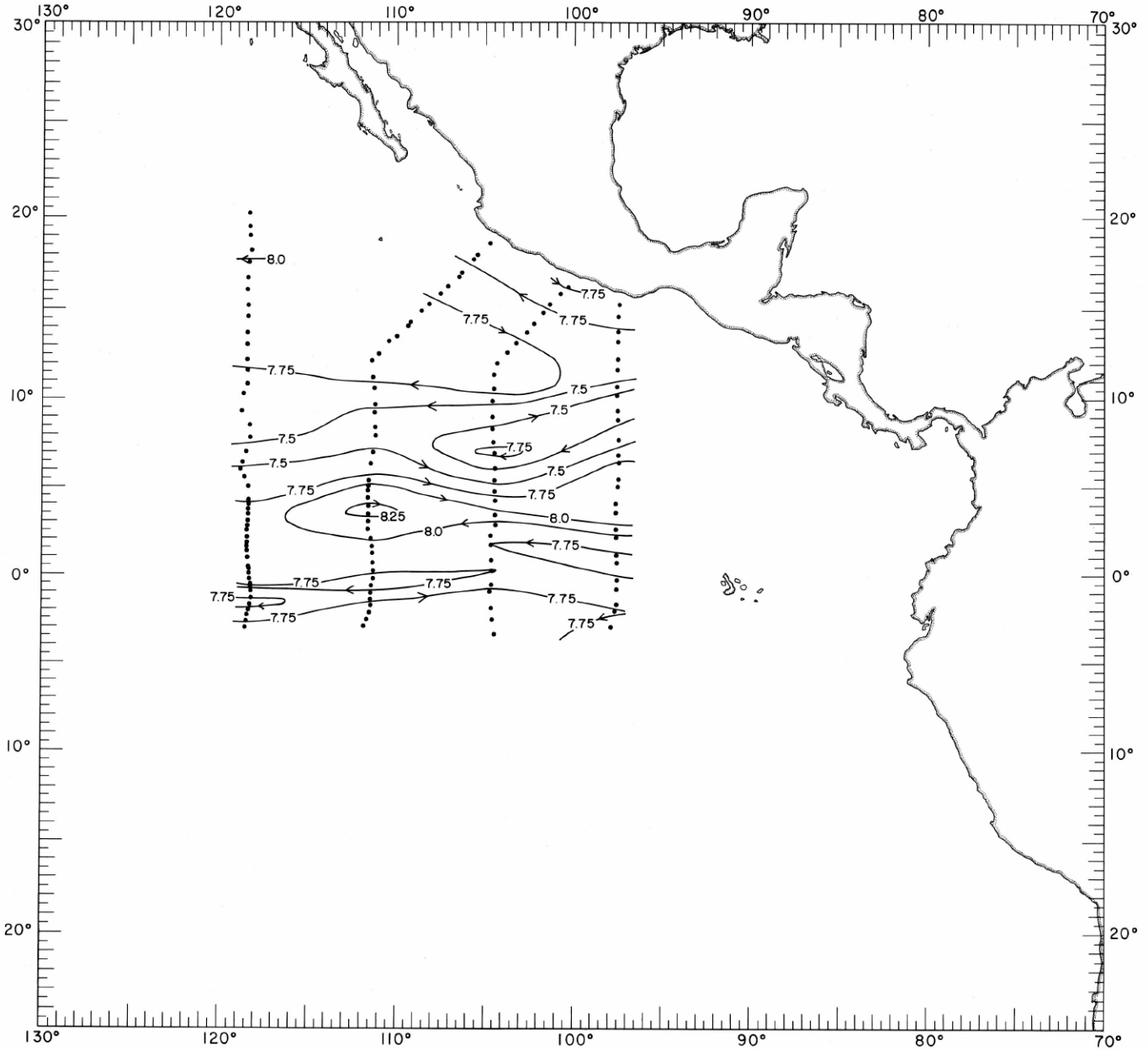

FIGURE 30-AP-8200.—Acceleration potential (j./kg.), relative to 500 db., on the surface where δ_T = 200 cl./t., June-July 1967. For computing acceleration potential, thermosteric anomaly, δ_T, was used instead of specific volume anomaly, δ.

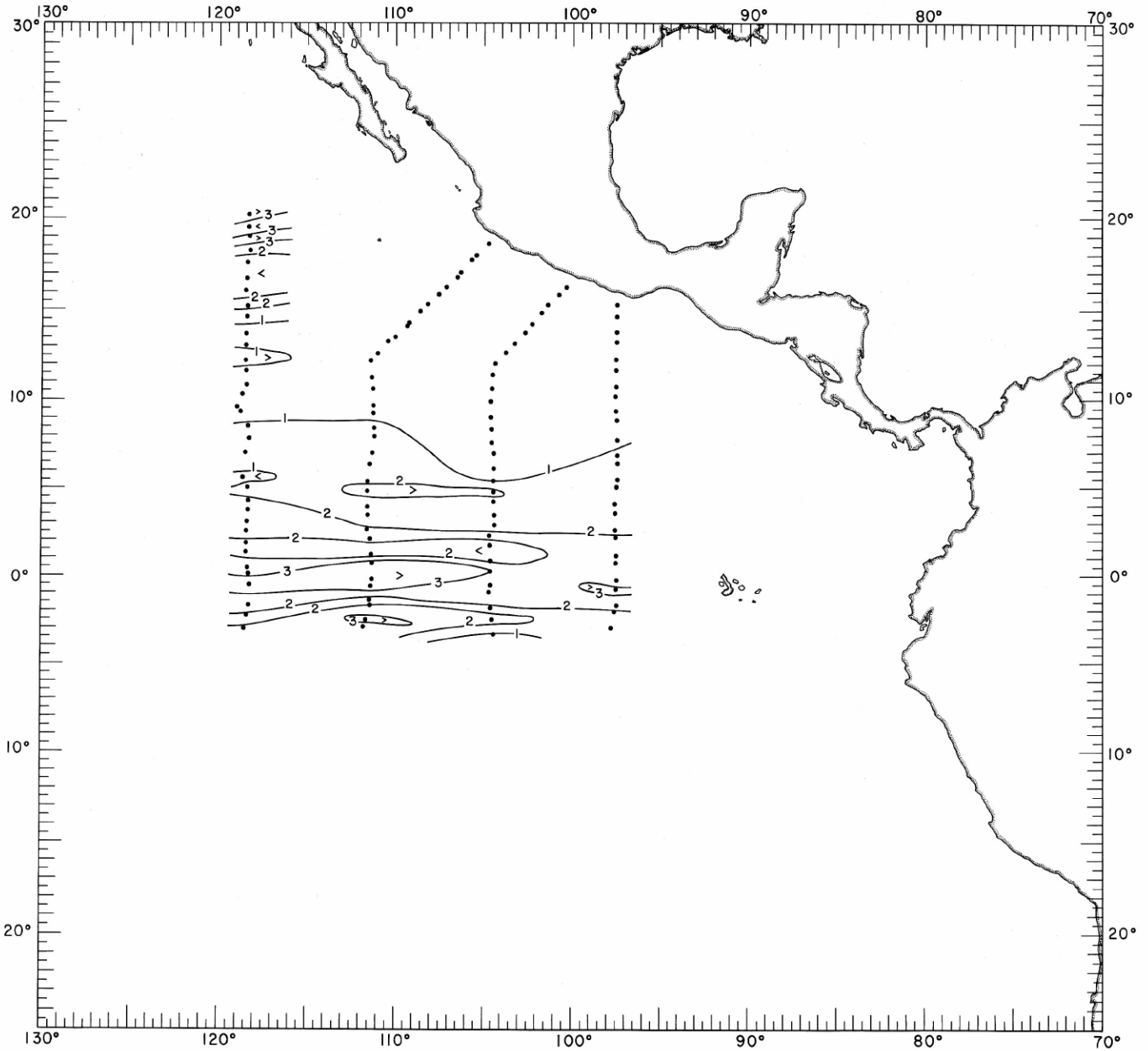

FIGURE 30-O2-δ200.—Oxygen (ml./l.) on the surface where $\delta_T = 200$ cl./t., June-July 1967.

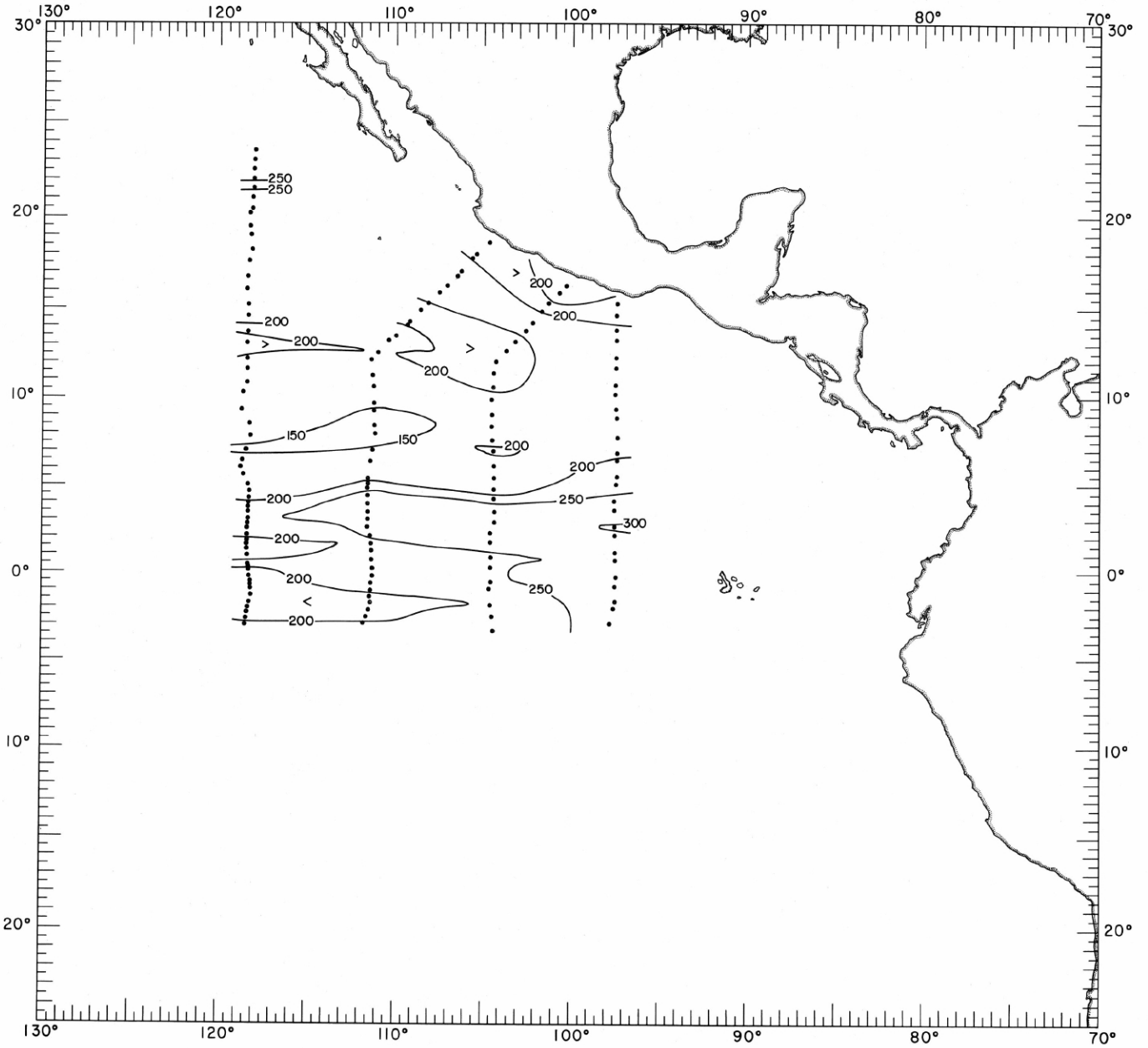

FIGURE 30-δ160-z.—Depth (m.) of the surface where $\delta_T = 160$ cl./t., June-July 1967.

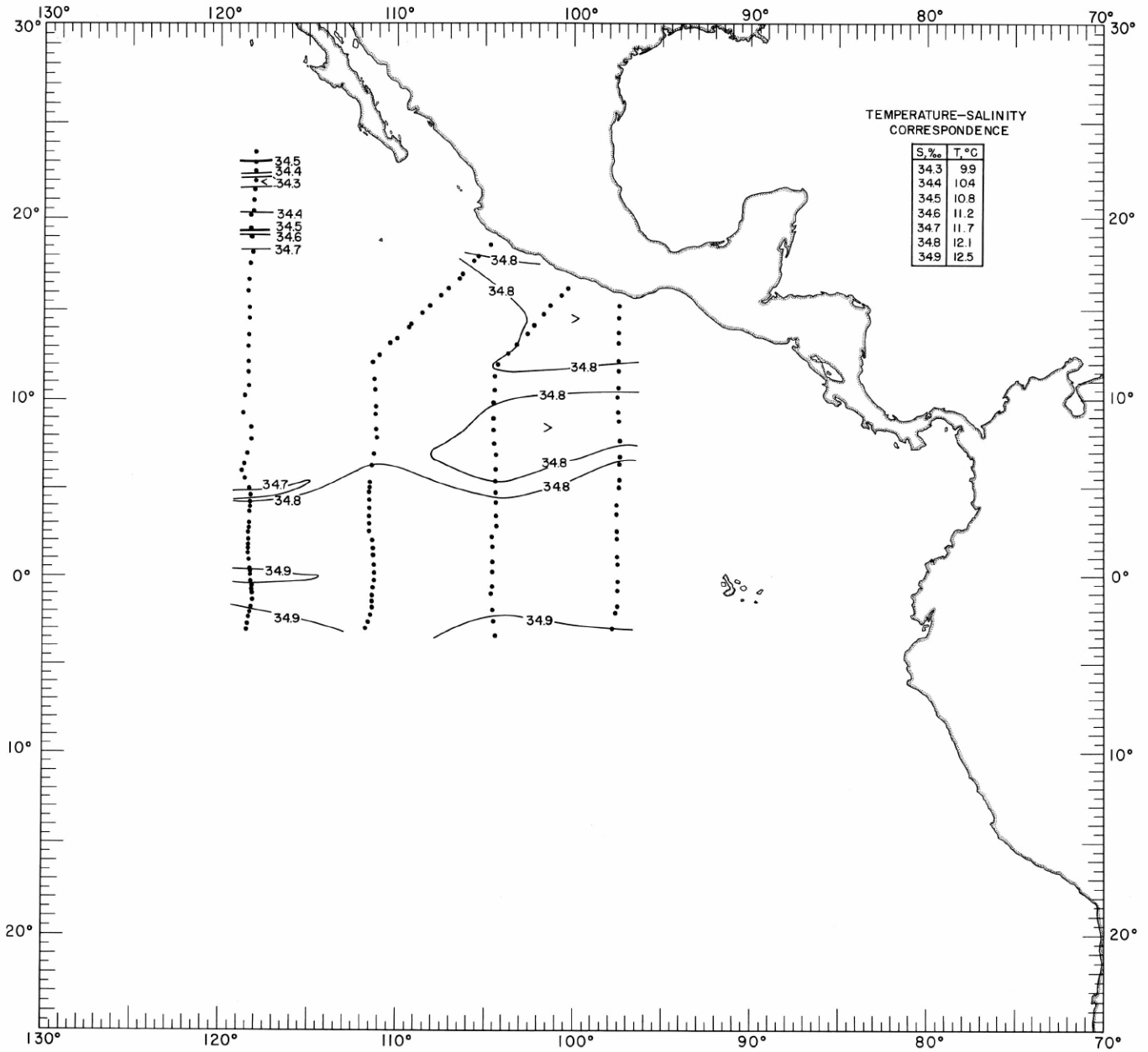

FIGURE 30-S-8160.—Salinity (‰) on the surface where $\delta_r = 160$ cl./t., June-July 1967. The table shows the temperature corresponding to each isohaline on the chart.

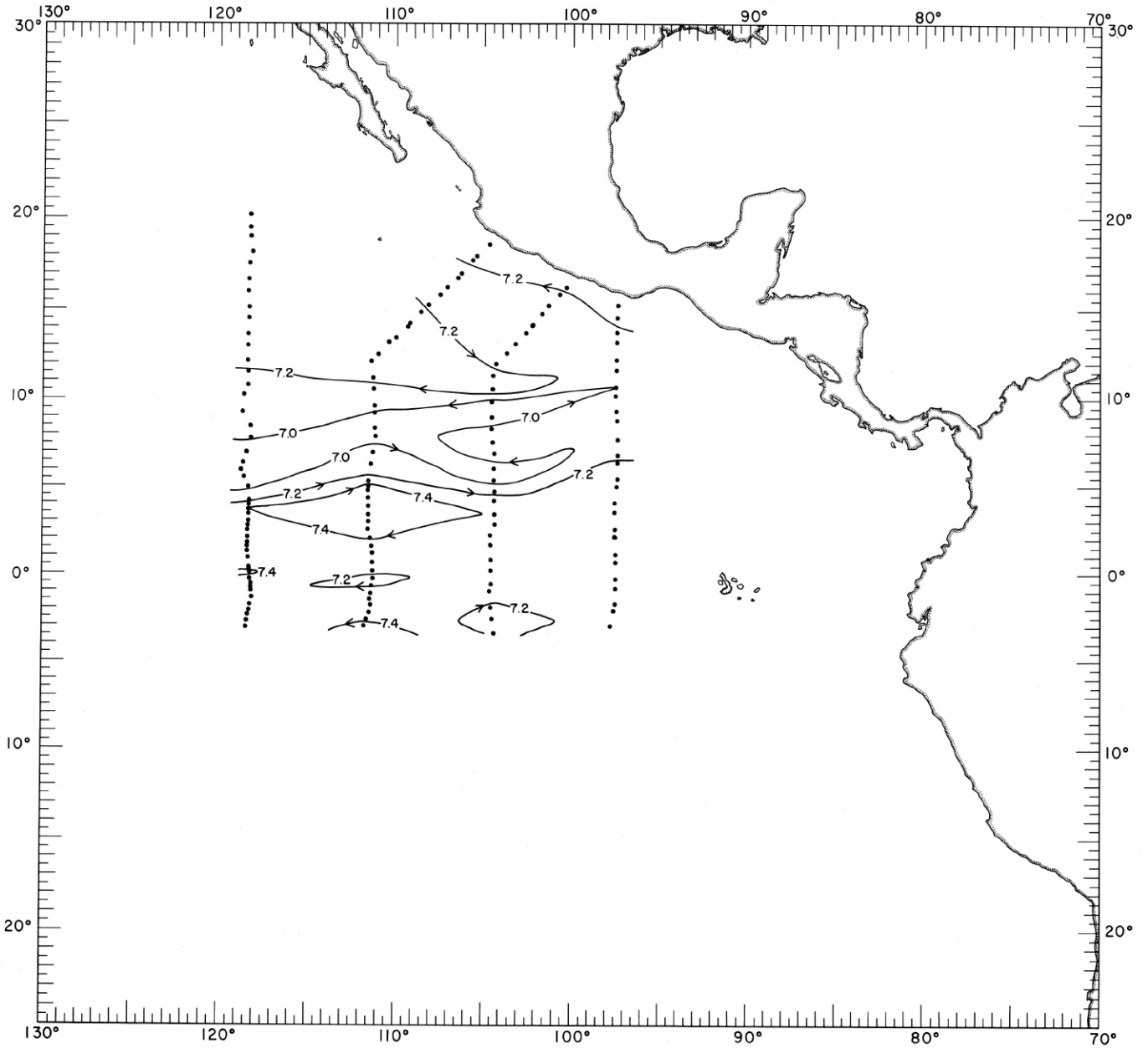

FIGURE 30-AP-δ160.—Acceleration potential (j./kg.), relative to 500 db., on the surface where δ_T = 160 cl./t., June-July 1967. For computing acceleration potential, thermosteric anomaly, δ_T, was used instead of specific volume anomaly, δ.

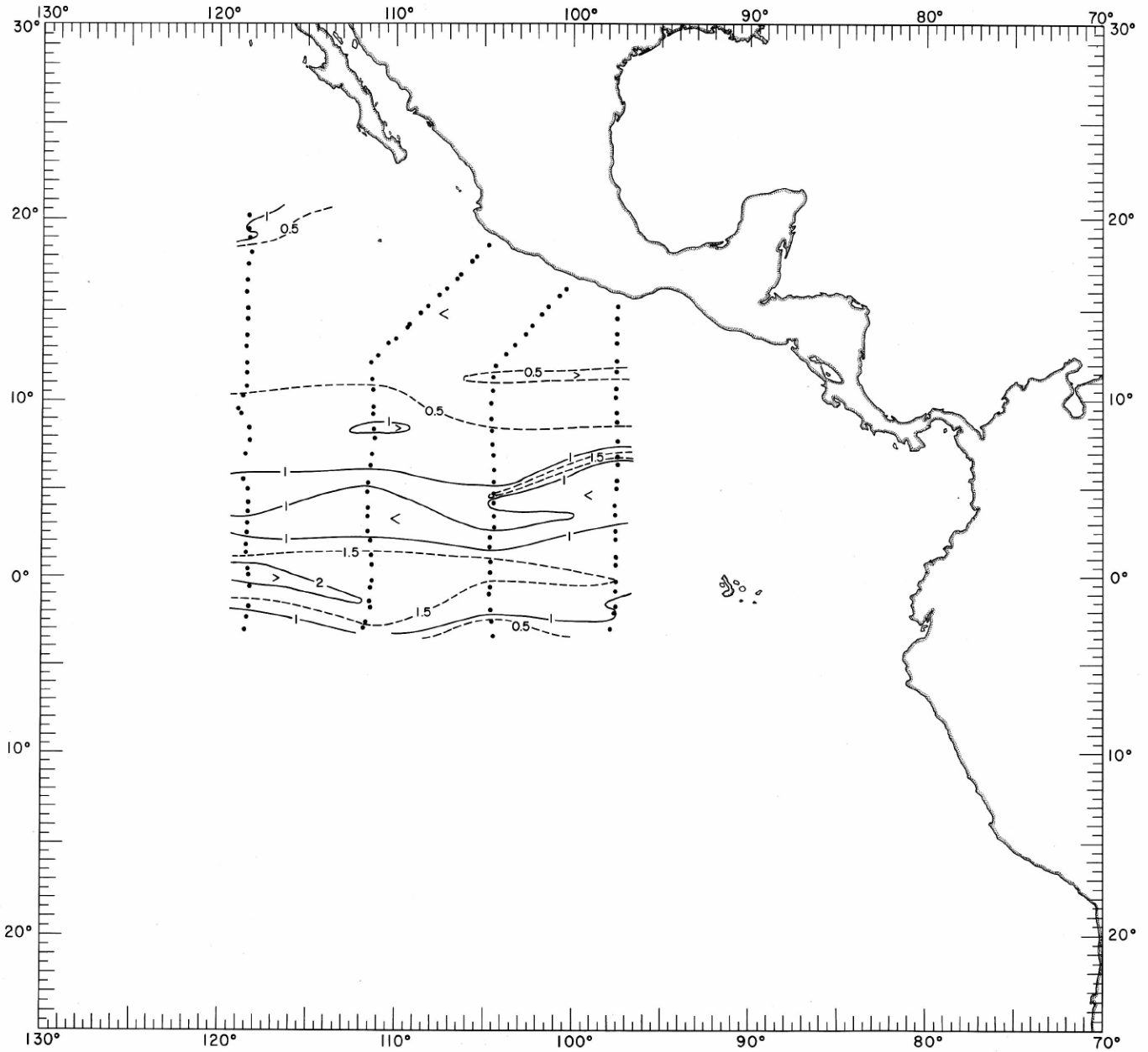

FIGURE 30-O_2-δ160.—Oxygen (ml./l.) on the surface where $\delta_T = 160$ cl./t., June-July 1967.

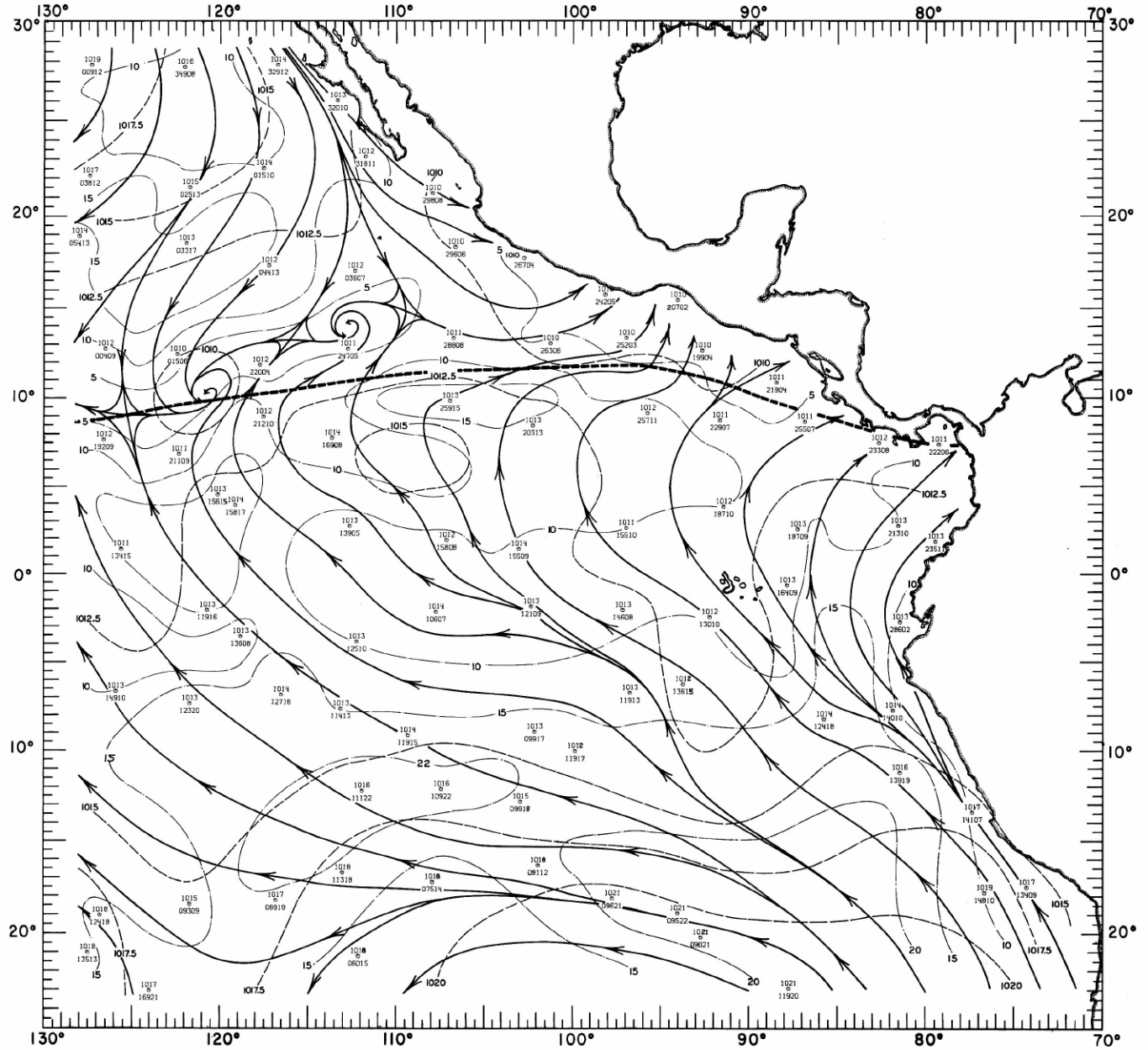

FIGURE 30-MW-1. — Analyses of the surface air pressure and surface winds from all available ship observations, averaged over 2-degree (latitude-longitude) squares for the period June 1-16, 1967. Heavy dashed lines are isobars. Solid lines are streamlines showing the mean resultant direction of wind flow. Light dash-dot lines are isotachs indicating mean resultant wind speed (kn.). Pressure (mb.) averaged for 5-degree squares is plotted above the mean position of the square, and resultant wind direction followed by speed (kn.) is plotted below. The monthly climatological position of the intertropical convergence zone is shown by a wide dashed band.

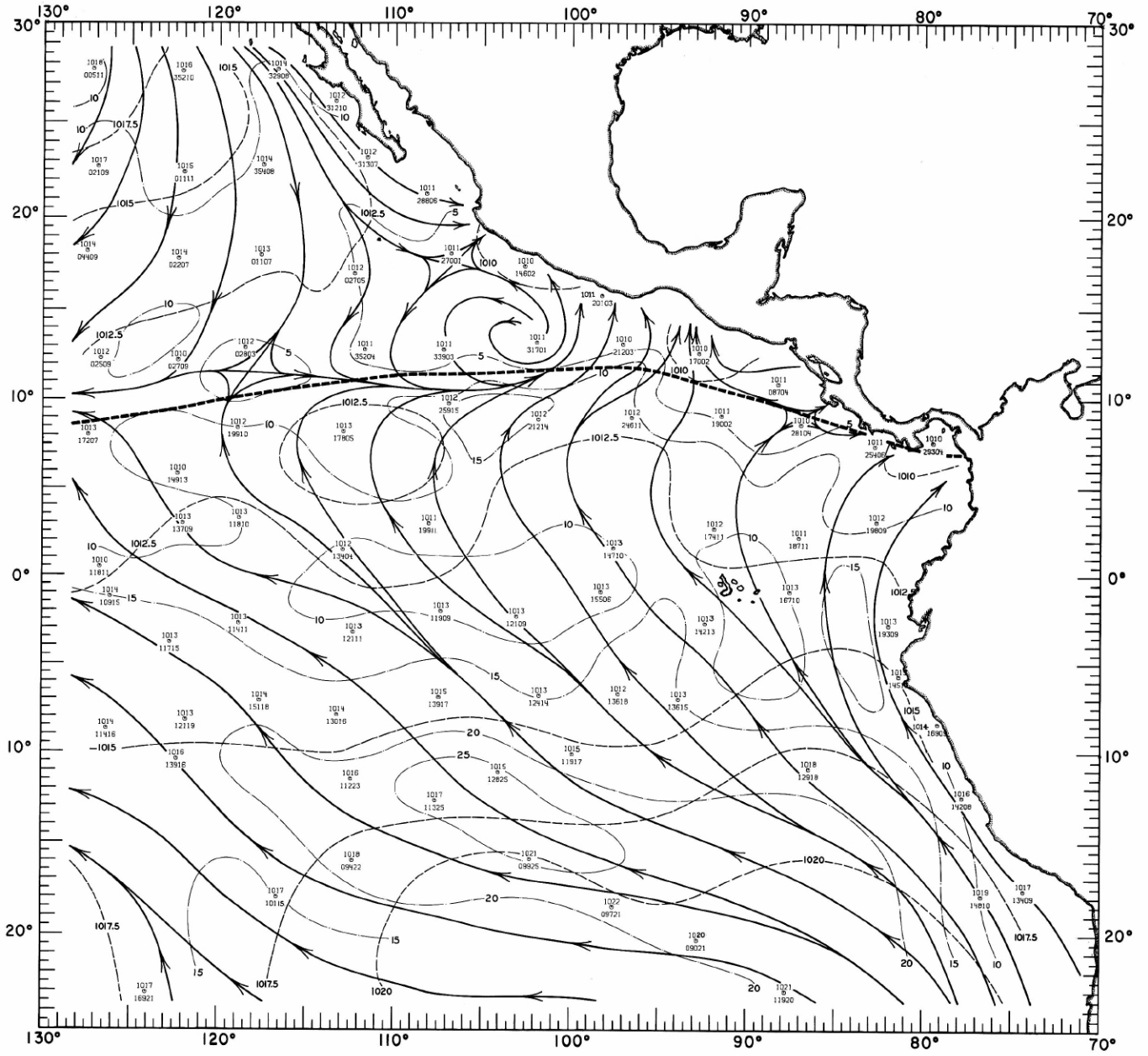

30-MW-2.

FIGURE 30-MW-2. — Analyses of the surface air pressure and surface winds from all available ship observations, averaged over 2-degree (latitude-longitude) squares for the period June 17-30, 1967. Heavy dashed lines are isobars. Solid lines are streamlines showing the mean resultant direction of wind flow. Light dash-dot lines are isotachs indicating mean resultant wind speed (kn.). Pressure (mb.) averaged for 5-degree squares is plotted above the mean position of the square, and resultant wind direction followed by speed (kn.) is plotted below. The monthly climatological position of the intertropical convergence zone is shown by a wide dashed band.

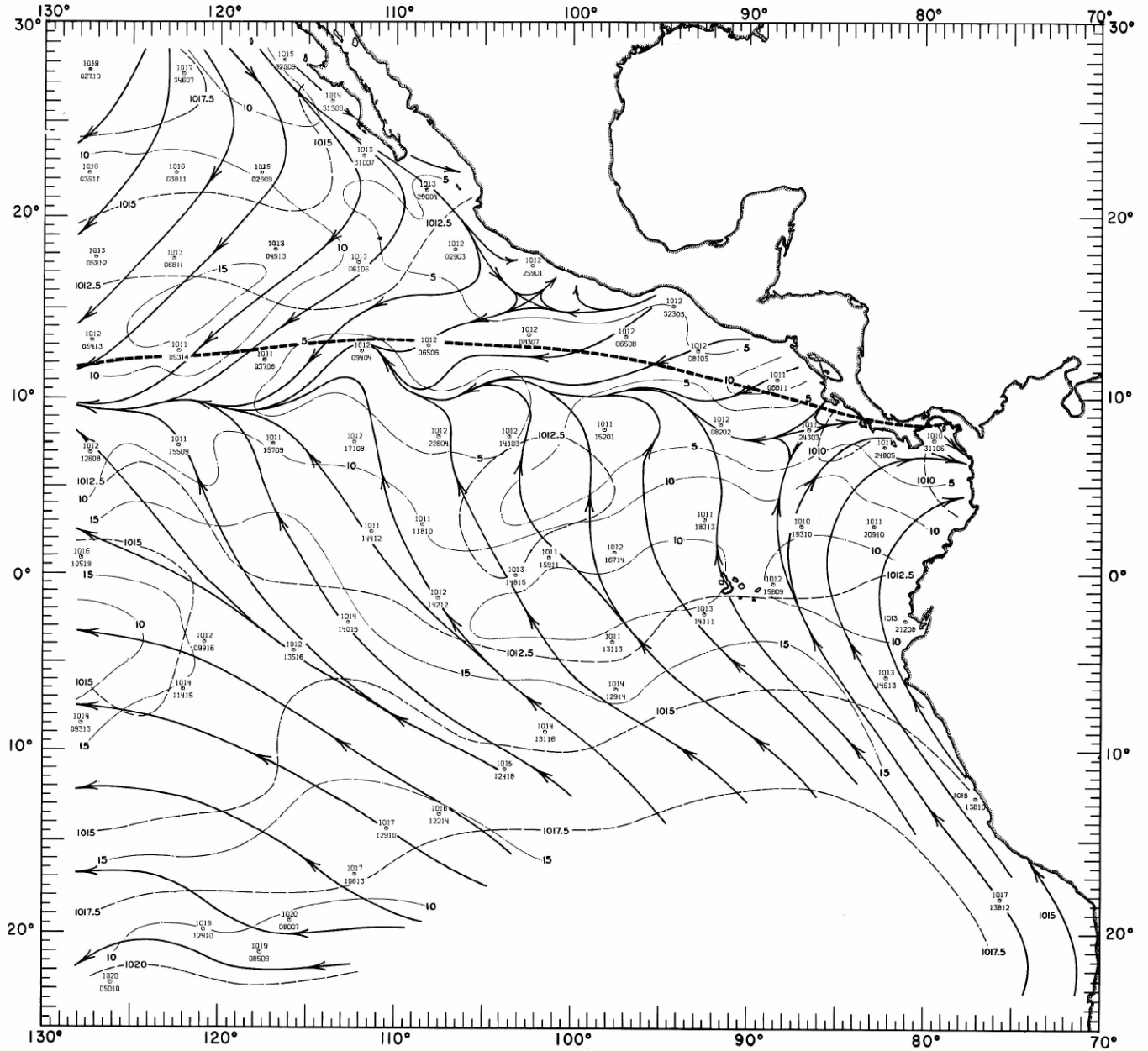

FIGURE 30-MW-3. — Analyses of the surface air pressure and surface winds from all available ship observations, averaged over 2-degree (latitude-longitude) squares for the period July 1-15, 1967. Heavy dashed lines are isobars. Solid lines are streamlines showing the mean resultant direction of wind flow. Light dash-dot lines are isotachs indicating mean resultant wind speed (kn.). Pressure (mb.) averaged for 5-degree squares is plotted above the mean position of the square, and resultant wind direction followed by speed (kn.) is plotted below. The monthly climatological position of the intertropical convergence zone is shown by a wide dashed band.

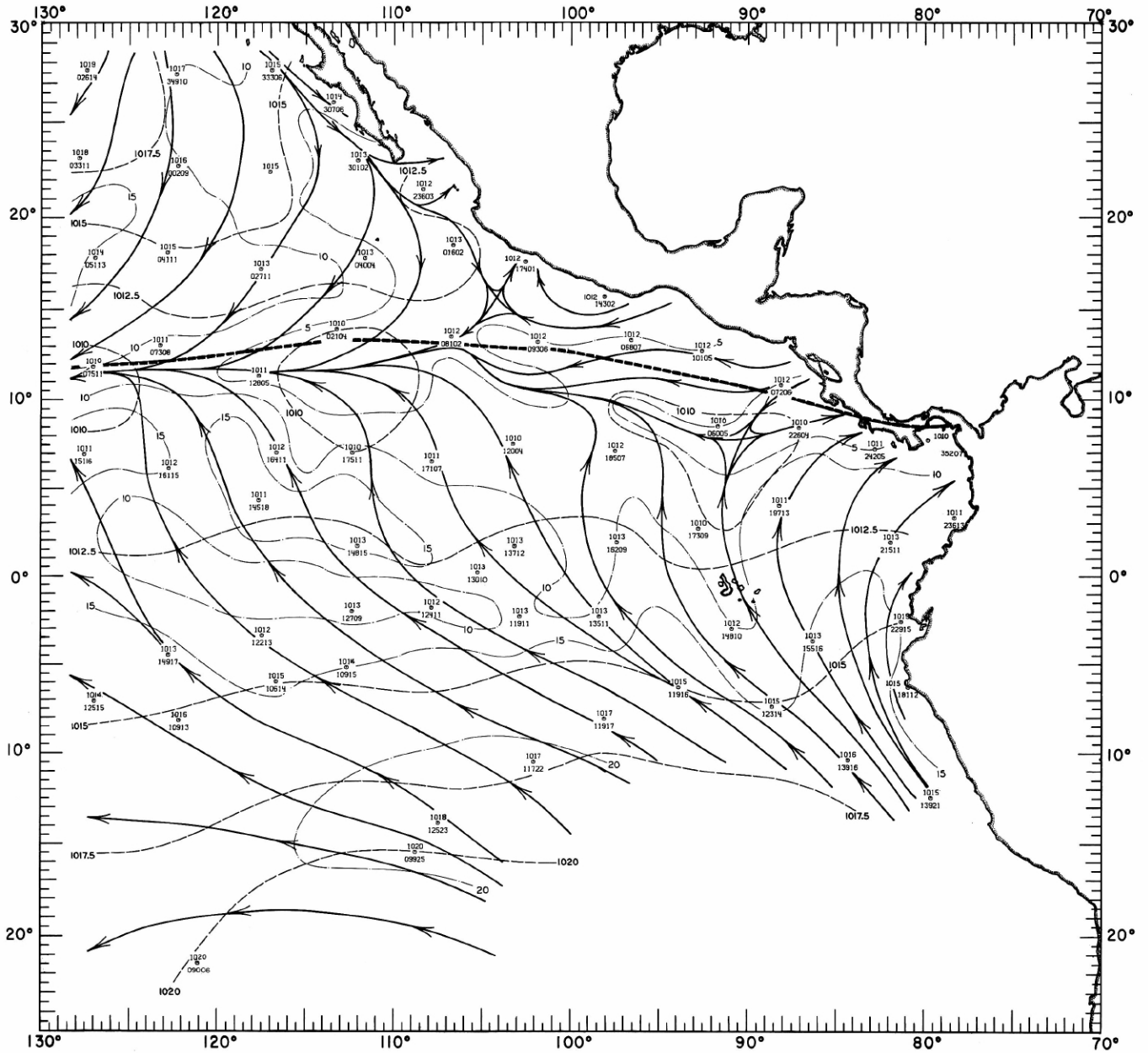

30-MW-4.

FIGURE 30-MW-4. — Analyses of the surface air pressure and surface winds from all available ship observations, averaged over 2-degree (latitude-longitude) squares for the period July 16-31, 1967. Heavy dashed lines are isobars. Solid lines are streamlines showing the mean resultant direction of wind flow. Light dash-dot lines are isotachs indicating mean resultant wind speed (kn.). Pressure (mb.) averaged for 5-degree squares is plotted above the mean position of the square, and resultant wind direction followed by speed (kn.) is plotted below. The monthly climatological position of the intertropical convergence zone is shown by a wide dashed band.

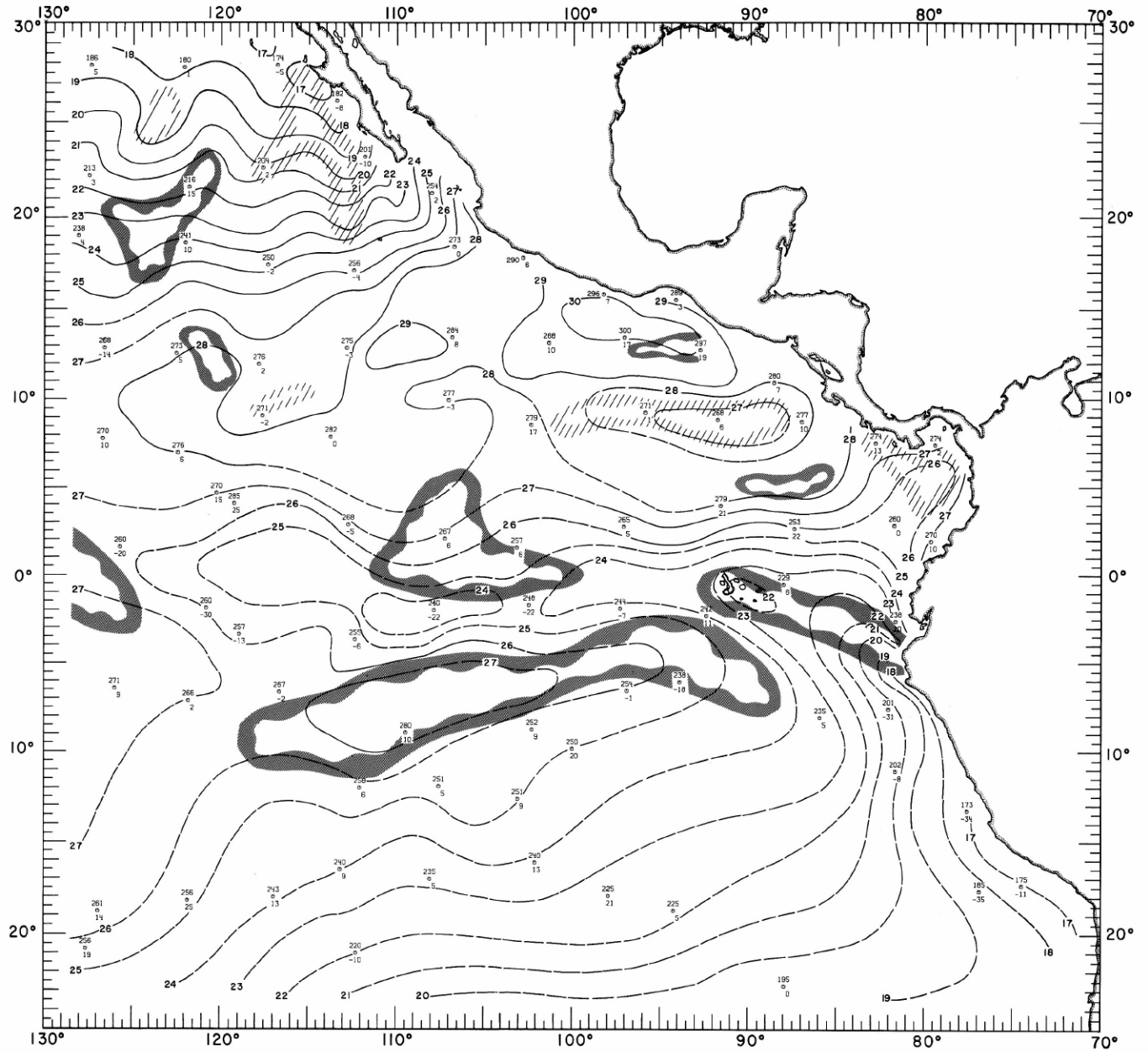

30-MT-1.

FIGURE 30-MT-1. — Analysis of sea surface temperatures based on averages for 2-degree (latitude-longitude) squares from all available ship observations for the period June 1-16, 1967. Solid lines are sea surface isotherms (°C.); the isotherms are dashed where data are sparse. Dark hatching outlines areas with positive temperature anomalies (computed from mean sea surface temperatures averaged over 22 years) greater than 1°C.; light hatching shows areas with negative anomalies greater than 1° C. Sea surface temperature (°C. x 10) averaged for 5-degree squares is plotted above the mean position of the square; sea temperature minus air temperature difference (°C. x 10) is plotted below the symbol.

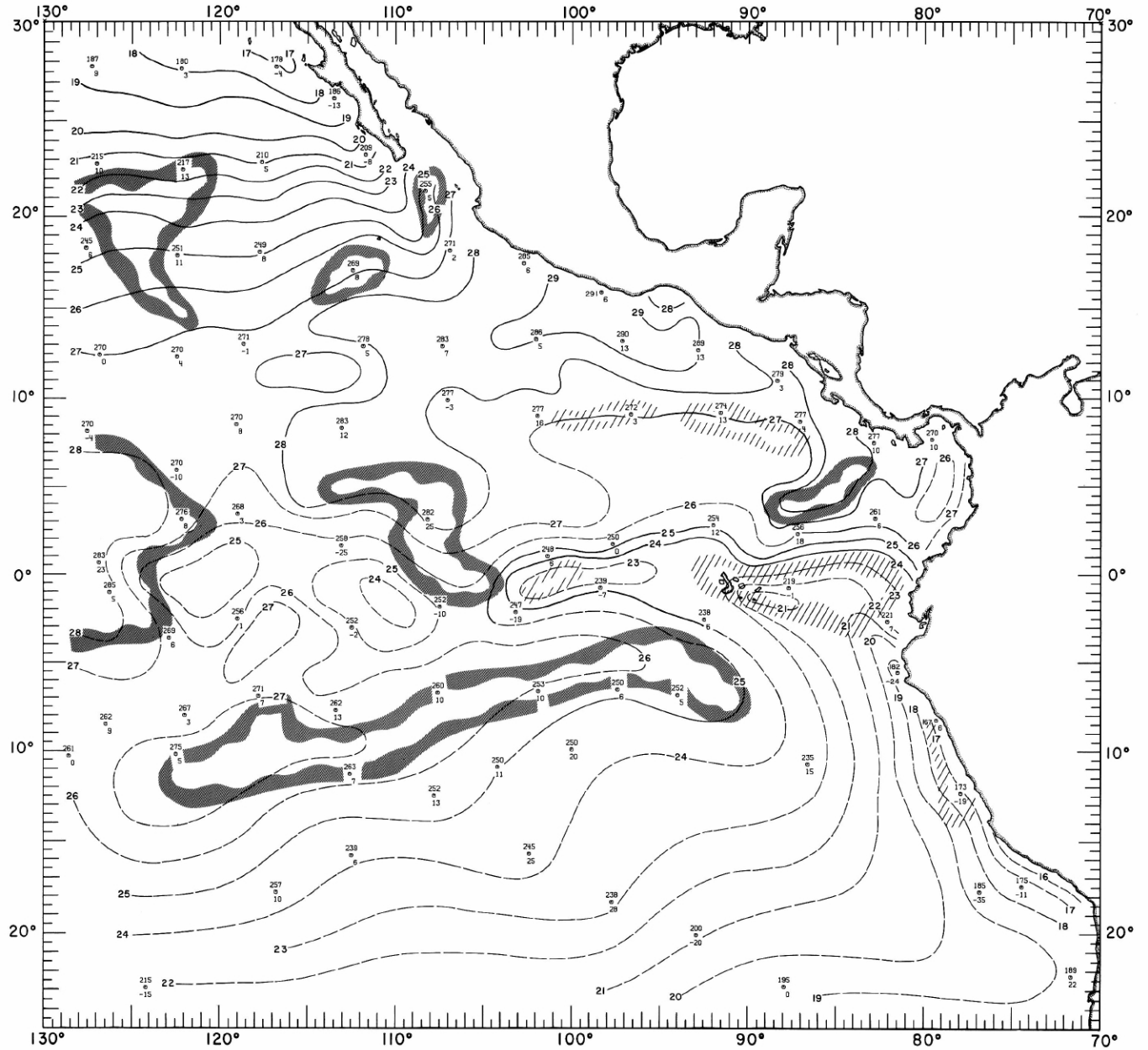

30-MT-2.

FIGURE 30-MT-2. — Analysis of sea surface temperatures based on averages for 2-degree (latitude-longitude) squares from all available ship observations for the period June 17-30, 1967. Solid lines are sea surface isotherms (°C.); the isotherms are dashed where data are sparse. Dark hatching outlines areas with positive temperature anomalies (computed from mean sea surface temperatures averaged over 22 years) greater than 1°C.; light hatching shows areas with negative anomalies greater than 1° C. Sea surface temperature (°C. x 10) averaged for 5-degree squares is plotted above the mean position of the square; sea temperature minus air temperature difference (°C. x 10) is plotted below the symbol.

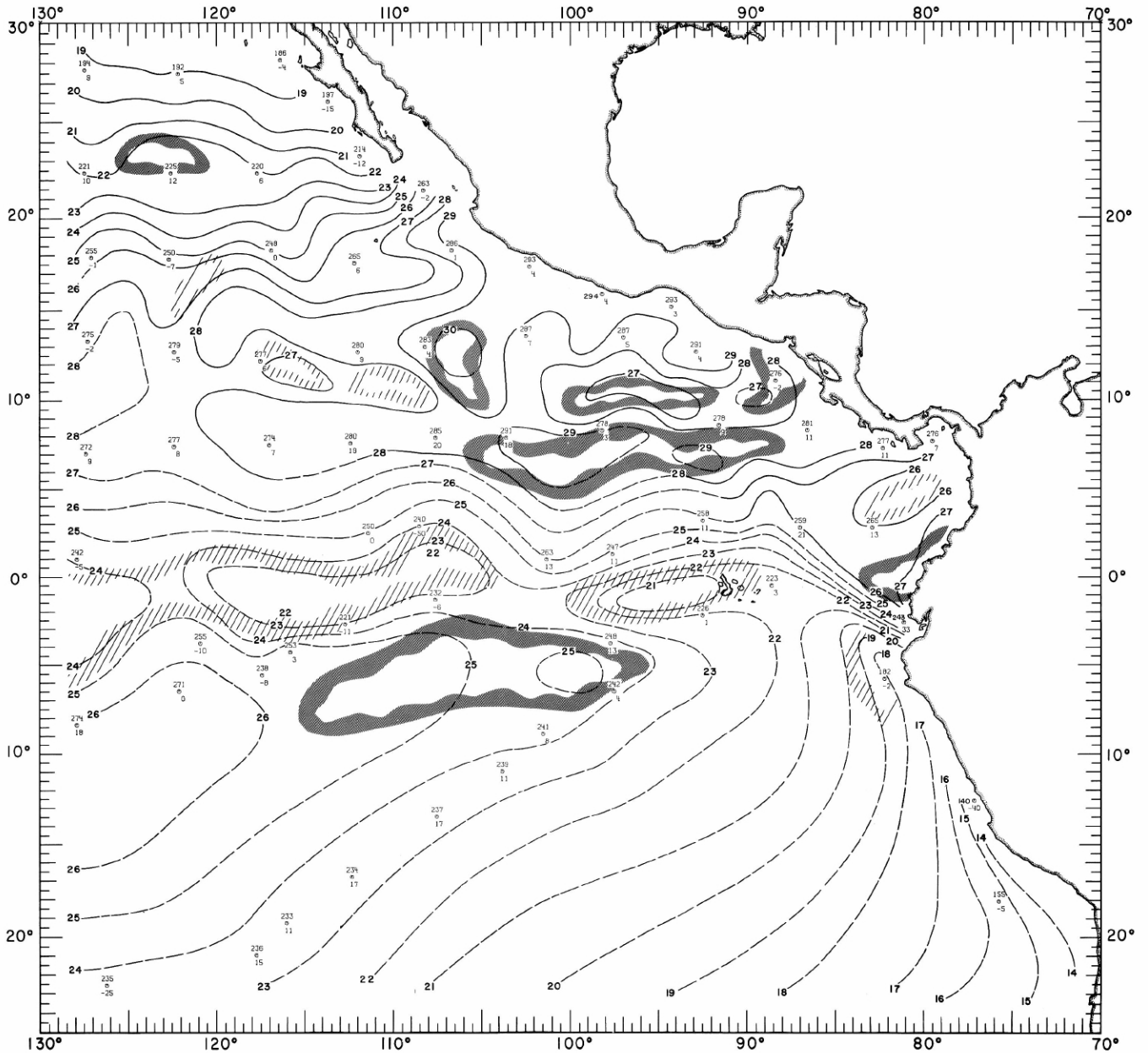

FIGURE 30-MT-3. — Analysis of sea surface temperatures based on averages for 2-degree (latitude-longitude) squares from all available ship observations for the period July 1-15, 1967. Solid lines are sea surface isotherms (°C.); the isotherms are dashed where data are sparse. Dark hatching outlines areas with positive temperature anomalies (computed from mean sea surface temperatures averaged over 22 years) greater than 1°C.; light hatching shows areas with negative anomalies greater than 1° C. Sea surface temperature (°C. x 10) averaged for 5-degree squares is plotted above the mean position of the square; sea temperature minus air temperature difference (°C. x 10) is plotted below the symbol.

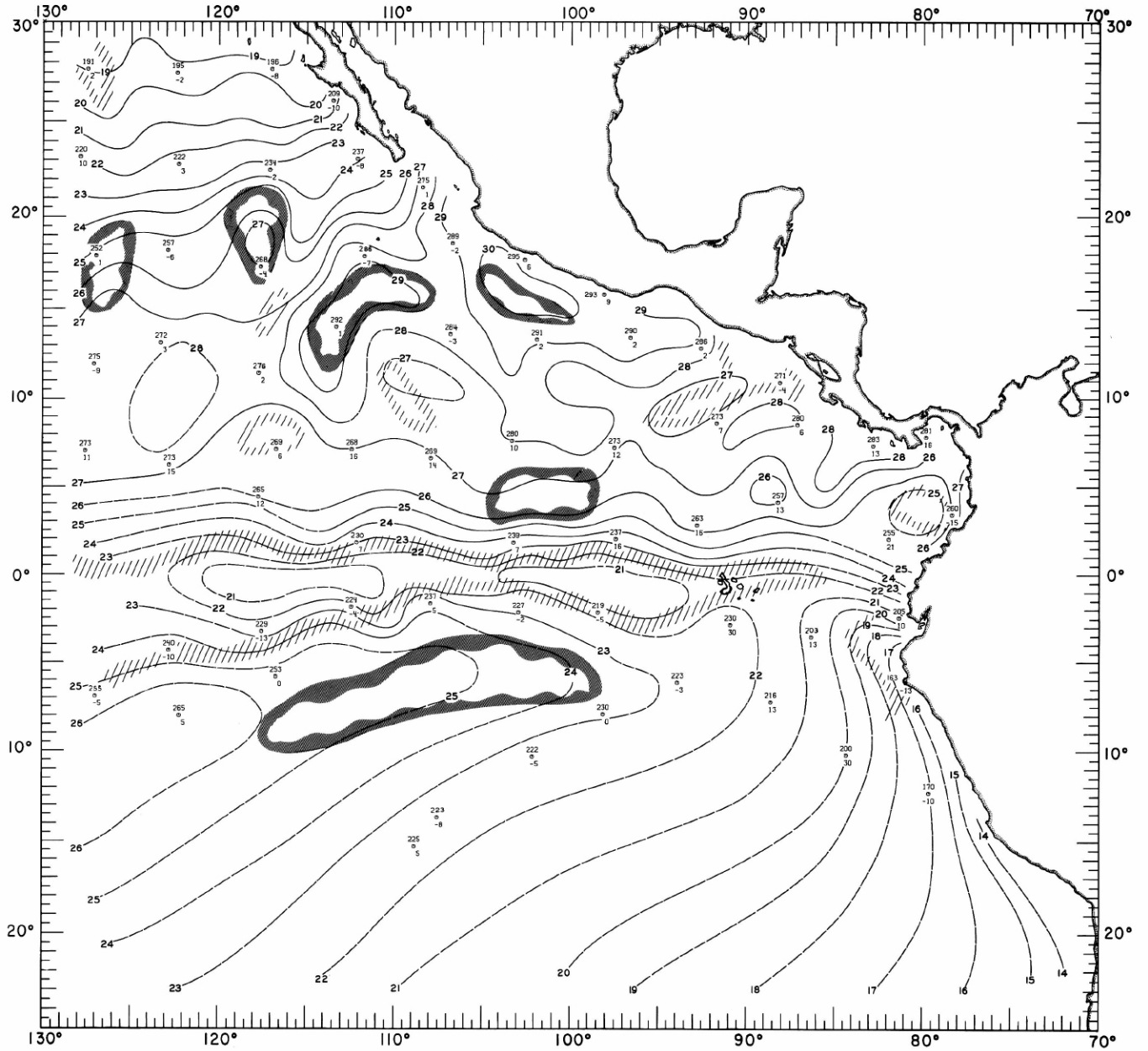

30-MT-4.

FIGURE 30-MT-4. — Analysis of sea surface temperatures based on averages for 2-degree (latitude-longitude) squares from all available ship observations for the period July 16-31, 1967. Solid lines are sea surface isotherms (°C.); the isotherms are dashed where data are sparse. Dark hatching outlines areas with positive temperature anomalies (computed from mean sea surface temperatures averaged over 22 years) greater than 1°C.; light hatching shows areas with negative anomalies greater than 1° C. Sea surface temperature (°C. x 10) averaged for 5-degree squares is plotted above the mean position of the square; sea temperature minus air temperature difference (°C. x 10) is plotted below the symbol.

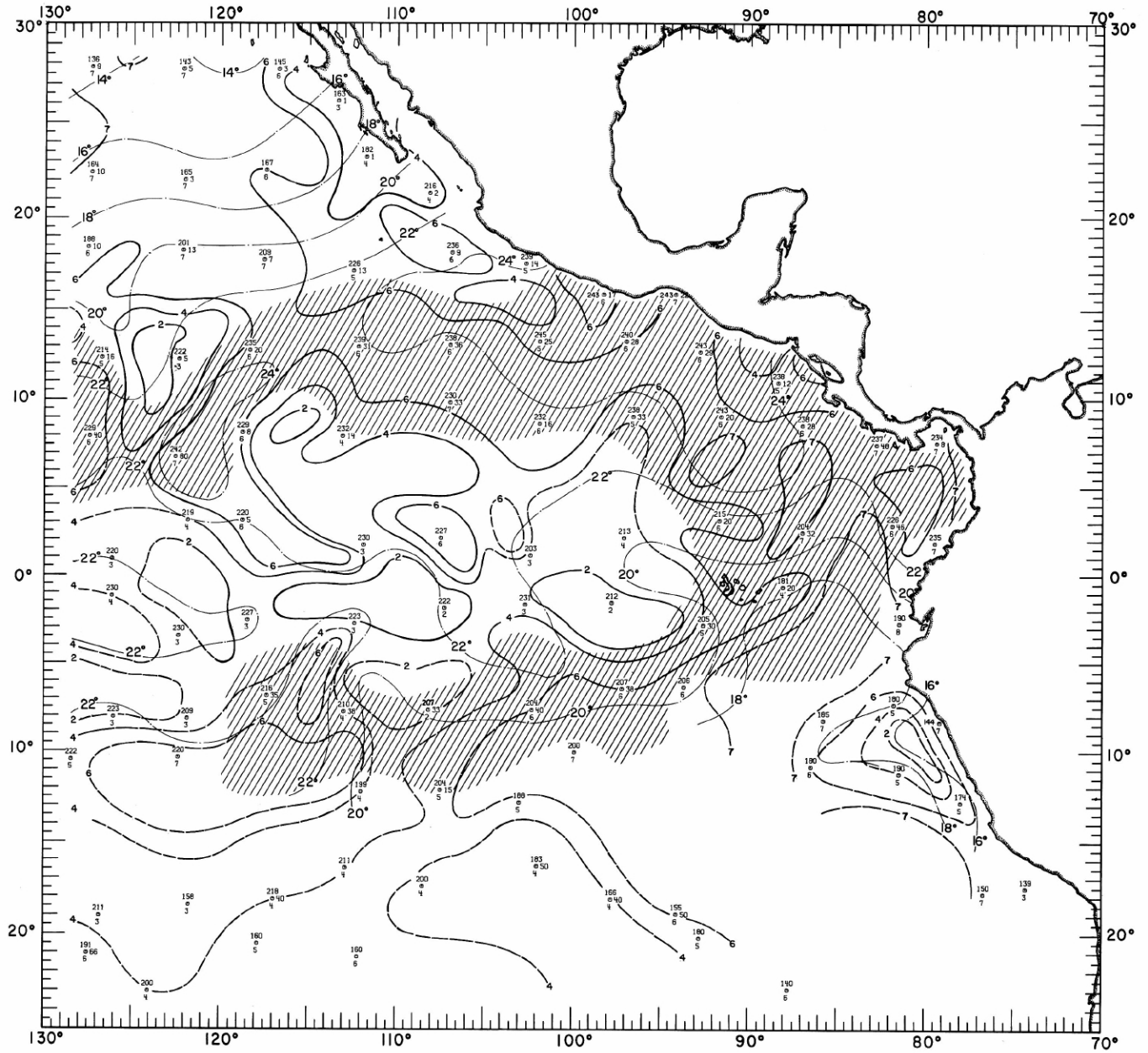

30-MC-1.

FIGURE 30-MC-1. — Analyses of the surface dew-point temperature of the air and total cloud cover based on 2 degree (latidude-longitude) averages from all available ship observations for the month of June 1967. Solid lines depict the monthly mean total cloud cover in oktas; the lines are dashed where data are sparce Dash-dot lines are isotherms of the mean monthly dew-point temperature at 2-degree (C.) intervals Areas where 15 percent or more of the ships reported rain of any type at or within sight of the ship are shaded. Dew-point temperature (°C. x 10) averaged for 5-degree squares is plotted above the mean position of the square, with total cloud cover (oktas) below and rainfall frequency (%) to the right of the symbol.

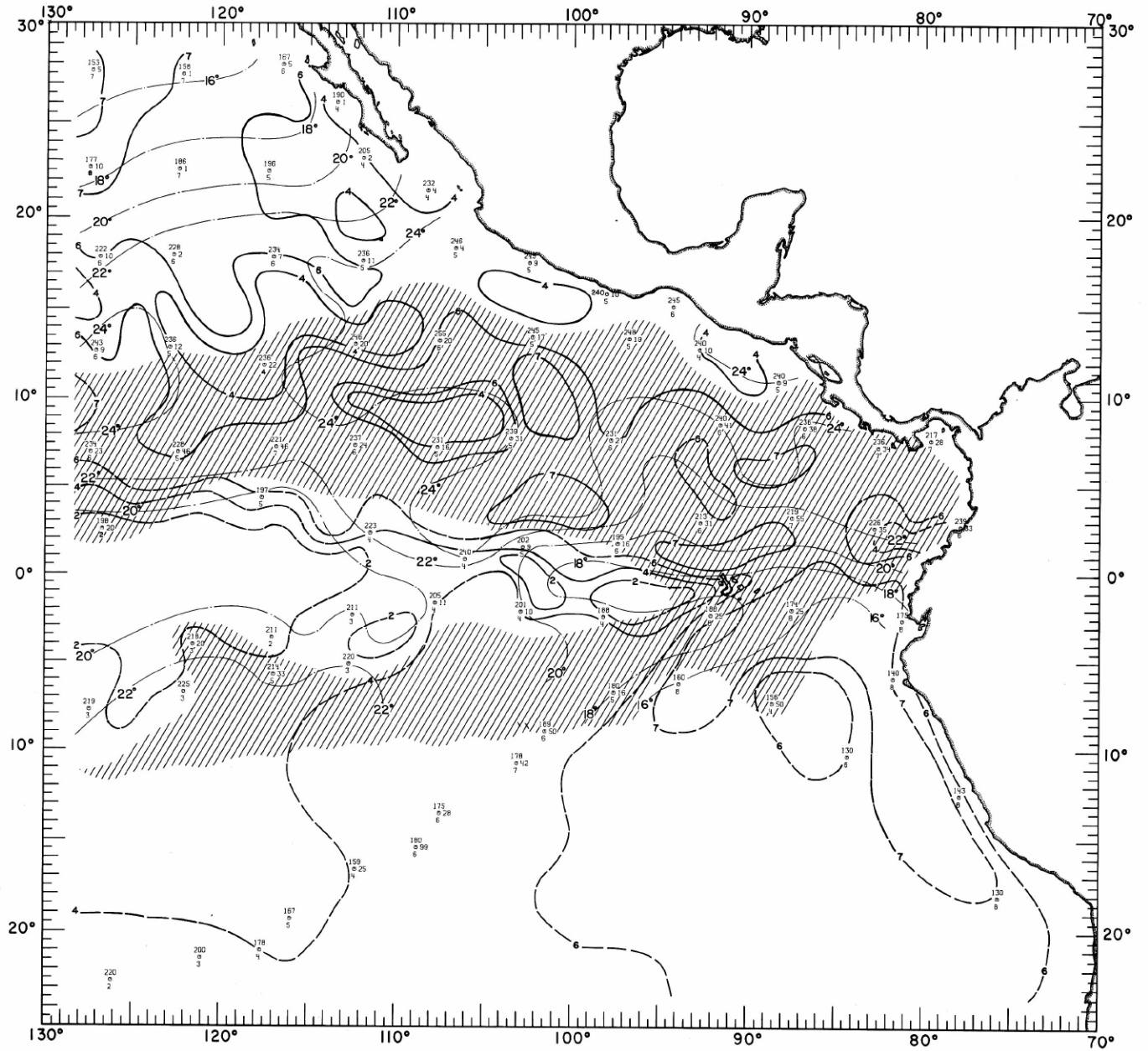

FIGURE 30-MC-2. — Analyses of the surface dew-point temperature of the air and total cloud cover based on 2 degree (latidude-longitude) averages from all available ship observations for the month of July 1967. Solid lines depict the monthly mean total cloud cover in oktas; the lines are dashed where data are sparce Dash-dot lines are isotherms of the mean monthly dew-point temperature at 2-degree (C.) intervals Areas where 15 percent or more of the ships reported rain of any type at or within sight of the ship are shaded. Dew-point temperature (°C. x 10) averaged for 5-degree squares is plotted above the mean position of the square, with total cloud cover (oktas) below and rainfall frequency (%) to the right of the symbol.

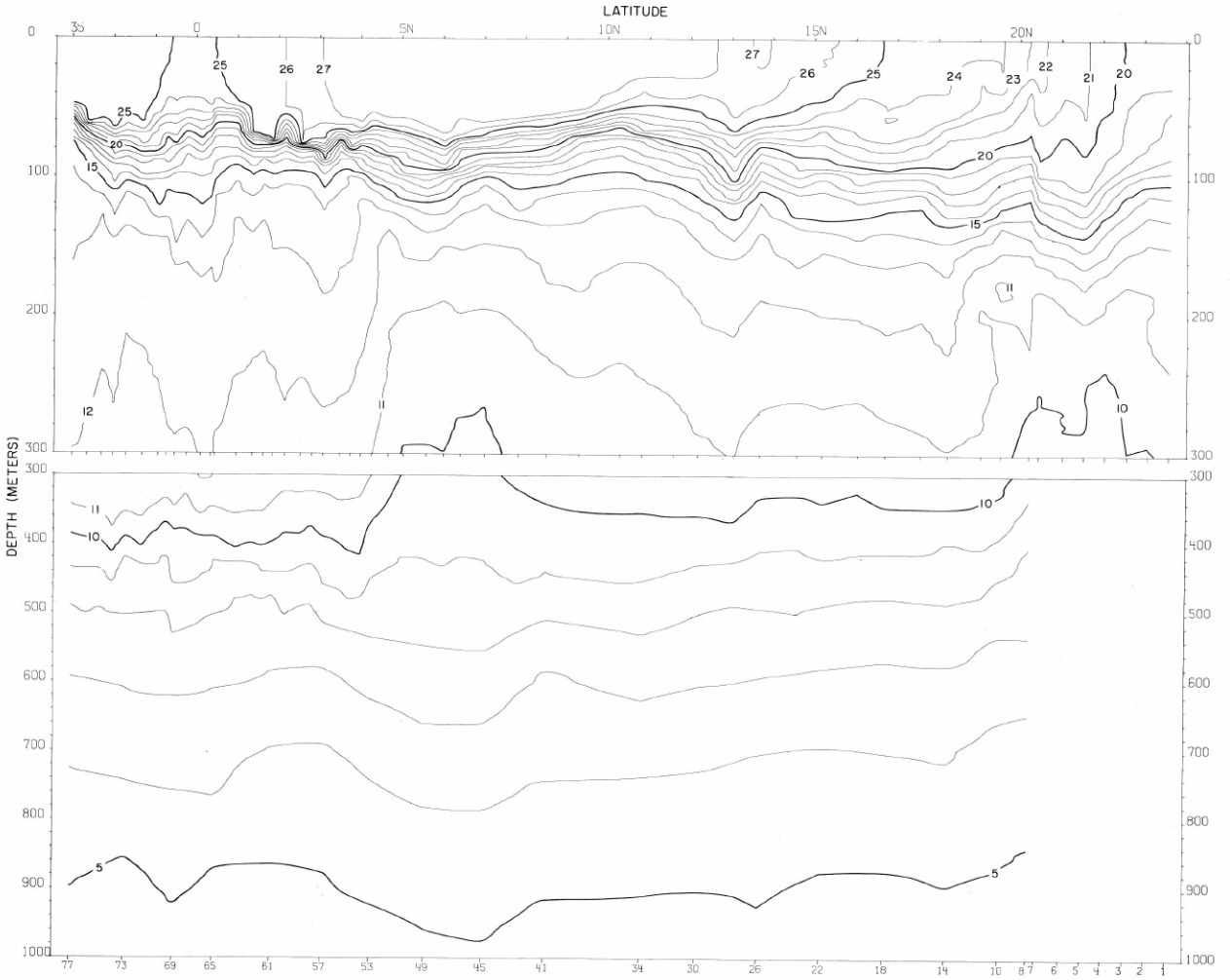

FIGURE 30-T-vl.—Vertical distribution of temperature (°C.) along 118°30′ W., June 16-26, 1967.

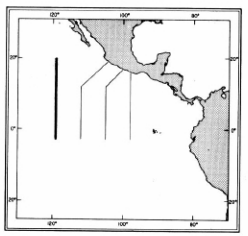

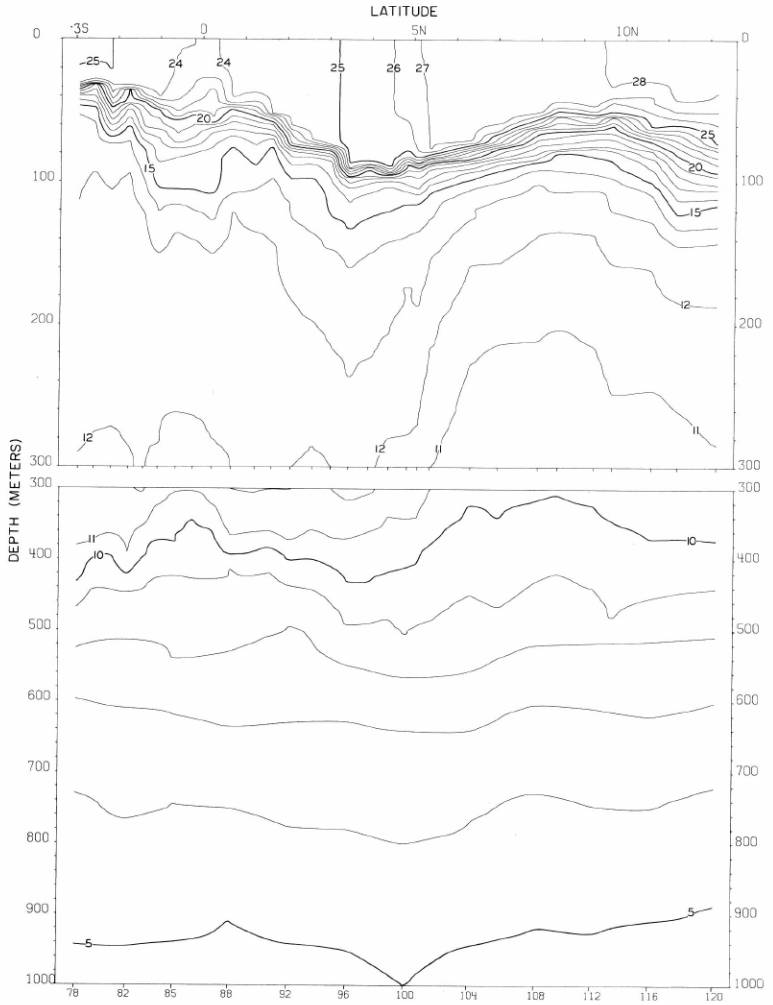

FIGURE 30-T-v2.—Vertical distribution of temperature (°C.) along 111°30′ W., June 28-July 3, 1967.

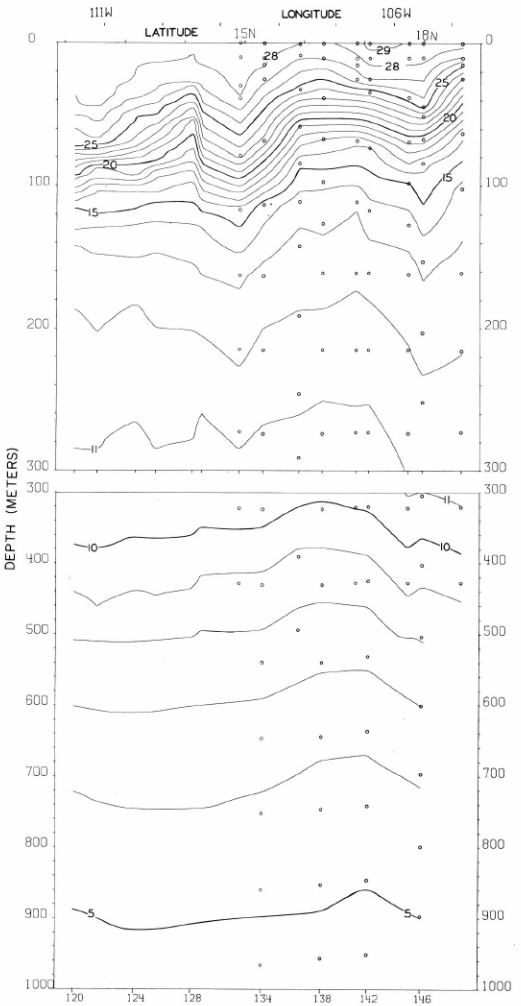

FIGURE 30-T-v3.—Vertical distribution of temperature (°C.) along a section from 12° N., 111°30′ W. to Manzanillo, July 4-7, 1967. The contours from Stations 132-148 are based on Nansen cast data only.

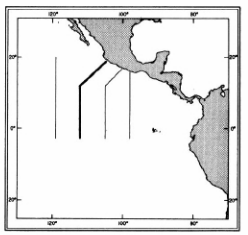

30-T-v2.

30-T-v3.

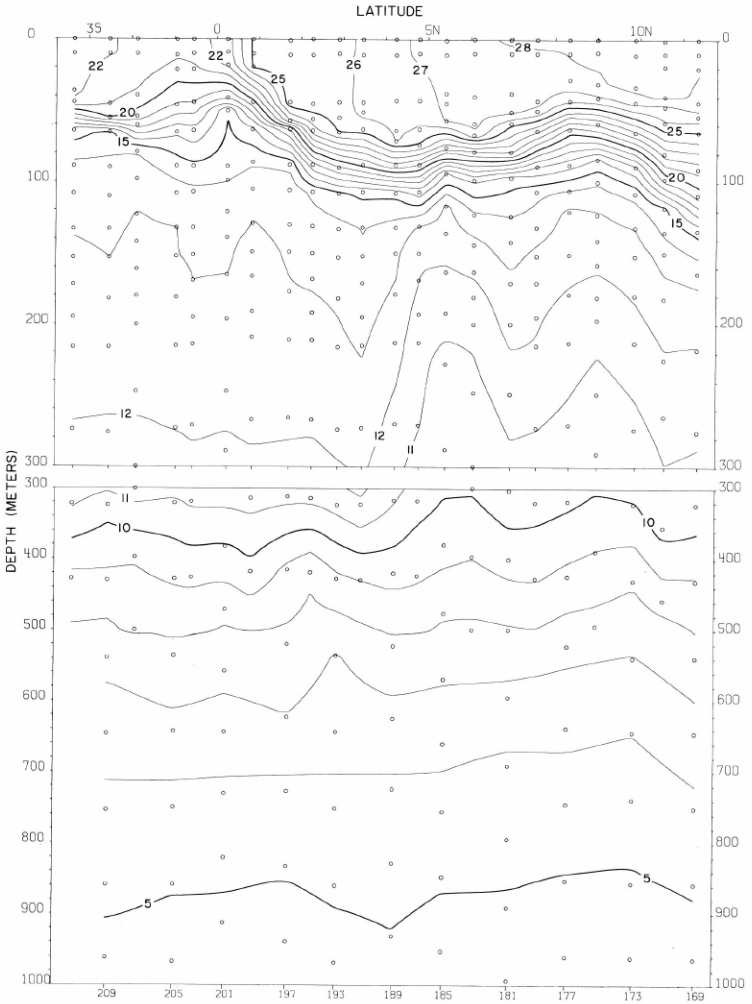

FIGURE 30-T-v5.—Vertical distribution of temperature (°C.) along 104°30′ W., July 13-18, 1967. These contours are based on Nansen cast data only.

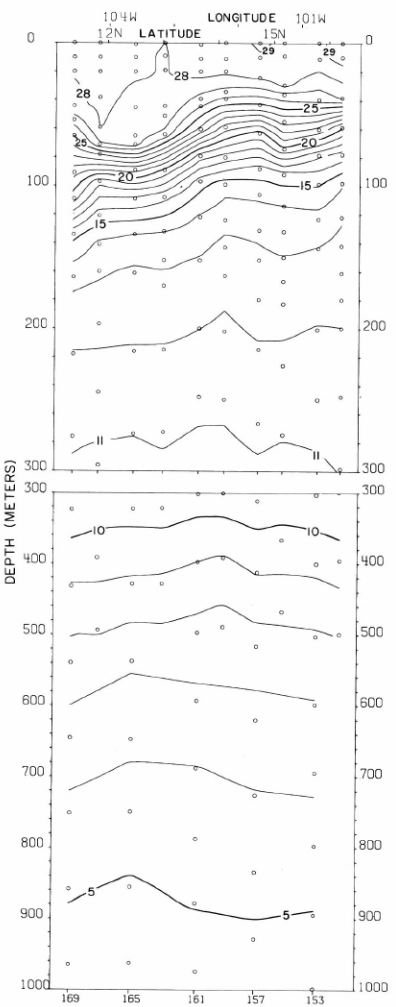

FIGURE 30-T-v4.—Vertical distribution of temperature (°C.) along a section from Acapulco to 12° N., 104°30′ W., July 10-13, 1967. These contours are based on Nansen cast data only.

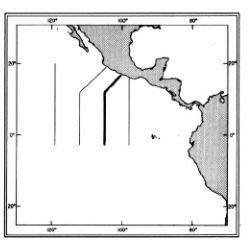

30-T-v4.

30-T-v5.

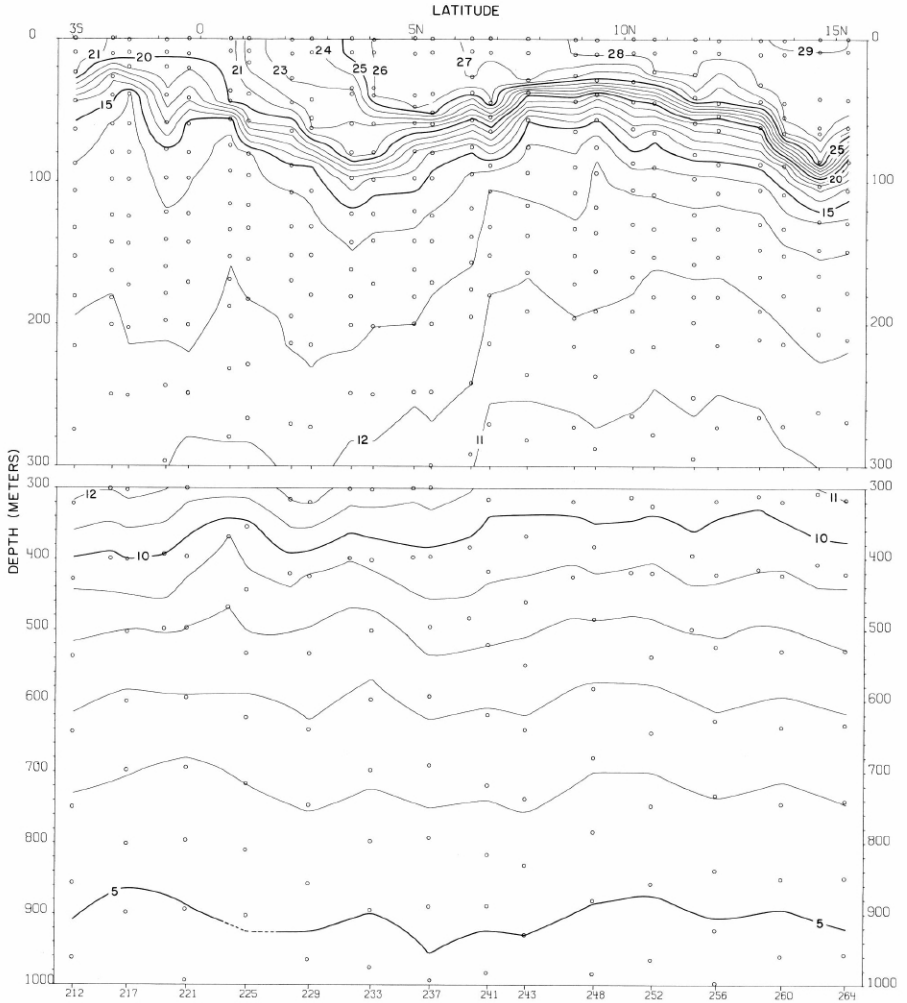

FIGURE 30-T-v6.—Vertical distribution of temperature (°C.) along 97°30′ W., July 20-27, 1967. These contours are based on Nansen cast data only.

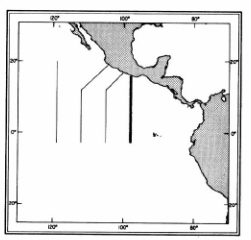

30-T-v6.

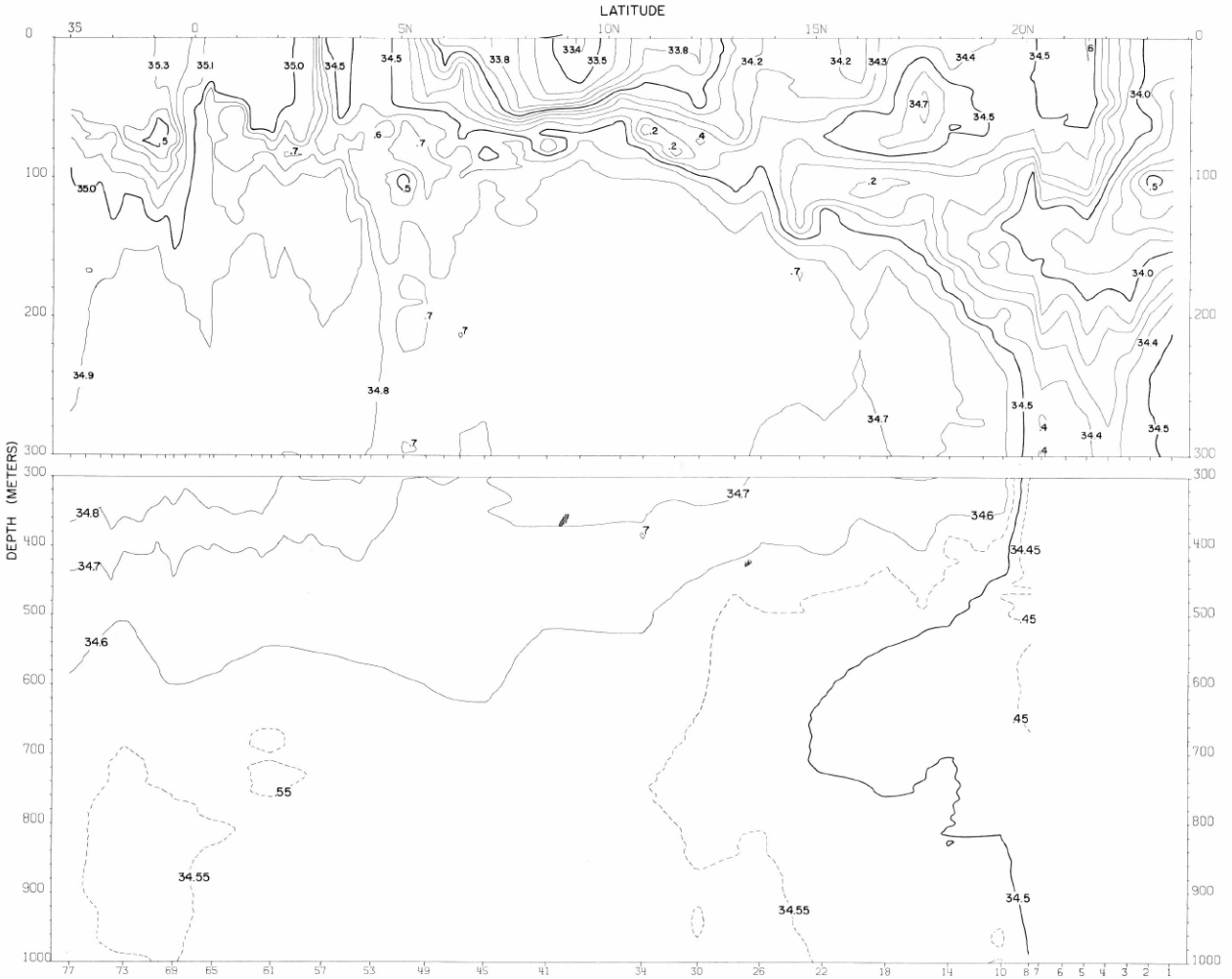

FIGURE 30-S-vl.—Vertical distribution of salinity (‰) along 118°30′ W., June 16-26, 1967.

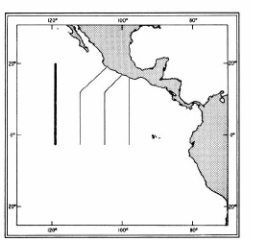

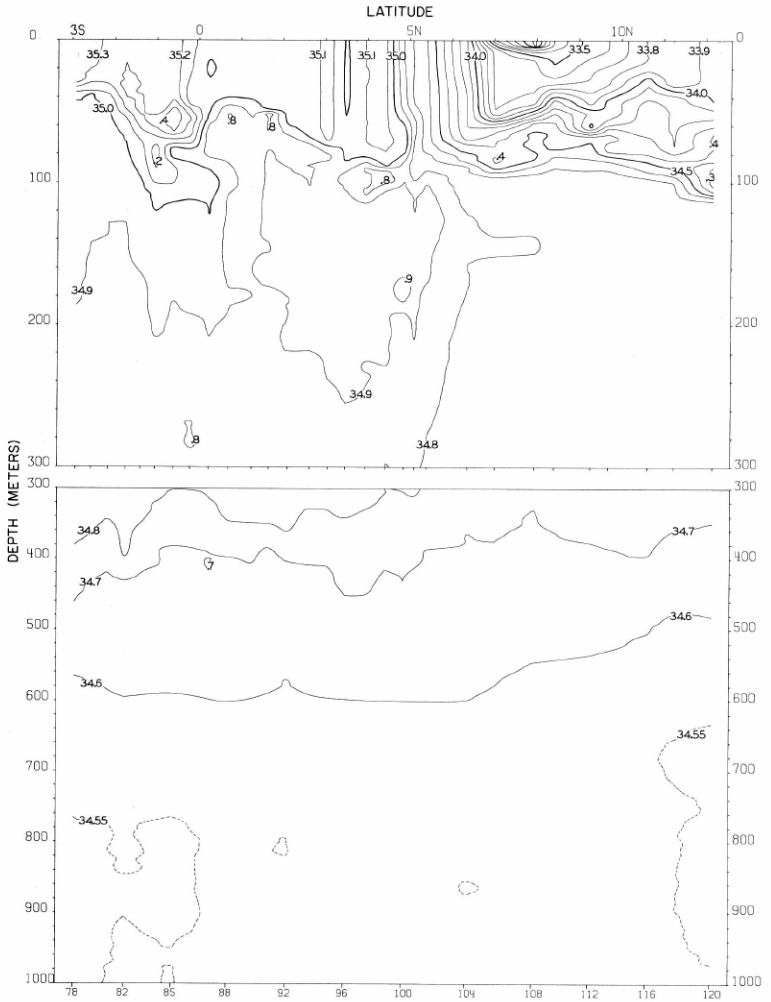

FIGURE 30-S-v2.—Vertical distribution of salinity (‰) along 111°30′ W., June 28-July 3, 1967.

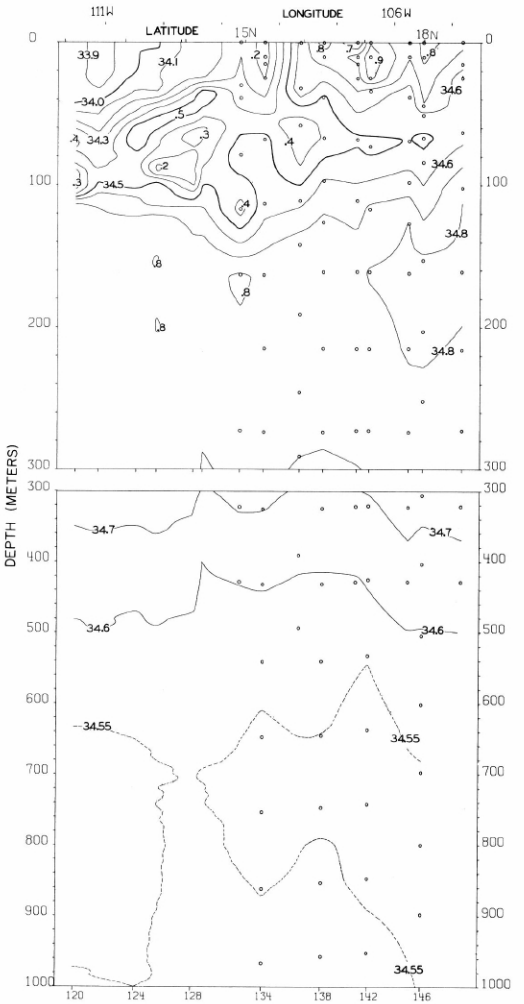

FIGURE 30-S-v3.—Vertical distribution of salinity (‰) along a section from 12° N., 111°30′ W. to Manzanillo, July 4-7, 1967. The contours from Stations 132-148 are based on Nansen cast data only.

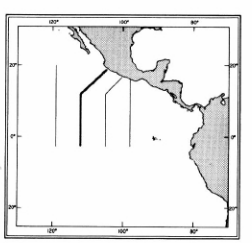

30-S-v2.

30-S-v3.

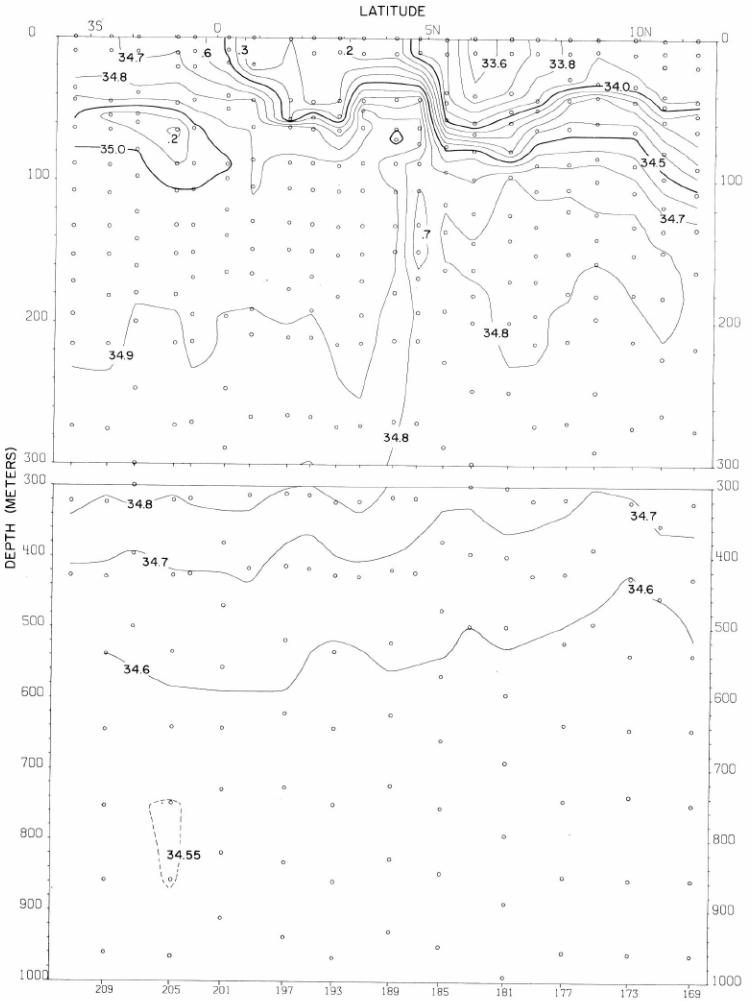

FIGURE 30-S-v5.—Vertical distribution of salinity (‰) along 104°30′ W., July 13-18, 1967. These contours are based on Nansen cast data only.

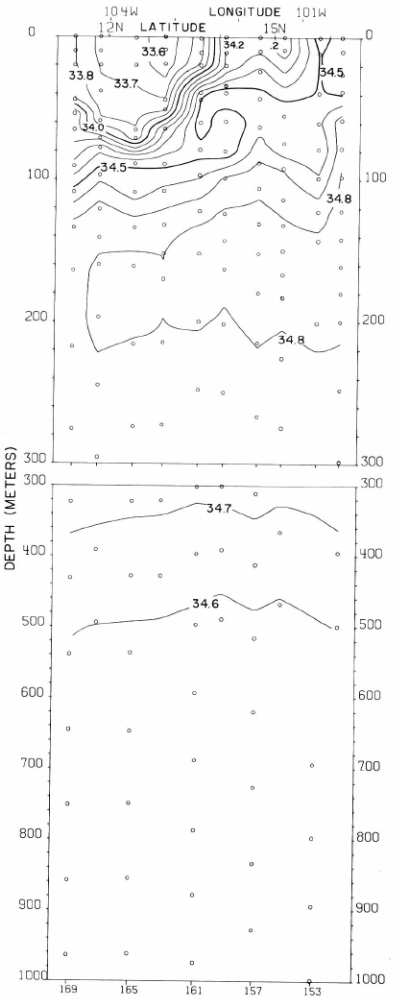

FIGURE 30-S-v4.—Vertical distribution of salinity (‰) along a section from Acapulco to 12° N., 104°30′ W., July 10-13, 1967. These contours are based on Nansen cast data only.

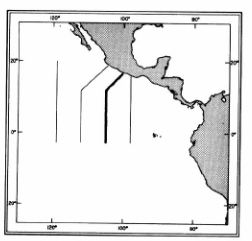

30-S-v4.

30-S-v5

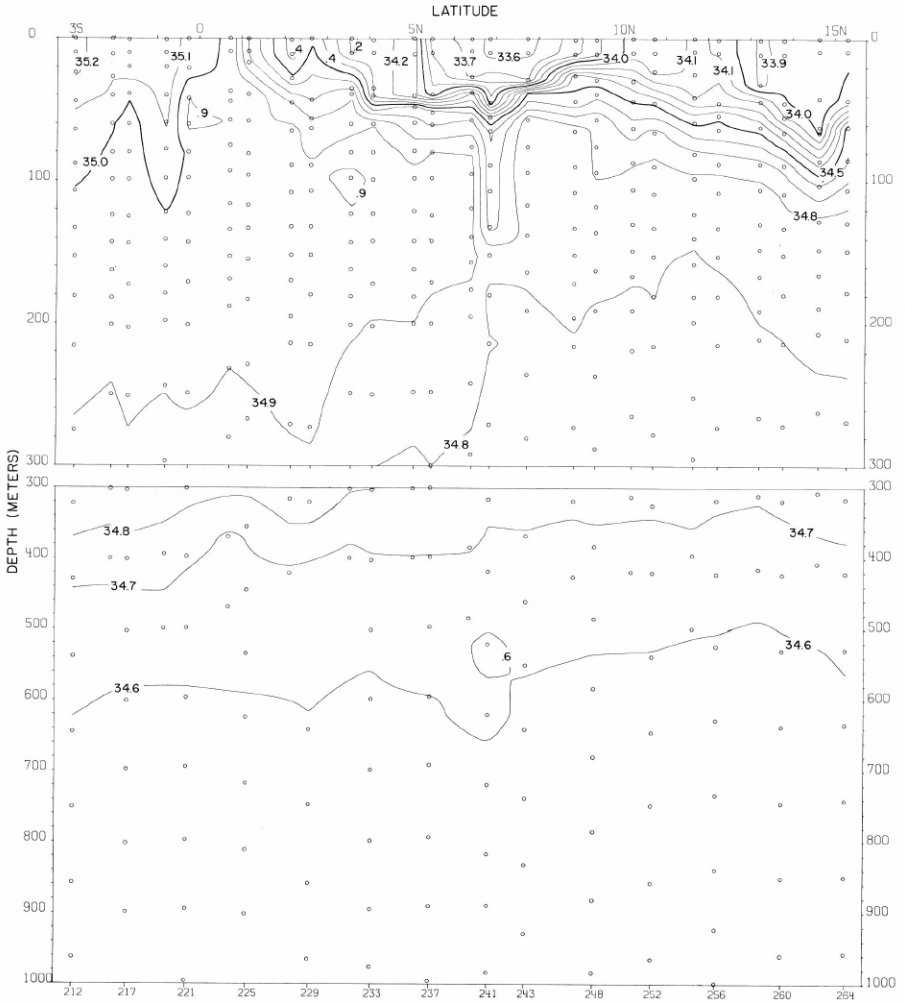

FIGURE 30-S-v6.—Vertical distribution of salinity (‰) along 97°30′ W., July 20-27, 1967. These contours are based on Nansen cast data only.

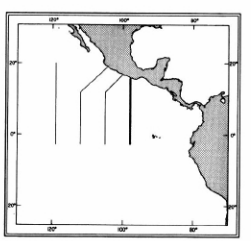

30-S-v6.

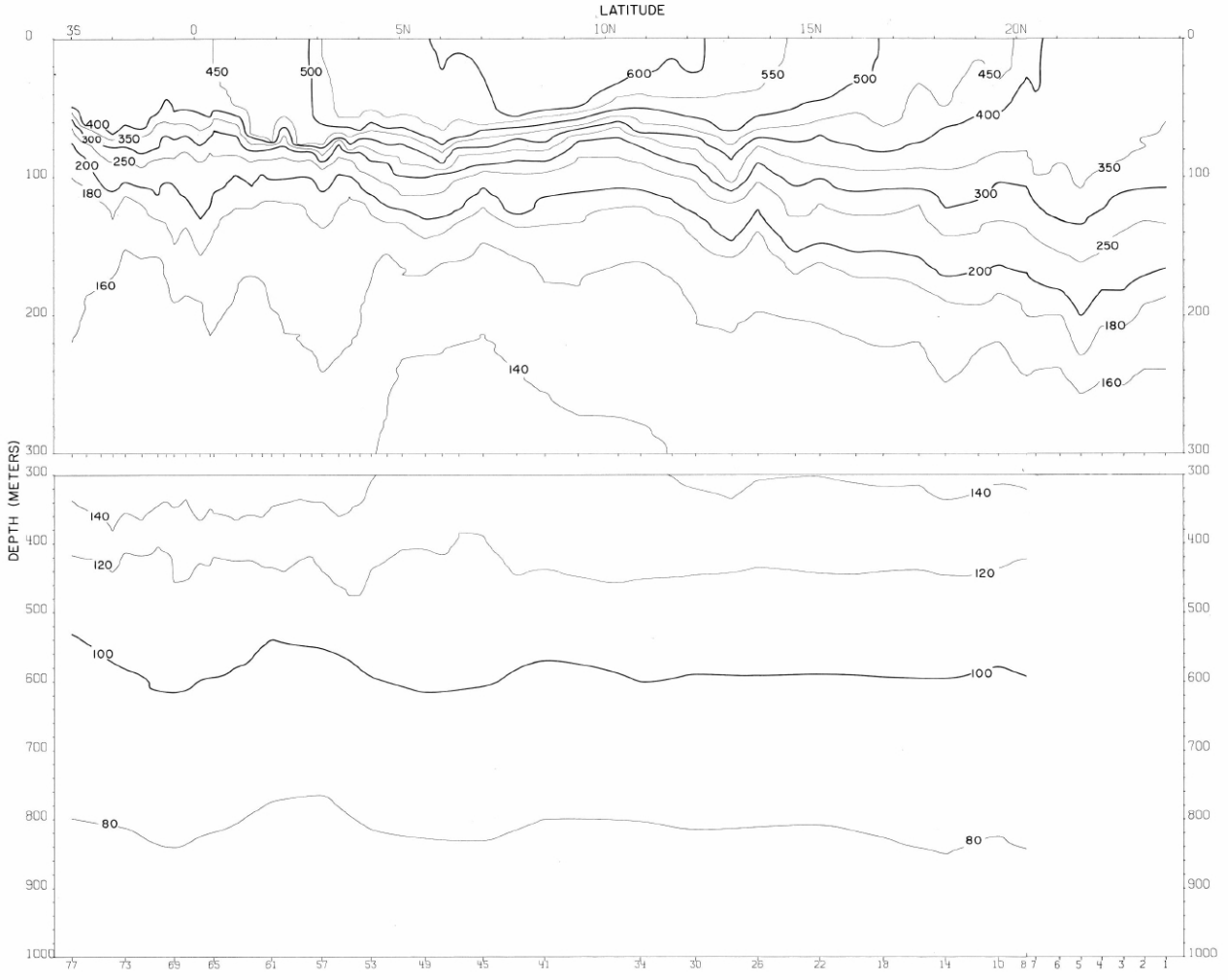

FIGURE 30-δ-vl.—Vertical distribution of thermosteric anomaly, δ_T, (cl./t.) along 118°30′ W., June 16-26, 1967.

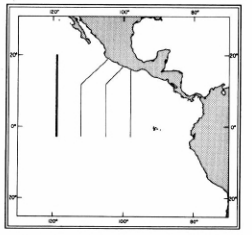

30-δ-vl.

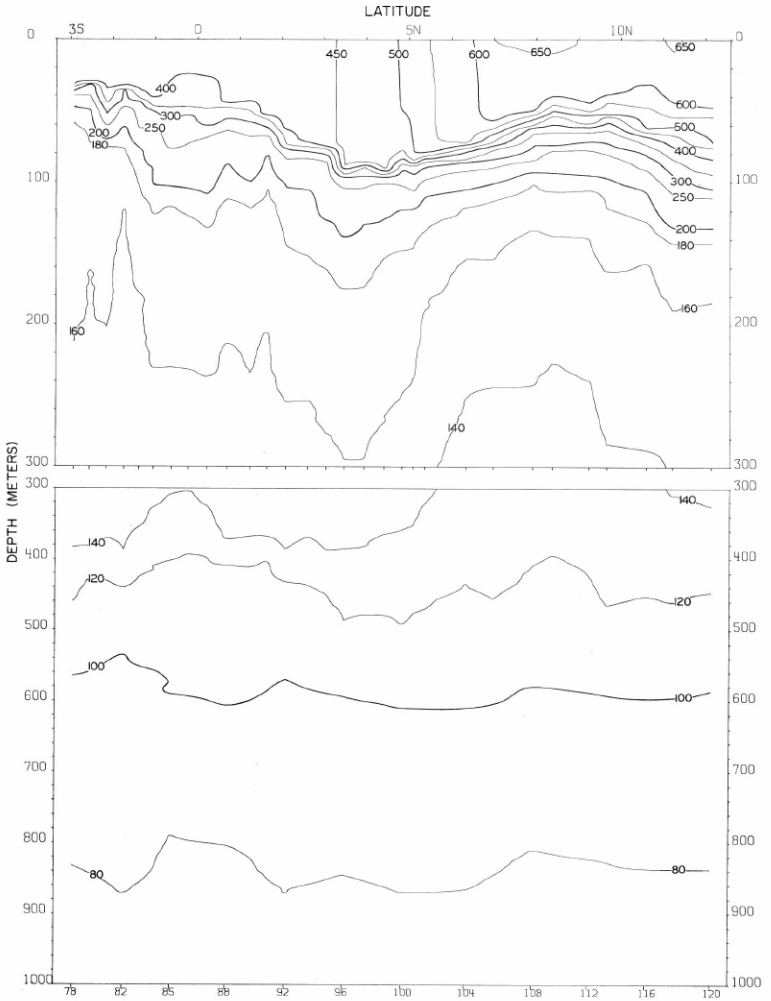

FIGURE 30-δ-v2.—Vertical distribution of thermosteric anomaly, δ_T, (cl./t.) along 111°30′ W., June 28-July 3, 1967.

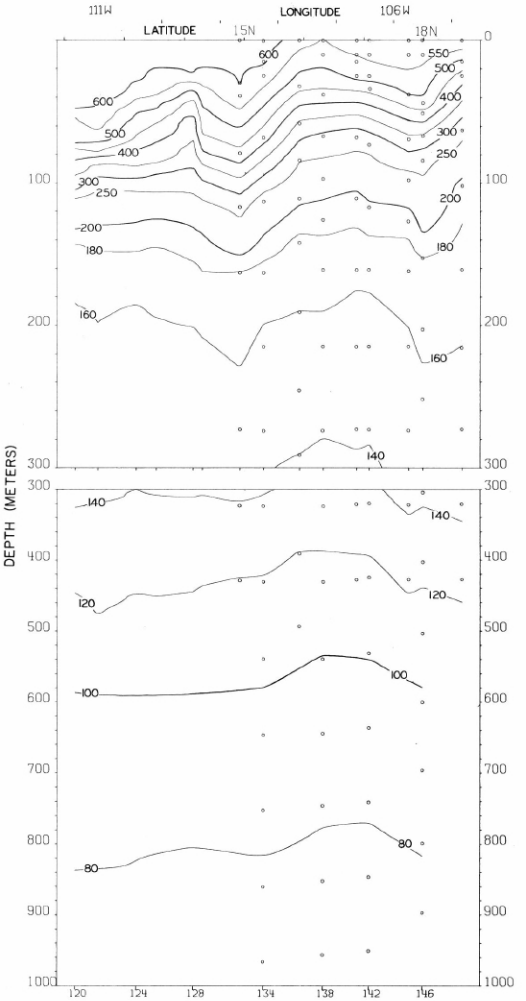

FIGURE 30-δ-v3.—Vertical distribution of thermosteric anomaly, δ_t, (cl./t.) along a section from 12° N., 111°30′ W. to Manzanillo, July 4-7, 1967. The contours from Stations 132-148 are based on Nansen cast data only.

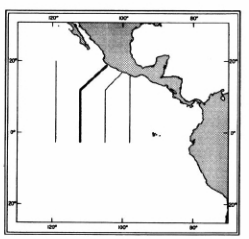

30-δ-v2.

30-δ-v3.

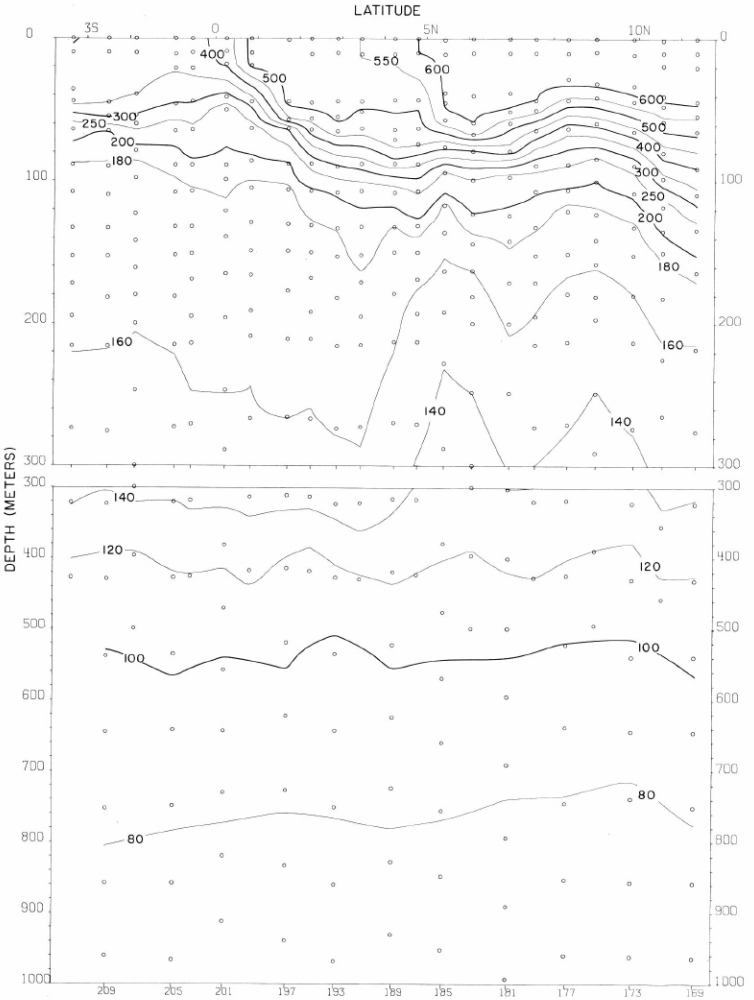

FIGURE 30-δ-v5.—Vertical distribution of thermosteric anomaly, δ_t, (cl./t.) along 104°30′ W., July 13-18, 1967. These contours are based on Nansen cast data only.

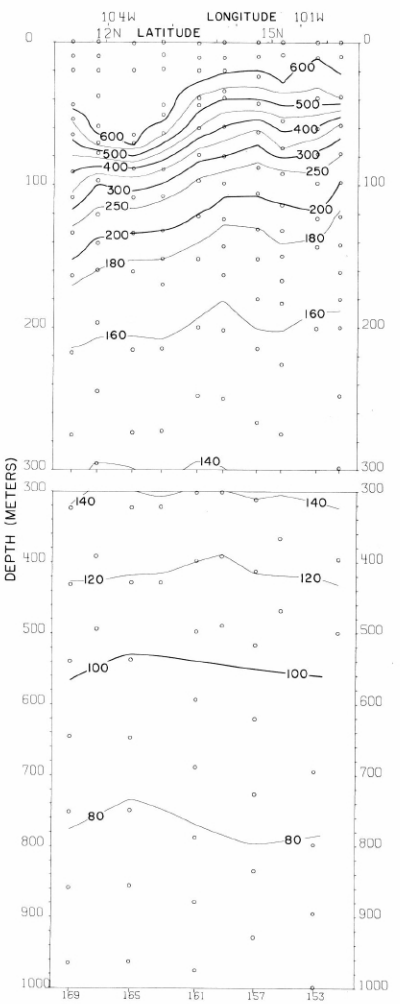

FIGURE 30-δ-v4.—Vertical distribution of thermosteric anomaly, δ_t, (cl./t.) along a section from Acapulco to 12° N., 104°30′ W., July 10-13, 1967. These contours are based on Nansen cast data only.

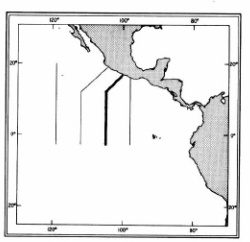

30-δ-v4.

30-δ-v5.

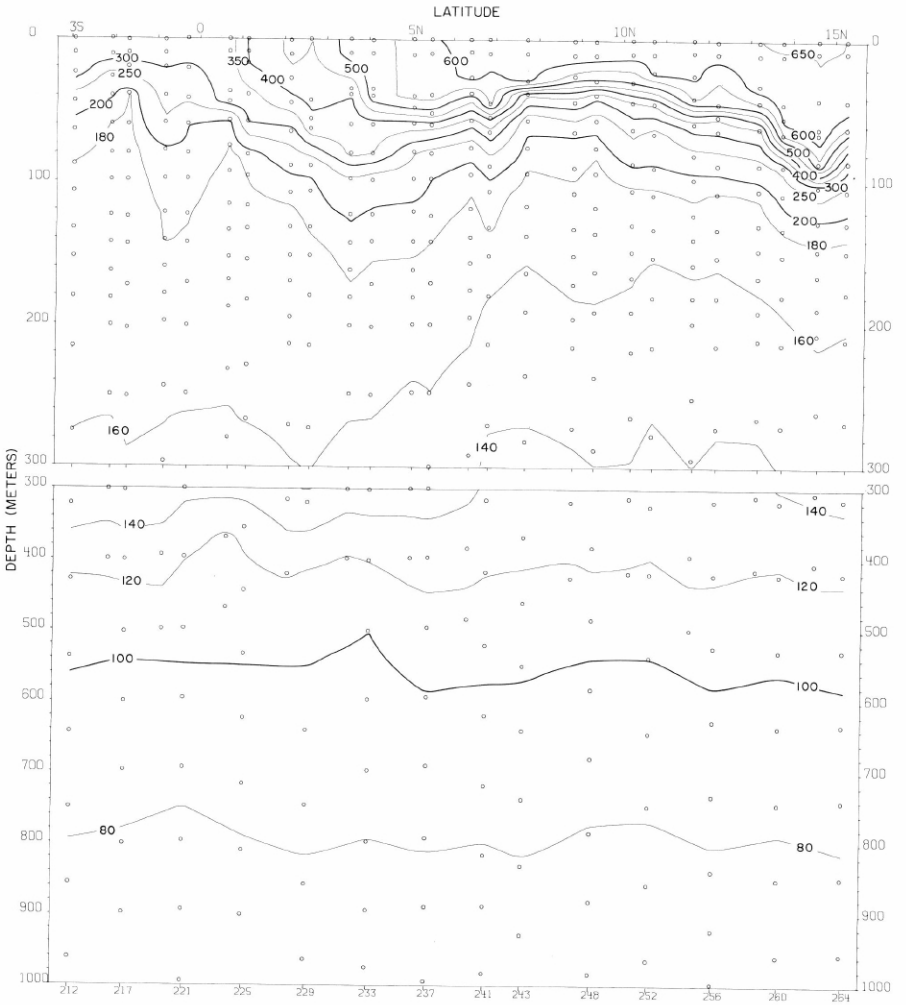

FIGURE 30-δ-v6.—Vertical distribution of thermosteric anomaly, δ_t, (cl./t.) along 97°30′ W., July 20-27, 1967. These contours are based on Nansen cast data only.

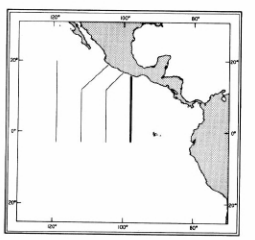

30-δ-v6.

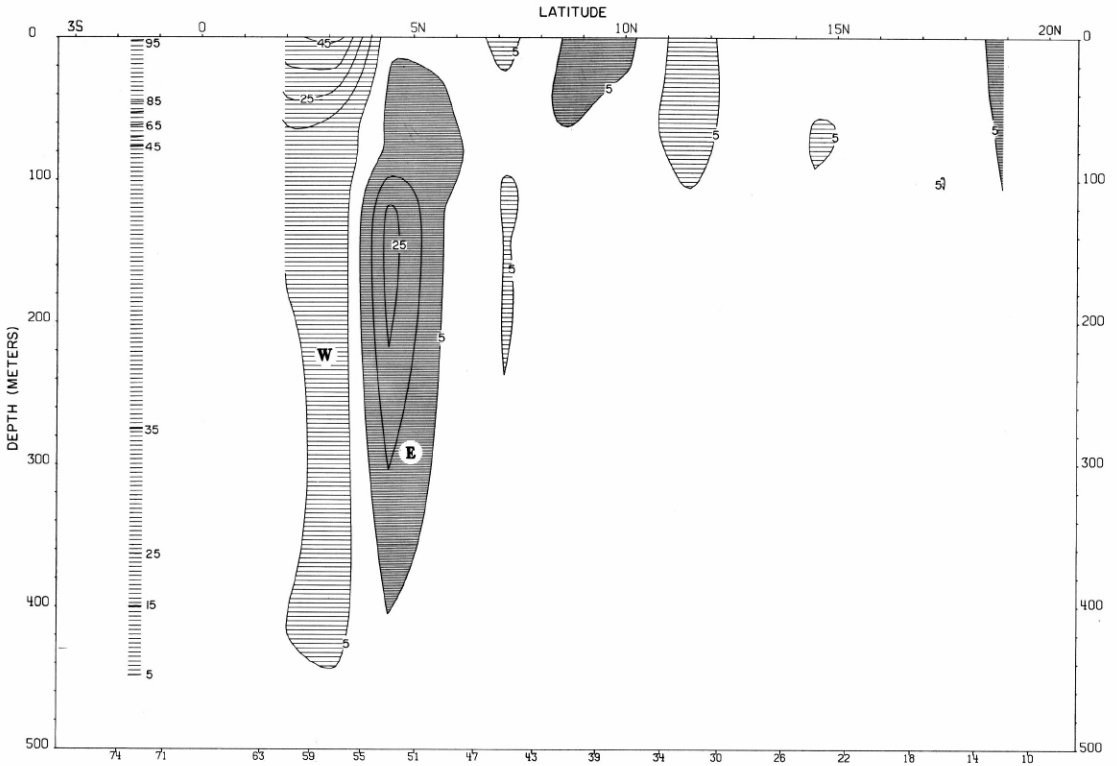

FIGURE 30-G-v1.—Vertical distribution of the zonal component of geostrophic velocity (cm./sec.), relative to 500 db., along 118°30′ W., June 17-26, 1967. Dark shading indicates eastward flow with a velocity greater than 5 cm./sec.; light shading indicates westward flow with a velocity greater than 5 cm./sec.

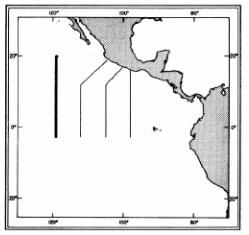

30-G-v1.

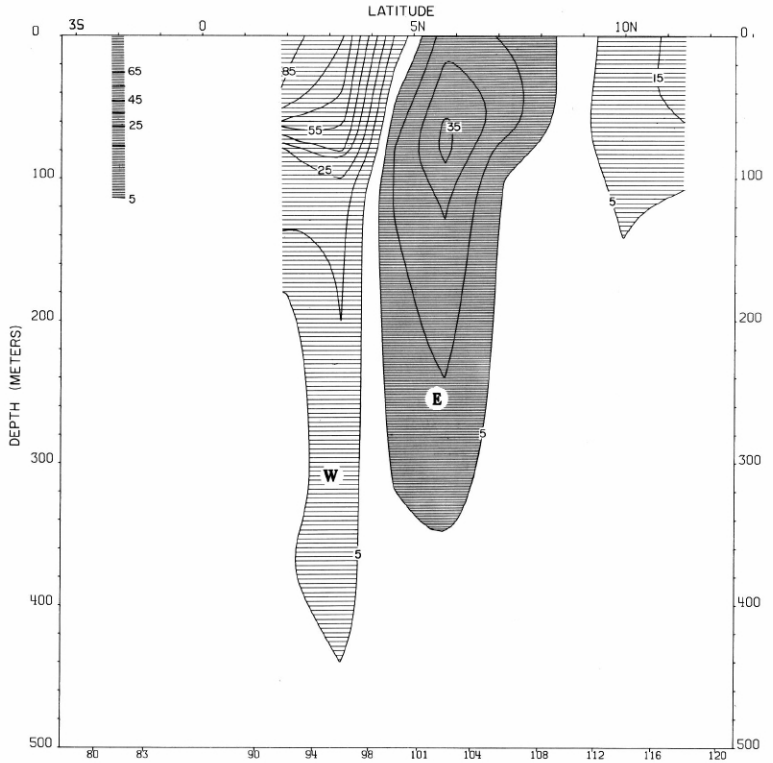

FIGURE 30-G-v2.—Vertical distribution of the zonal component of geostrophic velocity (cm./sec.), relative to 500 db., along 111°30′ W., June 28-July 3, 1967. Dark shading indicates eastward flow with a velocity greater than 5 cm./sec.; light shading indicates westward flow with a velocity greater than 5 cm./sec.

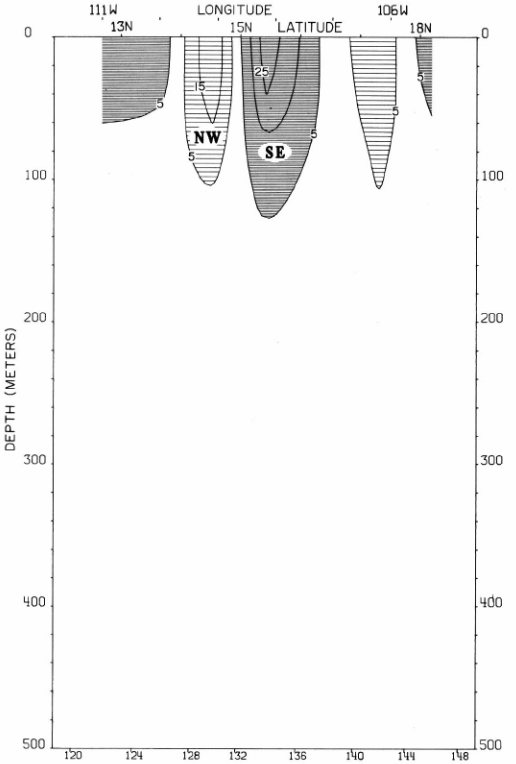

FIGURE 30-G-v3.—Vertical distribution of the component of geostrophic velocity (cm./sec.), relative to 500 db., normal to a section from 12° N., 111°30′ W., to Manzanillo, July 4-7, 1967. Dark shading indicates flow toward the southeast with a velocity greater than 5 cm./sec.; light shading indicates flow toward the northwest with a velocity greater than 5 cm./sec.

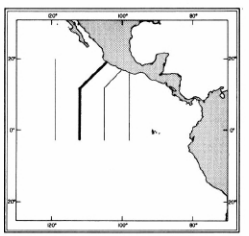

30-G-v2.

30-G-v3.

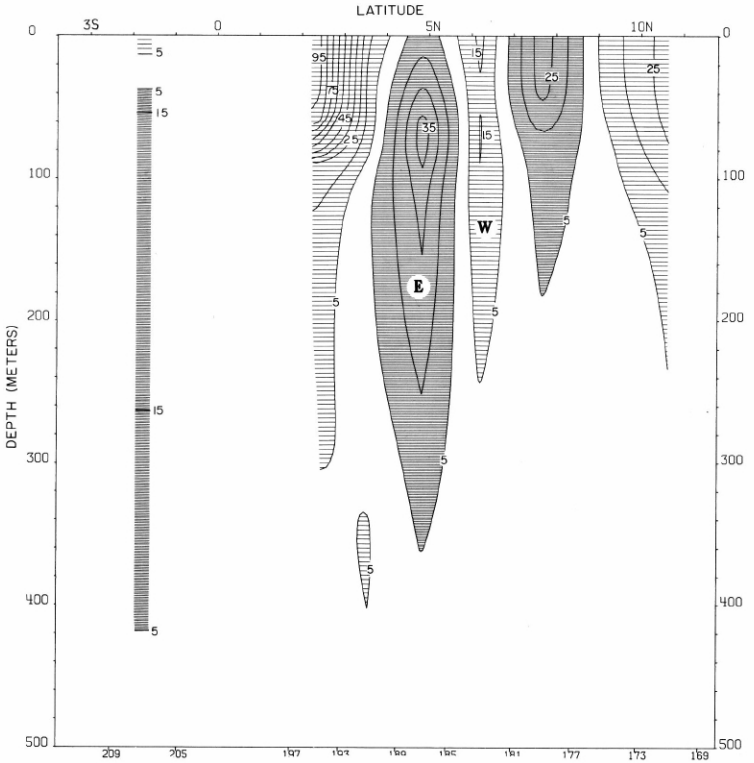

FIGURE 30-G-v5.—Vertical distribution of the zonal component of geostrophic velocity (cm./sec.), relative to 500 db., along 104°30′ W., July 13-18, 1967. Dark shading indicates eastward flow with a velocity greater than 5 cm./sec.; light shading indicates westward flow with a velocity greater than 5 cm./sec.

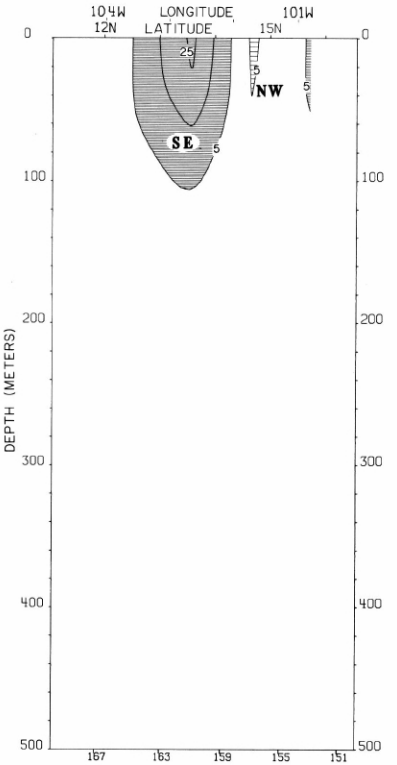

FIGURE 30-G-v4.—Vertical distribution of the component of geostrophic velocity (cm./sec.), relative to 500 db., normal to a section from Acapulco to 12° N., 104°30′ W., July 10-12, 1967. Dark shading indicates flow toward the southeast with a velocity greater than 5 cm./sec.; light shading indicates flow toward the northwest with a velocity greater than 5 cm./sec.

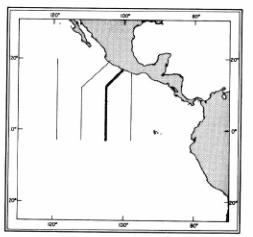

30-G-v4.

30-G-v5.

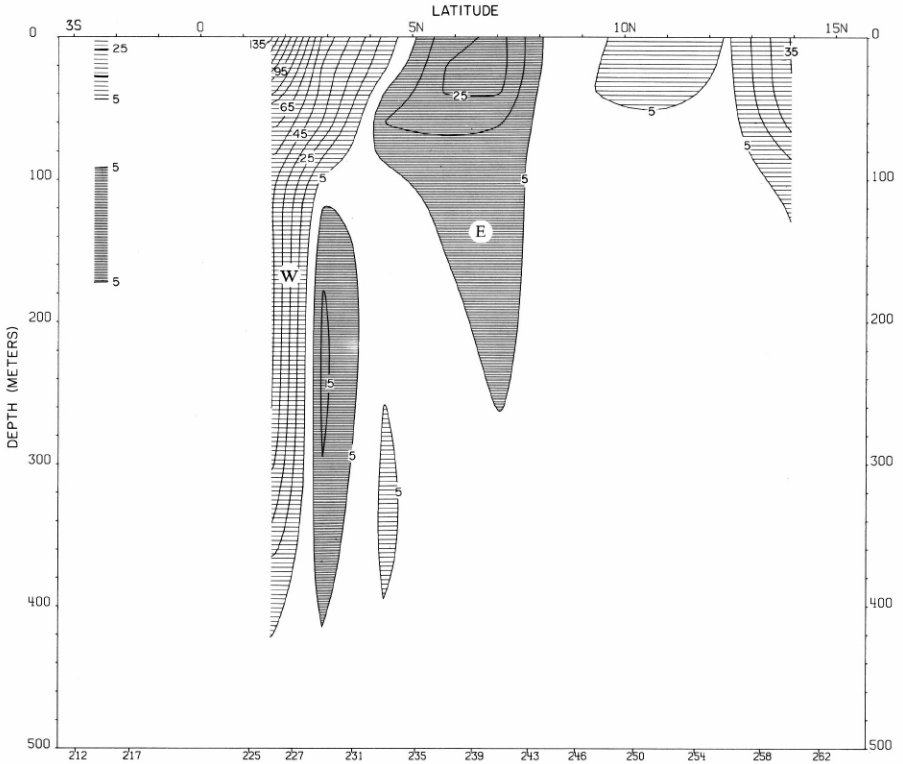

FIGURE 30-G-v6.—Vertical distribution of the zonal component of geostrophic velocity (cm./sec.), relative to 500 db., along 97°30′ W., July 20-26, 1967. Dark shading indicates eastward flow with a velocity greater than 5 cm./sec.; light shading indicates westward flow with a velocity greater than 5 cm./sec.

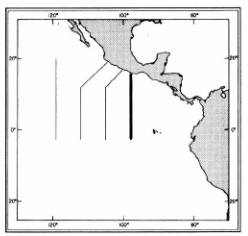

30-G-v6.

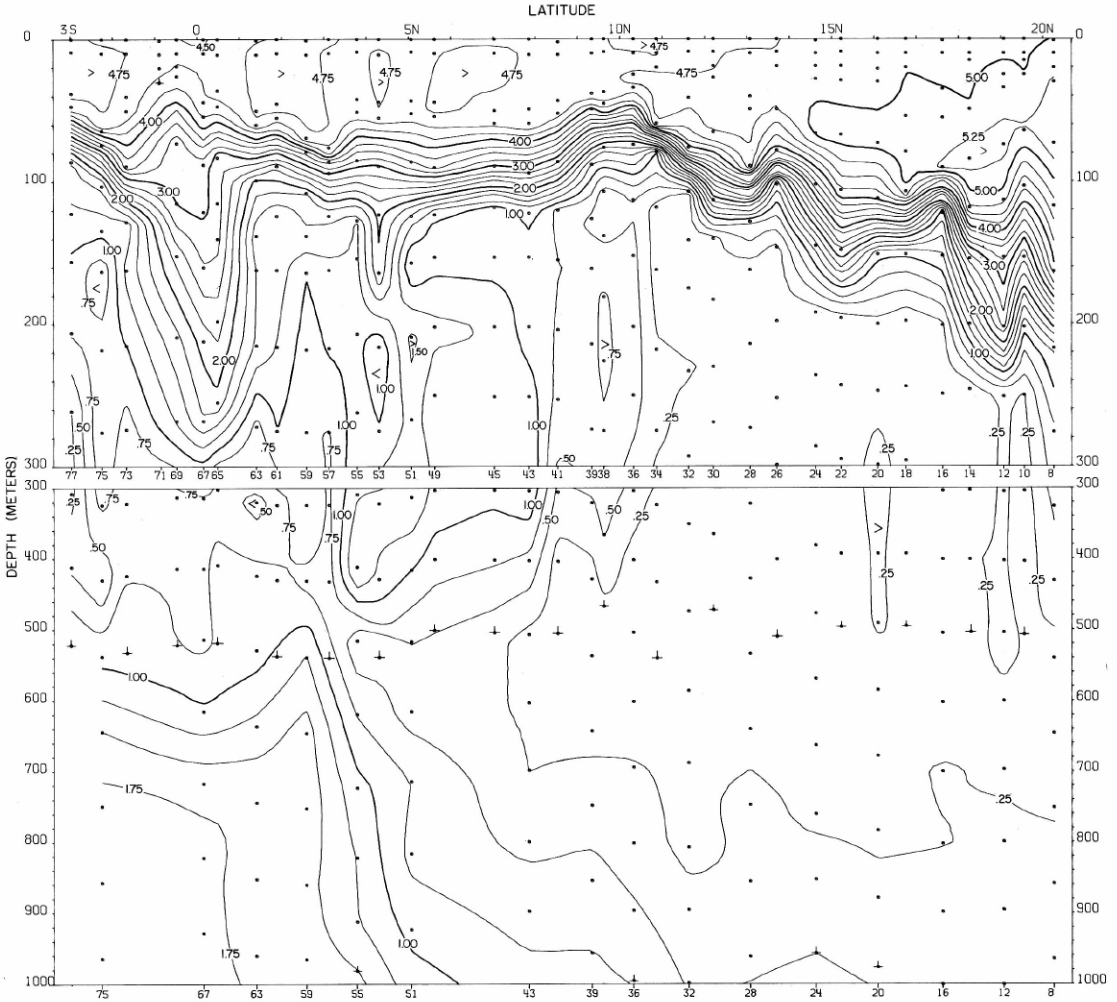

FIGURE 30-O2-v1.—Vertical distribution of oxygen (ml./l.) along 118°30′ W., June 17-26, 1967.

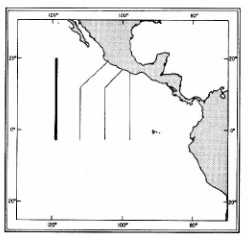

30-O2-v1.

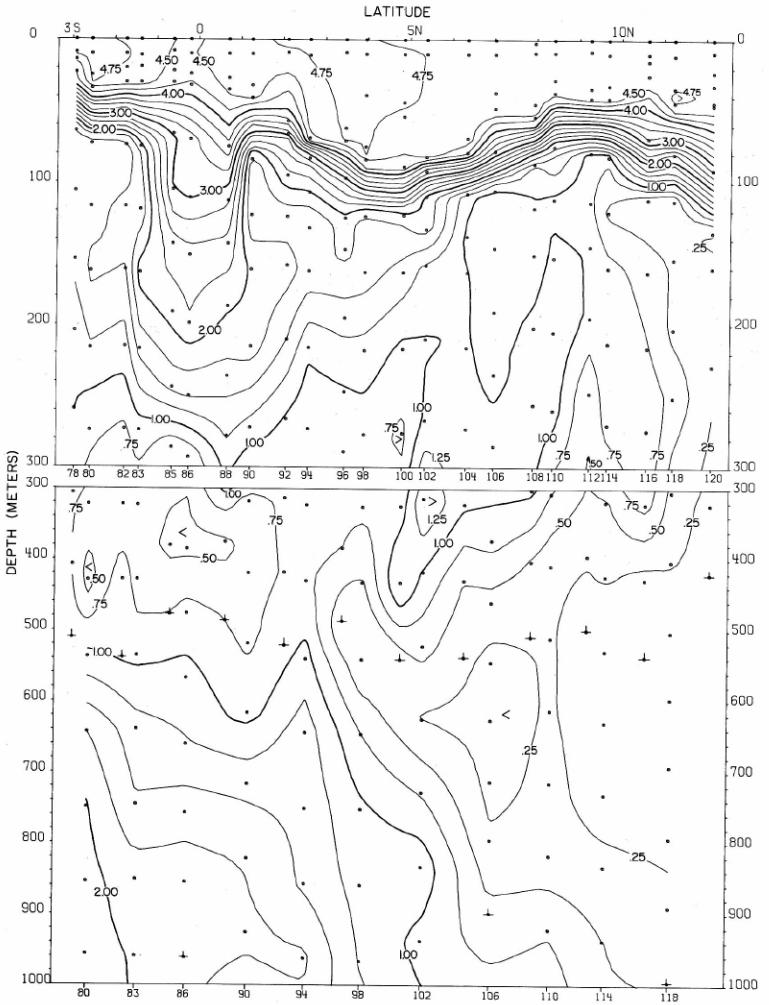

FIGURE 30-O₂-v2.—Vertical distribution of oxygen (ml./l.) along 111°30′ W., June 28-July 4, 1967.

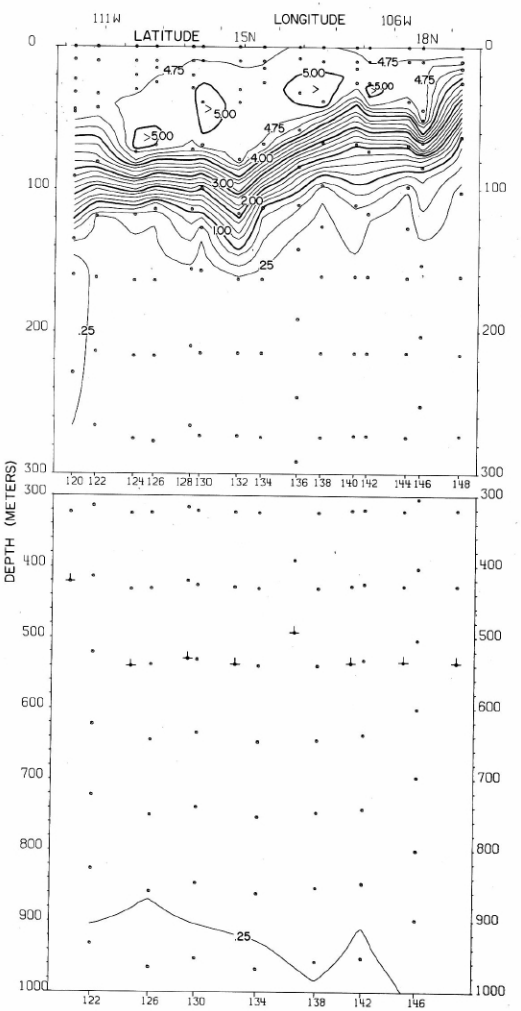

FIGURE 30-O₂-v3.—Vertical distribution of oxygen (ml./l.) along a section from 12° N., 111°30′ W. to Manzanillo, July 4-7, 1967.

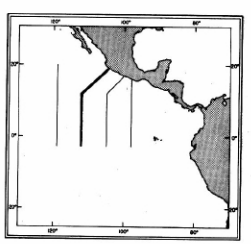

30-O₂-v2.

30-O₂-v3.

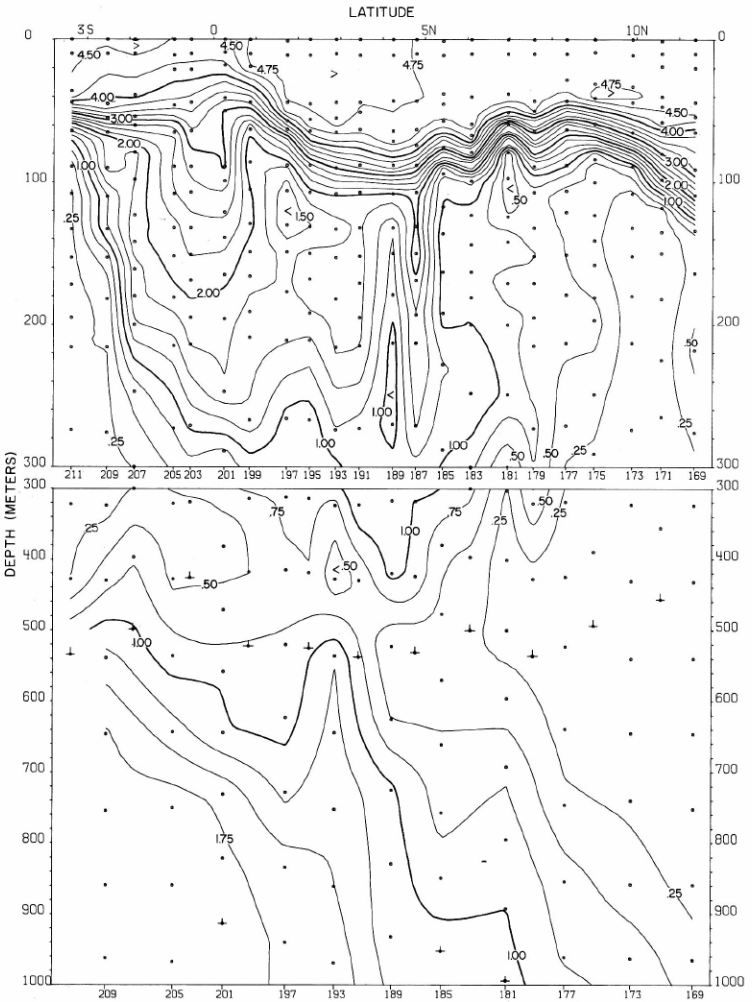

FIGURE 30-O2-v5.—Vertical distribution of oxygen (ml./l.) along 104°30′ W., July 13-18, 1967.

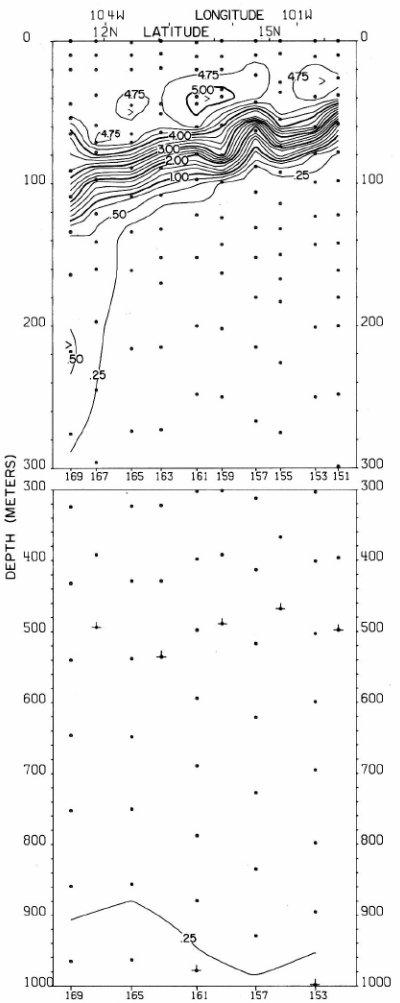

FIGURE 30-O2-v4.—Vertical distribution of oxygen (ml./l.) along a section from Acapulco to 12° N., 104°30′ W., July 10-13, 1967.

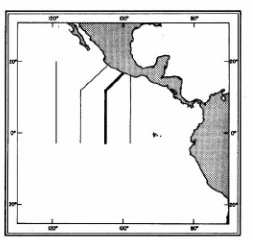

30-O2-v4.

30-O2-v5.

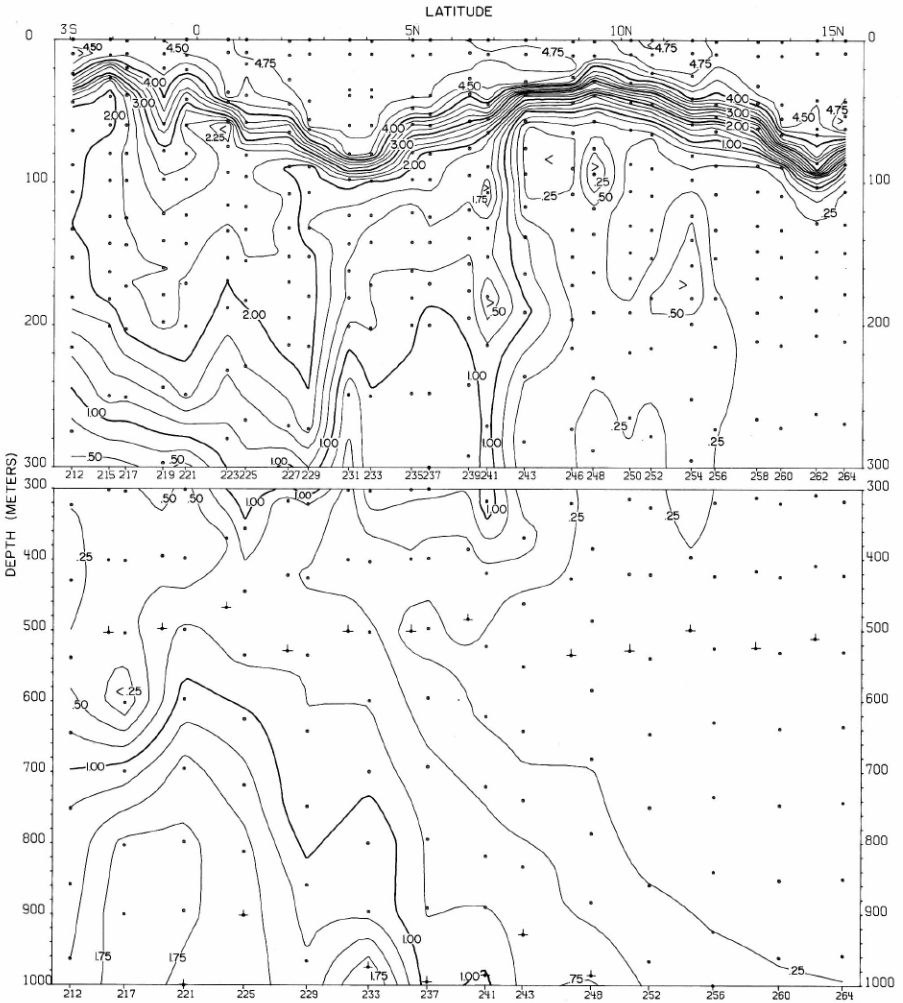

FIGURE 30-O₂-v6.—Vertical distribution of oxygen (ml./l.) along 97°30′ W., July 20-27, 1967.

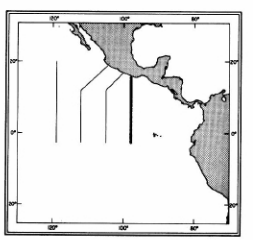

30-O₂-v6.

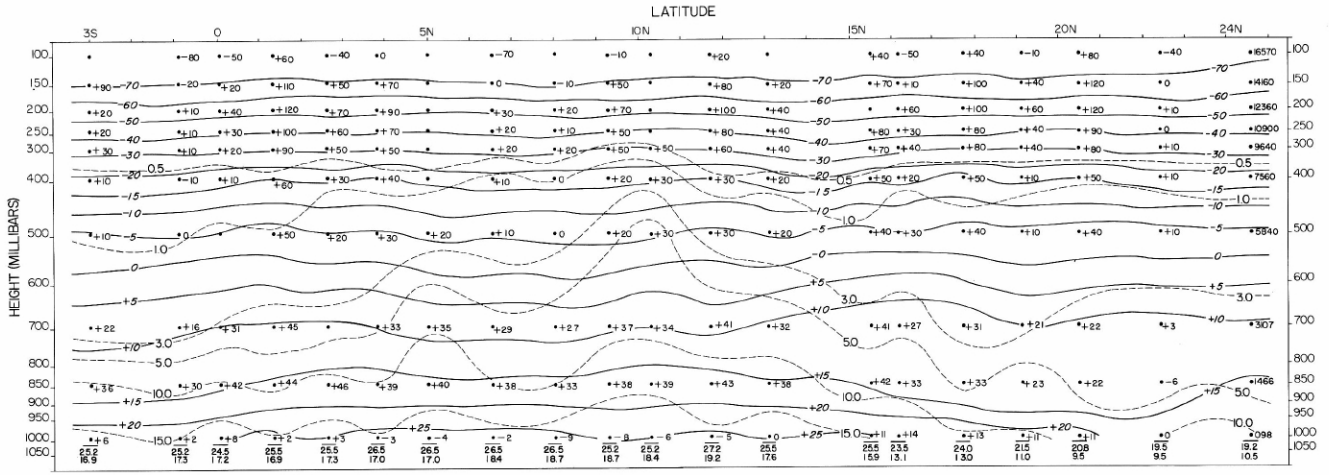

FIGURE 30-UA-vl.—Vertical section of the atmosphere along 118°30′ W., June 16-27, 1967. Solid lines are isotherms of air temperature (°C.). Dashed lines are isopleths of mixing ratio of the air (g./kg.). Surface air temperature is plotted above surface mixing ratio and below a base line representing the surface pressure (mb.). The computed height (m.) of each standard pressure surface is plotted for the northernmost radiosonde station of the section. At other stations the difference of computed height minus the corresponding height at the northern station is shown at each standard level.

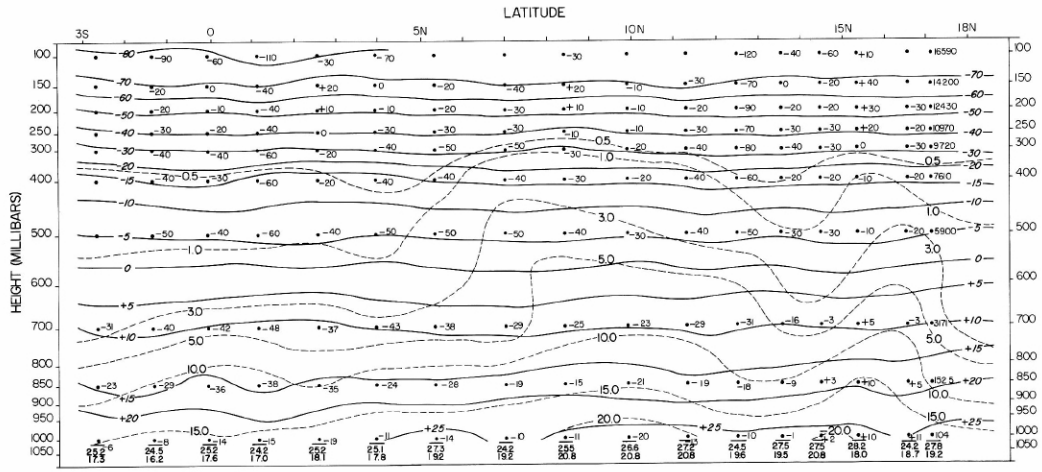

FIGURE 30-UA-v2.—Vertical section of the atmosphere along 111°30′ W., June 28 to July 7, 1967. Solid lines are isotherms of air temperature (°C.). Dashed lines are isopleths of mixing ratio of the air (g./kg.). Surface air temperature is plotted above surface mixing ratio and below a base line representing the surface pressure (mb.). The computed height (m.) of each standard pressure surface is plotted for the northernmost radiosonde station of the section. At other stations the difference of computed height minus the corresponding height at the northern station is shown at each standard level.

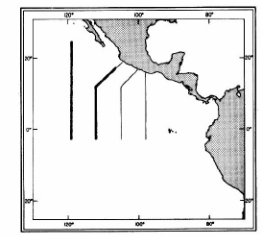

30-UA-vl.

30-UA-v2.